UNIVERSITY OF SOUTHAMPTON

FACULTY OF MEDICINE

Cancer Sciences Unit

The Role of Cancer-Associated Fibroblasts in Chemoresistance in Oesophageal Adenocarcinoma

by

Clarisa Thian Puay Choh

MBBS, MRCSEd, PG CertMedEd, AcadMedEd

Thesis for the degree of Doctor of Medicine

2015 - 2019

UNIVERSITY OF SOUTHAMPTON

ABSTRACT

FACULTY OF MEDICINE, Cancer Sciences Unit

Doctor of Medicine

THE ROLE OF CANCER-ASSOCIATED FIBROBLASTS IN CHEMORESISTANCE IN OESOPHAGEAL ADENOCARCINOMA

Clarisa Thian Puay Choh

Oesophageal cancer is the fastest rising cancer in the UK, being the 5th most common cause of cancer death and associated with a low 5-year survival of 15%. 39% of patients diagnosed with oesophageal cancer have a curative management plan, half of which undergo neoadjuvant chemotherapy and surgery. Despite 70% of this cohort of patients completing chemotherapy treatment, tumour response was observed in less than 40%. This was thought to be attributable to the close relationship within the stroma and the cancer cells, which may affect the resistance of cancer cells to chemotherapy. This thesis aims to explore the role of cancer-associated fibroblasts (CAFs) in oesophageal adenocarcinoma, and its relation to chemoresistance.

Chemoresistance was characterized by using chemotherapy response in oesophageal adenocarcinoma cell lines as a surrogate marker. The role of CAFs in influencing chemoresistance was investigated with CAF-conditioned medium, and spheroidal co-cultures as a form of 3D modelling. Subsequently, phosphodiesterase-5 inhibitors (PDE5i), which had been reported to de-activate CAFs, were used on CAFs to determine if oesophageal adenocarcinoma cells could be re-sensitised to chemotherapy after treatment. Biomarkers specific to CAFs were then examined for its association with survival and to determine its relation to prediction of response to chemotherapy.

Colony growth assays demonstrated a positive effect when oesophageal adenocarcinoma cells were placed in CAF-conditioned media, together with higher drug concentrations required in dose-response assays, both of which were remediated with PDE5i treatment. When used in spheroids, there appeared to be some enhanced metabolic activity when both types of cells were in combination, and activity reduction with PDE5i treatment.

In conclusion, CAFs appear to be involved in influencing chemoresistance in oesophageal adenocarcinoma, and that PDE5i treatment seem to re-sensitize cancer cells to chemotherapy and thereby require a lower drug concentration for a cytotoxic effect. Tumour stage and presence of a biomarker such as nestin in cancerous lymph nodes correlated with a poor survival outcome, and could be considered a viable prognostic marker that can be utilized in the future.

Table of Contents

List of Tables

List of Figures

DECLARATION OF AUTHORSHIP

I, Clarisa Thian-Puay Choh, declare that this thesis and the work presented in it are my own and has been generated by me as the result of my own original research.

'The Role of Cancer-Associated Fibroblasts in Chemoresistance in Oesophageal Adenocarcinoma'

I confirm that:

1. This work was done wholly or mainly while in candidature for a research degree at this University;
2. Where any part of this thesis has previously been submitted for a degree or any other qualification at this University or any other institution, this has been clearly stated;
3. Where I have consulted the published work of others, this is always clearly attributed;
4. Where I have quoted from the work of others, the source is always given. With the exception of such quotations, this thesis is entirely my own work;
5. I have acknowledged all main sources of help;
6. Where the thesis is based on work done by myself jointly with others, I have made clear exactly what was done by others and what I have contributed myself;
7. Parts of this work have been published as per Appendix I:

    - Authentication and characterisation of a new oesophageal adenocarcinoma cell line: MFD1*. Scientific Reports* 2016; **6**: 32417.
    - NCRI Cancer Conference 2016, Liverpool - PDE5 Inhibitors Can Ameliorate Chemoresistance in Oesophageal Adenocarcinoma Caused by Cancer-Associated Fibroblasts
    - 10th National Barretts symposium, London

      - Cancer-Associated Fibroblasts Can Promote Chemoresistance in Oesophageal Adenocarcinoma In Vitro

      - Optimising PDE5 Inhibitor Induced Dedifferentiation of Cancer-Associated Fibroblasts

      - Optimising Chemoradiation Methodology for the Study of the Tumour Microenvironment in Oesophageal Adenocarcinoma

Signed: .....

Date: .....

Acknowledgements

Undertaking this MD has been an amazing experience. Many people have helped me along this journey, to whom I am indebted to that I wish to acknowledge.

First and foremost, I must thank my supervisor Professor Tim Underwood for being instrumental in helping me in my MD and directing efforts in the thesis to my interests and strengths in Upper GI Surgery. His enthusiasm for research, persistence for results and constant support are very much appreciated. I would also like to thank my supervisors Dr Jeremy Blaydes & Dr Gareth Thomas for their help in helping me decipher biology!

I would also like to thank Dr Annette Hayden for her unwavering help and patience in teaching me laboratory techniques, sharing their science secrets, and making my journey in research fun and interesting, and our medical student Ewan Kyle, who was always in tissue culture hood with me carrying out joint experiments, and finding out about surgery.

I would personally like to thank Dr Sam Drennan (CLL Group) for her limitless patience in her help with the FACS machine and its mysterious workings. Whatever faults there are with the machine, or more importantly, my results, she seems to fix the problem and magic the headaches away!

My eternal gratitude is extended to Monette Lopez and Maria Machado (Histopathology Research Department) for their help with my tissue microarrays; Dr Eleanor Jaynes for her help and patience in marking slides to aid in the construction of TMAs. Humongous thanks goes to Gui Han Lee, a wonderful colleague, friend and teacher, who has helped me understand mind-boggling medical statistics a little better!

To my wonderful stars who have kept me sane throughout my time at the Cancer Sciences Unit in Southampton – Hollie, Sara, Durga, Andrew, Giorgia, thank you.

Finally I would like to thank my parents and sister Corinna, for their massive support in me, especially to my husband, Dan (and our dog Rosie), who have been extremely supportive, patient, optimistic and believing in me in achieving the results in this thesis and making a difference in oesophageal cancer!

Funding

This research was entirely self-funded, with consumables partially funded from Spire Southampton Hospital and grants from Professor Tim Underwood's Advanced Clinician Scientist Award.

Conflict of Interest

None declared.

Abbreviations

3D	three-dimensional
5FdUMP	5-fluoro-2'-deoxyuridine 5'-monophosphate
5FU	5-fluorouracil
7AAD	7-aminoactinomycin D
α-SMA	alpha smooth muscle actin
β-actin	beta actin
γ-IFN	gamma-interferon
ABC	ATP-binding cassette
ABCB1	ATP-binding cassette subfamily B member 1, also known as P-glycoprotein
APC	antigen presenting cells
APC (FACS)	allophycocyanin
BCL-x_L	B-cell lymphoma-extra large
BEST	Barrett's Esophagus Trial
BO	Barrett's oesophagus
BMI	body mass index
BPH	benign prostatic hypertrophy
BSA	bovine serum albumin
CAFs	cancer-associated fibroblasts
CAF-CM	conditioned medium from cancer-associated fibroblasts
cAMP	cyclic adenosine 3,5-monophosphate
c-ABL	Abelson murine leukaemia viral homolog 1
cDNA	complementary deoxyribonucleic acid
cGMP	cyclic guanosine 3,5-monophosphate
cGMP-NO	cyclic guanosine monophosphate – nitric oxide
Cav1	caveolin-1
CDK2	cyclin-dependent kinase 2
CDKN2A	cyclin-dependent kinase inhibitor 2A
CD(number)+	cluster of differentiation
CI	confidence interval

CLL	chronic lymphocytic leukaemia
CM	conditioned media
COL11A1	collagen type XI alpha I
COX2	cyclo-oxygenase 2
CRT	chemoradiotherapy
CRUK	Cancer Research UK
CT	computed tomography
CXCL2	chemokine (C-X-C motif) ligand 2
CXCR7	chemokine (C-X-C motif) receptor 7
DAB	3,3'-diaminobenzidine
DDR	DNA damage repair
DFS	disease free survival
DMEM	Dulbecco's Modified Eagle medium
DMSO	dimethyl sulphoxide
DNA	deoxyribonucleic acid
DNMT1	deoxyribonucleic acid methytransferase1
DOCK2	dedicator of cytokinesis 2
DTT	dithiothreitol
ECF	epirubicin, cisplatin and 5-fluorouracil
ECM	extracellular matrix
ECX	epirubicin, cisplatin and capecitabine
EDTA	ethylene diamino tetraacetic acid
EGF	epidermal growth factor
EGFR	epidermal growth factor receptor
EGFR-TKI	epidermal growth factor receptor-tyrosine kinase inhibitors
ELMO1	engulfment and cell motility protein 1
EMR	endoscopic mucosal resection
EMT	epithelial-to-mesenchymal transition
EORTC QLQ	European Organization for Research and Treatment of Cancer Quality of Life Questionnaire
ERACC	European Collection of Authenticated Cell Collections
ERCC1	excision repair cross-complementation group 1
ERK	extracellular signal-regulated kinases

EUS	endoscopic ultrasound
FACS	fluorescence activated cell sorting
FAK	focal adhesion kinase
FAP	fibroblast activation protein
FCS	foetal calf serum
FDG-PET	fluorodeoxyglucose positron emission tomography
FITC	fluorescein isothiocyanate
FGF	fibroblast growth factor
FSC	forward scatter
FSP1	fibroblast specific protein 1
FVD	fixable viability dye
GAPDH	glyceraldehyde-3-phosphate dehydrogenase
GI	gastrointestinal
GIST	gastrointestinal stromal tumour
GORD	gastro-oesophageal reflux disease
GST	glutathione S-transferase
H&E	haematoxylin and eosin
HCC	hepatocellular carcinoma
HER2	human epidermal growth factor 2, also known as ERBB2
HGD	high grade dysplasia
HGF	hepatocyte growth factor
HGMA1	high-mobility group AT-hook 1
HIF1	hypoxia-inducible transcription factor 1
HMGB1	high mobility group box 1
HNSCC	head and neck squamous cell carcinoma
HR	hazard ratio
HRP	horseradish peroxidase
HRT	hormone replacement therapy
HSC70	heat shock cognate 71kDa protein
IAP	inhibitors of apoptosis proteins
IC50	half maximal inhibitory concentration
IGF	insulin-like growth factor

IGFBP2	insulin-like growth factor binding protein 2
IHC	immunohistochemistry
iNOS	inducible nitric oxide synthase
IL	interleukin
IrRC	Immune-related Response Criteria
JAK	Janus kinases
kDa	kilodalton
LN	lymph node
MAPK	mitogen-activated protein kinase
MDR	multidrug resistant
MFI	mean fluorescence intensity
MHC	major histocompatibility complex
MMP	matrix metalloproteinase
mRNA	messenger ribonucleic acid
MRP1	multidrug resistance-associated protein 1
MSH	medical subject heading
mTOR	mammalian target of rapamycin
MTS	3-(4,5-dimethylthiazol-2-yl)-5-(3-carboxymethoxyphenyl)-2-(4-sulfophenyl)-2H-tetrazolium
MTT	methylthiazolyldiphenyl-tetrazolium bromide
MYO18E	myosin 18E
NAC	neoadjuvant chemotherapy
NER	nucleoside excision repair
NFκB	nuclear factor kappa B
NK	natural killer
NO	nitric oxide
NOF	normal oesophageal fibroblast
NOGCA	National Oesophago-Gastric Cancer Audit
NOX	nicotinamide adenine dinucleotide phosphate oxidase
Nrf2	nuclear factor E2-related factor 2
NSAIDs	non-steroidal anti-inflammatory drugs
OAC	oesophageal adenocarcinoma
OG	oesophagogastric

OS	overall survival
OSCC	oesophageal squamous cell carcinoma
PAI-1	plasminogen activator inhibitor-1
PBMC	peripheral blood mononuclear cells
PBS	phosphate-buffered saline
PCR	polymerase chain rOACtion
PDAC	pancreatic ductal adenocarcinoma
PDE	phosphodiesterase
PDE5i	phosphodiesterase 5 inhibitors
PDGF	platelet-derived growth factor
PERCIST	PET response Criteria in Solid Tumours
PET	positron emission tomography
PKG	protein kinase G
PI	propidium iodide
PI3K/AKT	phosphoinositide-3-kinase-protein kinase B (AKT)
PIK3CA	phosphatidylinositol-4,5-bisphosphate 3-kinase catalytic subunit alpha
PMS	phenazine methosulfate
POSTN	periostin
PPI	proton pump inhibitor
PRISMA	Preferred Reporting Items for Systematic Reviews and Meta-Analyses
PTEN	phosphatase and tensin homolog
qRT-PCR	quantitative real-time polymerase chain rOACtion
R_0	complete resection
RAGE	receptors of advanced glycation end products
RARRES	retinoic acid receptor responder protein
RECIST	Response Evaluation Criteria in Solid Tumours
RFA	radiofrequency ablation
RhoA/ROCK	Ras homolog member A/Rho-associated kinase
RIPA	radio-immunoprecipitation assay
RLT	RNeasy lysis buffer
RNA	ribonucleic acid
ROS	rOACtive oxygen species

rpm	revolutions per minute
RPMI	Roswell Park Memorial Institute 1640 medium
RT-PCR	reverse transcription polymerase chain rOACtion
SCC	squamous cell carcinoma
SCID	severe combined immunodeficiency
SDF1	stromal cell-derived factor 1
SDS-PAGE	sodium dodecyl sulphate polyacrylamide gel electrophoresis
SEM	standard error of means
SEMA5A	semaphorin 5A
siRNA	short interfering ribonucleic acid
SMAD4	mothers against decapentaplegic homolog 4
SNP	single nucleotide polymorphism
SNV	single nucleotide variant
SOC	standard of care
SPARC	secreted protein acidic and rich in cysteine
SPG20	spastic paraplegia 20
SSC	side scatter
STAT	signal transducer and activator of transcription
SUL	SUV normalized by lean body mass
SUV	standardized uptake value
TAMs	tumour associated macrophages
TBS	Tris-buffered saline plus tween-20
TGF-β	transforming growth factor β
TILs	tumour infiltrating lymphocytes
TIMPs	tissue inhibitors of metalloproteinases
TLR4	toll-like receptor 4
TMA	tissue microarrays
TME	tumour microenvironment
TNF	tumour necrosis factor
TNF-α	tumour necrosis factor α
TNM	tumour node metastasis
TP	tumour protein

TRG	tumour regression grade
TS	thymidylate synthase
UGI	upper gastrointestinal
UHSFT	University Hospitals Southampton Foundation Trust
ULA	ultra-low attachment
UK	United Kingdom
vCM	conditioned medium from vardenafil-treated CAFs
VEGF	vascular endothelial growth factor
WHO	World Health Organization

Chapter 1 Introduction

1.1 Oesophageal adenocarcinoma (OAC)

1.1.1 Burden of disease - epidemiology and its importance

Oesophageal cancer has become increasingly common in Northwest Europe and North America in the last 40 years, with an estimated number of 456,000 people developing oesophageal cancer in 2012[1], with the highest age standardised incidence in the UK[2] (Figure 1).

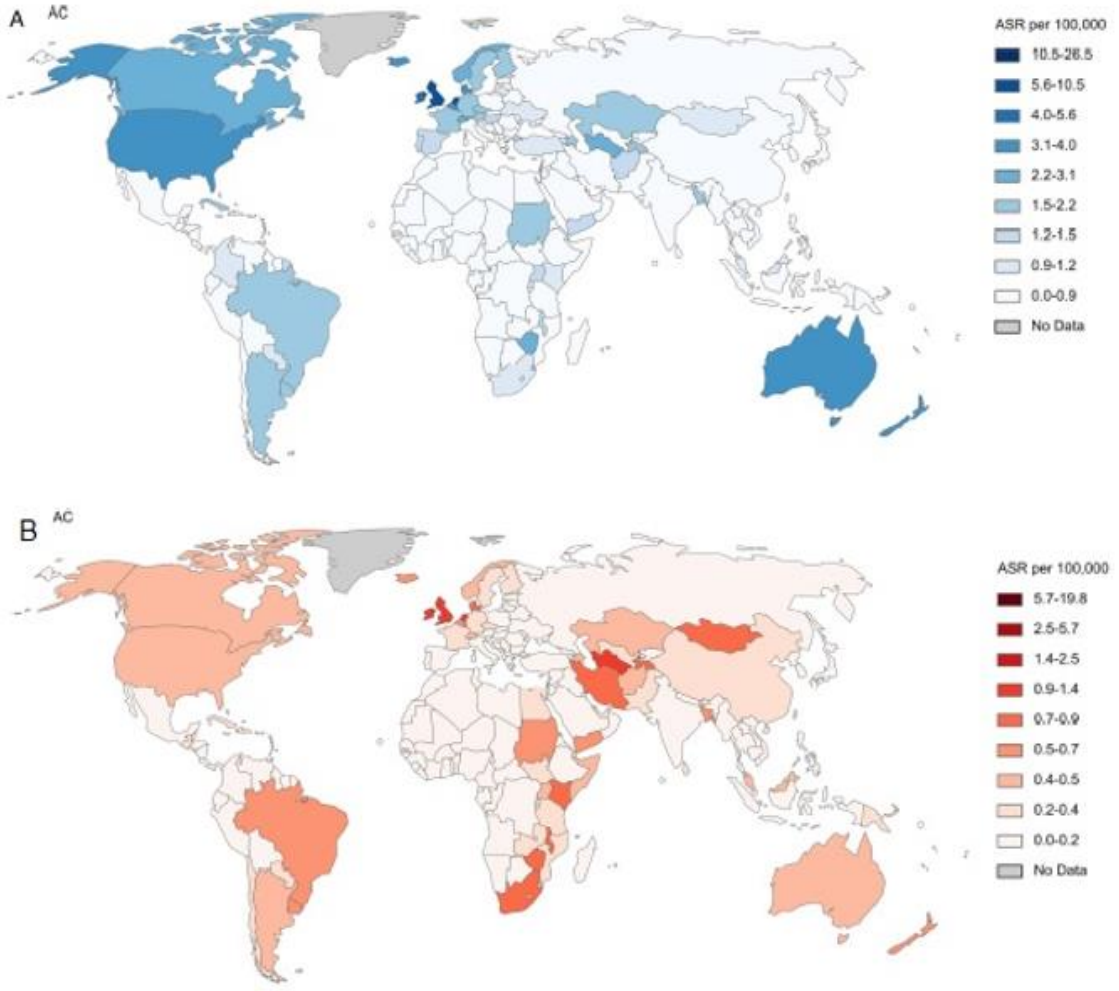

Figure 1. Age standardized incidence rate of OAC globally
(A) Age-standardized incidence rate per 100,000 of OAC in men.
(B) Age-standardized incidence rate per 100,000 of OAC in women. (Image adapted with permission from Arnold *et al* 2015[1])

It is the fifth most common cancer in the UK, with approximately 13,000 people diagnosed annually in England and Wales[3]. Over the last 2.5 decades, there has been an increased incidence of oesophageal cancer, particularly junctional cancers, with an increase in

proportion from 67.2% to 70.5% in the last 5 years[1-3]. OAC has become the predominant type of oesophageal cancer to be diagnosed in the UK[1 4], with males predominantly being affected. Initially in the 2016 National Oesophagogastric Audit (NOGCA), men over the age of 65 being more likely to be diagnosed with OAC[1 5]. However, NOGCA 2019 reported that the median age of affected patients had increased to 72 years of age[3].

Oesophageal cancer has a high mortality rate, despite modern therapies. Cancer Research UK reported 1-year survival rates for oesophageal cancer in England to be 41.9%, but it drops to 15.1% for 5-year survival, with 10-year survival rates at 12.3%[6]. Only 38% of patients diagnosed with the disease were managed with a curative treatment pathway, as by the time most patients are diagnosed, they were in the advanced stages of cancer and were not suitable for curative treatment[3]. For those with a curative treatment plan, a smaller number of patients were recorded to undergo surgery, which was attributed to the rising use of definitive chemoradiotherapy, progression of disease during neoadjuvant treatment, lower proportion of older or frailer patients undergoing surgery, and changes in patient preferences[3].

In the UK, oesophageal cancer, particularly OAC, is the fastest rising cancer. This rapid increase had led the Chief Medical Officer for England to call for increased research in oesophageal cancer in December 2008[7], and has led CRUK to make this cancer a high research priority in their latest 5-year plan. Public Health England had initiated a campaign called ‘Be Clear on Cancer’ in 2015 to improve early detection rates as well as raise awareness of early symptoms of oesophagogastric cancers. This research is therefore of utmost importance and relevance in today’s world of medicine.

1.1.2 Anatomy and Pathophysiology of the disease

The oesophagus is a 25cm long muscular tube connecting the pharynx to the stomach. Its main function is to allow passage of swallowed food and fluid, which it propels by peristalsis. It also prevents the reflux of gastric contents whilst allowing regurgitation, vomiting and belching to take place, with the help of the upper and lower oesophageal sphincters sited at its proximal and distal ends. If oesophageal function is impaired, it can lead to gastro-oesophageal reflux, oesophageal pain or spasm, and dysphagia, symptoms that patients with oesophageal cancer can present with.

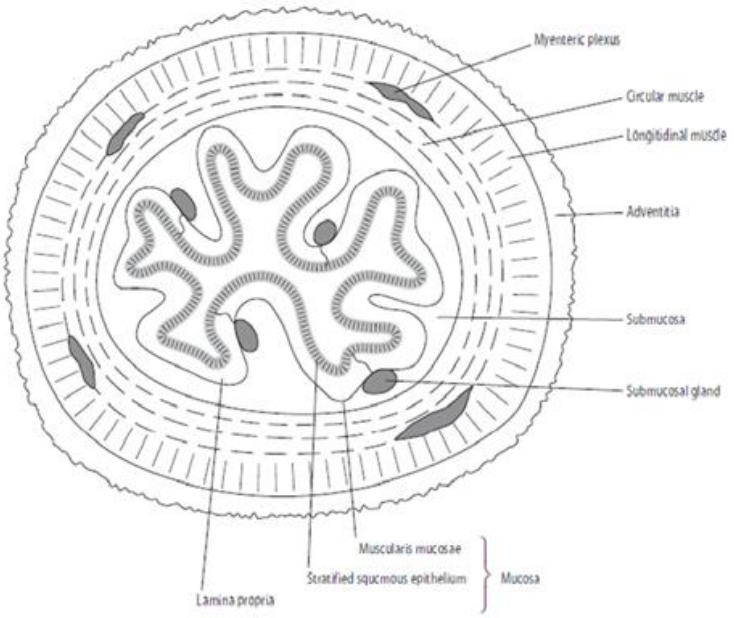

Figure 2. Cross-section of the oesophagus

The oesophagus is made up of four layers: adventitia, muscle, submucosa and mucosa (Figure 2). The muscular layer is composed of 2 layers: an outer longitudinal and an inner circular layer. These longitudinal muscle fibres split above the gastro-oesophageal junction, while the circular muscle layer is continuous proximally with the inferior constrictor and the muscle fibre arrangement is elliptical in nature. Both work to function in peristalsis, to propel food to the stomach and clear refluxed gastric contents. The submucosal layer consists of elastin fibres within a loose connective tissue and allows distension of the oesophagus during swallowing. The oesophageal mucosa is made up of a non-keratinised stratified squamous epithelium with a basement membrane separating it from the underlying lamina propria and muscularis mucosa. This changes close to the gastro-oesophageal junction to a columnar-lined gastric epithelium at the squamo-columnar junction.

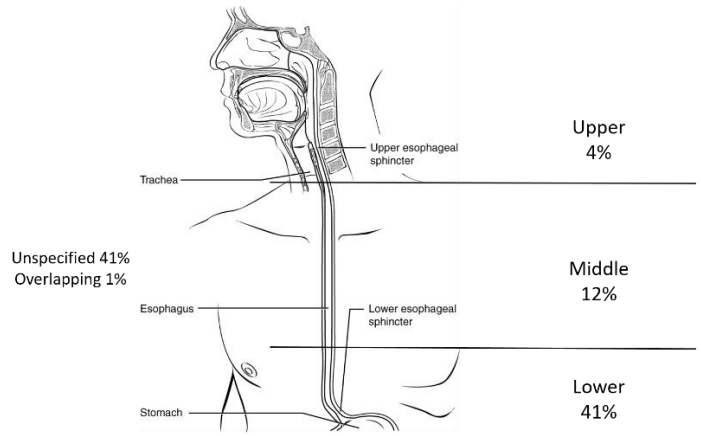

Figure 3. Distribution of oesophageal cancer in England and Wales

There are several subtypes of oesophageal cancer, with the predominant histological subtypes being oesophageal squamous cell carcinoma (OSCC) and oesophageal adenocarcinoma (OAC) accounting for more than 95% of oesophageal cancers. Other subtypes include undifferentiated cancers, and rarer subtypes such as melanoma, lymphoma, sarcoma and small cell carcinoma[6]. Globally OSCC is the most common, particularly in eastern Asia and African, while OAC is the more common subtype throughout Western Europe and Northern America[8 9]. In the UK, OAC is the most common type of oesophageal cancer, followed by OSCC[6]. Figure 3 demonstrate a distribution of oesophageal cancers in England and Wales as reported by CRUK, where a large proportion of patients have lower or junctional oesophageal cancer[6]. As OAC is the most predominant subtype of oesophageal cancer and has a high incidence in the UK, my thesis will focus on OAC.

1.1.3 Non-genetic risk factors of OAC

Table 1 list the risk factors for OAC, which was reported to be multifactorial.

Table 1. Risk factors for oesophageal cancer.
Factors denoted with an asterisk (*) were reported to be protective against OAC

Oesophageal Adenocarcinoma		Oesophageal Squamous Cell Carcinoma
Population demographics	Male sex	Tobacco use
	Advancing age	Alcohol consumption
	Smoker	
Dietary habits	Consumption of processed meats	Human Papilloma Virus (HPV) infection
	Obesity	
Chronic reflux	Gastro-oesophageal reflux (GORD)	
	Barrett's oesophagus	
Family history of oesophageal cancer		
*Physical activity**		
*Hormone replacement therapy & Breastfeeding**		
*Helicobacter pylori infection **		
*Use of aspirin/NSAIDs/statins**		

Gender, Age and Smoking Status

In the population, OAC incidence increases above the age of 60, with males having a 6-fold increased risk of being affected by this cancer, compared to females[10 11]. Even though the effects to tobacco use in both sexes are similar, men tended to smoke tobacco more often than women, and hence at higher risk[12 13].

Obesity

Obesity has recently been reported to be the second biggest cause of cancer[3 6 14]. In the Western countries where there is an abundance of high-fat, low-fibre diets, there is an increasing population with rising obesity. Whiteman *et al* had reported that risks of OAC increased with rising body mass index (BMI), with those BMI greater than 40kg/m^2 gaining a 7-fold higher risk of OAC. Moreover, marked weight gain (>5kg/m^2) during adulthood from age 20 was associated with 1.6-2.2 times rise in developing OAC[13]. People with a BMI of 30-34.9kg/m^2 have an increased risk of OAC by 2.39 times[15]. In particularly, abdominal obesity has been associated with OAC[11 16]. This was thought to be attributable to the mechanical effect of obesity promoting hiatal hernia formation and GORD, but also biochemical systemic effects of insulin resistance and hyperinsulinaemia, which were also associated with multiple epithelial cancers[1 17].

Gastro-oesophageal reflux disease (GORD)

A strong risk factor is GORD, which occurs when the lower oesophageal sphincter is relaxed. It can occur in obese patients, or those who smoke or have a hiatus hernia. People with GORD symptoms were found to increase their risk of getting OAC by 5 times[18]. It was reported to be more pronounced in obese patients with BMI>30kg/m^2 with weekly reflux symptoms, with a 3-fold higher risks of developing OAC[13]. GORD can affect up to 40% of the population at some point in their lifetime, but most people do not develop OAC[19]. It may be that the small cohort of people who developed OAC could have been asymptomatic GORD sufferers, before actually presenting with symptoms of the cancer.

Barrett's oesophagus (BO)

Barrett's oesophagus is a premalignant state for development of OAC, and is characterised by intestinal metaplasia and the presence of goblet cells. It usually occurs in patients with chronic GORD, where chronic reflux of gastric acid can lead to erosive oesophagitis and can result in development of BO if healing becomes atypical[11]. Figure 4 demonstrates the process, which involves a sequence of changes, from erosive oesophagitis to non-dysplastic or metaplastic BO, low grade dysplasia, high grade or severe dysplasia, adenocarcinoma in situ, and finally invasive adenocarcinoma[20].

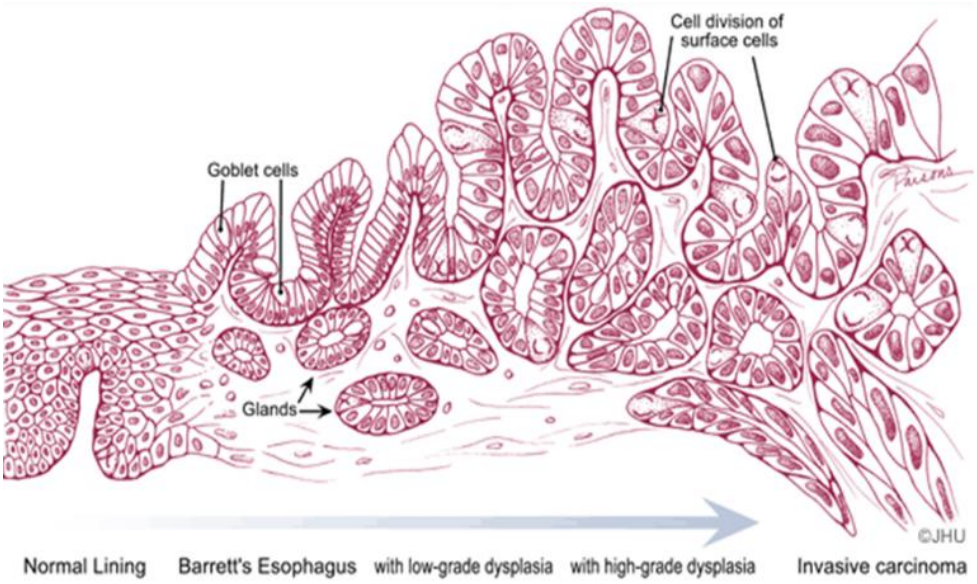

Figure 4. Development of Barrett's Oesophagus
(Image adapted from www.medpagetoday.com/blogs/celebritydiagnosis/37196)

BO is defined as biopsy confirmation of intestinal metaplasia with mucosal extension ≥1cm proximal to the gastro-oesophageal junction[21]. It is not easy to diagnose BO as it does not affect all the tissue in the oesophagus. In addition, an irregular z-line at the squamo-columnar junction makes it challenging to determine when BO starts proximal to the gastro-oesophageal junction. To mitigate these factors, diagnosis is usually by visual confirmation on high-resolution endoscopy, together with histological confirmation. Other modalities such as narrow-band imaging, chromoendoscopy and confocal laser endomicroscopy may also be utilized. The length of BO is visualized endoscopically and classified according to Prague C&M criteria, which is a validated system utilizing standardized landmarks to determine the length of BO[22] (Figure 5).

Risk factors that cause acceleration of BO to OAC had been identified to be long segment length (>3cm) of BO, presence of ulceration, strictures and nodules[21]. Presence of these factors require multiple targeted biopsies of these areas as they are indicative of malignancy. If BO is suspected, biopsies are taken according to the Seattle protocol, which has been the gold standard method of quarandrantic biopsies every 2cm over the entire segment of BO, starting from the distal areas and advancing proximally to minimise obscured views from bleeding[21]. The biopsies, if there is evidence of dysplasia, should ideally be reported by 2 gastrointestinal pathologists.

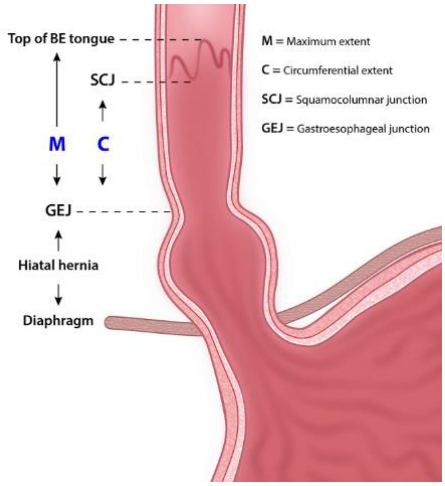

Figure 5. Prague Classification to document hiatal hernia and Barrett's

Dysplasia in biopsies can be reported as low grade (LGD) or high grade (HGD). With a lag time of approximately 10 years between onset of BO and progression to HGD[1], LGD had been reported to progress to HGD or cancer at the rate of 9.1% per year[23]. With HGD being considered a precursor to OAC with up to 50% of patients with HGD had been reported to progress to OAC[24], it is considered a major risk factor and was important to be included in the National Oesophago-gastric Cancer Audit since 2016[5]. First-line management options for LGD and HGD are radiofrequency ablation and endomucosal resection respectively, which was said to achieve complete eradication of dysplasia in more than 90% of patients, thereby reducing their cancer risk.

A meta-analysis had found that 12% of OAC patients had a prior Barrett's diagnosis, but that concurrent BO was found in at least 57% of patients at the time of OAC diagnosis[25]. Overall, only 0.19% of patients with BO will progress to OAC annually[26]. It brings into question the requirements for surveillance and feasibility of screening for BO. There is currently no strong evidence of surveillance for BO, despite widespread practice internationally. The BOSS trial, carried out in the UK in 2015, was a randomized controlled trial for endoscopic surveillance (2-yearly) versus 'at need' endoscopy reserved for symptomatic BO patients, of which the results are eagerly awaited. In the meantime, guidelines from the British Society of Gastroenterologist had been published regarding the surveillance and management of BO patients who have LGD, HGD or cancer. If biopsies indicated LGD or indefinite for dysplasia, the recommendations were for the endoscopy and biopsies to be repeated in 6 months, usually with acid suppression in the interim. If LGD or no dysplasia was subsequently found, then surveillance is recommended every 2-5 years based on current national guidance. If biopsies showed HGD or OAC, these go through a multi-disciplinary team discussion before proceeding with endoscopic, surgical or oncologic therapy.

Screening for BO with endoscopy has been highlighted as not being feasible or cost-effective for an unselected population, but that it should be reserved for patients with chronic GORD symptoms and multiple risk factors, or with a positive family history of BO or OAC[21]. Meanwhile, Professor Rebecca Fitzgerald from Cambridge had spearheaded the Cytosponge™ test, which involved patients swallowing a dissolvable capsule with a string attached to it, containing the Cytosponge™. Once the capsule dissolved, the string can be pulled to retrieve the sponge and sent to the lab for analysis. Not only was the Cytosponge™ found to be safe and acceptable to patients with or without BO, it was also found to have 80-87% sensitivity for patients with >3cm circumferential BO, and high specificity rate of 92.4% for diagnosing BO[27 28]. In the last 5 years, BEST2 and BEST3 trials were launched, with the former evaluating the differential sensitivity of BO screening and the ability to risk-stratify these patients, as well as determining the reproducibility and the logistics of sample processing and automated analysis in NHS settings[27 28]. The BEST3 trial is currently being carried out in primary care in East Anglia, in a randomized fashion on patients with reflux symptoms to evaluate the detection and cost-effectiveness of BO screening with the Cytosponge™ in primary care[29].

Protective factors

Physical activity reduced the risk of OAC, as demonstrated by Singh *et al*[30] in a meta-analysis, with the risk of developing oesophageal cancer being 19% lower in physically active people, particularly for OAC. In a collaborative organised in the National Cancer Institute Cohort Consortium in the United States called the Physical Activity Collaboration, it was found that a higher level of activity was associated with greater than 20% reduction in risk for OAC[31].

Hormone manipulation with hormone replacement therapy (HRT) or breastfeeding can have an impact on OAC risk. A meta-analysis reported that women who had ever used HRT were found to have a significant decrease of risk for OAC by 25%[32]. This corresponded to a population-based study from Sweden which concluded that any use of HRT reduced OAC risk[33]. Breastfeeding also conferred a protective effect of developing OAC, with a 58% reduction in risk that was reduced when breastfeeding continued for greater than a year [34].

Infection with the bacteria Helicobacter pylori had also been associated with a risk reduction in OAC. Two meta-analyses had demonstrated that a 40-60% reduction in OAC risk with this infection[35].

Medications can also have a protective effect on OAC formation, and can act as a form of chemoprevention. For instance, proton pump inhibitors (PPI) were reported to decrease progression of OAC by 71%[36]. Aspirin[37], non-steroidal inflammatory drugs (NSAIDs)[37] and statins[38] were also associated with a 32-41% reduction in risk of OAC[39]. More recently, a

randomized trial called the AspECT trial was carried out in 2557 patients with BO, and compared high-dose (twice a day) vs once daily PPI use, with or without the addition of aspirin. The study found that use of high-dose PPI increased survival in BO. Moreover, aspirin had an additive effect, and if both are taken together for at least 9 years, it would improve survival in patients with BO[40].

1.1.4 Genetics and molecular biology of oesophageal adenocarcinoma

OAC is a complex disease. Not only is it influenced by environmental risk factors, genetics also play a role in the development and progression of OAC. Several studies have demonstrated that OAC exhibit a high mutational burden and chromosomal instability leading to genetic heterogeneity. Mutations or amplifications in multiple genes were found to be the most recurrent driver events, with a median of 382 damaged genes found per OAC patient[41-43]. Other genomic catastrophes such as copy number aberrations or alterations[44], single nucleotide polymorphisms (SNPs) or variants (SNV)[41], microsatellite instability and chromosomal changes with telomere shortening or chromothripsis[42 45], all of which alter protein function and change the expression or activity of the encoded proteins, which in turn drive development of oesophageal cancer. Microsatellite instability, defined as hypermutability of genes resulting from impaired DNA mismatch repair, was reported to affect 7% of OAC patients[41]. Interestingly, when samples from chemonaive OAC patients were analysed, they had contained 24,449 SNVs, and this was similar to the group of OAC patients treated with chemotherapy. Moreover, both groups had displayed similar proportions of amplifications, deletions and losses of heterozygosity, therefore it appeared that chemotherapy treatment did not change the OAC genome in terms of copy number alterations, SNVs or mutations[44].

Dulak *et al* had carried out an extensive study of 149 OAC cases and found 26 genes to be commonly mutated, included tumour suppressor genes such as TP53 and CDKN2A[41]. Other genes found to be significantly mutated were identified as ARIDIA, PIK3CA, SMAD4, ELMO1, DOCK2, SPG20, TLR4 and ERBB2[41]. These genes were also reflected in a study by Weaver *at al* who also found several new OAC genes such as MYO18B, SEMA5A and ABCB1[42]. It was noted that in non-dysplastic BO, HGD BO and OAC, accumulative mutations in TP53 and SMAD4 seemed to coincide with the stepwise progression of OAC, while other mutated genes occurred independently of stage of the cancer. As such, boundaries could potentially be defined and created at specific stages of the disease for early diagnosis and treatment (Figure 6)[42].

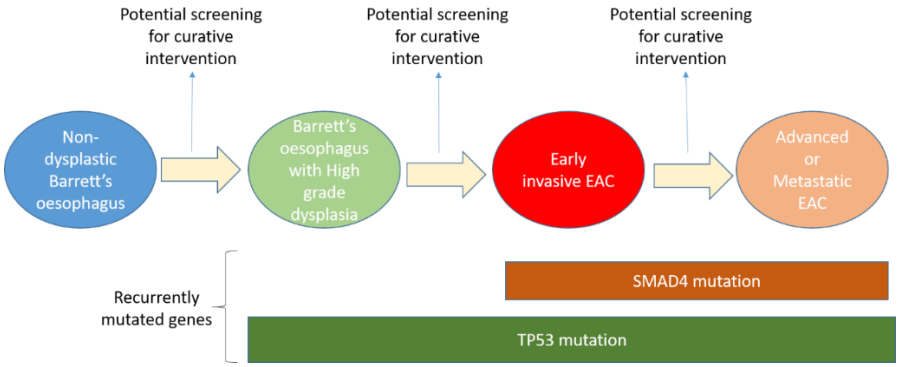

Figure 6. Mutations denoting stages of OAC

p53 is a tumour suppressor gene located on chromosome 17, which when mutated, can predispose people to cancer. Hardwick *et al* had found that out of 205 oesophageal cancer patients, 66% of OAC patients and 68% of OSCC patients had overexpression of p53[46]. Other studies also showed similar results, where majority of the tumours had p53 mutations, and were associated with protein overexpression, poor tumour differentiation, advanced pTNM stage, higher number of involved lymph nodes, and poor prognosis with a reduction in 5-year overall survival rates[47-49]. Duhaylongsod *et al* had found that being positive for p53 correlated with residual disease in the resection specimens[50]. A meta-analysis performed by Fisher *et al* showed over 16 studies with more than 800 patients, there was a high TP53 mutation rate of up to 70% in dysplastic BO and OAC, and it was the most common genetic modification. These patients had a lower overall survival, with a 7-month reduction in median survival time[51].

The other gene highlighted by Dulak's and Weaver's groups was the SMAD4 gene, located on chromosome 18 and is involved with the TGF-β SMAD signalling pathway. When TGF-β protein binds to a receptor on the cell surface, it activates a group of related SMAD proteins which bind to the SMAD4 protein to form a protein complex. This complex acts as a transcription factor and tumour suppressor, as it gets transported to the cell nucleus and binds to DNA to regulate cell proliferation, and controls gene activity. Mutations in the SMAD4 gene was reported to affect 18% of patients with OAC, and increased risk of other cancers developing, such as pancreas or colon[41].

There have been attempts to categorize mutational processes in human cancers, and mutational signatures related to age of cancer diagnosis, transcriptional strand bias, insertions or deletions causing impairment of DNA repair systems have been suggested[52]. Similarly in OAC, there have been attempts to profile this disease in the last decade. Kim et al had applied non-supervised clustering on transcriptome data from 64 patients and discovered 3 subgroups with differences in overall gene expression patterns that were associated with prognostic differences for each group[53]. Secrier *et al* had performed whole genome sequencing analysis of 129 OAC cases, and discovered 3 distinct molecular

subtypes: C>A/T dominant, DNA damage repair (DDR) impaired, and mutagenic. The first subgroup had a higher frequency of inter-chromosomal translocations and reduced duplications, while the DDR impaired subgroup appeared to have the most genomic instability. Additionally, the mutagenic group, which had included the MFD1 cell line used in my thesis, appeared to display higher mutational burden and levels of neoantigen presentation, reflecting a higher density of CD8+ T-cells[54]. Frankell *et al* investigated on a larger scale using 551 genomically characterized OAC samples, and discovered 76 OAC driver genes, where 71% had not been detected previously[55]. These novel drivers were associated with features such as highly recurrent mutations within a gene causing high functional impact, mutation clustering, recurrent high copy number amplification, and copy number loss associated with presence of mutations leading to loss of heterozygosity, all of which led to dysregulation of specific pathways and poorer prognosis.

Profiling can also be based on other aspects. Bornschein *et al* had carried out transcriptomic profiling of junctional OAC in 84 patients, which revealed 3 groups: Group 1 was associated with pathways involved in cell turnover and had shown features of mucosal damage by reflux, while group 2 was characterized by metabolic processes, and group 3 was linked to changes in genes involved in DDR pathways and was associated with inflammatory response regulation[56]. On the other hand, Turkington *et al* in Belfast had focused on OAC cancers that had neoadjuvant chemotherapy, and discovered that OAC tumours which were positive for DDR had a higher pathological response rate, lower nodal burden and reduced circumferential margin involvement, with no difference in overall survival[57]. Noorani *et al* had also looked at OAC patients who had chemotherapy, focusing on the pre- and post-chemotherapy (ECX/ECF) samples, and found that there was a significant overexpression of C>A substitution mutations in the post-chemotherapy cohort, and termed it as a cisplatin-induced mutational signature[44]. Interestingly, when Sawas *et al* investigated OAC patients from the Mayo clinic in the United States, his group had found OAC patients with a background of BO or intestinal metaplasia (excluding BO patients on surveillance) had presented at earlier stages of the disease and had better survival. These results were also reflected when a larger cohort of OAC patients from multiple hospitals in the UK was looked at in the same study[58]. More recently, BO and OAC had been grouped based on DNA methylation profiles using more than 400 samples. They were classed into 4 subtypes: Subtype 1 was characterized by DNA hypermethylation with a high mutational burden involving multiple mutations in genes in cell cycle and tyrosine receptor signalling pathways. Subtype 2, represented by 83% of BO samples and 17% of OAC tissues, was characterized by a gene expression pattern associated with metabolic processes. Subtype 3 had a gene expression pattern consistent with immune cell infiltration, while subtype 4 was illustrated by DNA hypomethylation associated with structural rearrangements, copy number changes, and amplifications of the CCNE gene said to be sensitive to CDK2 inhibitors[59].

In summary, genetics do play a major role in OAC development. Several driver genes and mechanisms have been discovered and methods had been attempted to profile OAC tumours, however with no consensus in sight. More information is constantly being discovered about genomic alterations in OAC, therefore discussions will need to be carried out on an international level to achieve a consensus regarding the most appropriate manner to classify OAC on a genomic basis.

1.1.5 Diagnosis, Staging & Treatment modalities

Over 60% of OAC patients are diagnosed after a referral from their GP[3]. Patients usually present with progressive dysphasia, which starts off subtly with difficulty in swallowing solids, followed by difficulty in swallowing liquids. However, by the time they are symptomatic with the disease, disease is advanced[2] and only 30% of patients are potentially suitable for curative treatment[5].

NICE guidelines recommend patients are referred for fast track upper gastrointestinal endoscopy within 2 weeks, when patients present with dysphagia, or are over the age of 55 and have weight loss and dyspepsia, reflux or upper abdominal pain[60]. If found to be positive at endoscopy, biopsies are taken to confirm the diagnosis, and patients then proceed to an initial computed tomography (CT) scan to assess the spread of disease and exclude evidence of metastatic disease. If suitable for radical therapy, other investigations such as positron emission tomography (PET), endoscopic ultrasound (EUS), or staging laparoscopy is arranged[2]. They are then discussed at the upper gastrointestinal multi-disciplinary team meeting, and staged using the 2016 (8th Edition) TNM (Tumour, Node, Metastasis) system by the American Joint Committee of Cancer (Figure 7).

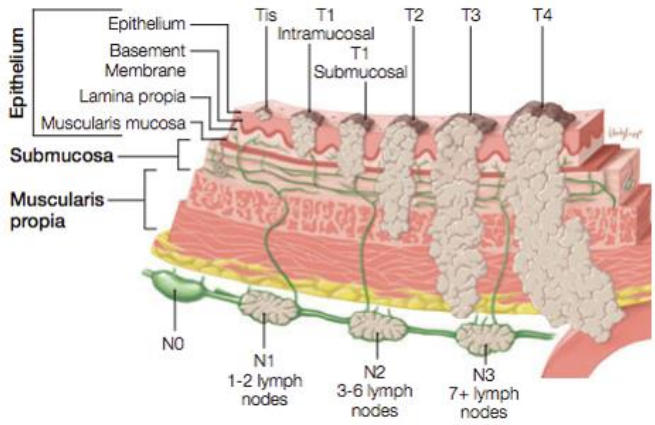

Figure 7. Staging of oesophageal cancer
(Image adapted from http://www.pathologyoutlines.com/topic/esophagusstaging.html)

Treatment depends on the patient and their comorbidities, tumour depth of invasion, nodal status and the presence of metastases. T1a cancers, otherwise known as intramucosal cancers, can invade the lamina propria, and are suitable for endoscopic therapy, such as endoscopic mucosal resection (EMR), followed by radiofrequency ablation (RFA) to remove any remnant dysplasia. However, T1b cancers involve the submucosa, and are associated with a higher rate (27-41%) of lymph node involvement[2], therefore making EMR an unsuitable choice for curative management for that stage of disease. Poorly differentiated OAC, as well as those with stage 2/3 disease who are fit enough to undergo radical therapy are recommended surgery with or without oncological therapy.

The work carried out in my research focuses on early stage OAC, and does not include metastatic or palliative chemotherapy treatment.

1.1.6 Implications for treatment and survival

The 5-year survival rate for oesophageal cancer was reported to be 15%[5]. This had been attributed to patients presenting with unresectable or metastatic disease at the time of diagnosis, with more than two thirds affected[5]. Even if patients did have resectable disease, they had a relatively high rate of local and distant recurrences, which accounted for the dramatic drop in survival rates, especially in patients with Stage 2 and above disease[6 61 62].

Table 2. Summary of treatment options and survival rates by stage of oesophageal cancer

Stage	TNM description	Standard treatment	5-year survival rate
0	TIS N0 M0 or HGD	EMR or RFA	80-90%
1A	T1 N0 M0	Surgery	34%
1B	T2 N0 M0	Surgery +/- adjuvant chemoradiotherapy	
2A	T3 N0 M0	Neoadjuvant chemotherapy +/- Surgery	17%
2B	T1-2 N1 M0		
3A	T1-2 N2 M0 or T3 N1 M0 or T4a N0 M0	Neoadjuvant chemotherapy +/-Surgery	15-30%
3B	T3 N2 M0		
3C	T4a N1-2 M0 T4b Any N M0 Any T N3 M0		
IV	Any T Any N M1	Symptomatic control +/- Radiotherapy +/- chemotherapy +/- Herceptin	2.8%

Table 2 illustrates a summary of the varied management of oesophageal cancer according to the stage of disease and its associated survival rates[6 61 62]. Approximately 38% of patients

found to have stage 2 or 3 disease and fit enough to undergo surgery had a curative treatment plan[3 63], which consisted of multimodal therapy encompassing either neoadjuvant chemotherapy (NAC) or chemoradiotherapy (CRT) with surgery as the standard of care. Table 3 reports NICE recommendations of curative treatment options for OSCC and OAC, with CRT recommended for OSCC, while NAC or neoadjuvant CRT recommended for OAC tumours[60].

Table 3. NICE guidelines for recommended curative treatments for UGI cancers

Cancers	Location	Treatment
OSCC	Proximal	Definitive chemoradiation
	Middle and lower oesophagus	Chemoradiation +/- surgery
OAC and GOJ tumours	Preoperative chemotherapy or chemoradiation recommended	
	Peri-operative (pre- and post-operative) recommended for junctional tumours	
Gastric	Peri-operative chemotherapy recommended	
	Patients at high risk of recurrence: adjuvant chemoradiotherapy recommended if did **not** have neoadjuvant chemotherapy	

Curative surgery is only reserved for fit patients who have localised disease on staging investigations. It was discovered that fewer patients had curative surgery, compared to the number of patients with a curative treatment plan[3]. This was explored and several factors contributing to this phenomenon were listed, such as increasing use of definitive CRT and patients beginning neoadjuvant therapy not proceeding on to planned surgery because of disease progression or patient preference changes. Surgery is a major undertaking that has a 90-day mortality rate of 3.8%[3], and a 36.9% morbidity rate post-surgery[63], mostly in the form of wound or pulmonary infections and anastomotic leaks[2]. Moreover, patients require a minimum of 6-9 months recuperation time to regain a decent quality of life[64]. Quality of life was assessed based on validated questionnaires such as those for cancer in general (EORTC QLQ-C30) or oesophageal cancer specifically (EORTC QLQ-OES18). A meta-analysis from 15 studies showed that symptoms of pain and fatigue persisted up to a year[65], while Schandl *et al* described a deterioration in symptoms as well as role and social functioning in oesophageal cancer survivors 5 to 10 years after surgery[66].

Focusing on patients with resectable disease, patients with stage 2 or 3 disease are recommended neoadjuvant chemotherapy (NAC) before curative surgery, as NAC has been proven to improve survival[67-69]. This was through downstaging of the tumour[70 71] or lymph nodes[70 72], which increased chances of achieving a microscopically complete resection (R_0) of the tumour[67 68 73], and possibly eradicated micrometastases[74]. Table 4 showcases the key clinical trials for oesophageal cancer in the last 1.5 decades.

Table 4. Key clinical trials in oesophageal cancer

Clinical Trials	n	Types of cancer	Therapy		Main Findings	5-year survival	Conclusion
Kelsen et al 2007 (Intergroup 113, USA)	443	OAC (53%) and OSCC (47%)	CF+surg (216)	Surg alone (227)	Patients with objective tumour regression after preoperative chemotherapy had improved survival	45% vs 26%	R0 resection results in substantial long-term survival. Postoperative CRT offers improved DFS to small group of patients
Cunningham et al 2006 (MAGIC, UK)	503	Oesophageal (26%) and gastric adenocarcinomas	ECF+Surg (250)	Surg alone (253)	Decreases tumour size Downstage tumour	36% vs 23%	Improved survival outcome with perioperative chemotherapy and surgery
Allum et al 2009 (OEO2, UK)	802	OAC (67%) and OSCC (31%)	CF+Surg (335)	Surg alone (320)	Surg only – higher rate of R1 resections or unresectable tumours	23.0% vs 17.1%	Improved 5-year survival 60% vs 54% R0 resections
Ychou et al 2011 (FFCD, France)	224	OAC (75%) and junctional cancers	CF+Surg (113)	Surg alone (111)	Improved OS and DFS using CF perioperative chemotherapy and surgery	38% vs 24%	Perioperative chemo improved curative resection rate and OS and DFS
van Hagen et al 2012 (CROSS, US.Europe)	368	OSCC and OAC	CRT+Surg (178)	Surg alone (188)	Median OS 49.4 months (CRT+Surg) vs 24 months (surg alone)	46% vs 34%	Preoperative CRT improved survival
Cunningham et al 2017 (ST03, UK)	1063	Gastric and oesophagogastric junctional cancers	ECX (533)	ECX+B (530)	Anastomotic leak rates for oesophagectomies higher in ECX+B group	50.3 vs 48.1% (3 year survival)	No difference in survival, therefore no evidence for use of bevacizumab Associated with impaired wound healing
Alderson et al 2017 (OEO5, UK)	907	OAC	CF (451)	ECX (456)	More toxicity with ECX. No survival differences	39% vs 42% (3 year survival)	No difference in survival with chemotherapy change from CF to ECX
Al-Batran et al 2019 (FLOT4, Germany)	716	OAC or gastric junctional adenocarcinoma	FLOT (356)	ECF/ECX (350)	Greater OS and DFS survival. Greater number of R0 resections and T0/T1 tumours	45% vs 36%	Perioperative FLOT improved overall survival compared with ECF/ECX
Mukherjee et al2017 (NEOSCOPE, UK)	85	OAC	CRT(C/P) +surg (41)	CRT(OX) +surg (36)	CP arm – 27.9% complete response OX arm – 8.5% complete response		Carbo/paclitaxel better tolerated than Oxali/capecitabine
NEOAEGIS (2015-20, UK)	Ongoing	OAC	CRT+ surg	NAC+ Surg	Awaited	Awaited	Awaited
ESOPEC (2016-, Germany)	438	OAC	CRT+ Surg	FLOT+ surg	Awaited	Awaited	Awaited

Kelsen *et al* from United States had compared OSCC and OAC patients who had chemotherapy and surgery versus surgery alone, and found that those with R_0 resections had longer survival, as expected[75]. In the UK, the OEO2 trial, where 67% of patients had OAC, had compared NAC of cisplatin and fluorouracil with surgery, against surgery alone. It showed a significant improvement of 5-year survival of 22.6%, compared with 17.6% in surgery only patients[68]. It was also found that the surgery only group had a higher rate of unresectable tumours or incomplete resections. Similarly, Cunningham *et al* had demonstrated, in junctional oesophageal and gastric cancers, that perioperative chemotherapy of epirubicin, cisplatin and 5-fluorouracil (ECF) had decreased tumour size and stage as well as improved 5-year survival to 36%, compared to patients who underwent surgery alone (23%) (Figure 8)[67]. This was further corroborated by Ychou's group in France, who had determined that perioperative chemotherapy with cisplatin and 5-fluorouracil improved survival outcomes and curative resection rates[76]. Consequently, the OEO5 trial provided evidence that there was no difference in survival when chemotherapy agents were altered between 2 cycles of cisplatin/5-fluorouracil or 4 cycles of epirubicin/cisplatin/capecitabine[77]. More recently, the FLOT4 trial compared FLOT chemotherapy (fluorouracil, leucovorin, oxaliplatin and docetaxel) against ECF/ECX, and found that there was improved 5-year survival and a greater number of R_0 resections with FLOT chemotherapy treatment[78].

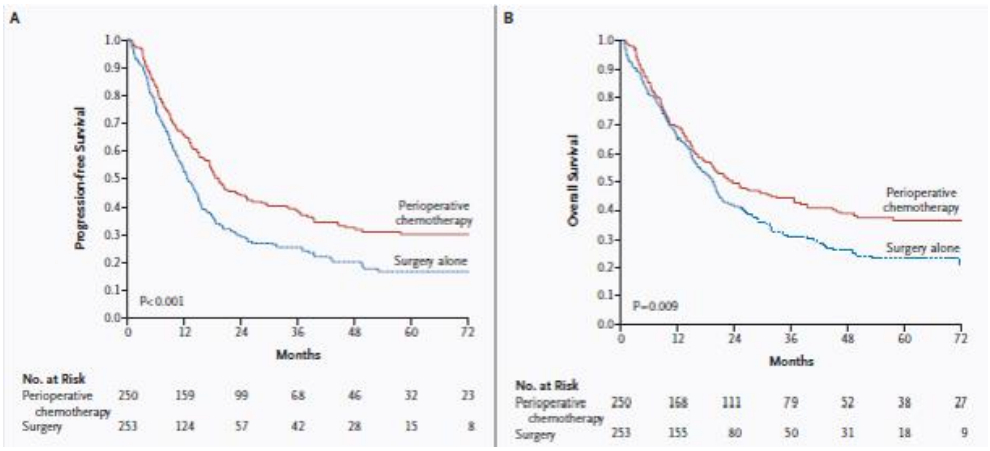

Figure 8. Kaplan-Meier survival estimates for patients of OEO2 trial who underwent perioperative chemotherapy and surgery versus surgery alone of (A) progression-free survival and (B) overall survival

There has been discussions internationally regarding the impact on radiotherapy on cancer treatment for UGI adenocarcinomas. MacDonald *et al* demonstrated that CRT given after surgery, compared with surgery alone, improved median overall and disease-free survival, with a drop in cancer relapse in the CRT group[79]. Following on from that, the CROSS trial carried out in the Netherlands, had compared neoadjuvant CRT and surgery with surgery alone, and detected a median survival difference of 6 months in favour of CRT and surgery (22 months) versus surgery only (16 months)[80]. It also demonstrated an improved survival in the CRT and surgery group, which seemed more beneficial in the OSCC patients, than in the OAC patients (Figure 9)[80]. Studies[81] and meta-analyses performed by Sjoquist *et al*[69], Wang *et al*[82] and Ronellenfitsch *et al*[83] showed that CRT resulted in higher rates of R_0 resections and improved survival of 9% at five years, compared to surgery alone.

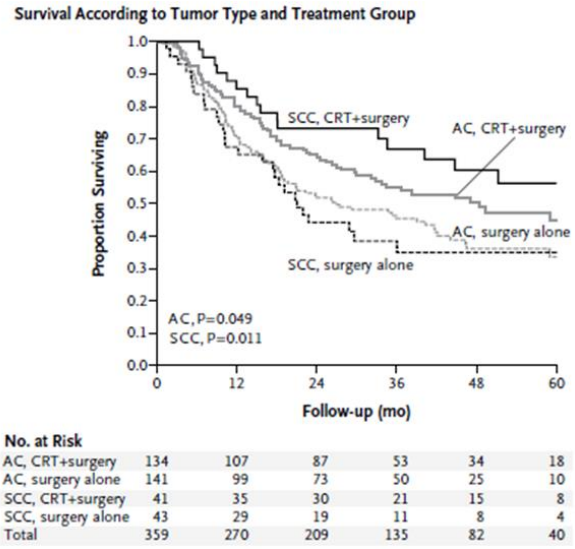

Figure 9. Survival rates for OAC and OSCC with different treatment modalities in the CROSS trial

The phase II NEOSCOPE multi-centre trial compared different types of pre-operative chemotherapy with radiotherapy, followed by surgery, and found evidence that the combination of carboplatin/paclitaxel was better tolerated, with acceptable toxicity. In addition, 27.9% of patients in that arm had a complete pathological response, compared with the oxaliplatin/capecitabine arm, which only had a complete response rate of 8.5%[84]. Moreover, the TOPGEAR trial by Leong *et al* had suggested that there was a high surgical compliance rate for the CRT group and that pre-operative CRT with 2 cycles of ECF is safe and feasible compared with 3 cycles of ECF, prior to surgery[85]. Work had also been done to look at the effects of post-surgical treatment with CRT, using fluorouracil and leucovorin versus ECF chemotherapy in the CALGB 80101 trial, which did not show any survival differences with alterations in chemotherapy drugs[86]. Table 5 shows a summary of the chemoradiotherapy trials in UGI cancers.

Table 5. Summary of UGI trials involving chemoradiotherapy

Clinical Trials	n	Types of cancer	Therapy		Main Findings	5-year survival	Conclusion
MacDonald et al 2001	556	Gastric and oesophagogastric junctional adenoCa	Surg+post-surg CRT (281)	Surg alone (275)	Median OS: 36 months vs 27 months Median DFS: 30 months vs 19 months Relapses: 43% vs 64% in surg only group	50% vs 41% (3 year survival)	Better OS and DFS in CRT group
van Hagen et al 2012 (CROSS, US.Europe)	368	OSCC and OAC	CRT+Surg (178)	Surg alone (188)	Median OS 49.4 months (CRT+Surg) vs 24 months (surg alone)	46% vs 34%	Preoperative CRT improved survival
Cunningham et al 2017 (ST03, UK)	1063	Gastric and oesophagogastric junctional cancers	ECX (533)	ECX+B (530)	Anastomotic leak rates for oesophagectomies higher in ECX+B group	50.3 vs 48.1% (3 year survival)	No difference in survival, therefore no evidence for use of bevacizumab Associated with impaired wound healing
Mukherjee et al2017 (NEOSCOPE, UK)	85	OAC	CRT(C/P) +surg (41)	CRT(OX) +surg (36)	CP arm – 27.9% complete response OX arm – 8.5% complete response		Carbo/paclitaxel better tolerated than Oxali/capecitabine
Leong et al 2017 (TOPGEAR)	120	Gastric and oesophagogastric junctional adenoCa	Pre-op CRT + 2xECF + Surg (60)	3xECF + Surg (60)	Preop CRT safe and feasible, with 98% completion of RT High surgical compliance rates in CRT group	Awaited	Awaited
Fuchs et al 2017 (CALGB 80101)	546	Gastric or oesophagogastric junctional adenoCa	Post-surg FU+LV CRT	Post-surg ECF CRT	5-ear DFS rates: 39% (FU/LV arm) vs 37% (ECF arm) Treatment effect similar across all examined patient subgroups.	44% vs 44%	Post-op CRT with ECF did not improve survival compared with FU/LV
NEOAEGIS (2015-20, UK)	Ongoing	OAC	CRT+ surg	NAC+ Surg	Awaited	Awaited	Awaited
ESOPEC (2016-, Germany)	438	OAC	CRT+ Surg	FLOT+ surg	Awaited	Awaited	Awaited

So far, results are eagerly awaited from the randomized controlled NEO-AEGIS trial that had been carried out across centres in the UK, Ireland and Europe investigating NAC using a modified MAGIC regime or neoadjuvant CRT using the CROSS protocol, prior to surgery. The results are due to be published in 2022, which will hopefully answer the question of the most optimal therapy to improve survival outcomes of OAC patients[87]. Similarly, the ESOPEC trial is currently being carried out in Germany to determine the outcomes of neoadjuvant CRT and surgery versus FLOT chemotherapy and surgery[88].

Additionally, other work had been performed to determine if the effect of NAC alone can be augmented. The ST03 trial used bevacizumab as an addition to chemotherapy for gastric and junctional oesophageal cancers, and found that it was associated with higher anastomotic leak rates, impaired wound healing, and it made no difference to survival outcomes[89]. Although this agent has been mooted, another monoclonal antibody such as trastuzumab, otherwise known as Herceptin, has been utilised in the INNOVATION trial to

determine if addition of trastuzumab can impact on pathological response rate in HER2-positive UGI cancers[90].

1.2 Response to chemotherapy

1.2.1 Chemotherapy agents used in the management of oesophageal adenocarcinoma and its influence on the cancer cell cycle

Trials have demonstrated that NAC is of benefit to increasing survival rates, and that both ESCC and OAC are responsive to chemotherapeutics. Standard UK NAC used in OAC is ECF (epirubicin, cisplatin, fluorouracil), which currently consists of a 3-week cycle of epirubicin (50g/m^2 of body-surface area), cisplatin (60mg/m^2), and 5-fluorouracil (5FU) (200mg/m^2/day) for 21 days by intravenous infusion, followed by surgery 3-6 weeks after the third cycle of chemotherapy (Figure 10)[67]. An alternative used is ECX (epirubicin, cisplatin, capecitabine), where the fluorouracil is substituted with oral capecitabine (625mg/m^2).

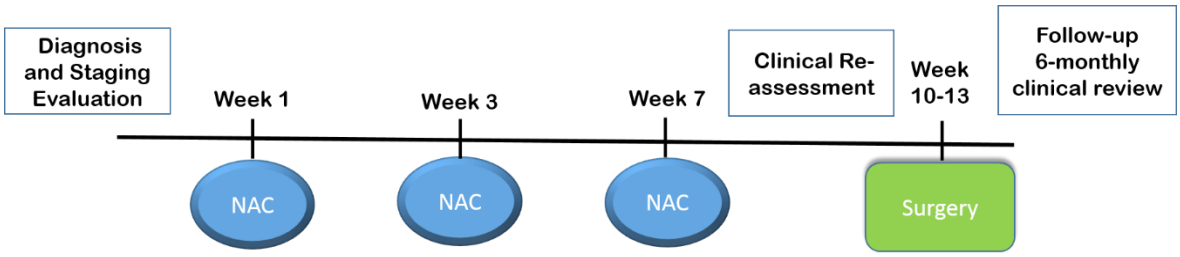

Figure 10. Curative treatment of OAC in the UK

5FU and capecitabine are antimetabolites (fluoropyrimidines), which act to impede DNA and RNA synthesis in the S phase (DNA synthesis) of the cell cycle. Deoxyribonucleic acid (DNA) and ribonucleic acid (RNA) are nucleotides comprising of a sugar, a phosphate group, and a nucleobase, such as purines (guanine, adenine) and pyrimidines (cytosine, thymine, and uracil). These drugs look similar to nucleobases or nucleotides but have altered chemical groups, and act to be incorporated into DNA or RNA, thus causing DNA/RNA damage and inducing apoptosis (programmed cell death). It can also block enzymes essential for DNA synthesis, thereby preventing mitosis and duplication of DNA[91].

Cisplatin, carboplatin and oxaliplatin are platinum-based antineoplastic agents which can work at any point in the cell cycle. They impair cell function by directly binding to DNA, forming intrastrand adducts, often between adjacent purines, some interstrand crosslinks and monoadducts. This crosslinking inhibits DNA synthesis in cancer cells, thereby resulting in apoptotic cell death. Usually the intrastrand complexes are repaired by the nucleoside

excision repair (NER) pathway in cells. However, if the NER capacity of the tumour cells is dominant, it may affect the response of the tumours to platinum-based chemotherapy[92].

Epirubicin is part of a class of cytotoxic antibiotics, which includes anthracyclines. It acts to intercalate between DNA, which inhibits DNA and RNA synthesis. It also generates highly reactive free radicals that damage intercellular molecules and inhibits topoisomerase enzymes[93]. However, there have been questions whether prolonged neoadjuvant chemotherapy and with the addition of epirubicin will actually improve outcomes. The initial results of the OEO5 trial showed that although the complete resection (R_0) rate was better with ECX (66% vs 60%), patients treated with the triple regimen of ECX had more severe toxicity (46% vs 30%), and there were no differences in survival, post-operative complications and 30-day mortality[77].

With the advent of CRT being progressively used as the standard of curative treatment for OAC, neoadjuvant chemotherapy used in this setting consists of intravenous carboplatin (2mg/ml/min) and paclitaxel (50mg/m^2 of body surface area), which is combined with radiotherapy. In the CROSS study, a total radiation dose of 41.4Gy was given in 23 fractions of 1.8Gy each, with 5 fractions administered weekly, starting on the first day of the first chemotherapy cycle[80].

Paclitaxel, originally extracted from the Pacific Yew tree, is classed as a taxane which is an anti-microtubule agent. Microtubules, composed of α-tubulin and β-tubulin proteins, are hollow rod-shaped cellular structures involved in cell division that are in permanent dynamic states of assembly and disassembly. Taxanes act to prevent microtubule disassembly, thereby preventing separation of cells and the completion of mitosis, which in turn induces apoptosis. This occurs at the G2-M phase of the cell cycle[94]. Figure 11 illustrates the action of various chemotherapy drugs on the cell cycle.

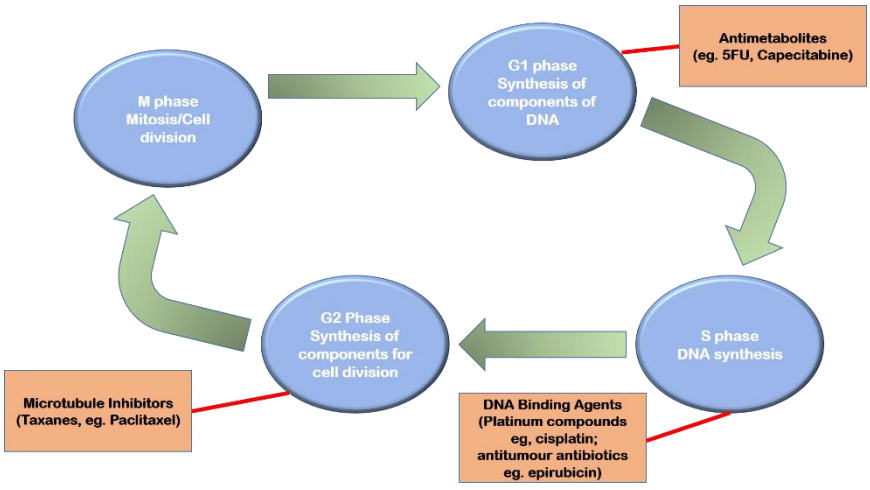

Figure 11. Action of chemotherapy drugs on the cell cycle

1.2.2 Methods to evaluate response to chemotherapy

Anatomical response

Tumour size

With a variety of actions on the cell cycle, an objective clinical response is essential to evaluate the effectiveness of chemotherapy on the cancer being treated. The World Health Organization (WHO) tried to standardize the criteria used for tumour response to chemotherapy, by measuring tumours in 2 dimensions and adding the products of the 2 measurements. The changes were then categorized into 4 groups: complete response, partial response, progressive disease, and stable disease[95]. However, this method had been criticized for inconsistent measurements which are not reproducible, inability to differentiate between viable and non-viable tumour, and no information about tumour attenuation as treatment may lead to macroscopic tumour necrosis or cystic changes which can increase tumour size temporarily.

In response to these issues as well as the inclusion of lymph node assessment and the availability of newer imaging techniques, the RECIST (Response Evaluation Criteria in Solid Tumours) working group proposed new response evaluation criteria in solid tumours in 2000, which was revised in 2009[96]. The ultimate aim of these criteria was to maintain standard imaging parameters to allow comparison between scans, so as to minimize measurement error and overestimation of response rates[97]. It incorporates FDG-PET (fluorodeoxyglucose positron emission tomography) scanning in addition to CT scanning if required. However, although the RECIST criteria assigns a new overall response status taking into account target, non-target and new lesions, it does not consider tumour necrosis as a type of tumour response[98].

Looking at the applicability of these criteria specifically in oesophageal cancer, none of the trials in the RECIST publications appear to involve oesophageal cancer patients. When Schwartz *et al* (n=19) applied both the WHO and RECIST criteria to metastatic oesophageal cancer patients, there were only a 73.7% concordance rate between both criteria. The study also highlighted the importance of lymph nodes being used to assess response[99]. Kurokawa *et al* studied 330 OSCC patients and found that the RECIST criteria had a lower response validity than histological criteria, and that the latter was better correlated to overall and progression-free survival[100].

Tumour Attenuation

Choi *et al* studied gastrointestinal stromal tumours (GISTs) and found that tumour attenuation was an important feature of tumour response, otherwise known as tumour

density and is expressed in Hounsfield units[101]. His group also found that FDG-PET scanning was useful in detecting an early response[101 102]. This brought about the Choi response criteria, which differed from the 2009 revised RECIST criteria, with the addition of tumour attenuation and modified tumour size to determine partial response. This in turn separated responders from non-responders and provided prognosis about progression-free-survival[101]. This assessment of tumour density was also used in evaluating the response of sarcoma to chemoradiation, and was found to be superior to the RECIST criteria[103].

Functional response

Metabolic Rate

Apart from evaluating physical aspects of the tumour, tumour response can be assessed by determining the alteration in metabolism, especially if chemotherapy is predominantly cytostatic rather than cytocidal. The PERCIST (PET Response Criteria In Solid Tumours) criteria was introduced in 2009, which utilized PET scanning as it gave information about the relationship between cancer cells and its FDG uptake, as metabolic changes are closely related to the malignant potential of tumours[104]. It is expressed as a percentage change in SUL (lean body mass-normalized SUV [standardized uptake value]) peak for the same lesion which is most active on PET/CT scans before and after treatment. If all metabolically active tumours had disappeared, it was considered a complete metabolic response[104]. This was seen in a study by Yanagawa *et al*, which demonstrated that PERCIST was significantly better that RECIST at predicting treatment response and its relation to prognosis in OSCC[105].

Immune Function

Workshops hosted by the Cancer Vaccine Consortium in 2005 had recommended additions to the WHO criteria as studies have shown that response (complete or partial) status could still be achieved after an increase in tumour burden[106]. As such, the Immune-related Response Criteria (IrRC) was developed, with the main difference with the WHO criteria being that new measurable lesions are not always considered to be progressive disease. This is because immune responses may take longer to manifest, and treatment should not be stopped until progressive disease is confirmed, which was defined as greater than 25% increase in tumour volume from baseline in 2 consecutive observations at least 4 weeks apart[107].

Histopathological response

Tumour Stage

Tumour stage is dependent on the American Joint Committee on Cancer TNM staging system, which is based on depth of tumour invasion, presence of positive nodes and presence of distant metastasis. The clinical TNM (cTNM) stage is allocated during a multi-disciplinary meeting before the start of neoadjuvant therapy. Following that, patients are re-staged clinically with the use of CT or PET-CT, then proceed on to surgery, where resection specimens are examined histologically and given a pathological TNM stage (pTNM). The latter is then compared to the cTNM stage to determine if there was downstaging of the T or N stage, which was considered to be a response to neoadjuvant therapy. In OAC, downstaging of their primary tumour (T-stage) or nodal status (N-stage) had survival benefit comparable to patients with early-stage tumours who did not have chemotherapy (Figure 12), and that it was an important independent prognostic factor on multivariate analysis[108].

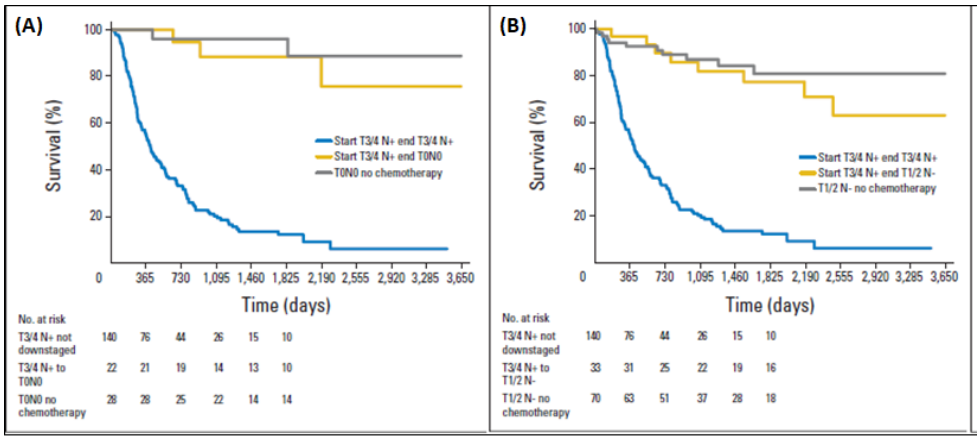

Figure 12. Kaplan-Meier curves that demonstrates T stage downstaging with survival
(A) demonstrate OAC patients that were downstaged from cT3/4N+ to pT0N0 having similar survival to T0N0 OAC patients who had no chemotherapy treatment
(B) show downstaging of OAC patients from cT3/4N+ to pT1/2N- having similar survival to T1/2N- OAC patients who had no chemotherapy treatment
(Image adapted with permission from Davies AR *et al* 2014)

Tumour Regression Grade (TRG)

Another way to determine response to neoadjuvant therapy is to look at fibrotic or regressive changes of the tumour following treatment. Not all cancers show these changes in a similar manner. Table 6 describe several classification systems for tumour regression in GI cancers described in the literature, which look at either fibrotic changes after therapy or percentage of residual tumour left. In upper GI cancers, Becker *et al* had described his grading system developed on his cohort of gastric cancer patients (n=36), which was based on amount of

residual tumour left after chemotherapy, and it had showed that tumour regression was associated with improved survival[109], which was validated in a larger study done in 2011[110].

In oesophageal cancer, Schneider *et al* (n=85) had looked at a cohort of oesophageal cancer patients following CRT treatment[111], and graded response according to the percentage of vital tumour cells. Similarly, Wu *et al*[112] and the Japanese Society for Esophageal Disease[113] had graded their tumour regression from 0-3, and based it on residual cancer cells. Using Wu's classification, Guo *et al* (n=122) had found that patients with a lower TRG correlated with a better survival, and that TRG had reflected the changes in tumour lesions after neoadjuvant therapy compared with pathological T-stage[114]. Interestingly, all classifications were used on a mixture of predominantly OSCC patients and a smaller proportion of OAC patients.

Table 6. Tumour regression grading systems in oesophageal cancer

TRG Grade	Mandard *1994*	Becker *2003*	Schneider *2005*	Wu *2007*	JSED 2017
0				No residual cancer cells	No recognizable cytological or histological therapeutic effect
1	No residual cancer	a. No residual tumour/tumour bed b. <10% residual tumour/tumour bed	>50% vital residual tumour cells (VRTC)	1-50% residual cancer cells	a. Viable cancer cells accounting for ≥2/3 tumour tissue b. Viable cancer cells accounting for 1/3≤2/3 tumour tissue
2	Rare residual cancer cells	10-50% residual tumour/tumour bed	10-50% VRTCs (partial response)	>50% residual cancer cells	Viable cancer cells account for ≤1/3 tumour tissue, while other cancer cells are severely degenerative/necrotic
3	Fibrosis outgrowing residual cancer	>50% residual tumour/tumour bed	<10% VRTCs (nearly complete response)		No viable cancer cells evident
4	Residual cancer outgrowing fibrosis		No VRTCs (Complete response)		
5	Absence of regressive changes				

On the other hand, Mandard *et al* (n=93) had described their grading system based on the balance between fibrosis and cancer in their cohort of mainly OSCC patients (84%) as a pathological response to CRT treatment (Figure 13)[115]. They found that those with TRG 1-3 had correlated with better disease-free survival and categorized this group as responders[115].

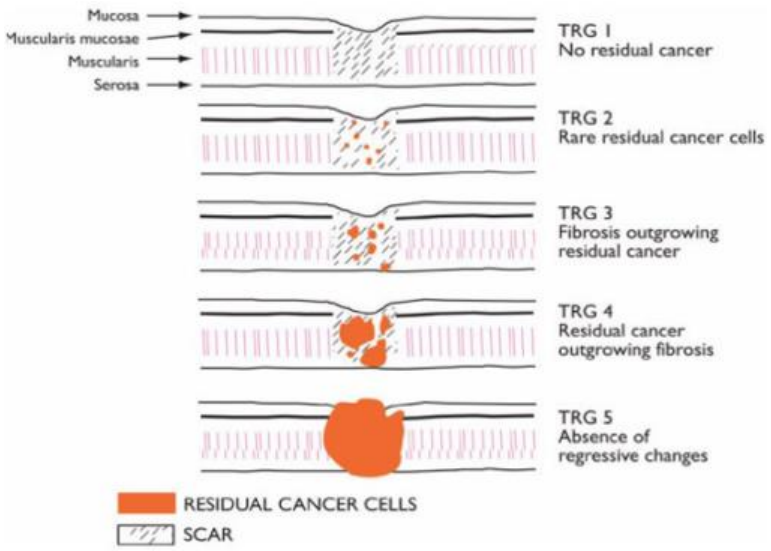

Figure 13. Mandard's tumour regression grading (TRG) system
(Image adapted with permission from Mandard AM *et al* 1994)

Conversely, Noble *et al* (n=218) classified OAC patients who underwent NAC with histology graded TRG 1-2 (26.5%) as responders, and TRG 3-5 (73.5%) as non-responders, as his study had demonstrated no difference in the survival of patients graded TRG 1 or 2 (Figure 14)[116].

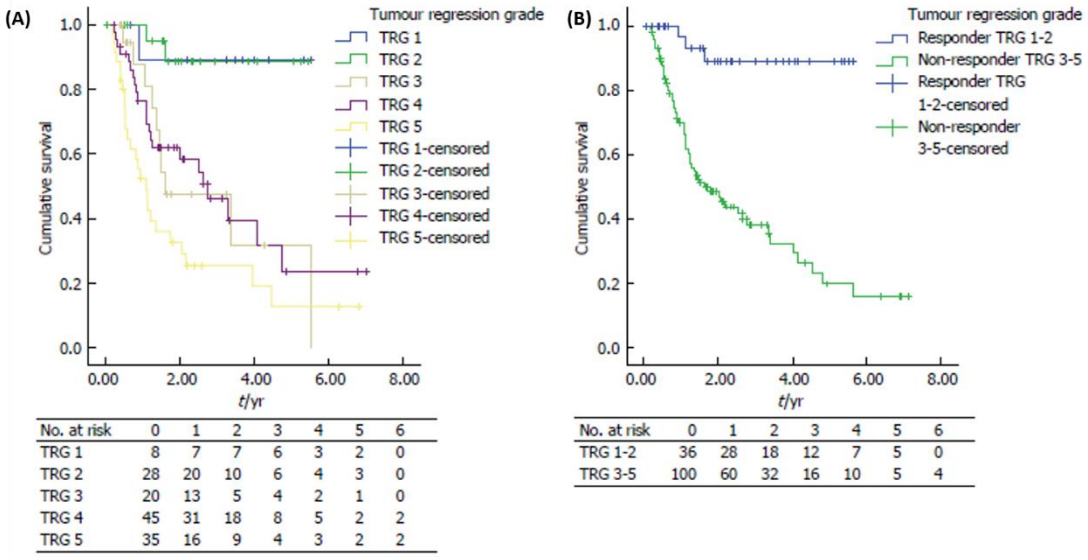

Figure 14. Kaplan-Meier survival curves of patients who received NAC grouped by tumour regression grade
(A) show survival curves of patients with individual TRG scores, which demonstrated that there was no survival difference if OAC patients had histology graded as TRG 1 or 2
(B) show significant survival differences when patients were classified into responders (TRG 1-2) or non-responders (TRG 3-5)
(Image adapted with permission from Noble *et al* 2013)

His study also found that responders had significant downstaging of their T-stage and N-stage, as well as had maximal pathological tumour diameter. The disease-free survival of responders (5.064 years) was found to be significantly different to non-responders (2.759 years) (Figure 14B)[116]. This was also reflected when Smyth *et al* investigated the MAGIC trial patients (n=503), and found that tumour regression was associated with better overall survival in NAC patients (Figure 15)[117].

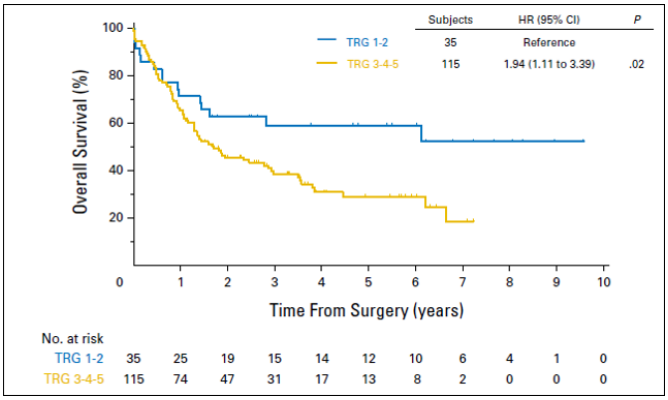

Figure 15. Overall survival of MAGIC trial patients treated with neoadjuvant chemotherapy and surgery, demonstrated that overall survival was better for patients who had tumour regression
(Image adapted with permission from Smyth EC *et al* 2016)

Lymph node status

Chemotherapy can shrink a tumour, but it can also alter the status of surrounding lymph nodes and affect prognosis. Lymph node downstaging can be considered as a manifestation of a response to chemotherapy, and is defined as a positive clinical N-stage which progresses to a negative pathological N-stage after treatment.

Noble *et al* had found that over 83% of responders (TRG 1-2) had lymph node downstaging, compared to only 30% of non-responders (TRG 3-5), and that patients with lymph node downstaging after NAC had better disease-free survival compared with those who did not achieve downstaging[116]. These results were validated later in 2017 in a multi-centre study by Noble *et al*, who showed a significant difference in survival between responders and non-responders (Figure 16). Moreover, for those who were non-responders (TRG 3-5), a third of them still had a survival advantage when there was lymph node downstaging[118].

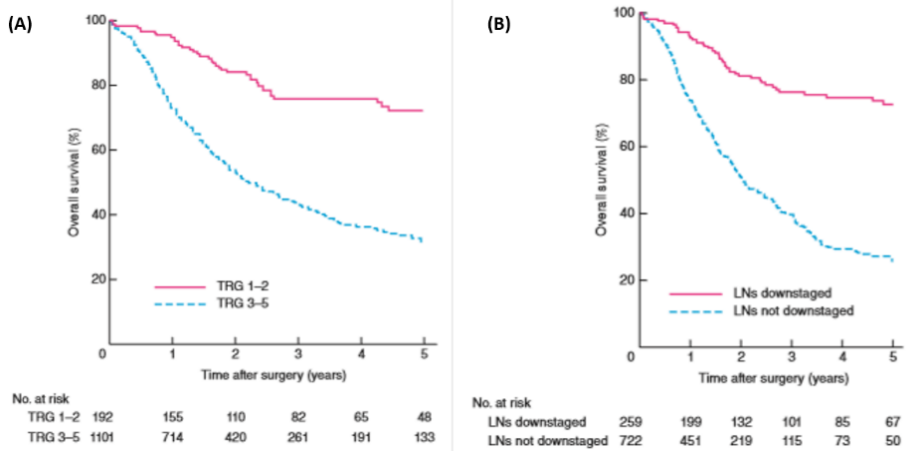

Figure 16. Kaplan-Meier survival analysis of patients grouped according to Tumour Regression Grade (TRG)

(A) TRG 1-2 (responders) versus TRG 3-5 (non-responders) showing a significant survival improvement

(B) Kaplan-Meier survival analysis of patients grouped according to lymph node downstaging showing a significant survival advantage with lymph node downstaging

Similarly, these findings were reflected in a study which found that patients staged T3/4N+ had better 5-year survival when there was lymph node downstaging from NAC (Figure 17)[108], and likewise, in the cohort of patients from the MAGIC trial[117]. In a later paper, Davies *et al* had examined lymph nodes retrieved after oesophagectomy for 377 patients and concluded that lymph node responders had a significant survival benefit regardless of response in the primary tumour. Moreover, this group of patients had decreased local and systemic recurrence, and lower overall and disease-free mortality[119].

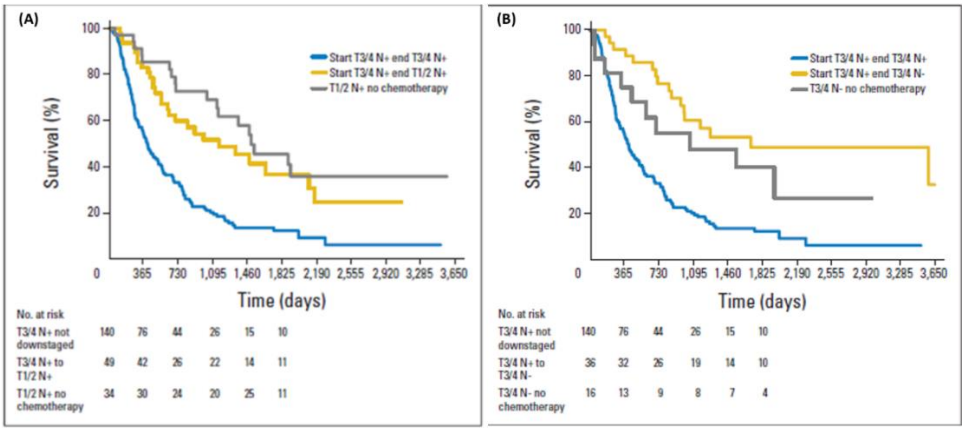

Figure 17. Comparison of patients with lymph node downstaging after multimodal treatment versus those without downstaging

(A) show that despite T-downstaging from cT3/4N+ to pT1/2N+, there is poor prognosis if nodal burden showed no response to treatment

(B) show that N-downstaging improved disease-free survival

(Image adapted with permission from Davies AR *et al* 2014)

1.2.3 Problems with response rates & contributing factors

As shown above, there are multiple ways that can evaluate response to chemotherapy and be beneficial for detecting patients who respond to treatment, so that effectiveness of patient care can be maximised. However, response rate to chemotherapy is only 40% at best in oesophagogastric cancer[120]. Therefore identifying responders is important in the treatment of patients who receive preoperative chemotherapy. If non-responders are identified early, these patients may not be disadvantaged by toxicity of chemotherapy, a 6-week delay to potentially curative surgery or allowing disease progression.

Using a sole method such as CT scanning against the RECIST criteria, is not usually suitable as resectable oesophageal cancer often has no measurable lesions, and even if there was, it has poor reproducibility[96]. However, increasing usage of PET-CT with the PERCIST criteria may improve assessment of response and restaging accuracy[105]. A reduction in FDG-PET activity could predict a tumour response, especially if done after the first cycle of chemotherapy. However, it is dependent on the uptake of FDG which can be variable in oesophageal cancer and may be dependent on specific histologic features. As such, this is currently being determined by the Dutch NEOPEC trial, which is looking at neoadjuvant therapy monitoring with PET and CRT in oesophageal cancer[121].

Subsequently, utilizing the TNM stage can provide some prognostic information, but is limited as many patients present with advanced disease (T_3N_1). Other means to provide this information include TRG or lymph node status, which has proven to be more predictive of chemotherapy response and survival.

Combining information from PET-CT with histopathological means such as TRG or lymph node status may predict response to chemotherapy and can provide prognostic information that would be much more useful in the clinical setting. Additional prognostic markers could aid in the selection of individual patients for adjuvant therapy to enable maximal benefit and improve survival rates for patients who are sensitive to chemotherapy.

1.3 Tumour microenvironment (TME)

1.3.1 Importance of the stroma in survival and therapeutic response

Cancer research has traditionally focused on cancer cells, such as gene mutations in the epithelial cells being looked at for being a driver in cancer progression[41 42]. However, there has been increasing evidence that the microenvironment plays a critical role in cancer

development and progression. Its interaction with the tumour can affect response to therapy, survival and influence patient prognosis.

Stroma

Cells do not exist in isolation but are surrounded by the microenvironment, otherwise known as the stroma, and consists of host cells such as fibroblasts, endothelial cells, immune cells, extracellular matrix (ECM) components, and blood and lymphatic vessels, to regulate cellular homeostasis. When host cells are activated by tumour cells, they crosstalk amongst themselves and the tumour cells, causing tumour progression by releasing growth factors such as interleukins, fibroblast growth factors, transforming growth factors (TGF-β), amongst others, which act to upset normal tissue homeostasis and cause an inflammatory response or angiogenesis[122].

Patients with stromal-rich cancers have a dismal survival rate. Pancreatic ductal adenocarcinoma is a solid cancer that has stroma forming 80% of the tumour mass, and 5-year survival rates are reported to be less than 5%[123]. In oesophageal cancer, Wang *et al* (n=95) demonstrated that ESCC patients whose tumours were stroma-rich had a lower 3-year disease-free survival (23%) than those who had stroma-poor tumours (57%)[124]. Similarly, Courrech *et al* investigated this phenomenon in 93 OAC patients and determined that patients who had low tumour-stroma ratios had a better disease-free survival and this ratio could be used as a prognostic factor for overall survival[125]. These results have been attributed to the quantity of intra-tumour stroma resulting in a decreased response to chemotherapy, either by impeding drug delivery, reducing the effectiveness of the drug, or by providing a microenvironment for optimal tumour growth and development[126-129].

Immune Cells

A major element of the tumour microenvironment are immune cells such as macrophages, T-lymphocytes, natural killer (NK) cells and antigen-presenting cells (APCs). This group of cells play a role in tumour suppression and progression. Macrophages derive from myeloid cells in the bone marrow, where they mature and circulate in the bloodstream as monocytes, entering tissues after differentiating into macrophages. They are phagocytic in nature, and can inhibit tumour growth (M1 - classically activated) or encourage tumour development (M2 – alternative activated). M2 macrophages, also known as tumour-associated macrophages (TAMs), are highly immunosuppressive due to secretion of cytokines such as interleukin-10, which facilitate tumour progression[130]. TAMs have also been correlated with poor prognosis in breast cancer as it secretes other growth factors that can promote the hallmarks of cancer (Figure 18)[131].

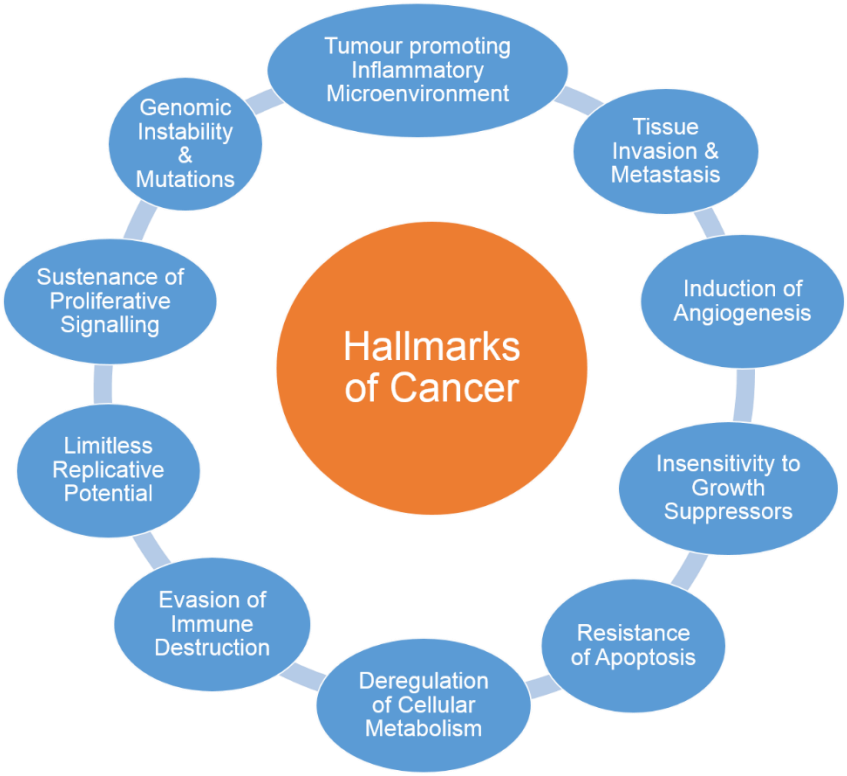

Figure 18. Hallmarks of cancer for cancer cell development

Image adapted from Hanahan & Weinburg (2011)[132]

T-lymphocytes in the stroma, also known as tumour-infiltrating lymphocytes (TILs), consist mainly of CD8+ cells, CD4+ cells, regulatory T cells, and helper T-cells. A high density of CD8+ cells has been associated with a better response to chemotherapy, as it is said to arrest growth of cells and induce apoptosis of cancer cells by releasing cytokines such as gamma-interferon (γ-IFN)[133]. Noble 2016 had also found that high levels of CD8+ TILs were associated with improved disease-free survival[134].

CD4+ cells can differentiate into various T-helper cells, such as T_H1, T_H2 or regulatory T cells (T_{reg}). T_H1 and T_H2 support immune responses, while T_{regs} (CD4+, FOXp3+) impede the activity of CD8+ cells, macrophages, APCs and NK cells[135 136]. Thereby if the equilibrium between CD8+ cells and regulatory T cells is skewed, this indicated that a poor response to chemotherapy might be anticipated, as this imbalance could enhance tumour growth instead[137].

APCs function to display antigens with MHC proteins to stimulate T-cells, while NK cells are innate immune cells that destroy cancer cells when a reduction of MHC-I is detected. However, this activity is decreased in the TME by cytokines secreted by cancers, such as TGF-β[138].

Endothelial cells and vasculature

The microenvironment has capillaries made up of endothelial cells which are surrounded by pericytes[138]. In the TME, vasculature is chaotic, with tortuous saccular vessels. The vessel walls are made up of leaky junctions of endothelial cells with large gaps in between, non-functional pericytes which are detached, and abnormal basement membranes, which can lead to an uneven perfusion of blood in tumours. As a result, it inhibits drugs and immune cells from penetrating through to poorly perfused areas of the tumour, as well as causing hypoxia and extracellular acidosis[139]. Many treatments, be it radiotherapy or chemotherapy, require oxygen to be effective. Consequently, resistance can be conferred if the TME becomes hypoxia and acidotic, as it shifts metabolism to be more catabolic, as well as encouraging inflammation, immunosuppression and inducing angiogenesis[140-143].

Extracellular matrix (ECM)

The ECM is the structural scaffold that supports cells in the microenvironment, and consists of collagens, proteoglycans, and glycoproteins such as fibronectin and laminin, amongst others. These are produced predominantly by fibroblasts, but also by other cell types such as epithelial cells, chondrocytes and osteoblasts in the microenvironment, and function to permit ECM signalling, allow penetration of drugs and contribute to mechanical forces in tumours[139].

However, in the TME, cancer cells actively remodel the ECM by excessive production of collagens and fibronectin to surround the tumour, which increases ECM stiffness and influences growth factor signalling to activate cell migration, and adhesion of tumour cells on the ECM via ligands. This in turn, limits penetration of chemotherapy to cancer cells to allow for apoptosis[144 145].

The ECM turnover is also regulated by key enzymes such as matrix metalloproteinases (MMPs) and tissue inhibitors of metalloproteinases (TIMPs). The MMPs, secreted by both tumour and stromal cells, are zinc-dependent enzymes that degrade the ECM and basement membranes and are important in angiogenesis and metastasis[138]. TIMPs, on the other hand, inhibit MMP activity to degrade the ECM and apoptosis, and stimulate cell growth[144]. MMP7 overexpression in colorectal cancer cell lines have been found to be resistant to doxorubicin and oxaliplatin[146], while high TIMP1 expression were found to be associated with a poor response to chemotherapy and poor survival in breast cancer and colorectal cancer[147 148].

1.3.2 Origins and Characteristics of Cancer-Associated Fibroblasts (CAFs)

Fibroblasts are the most abundant cells in normal connective tissues that secrete ECM proteins to maintain structural support in tissues, and are involved in wound healing and fibrosis through tissue remodelling[149]. Physically, they are non-contractile and are spindle-shaped cells that express low levels of smooth muscle actin (SMA), which is associated with contractility[145]. In wound healing, they are activated and transdifferentiate into myofibroblasts. These myofibroblasts express high levels of SMA, and their ability to contract is an essential characteristic for healing and subsequent closure of wounds[149].

Likewise, within the tumour stroma, the major cellular component are cancer-associated fibroblasts (CAFs), which are responsible for providing the architectural support by remodelling the ECM dependent on factors within the TME[138]. CAFs are a heterogeneous population of cells within the same cancer, and originate from a number of sources, the most common source are resident fibroblasts (Figure 19)[131 144 149].

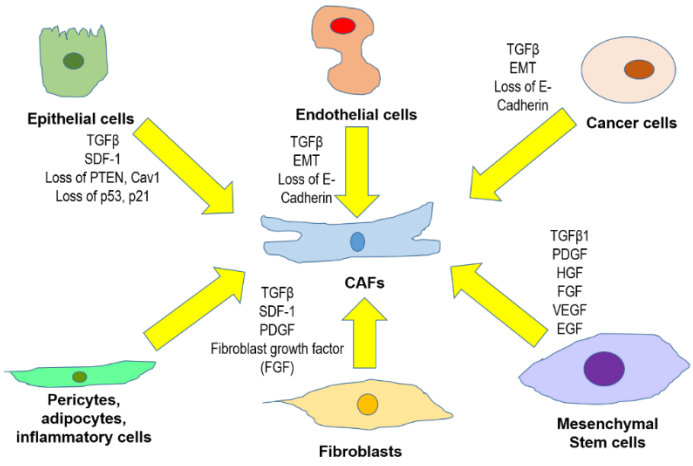

Figure 19. Origins of CAFs in the tumour microenvironment

Image adapted from Cirri & Chiarugi 2011, Hale *et al* 2013, Mao *et al* 2013

The activation of fibroblasts to myofibroblasts is usually induced by transforming growth factor (TGF-β) and stromal cell-derived factor 1 (SDF-1, also known as CXCL12), but can also be mediated by interleukin-1 (IL-1β)[145 150]. This distinguishes CAFs as a distinct cellular population with abundant expression of αSMA, fibroblast activation protein (FAP), fibroblast specific protein 1 (FSP1), tenascin-C, desmin, hepatocyte growth factor (HGF), or platelet-derived growth factor (PDGF-α/PDGF-β)[130 131 145 149]. They also express vimentin, fibronectin and podoplanin, like normal fibroblasts. However, due to the heterogeneity of CAFs, they can express different markers, depending on the origin of tissue[131].

As the largest component in the stroma, we will explore the multiple roles CAFs have to play as they produce multiple proteins and secrete soluble tumour-promoting factors such as ECM proteins, cytokine and chemokines, which impact on cancer cell proliferation, invasion and survival.

1.3.3 Role of CAFs in cancer progression

When CAFs are activated, it leads to downregulation of various tumour suppressor genes like p53, p21, phosphatase and tensin homolog (PTEN) and caveolin-1 (Cav-1), which disrupts the apoptotic response of cells to stress[151-155]. CAFs also secrete numerous growth factors and pro-inflammatory factors such as hepatocyte growth factor (HGF) vascular-endothelial growth factor (VEGF), platelet-derived growth factor (PDGF), interleukins interferons and members of the tumour necrosis factor (TNF) family, and plasminogen activators and members of the matrix metalloproteinases (MMPs) that alter the composition of the ECM. Cytokines and chemokines produced by CAFs leads to immune infiltration and promote angiogenesis and metastasis. All these in turn have profound effects on the TME to enhance tumour progression.

Proliferation and tumour growth

Kiaris *et al* had tested the effect of p53 downregulation in SCID mice with breast cancer MCF7 tumours, and found that those mice with p53-null fibroblasts had tumour growth speeded up, compared with mice with wild-type fibroblasts[152].

Trimboli *et al* showed that when PTEN was genetically ablated, it had increased ECM production and remodelling, chemokine and cytokine production in the TME, through pathways associated with cell architecture, chromosomal integrity, cell cycle progression, cell growth and stem cell self-renewal. Through the disruption of the TME, it led to slowed down tumour growth[153].

This effect was similarly seen in breast cancer xenograft models with cav-1 deficient fibroblasts increased tumour growth in terms of mass and volume[154].

Invasiveness

Activation of CAFs can lead to downregulation of tumour suppressor genes such as p53. Moskovits *et al* suggested through human and mice fibroblasts that SDF1 production is promoted, thereby enhancing the migration and invasiveness of cancer cells[155]. Important CAF-secreted factors such as HGF had been shown to promote invasion via the HGF/Met signalling pathway in ESCC[156] and in early breast cancer[157].

This was also seen in pancreatic cancer, where co-culture of cancer cells with fibroblasts led to tumour growth and cancer cell invasion, through the release of growth factors and cytokines[158].

Angiogenesis & Metastasis

CAFs produce growth factors such as VEGF and PDGF to directly stimulate tumour angiogenesis[122]. CAFs also secrete MMPs, which alter the ECM structure to support tumour growth and spread, as well as activate immune cells to increase degradation of the ECM[159].

Co-cultures of ESCC cells and fibroblasts produce conditioned medium that activated fibroblasts via TGFβ signalling, which in turn released VEGF and promoted angiogenesis[160].

Orimo *et al* had discovered that secretion of SDF1 by CAFs not only promoted tumour growth, it also contributed to angiogenesis by recruiting circulating endothelial cells and aided in breast cancer vascularization and metastasis[161].

Clinical Prognosis

The stroma is important in considering disease-free survival, with CAFs in particular being closely associated with prognosis. Alpha-SMA, which is a marker of CAFs, was demonstrated to have a poor overall survival outcome if it is associated with high α-SMA expression in 183 OAC patients[162]. This effect was also seen in patients with colorectal cancer, where fibroblast activation protein (FAP) expression was associated with a poor overall and disease-free survival, with a positive correlation to metastases, recurrences, and metastatic lymph nodes[163]. Similarly, IL-6 secreted by CAFs had been proven to be positively correlated with clinical stage of hepatocellular carcinoma (HCC)[164].

1.3.4 Role of CAFs in chemoresistance

Chemoresistance is defined as resistance of cancer cells to specific chemotherapy agents, and is a common problem that cancer patients face. It is believed that CAFs can promote chemoresistance of cancer cells in a number of ways, such as cancer cell survival, interstitial fluid pressure within the cancer, dampening of anticancer immune responses, and interactions between cancer cell and stroma either directly or indirectly[165]. For instance, direct contact occurring between cancer cells and fibroblasts induced epithelial-to-mesenchymal transition (EMT) in melanoma and lung cancer[145 166]. Adhesion of cancer cells to ECM proteins such as periostin could activate the PI3K/AKT pathway and stop the release of apoptotic factors[167].

The major contributor to chemoresistance was thought to be the secretion of soluble factors. Culturing pancreatic cancer cells in CAF-conditioned medium caused greater resistance of the cancer to chemotherapy and decreased the apoptotic rate by 76%[168]. This was also seen in breast cancer, where tamoxifen resistance was mediated through the activation of EGFR and PI3K/AKT pathways as well as initiation of EMT from inflammatory cytokines[131]. CAF-secreted HGF aided DNA repair by reactivating the Met/PI3K/ERK cascades and downregulated expression of apoptotic proteins[156]. HGF also produced resistance against EGFR tyrosine kinase inhibitors in lung cancer[169]. Similarly, CAF-secreted PDGF secretion was purported to enhance resistance of the cancer to anti-VEGF treatment[170]. Even secreted ECM proteins can affect the response to chemotherapy due to downregulation of apoptotic factors[144].

I conducted a structured literature search to identify all primary literature that examined the role of fibroblasts in chemoresistance of solid tumours. A search strategy combining Plain Text and Medical Subject Heading (MSH) terms was developed:

(1) tumour/tumour microenvironment OR stromal cells

AND

(2) fibroblast

AND

(3) chemosens* OR drug resist* OR chemotherapy resp*

The search terms were entered into Ovid MEDLINE (1996 to November 2016) and EMBASE without limits, and 247 articles were returned. Existing reviews and reference lists were manually searched to identify additional potentially relevant studies that were missed by the search terms. The search was limited to human studies published in English. Only published results were included in this review. Duplicated studies were removed and the titles and abstracts of the remaining citations were screened for eligibility using pre-determined selection criteria. Unpublished data from conference abstracts were excluded. In cases where studies used the same dataset, the more recent article was retained. Repeated use of datasets was found by cross-examining names of author and institution.

199 subject abstracts were examined. From these, 82 potentially eligible full-text articles were retrieved with relevant appendices and supplementary information. Of these, 59 were excluded after reviewing the papers. 4 further articles were added in after cross-checking references and additional sources. This left 27 papers to be included in the final review. Figure 20 shows a flow-chart that demonstrated the selection of articles for the literature review, using the PRISMA flow diagram as a guide.

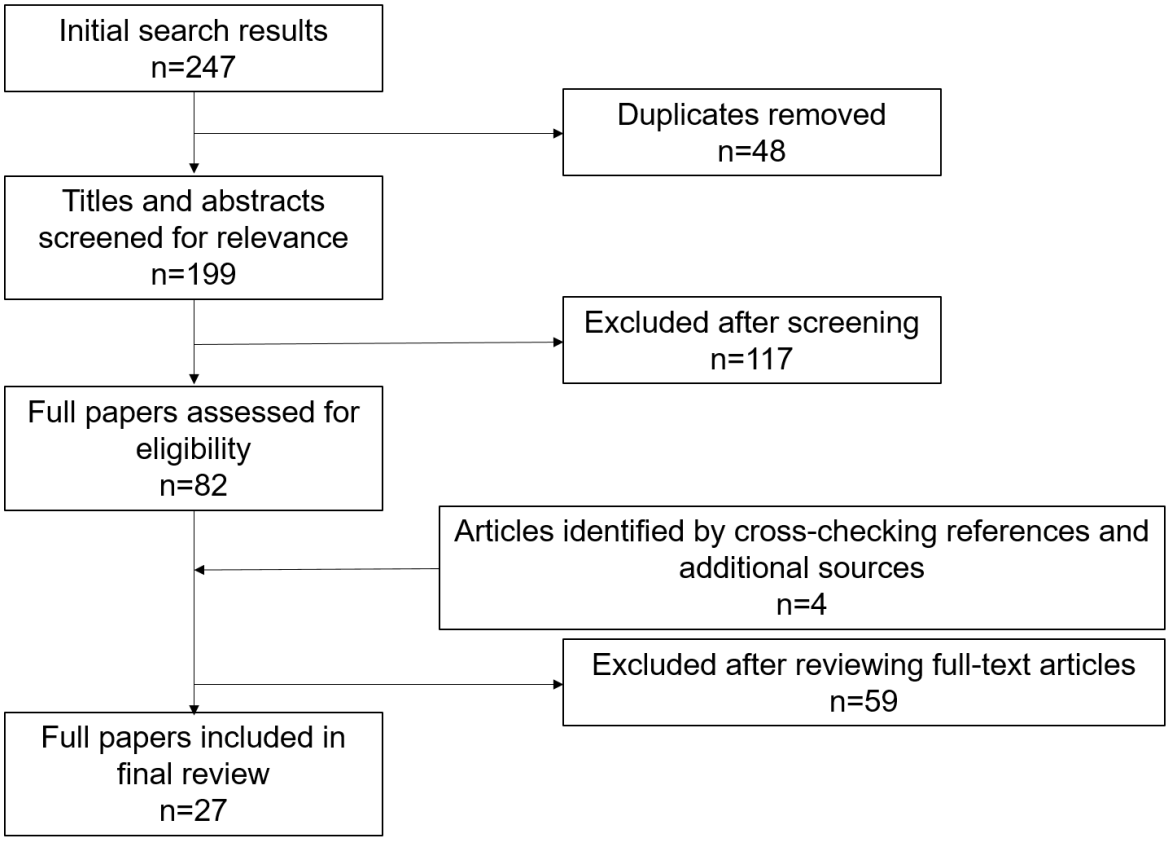

Figure 20. PRISMA flow chart illustrating selection of articles for review

After the literature search, the papers were categorized according to the method by which the experiments were carried out, for instance, direct contact versus CAF secretome. Further categories were considered: monolayer plating, spheroid assays, co-culture and CAF-conditioned medium.

Regulation of genes

CAFs from breast cancer patients that were isolated and had IHC testing and gene expression profiling showed that there was a difference in regulation of certain genes before and after chemotherapy treatment. 17 genes were up-regulated and 18 were down-regulated, and these genes were mainly involved in binding of nucleotide, actin or cytoskeletal protein, and structural molecule activity. The genes found to have a significant difference in expression included CXCL2, MMP1, IL-8, FGF1, CXCR7 and RARRES1[171].

Direct contact via cell adhesion

Using immunohistochemistry in breast and lung cancer tissue specimens, CAFs from breast cancer were mostly resistant to cisplatin while CAFs from lung cancer specimens showed a variable response, similar to lung and breast cancer cell lines. Consequently, CAFs in tissue specimens appeared to be less sensitive to cisplatin compared to isolated CAFs,

which indicate that the cell-cell interaction within the microenvironment can determine the sensitivity of cells to chemotherapy[172].

One way of influencing chemoresistance is by direct contact of CAFs with cancer cells. Flach *et al* had grown melanoma cells on top of cell culture plastic and on an activated fibroblast monolayer in the presence of chemotherapy, and found that more melanoma cells survived by growing on top of the fibroblast monolayer, and that it was a significant result[173]. Similarly, when melanoma cells were grown on a collagen matrix composed of fibroblasts (dermal equivalent), they maintained a lower percentage of dead cells compared with seeding on plastic or growth on collagen gel with no fibroblast presence. There was also a reduced response to doxorubicin treatment, resulting in a higher number of viable melanoma cells[174]. When plated in co-culture spheroidal assays, the fibroblasts adhered to the melanoma spheroid surface before infiltrating into the spheroids and being equally distributed in 4 days[173]. This may have been due to the cell-cell interaction between melanoma cells and fibroblasts through N-cadherin, thereby increasing survival of melanoma cells via AKT signalling. Another explanation may be due to an increase in cytokines IL-6 and IL-8 production when cultured on the dermal equivalent, as observed by Tiago *et al*, who had suggested that direct contact was required between melanoma cells and fibroblasts before cytokine production could be increased[174].

In lung cancer, when CAFs were cultured with cancer cells, either mixed together or separated by a Transwell chamber, Yoshida *et al* found that direct contact with CAFs was necessary to gain a significant resistance to gefitinib, and that podoplanin expression in CAFs was predictive of the response to EGFR-TKI, where patients with podoplanin-positive CAFs responded worse to EGFR-TKI. This resistance was reversed with the knockdown of podoplanin expression, with the suggestion that the intracellular MAPK signalling pathway in cancer cells was altered with the combination of signal transduction through the ligand for podoplanin[175].

In breast cancer, when breast cancer cell lines were individually cultured onto fibronectin-coated plastic, there was no increase in cell death when treated with tamoxifen. This adherence of fibronectin to cancer cells was found to be mediated by B1 integrin, and when the cells were treated with a B1 integrin blocking antibody (AIIB2), this protective effect was significantly reduced and there was tamoxifen-induced cell death[176].

Secreted factors

Another way that CAFs influence chemoresistance is through its secretome, which consist of growth factors, MMPs, cytokines, chemokines amongst others that affect chemoresistance.

Hepatocyte growth factor (HGF)

HGF is not expressed by epithelial cells but in fibroblasts[177-179]. Using conditioned medium from CAFs, HGF appeared to increase the survival of breast cancer cell colonies in the presence of gefitinib and erlotinib, by inducing Met phosphorylation and crosstalk between HGF and EFGR. Similar results were shown in co-culture experiments. In addition, as HGF is a ligand for Met, inhibition of Met kinase activity with activation of Met sensitized the breast cancer cells to EGFR TKIs[177].

CAFs also induced resistance to lapatinib in OSCC, by restoring growth of cancer cells by 20% after fibroblast supernatant was added to the culture, and this was attributed to the high expression levels of FGF2, FGF7 and HGF, and by stimulation of the HGF/Met and FGF/FGFR signalling pathways to increase cell growth[180].

In lung cancer co-cultures, particularly those with the EGFR-T790M mutation, HGF induced resistance to irreversible EGFR-TKI, which was reversed with the addition of HGF-Met inhibitors, therefore it was postulated that this resistance was mediated by Met/PI3K/AKT phosphorylation and initiating ERK1/2 signalling[178 179 181]. However, in further co-culture and conditioned medium experiments, the cetuximab resistance was dose-dependent on HGF, regardless of EGFR status[182]. Moreover, HGF in CAF-CM reduced normal and paclitaxel-induced apoptosis in vitro[179]. In addition, HGF can act in a paracrine signalling fashion to activate resistance to EGFR-TKIs through bypass signals[183].

Interleukins (IL)

Lung fibroblasts have been shown to secrete IL-6, which are a class of glycoproteins produced by leucocytes that regulates immune responses. When CAFs were used in co-culture or as CAF-CM involving lung cancer cells, they became more resistant to afatinib. This was attributed to the activation of the IL-6R/JAK1/STAT3 signalling pathway in a paracrine manner, resulting in cell cycle progression, tumour invasion, metastasis, angiogenesis and drug resistance. STAT proteins are intracellular transcription factors that get activated in certain cancers, primarily by membrane receptor-associated JAK. As STAT3 is a transcription factor for IL-6 transcription, this activated a positive feedback loop for that signalling pathway. However, when STAT3 was inhibited, cancer cell growth was suppressed and their sensitivity to cytotoxic drugs had improved[184].

Similarly, in pancreatic ductal carcinoma (PDAC), 60 factors were detectable in the CAF secretome, with IL-6 being one of the most abundant factors. When IL-6 was blocked by an antibody in CAF-CM, it reversed the resistance to gemcitabine, 5FU or oxaliplatin[123]. Experiments utilizing CAF-CM as well as co-culture in the Transwell system increased resistance of the pancreatic carcinoma cells to etoposide, due to IL-1β secretion by cancer

cells, which was increased 3-fold by culture with CAF-CM. In addition, iNOS expression was increased in fibroblasts and NO was found to be secreted by fibroblasts in large amounts, which in turn induced IL-1β and made the cells more resistant[185]. Moreover, the results of the co-culture experiments alluded to the conclusion that if activity of DNA methyltransferase 1 (DNMT1) was elevated, a reduction in STAT1 expression or DNA hypermethylation of CpG islands in cancer cells was noticed, which accounted for the downregulation and decreased protein levels of caspases. This was reversed when DNMT1 was knocked down, and chemosensitivity of the cancer cells was restored[186].

MMPs

In HNSCC, CAFs induced cetuximab resistance in co-culture and conditioned medium experiments. Johansson *et al* also observed that secreted factors greater than 50 kDa mediated more resistance to cetuximab. Furthermore, there was a 2-fold increase in expression level of MMP1 and an EGFR ligand, amphiregulin, which when reduced with an inhibitor of MMP1, significantly decreased the protective effect of the CAF-conditioned medium[187].

In breast cancer, CAF-CM revealed activity of both MMP2 and MMP9. With tamoxifen treatment, the cancer cells were resistant to treatment, while cells in CAF-CM that contained an MMP inhibitor had its protective effect reversed and these cells became non-viable with tamoxifen. As such, the study's authors concluded that MMPs are involved in the paracrine signalling to induce resistance through the EGFR and PI3K/Akt pathways[176].

PDGF

PDGF-C was consistently upregulated in CAFs in murine lymphoma models, together with a downregulation of SDF-1 in CAFs. Crawford *et al* found that both PDGF-C and VEGF-A, were expressed by CAFs, and when induced, mediated tumour growth and angiogenesis in vivo. Moreover, anti-PDGF-C antibody had inhibited angiogenesis in cancers that were resistant to anti-VEGF treatment[170]. This opened the floor to consider if responses could be improved to anti-VEGF therapy or a second-line anti-PDGF antibody if a way could be worked out to reverse or inactivate CAFs.

Similarly when conditioned medium was used on pancreatic cancer cell lines after treatment with a JAK1/2 inhibitor, PDGF was inhibited and the PI3K/mTOR pathway in CAFs was not activated, resulting in dephosphorylation of Akt and 4E-BP1, which was reversed with a phosphotyrosine phosphatase inhibitor. In addition, when the cancer cells were treated with chemotherapy in CAF-CM, there was a large increase in survivin, which is part of the family of inhibitors of apoptosis (IAP) that made cancer cells resistant to cytotoxic therapy. When

survivin was decreased by blocking IL-6 activity with a neutralizing antibody, the cancer cells became sensitive to chemotherapy once again[123].

Metabolic factors such as Cav-1 and HMGB1

Caveolin (Cav-1) is found in breast cancer stroma and loss of cav-1 has been associated with early recurrence and progression of disease and lymph node involvement. In co-culture, breast cancer cells were found to cause oxidative stress to fibroblasts and resulted in cav-1 loss. These cav-1-deficient CAFs appeared to confer resistance to tamoxifen in the cancer cells, which was reversed with dasatinib (a tyrosine kinase inhibitor), by inducing aerobic glycolysis in MCF7 breast cancer cells and apoptosis in the CAF population[188]. In addition, these cav-1-negative CAFs produced lactate and ketone bodies, where these metabolites increased cancer cell mitochondrial activity[189]. Mitochondrial activity was measured via glucose uptake, where usually fibroblasts take up 2-3 fold more glucose than cancer cells due to aerobic glycolysis. Martinez-Outschoorn *et al* found that breast cancer cells with high mitochondrial activity and low glucose uptake had more resistance to tamoxifen[189]. When breast cancer cells were treated with tamoxifen and a TKI or metformin, which is a mitochondrial complex I inhibitor, the mitochondrial activity of the cancer cells and the CAFs was reduced, with a decrease in production of ROS, which in turn reduced DNA damage[188 189].

In another breast cancer study, the cancer cell cultures grown in CAF-CM were resistant to doxorubicin and an increase in protein expression and high serum level of intracellular high mobility group box 1 (HMGB1) was noted to correlate to drug resistance. Furthermore, it was observed that dying cancer cells released HMGB1, and that extracellular HMGB1 bound to receptors of advanced glycation end products (RAGE) in cancers, aiding recruitment of inflammatory cells and increasing IL-6 production, which activated various signalling pathways[190].

Other factors

In melanoma, CAFs which were positive for CD44 appeared to support cancer cell survival, especially in avascular areas. In vivo studies suggested that CD44+ CAFs produced factors that were chemoresistant to 5FU treatment, and correlated with an increased expression level of MDR1 in cells[191].

In co-culture experiments in prostate cancer, CAFs conferred chemoresistance to sorafenib, which was reversed and sensitivity was re-established when treated with a Bcl-2/Bcl-X_L antagonist. It was then hypothesized that CAFs released other factors that could upregulate Bcl-X_L and cause chemoresistance[192].

On the other hand, CAFs were shown to significantly limit EGFR-TKI activity in lung cancer cells through paracrine secreted factors that did not affect Akt phosphorylation, regardless of EGFR–activating mutations[193]. Similarly, breast cancer cells that were co-cultured with fibroblasts were found to be resistant to tamoxifen via growth factor signalling pathways other than EGF/EGFR and IGF/IGF-1R pathways[194].

Not only do CAFs play an important role in chemoresistance, they also have a relationship with tumour-associated macrophages (TAMs). A high expression status of CAFs and TAMs was correlated with a poor pathological response to 5FU chemotherapy for oral SCC. As expected, it resulted in a poorer prognosis for this group of patients[195].

Particularly in oesophageal cancer, only a few papers have been published with regards to oesophageal CAFs playing a role in chemoresistance, with most of them in OSCC. Tanaka *et al* investigated 64 OSCC patients and identified 10 micro RNAs that were upregulated in non-responders, compared with responders. In particular, they discovered that micro RNA-27a/b derived from OSCC cells did not directly affect the chemosensitivity of cancer cells, but acted on normal fibroblasts to convert them to CAFs and that enhanced the cancer cells to become resistant to cisplatin via increased production of TGFβ. This effect was reversed with administration of neutralizing antibody of TGFβ to the supernatant and chemosensitivity to cisplatin was restored[196]. Zhang *et al* found that CAFs had conferred chemoresistance to cisplatin and taxol OSCC in vitro and in vivo, which was re-established with a blockage of TGFβ1 signalling, and resulted in less cell apoptosis, and that CAFs expressing TGFβ1 was significantly associated with tumour size, poorer diagnostic stage and LN metastasis and a lower overall survival of OSCC patients treated with CRT[197]. Similarly, Galvan *et al* investigated both OAC and OSCC cases treated with primary resection versus those receiving neoadjuvant treatment before resection, and found that presence of CAFs positive for COL11A1 and SPARC was associated with higher pT-stage, lymphatic invasion and worse overall survival[198]. On the other hand, OSCC patients with a high expression of PAI-1, a cytokine secreted from CAFs after treatment with cisplatin, demonstrated a significantly poorer disease-free survival[199]. Likewise, IL-6 derived from CAFs was associated with a worse overall and disease-free survival in OSCC patients who had received cisplatin after their operation[200].

In summary, CAFs play a huge role in chemoresistance through a combination of processes, which include cell adhesion of CAFs with the cancer cells, as well as the crucial secretome that contains amounts of cytokines, chemokines, growth factors and other soluble factors that work on several intracellular signalling pathways to bring about chemoresistance. Amongst other factors, collagen, fibronectin and laminin secreted by CAFs can bind to integrin receptors on cancer cells, which in turn activate the PI3K/AkT pathway in cancer cells that inhibits release of pro-apoptotic factors. Secreted factors can

also impact on chemosensitivity and act in an autocrine or paracrine way to stimulate signalling pathways in a simultaneous nature. It appears that TGFβ1 is involved in an important signalling pathway in oesophageal cancer that we were explore further when examining mechanisms of chemoresistance.

1.3.5 Importance of chemoresistance

Chemoresistance usually manifests as a lack of response to chemotherapy drugs, and can be innate or acquired. Clinical response to chemotherapy has been discussed in Chapter 1.2.2, and can be objectively evaluated according to anatomical, functional or histopathological response. Ultimately, chemoresistance can be represented as treatment failure, with recurrence and death. In the laboratory setting where cell lines are utilized, chemoresistance can be expressed with surrogate indicators, such as a raised metabolic activity or a higher drug dose required in dose-response assays, or minimal decrease in cellular proliferation or colony growth rate, in the presence of specific chemotherapy agents.

This issue is of important enormity, as 90% of treatment failure of metastatic cancers was believed to be secondary to resistance to chemotherapy[201]. A meta-analysis of patients with solid tumours undergoing chemotherapy showed a complete response rate of approximately only 7%, with partial responders accounting for 28.1%[202]. Even when patients had responded to chemotherapy, frequent relapses were common, with 50-70% of patients relapsing within a year[130].

A multitude of factors, such as genomic alterations or changes in transcription factors or the cell cycle, account for this problem in solid cancers. In ovarian cancer, women with a highly active fibroblast growth factor (FGF1) gene had aggressive advanced cancer that corresponded with resistance to platinum-based chemotherapeutics, which was reversed when the FGF1 gene was blocked[203]. Overexpression of high mobility group AT-hook1 (HGMA1) in patients with pancreatic ductal adenocarcinoma has been associated with chemoresistance to gemcitabine through an Akt-dependent mechanism and increased resistance to apoptosis[204]. CAFs also enhance chemoresistance in a pancreatic cancer model by inducing expression of DNA methyltransferase 1 and decreases expression of caspases[130]. In colorectal cancer, activation of nuclear factor E2-related factor 2 (Nrf2), a transcription factor regulating genes that affect oxidative stress, by oxaliplatin was shown to reduce the sensitivity of colon cancer cells to chemotherapy agents. This action was reversed with knockdown of Nrf2, which in turn decreased oxaliplatin-induced chemoresistance[205]. In lung cancer, resistance has been attributed to tubulin binding agents, by changes in microtubule structure or mitotic checkpoints, or even efflux through

multi-drug resistant (MDRs) proteins. Reducing β-tubulin expression was shown to increase the sensitivity of non-small-cell lung cancer cell lines to taxanes[206].

Specifically in UGI cancers, overexpression of thymidylate synthase (TS), an enzyme involved with 5FU metabolism, reduces binding of 5-fluorodeoxyuridine monophosphate (5FdUMP) to TS and depletes the nucleotide pool for DNA synthesis, thereby leading to 5FU resistance in gastric cancer and correlated to poorer survival[120]. In oesophageal cancer, presence of nuclear factor kappa B (NFκB), a transcriptional factor, had correlated with lack of chemotherapy response and poor overall survival[207]. Langer *et al* had suggested that in patients with Barrett's OAC, a high gene expression of MRP1, a multidrug resistance gene, was associated with a higher response to chemotherapy and a longer survival benefit[208].

In summary, chemoresistance is a major problem for oesophageal cancer as well as other solid cancers, and impacts on overall and disease-free survival. As it is a major component of cancer treatment, understanding of the mechanisms might allow for the development of targeted approaches to treat cancer.

1.3.6 Mechanisms of chemoresistance relevant in oesophageal cancer

Multidrug resistance affects up to 500,000 new cases of cancer annually[209]. Reasons for the occurrence of chemoresistance are multifactorial, and can be dependent on a combination of extrinsic influences such as patient factors, tumour-host interactions or cellular resistance, as well as intrinsic features. Intrinsic chemoresistance typically occurs when there is survival of a subpopulation of cancer cells after treatment, which subsequently leads to early recurrence, and is common in tumours with a heterogenous cell population. Other factors to consider include gene mutations resulting in defective tumour suppression or promotion of tumour formation, and loss of function or change in activity of various cell transporters which result in alterations in drug accumulation in cancer cells. Alternative features that can impact on chemoresistance include patient age, histological grade of the primary tumour, lymph node status, and particular RNA or protein expression profiles. Tumour suppressor genes such as p53 or oncogenes such as c-myc can acquire gene amplifications or mutations such that tumour suppression becomes defective and tumour formation gets promoted instead. It can even induce metastatic features and alter cell sensitivity to make it more resistant to chemotherapy agents[210]. For the purposes of this thesis, I will be focusing on mechanisms of chemoresistance that have been observed in oesophageal cancer, classified according to the chemotherapy agents that are commonly used in neoadjuvant treatment for OAC.

Metabolism enzymes such as metallothioneins and glutathione S-transferase (GST) were judged to be crucial enzymes as they are involved in stress response, cell proliferation, apoptosis, cell cycle metabolism and inactivation of certain chemotherapeutic agents, such as binding to cisplatin and allowing its export from cells through an efflux pump process. When polymorphisms alter the functional capability of GSTs, there was a lower response to platinum chemotherapy and poorer survival rate[211-214].

Another mechanism predominantly used is the NER pathway, which repairs substantial DNA damage that can be induced by platinum agents causing DNA binding and cross-linking of DNA strands. ERCC1 interacts with other enzymes such as XPF, XPA, RPA to repair DNA double-strand breaks and crosslinking damage, as part of the NER pathway Joshi *et al* had found that a high mRNA expression of ERCC1 had correlated with a poorer overall survival and an increase in cancer recurrence risk[212]. Similarly, this was also predictive of minor histopathological response[215]. When Kim *et al* analysed IHC assays of tumour specimens from patients treated with pre-operative CRT with cisplatin and 5FU, his study found that those whose tumours were ERCC1-negative had a longer overall and disease free survival, and that ERCC1 was the only independent variable predicting pathological response, and suggested that it could be used as a predictive and prognostic marker[216].

As alluded to in Chapter 1.3.4, TGFβ1 is an important molecule in the signalling pathway that is expressed by CAFs. In OSCC cell lines, there was higher concentration of TGFβ1 in the culture medium that correlated with chemoresistance of cisplatin and taxol use. This chemosensitivity was re-established once inhibition of the TGFβ1 receptor was instituted to block the TGFβ1 autocrine/paracrine signalling loop, which was found to be through the activation of FOXO1, a transcription factor stimulating TGFβ1 activity. This was also reflected with in vivo models and with other chemotherapy agents tested, such as 5FU, carboplatin, docetaxel, anthracyclines and vincristine. It was concluded that one mechanism of chemoresistance in OSCC was mediated by FOXO1/TGFβ1 signalling loop[197]. Similarly, micro RNA-27 converted normal fibroblasts to CAFs and induced cisplatin resistance via a rise in TGFβ production. This effect was reverted with usage of TGFβ antibody, to OSCC cells becoming sensitive to cisplatin therapy again[196].

On the other hand, overexpression of AXL in OAC cell lines was associated with cisplatin resistance via blockage of cisplatin-induced endogenous p73 protein transcriptional activity and expression of downstream targets. AXL is a tyrosine kinase receptor, and is associated with cancer cell proliferation, epithelial-mesenchymal transition and resistance to drug treatment. AXL had significantly lessened phosphorylation of c-ABL and p73 proteins in the

cytoplasm, thereby blocking nuclear accumulation of these molecules, which induced cisplatin resistance[217].

Expression of IGFBP2 in OAC cell lines was also found to be involved in cisplatin resistance. IGFBP2 are part of a family of proteins that modulate IGF and integrin signalling to stimulate cell growth, invasion and drug resistance in various tumours. Knockdown of IGFBP2 through the addition of either AKT or MEK1/2 inhibitors had re-sensitized the cells to cisplatin through activation of the AKT pathway and decreased cisplatin-induced ERK activation[218].

Molecules secreted by CAFs after drug treatment can also contribute to chemoresistance. Che *et al* observed that PAI-1, a cytokine secreted by CAFs after cisplatin treatment, was found to induce chemoresistance of OSCC cells in vitro and in vivo, and protected OSCC cells from apoptosis though inhibition of ROS accumulation as well as activation of the AKT and ERKK1/2 signalling pathways as well as inhibition of caspase-3 activity[199]. IL-6, a cytokine produced by CAFs, induced an upregulation of CXCR7 in OSCC cell lines, and was responsible for IL-6 mediated cisplatin resistance via the STAT3-NFkB signalling pathway[200].

Antimetabolites – 5FU and capecitabine

Antimetabolites act through inhibition of DNA and RNA synthesis, therefore over- or under-expression of any enzymes involved in the 5FU metabolism pathway such as thymidylate synthase (TS) or methylenetetrahydrofolate reductase (MTHFR) confer 5FU resistance, by reducing components for 5FdUMP binding or increasing 5FU catabolism to inactive metabolites and reduce cytotoxicity. Langer *et al* had analysed mRNA levels of TS, MTHFR and MDR1 of 21 OAC patients treated with NAC of cisplatin and 5FU chemotherapy, and found that downregulation of TS and MDR1 mRNA expression levels after chemotherapy were associated with tumour response[219]. Joshi *et al* had also found that a higher expression of TS was predictive of lower overall survival.[212] In addition, higher expression of MTHFR was associated with better pathological responses[208].

Anthracyclines – epirubicin, doxorubicin

AXL overexpression augmented epirubicin resistance in OAC cell lines, which became re-sensitised when AXL was genetically knocked down. It was discovered that AXL generated transcriptional upregulation of c-MYC, which encouraged epirubicin resistance via activation of the AKT/β-catenin signalling pathway, and when AXL was inhibited in xenograft mouse models in the presence of epirubicin treatment, it suppressed tumour growth and proliferation[220].

Taxanes – paclitaxel, docetaxel

High expressions of multidrug resistance protein 1 (MDR1) was noted in OSCC to be involved in paclitaxel resistance[221]. Otherwise known as ABCB1 or P-glycoprotein, MDR1 is usually expressed and distributed extensively in the intestinal epithelium. Similar to ABCC and ABCG2, they are ATP-binding cassette transporters located in cell surface membranes and actively efflux drugs such as etoposide, doxorubicin, paclitaxel and vinblastine out from cells by ATP hydrolysis. Overexpression of these receptors result in a decreased intracellular concentration of chemotherapy, thus minimising tumour cell killing and creating multi-drug resistance[222]. A correlation was demonstrated between MDR1 expression and chemoresistance to combination treatment[209].

Other mechanisms

Fareed *et al* reported that VEGF overexpression was linked with resistance to chemoradiotherapy treatment in oesophageal cancer[120]. Angiogenesis in tumour progression is haphazard and unstructured, resulting in incompetent blood vessels and a reduction in lymphatics. This increases the interstitial fluid pressure and may inhibit drugs diffusing into the tumour[136]. Hypoxia, on the other hand, initiates the HIF-1 pathway and generates tumour angiogenesis, which in turn activates VEGF. HIF-1α was noted in OSCC to be associated with resistance to chemoradiotherapy when over-expressed, and that 44.4% of those negative for HIF-1α had a complete response to therapy[223].

MMPs can also act to change vascular permeability and alter drug delivery[224]. However, hypoxia may alter the phenotype of the tumour and reduce drug delivery into the tumour[136]. In addition, MMPs and collagens, fibronectin and laminins was found to be significantly increased in OSCC, which upregulated the MEK-ERK and PI3K/Akt signalling pathways, and increased resistance to cisplatin, 5FU and epirubicin. With siRNA inhibition of these molecules, chemosensitivity was increased by 30-50%[225].

Gene expression profiling performed by Luthra *et al* had paved the way for stratification of oesophageal cancer, into 2 molecular subtypes associated with pathological responses. She had segregated 19 patients with a combination of OAC, OSCC and 1 case with adenosquamous carcinoma who were treated with CRT before surgery. Her group had discovered that patients classified into subtype II had partial pathological responses, with downregulation of the apoptotic pathway identified via pathway analysis[226]. In addition, downregulation of genes were linked with epidermal differentiation complex at chromosome 1q21 and was associated with resistance to chemotherapy in OSCC[226 227].

In summary, there appears to be a multitude of mechanisms by which the effect of chemoresistance can be exerted in oesophageal cancer patients. Depending on the chemotherapy agent used, consideration of inhibitor use should be included to tailor treatment, and modulate the chemosensitivity of the cancer cells and make them more susceptible to drug treatment.

1.4 Phosphodiesterase 5 inhibitors (PDE5i)

1.4.1 Rationale for consideration of PDE5 inhibitors

During my literature search on CAFs, I came across articles by Zenzmaier's group, who found that the phenotype of CAFs in prostatic stromal cells could be reverted with vardenafil and tadalafil, PDE5 inhibitors, and lessened cell proliferation[228 229]. This was also reflected in Catalano's study in a breast cancer cell line, where CAFs treated with PDE5i attenuated cancer cell proliferation and invasion. He also found that breast cancer cells had overexpression of PDE5, which had correlated with a lower overall survival[230].

Delving further into the relationship between PDE5i and chemoresistance, studies had indicated that PDE5 was associated with resistance to chemotherapy in cancer. Pratt and colleagues had suggested that the multidrug resistance protein 5 (ABCC5) had contributed to 5FU resistance in colorectal and breast cancers, which had a high PDE5 expression, through transportation of monophosphorylated metabolites[231]. Moreover, PDE5i was demonstrated to reverse multidrug resistance, mainly paclitaxel, by inhibiting the efflux transportation function[232].

Furthermore, Das *et al* investigated the effects of sildenafil on prostate cancer cells and found that the PDE5i had sensitized the cancer cells to doxorubicin through mechanisms which included augmentation of ROS generation, upregulation of caspase-3 and caspase-9, and decreased expression of Bcl-xL[233]. Their group also discovered that sildenafil enhanced the effects of doxorubicin through activation of the CD95 death receptor pathway to mediate apoptosis, and when knockdown of CD95 was instituted, this killing effect was abolished[234]. Chang *et al* also found similar results, but through impairment of a different pathway, the HR and NHEJ DNA repair systems[235].

On the other hand, Catalano *et al* had discovered a high expression of PDE5 in in breast cancer, and set about finding out its implications for cancer therapy[236]. Klutzny *et al* had found that PDE5i eliminated cancer stem cells in vitro using breast cancer cell lines via PKA signalling. In vivo, sildenafil was found to improve doxorubicin delivery and anticancer

activity in vitro and in a breast cancer mouse model[237]. PDE5i was also found to be involved in the mitochondrial-mediated death apoptosis pathway, and restored all biological markers to normal in vivo, together with inhibition of inflammatory markers[238].

Additionally, PDE5 has been found to be overexpressed in colorectal, bladder, lung, and head and neck cancers[239-242]. Tuttle *et al* had found that a high expression of PDE5 in all human HNSCC cell lines and that treatment with PDE5i induced apoptosis and made the cells less viable, and suggested this effect to be mediated by the cGMP-protein kinase G pathway[243]. PDE5i showed such promise that a Phase II trial carried out in HNSCC illustrated that PDE5i can reverse tumour-specific immune suppression[244].

There has been minimal information published about PDE5i in oesophageal cancer at present. Therefore, I wanted to investigate whether there was an impact of PDE5i use on OAC. This is in part related to one of the OAC cell lines I was using in my experiments, MFD1, which was found to have several mutations such as ABCB1, DOCK2, SEMA5A and TP53[245]. Articles about PDE5i use in drug repurposing suggested that sildenafil had reversed ABCB1-mediated chemoresistance and that vardenafil was a potent inhibitor of the ABCB1 transporter[246], both of which intrigued me and made me wonder if the MFD1 cell line could be more resistant to 5FU treatment. If so, this effect should be investigated to determine if it is attributable to the ABCB1 mechanism. Moreover, as we are still using epirubicin as part of our standard NAC, the effects mentioned earlier about sensitization of doxorubicin using PDE5i led me to consider if using PDE5i could influence a chemoresistant effect in OAC.

1.4.2 Structure of PDE5 enzymes, their inhibitors (PDE5i) and their actions

Phosphodiesterase (PDE) proteins are an important family of enzymes that regulate intracellular levels of AMP and GMP by hydrolysing cyclic adenosine 3,5-monophosphate (cAMP) and cyclic guanosine 3,5-monophosphate (cGMP). These latter molecules, that are membrane-bound or soluble in the cytosol, are second messengers that regulate physiological processes such as smooth muscle relaxation. They are categorized into 11 functional subtypes PDE1-PDE11 in mammals. They differ mainly in the selectivity of substrates they hydrolyse; for instance, PDE4, 7 and 8 are cAMP-specific, while PDE5, 6 and 9 are cGMP-selective, and PDE1, 2, 3, 10, 11 can hydrolyse both cAMP and cGMP[247].

The PDE enzymes are found in a variety of human tissues, however, we have chosen to look at PDE5 and their inhibitors as it appears to have an effect on fibroblasts[229]. The PDE5 enzyme has an active site for binding or catalytic actions at the junction of 3 functional domains: an N-terminal cyclin fold domain, a linker helical domain and a C-terminal helical

bundle domain. The active site has 3 regions based on its crystal structure: M site, Q pocket, and L region.

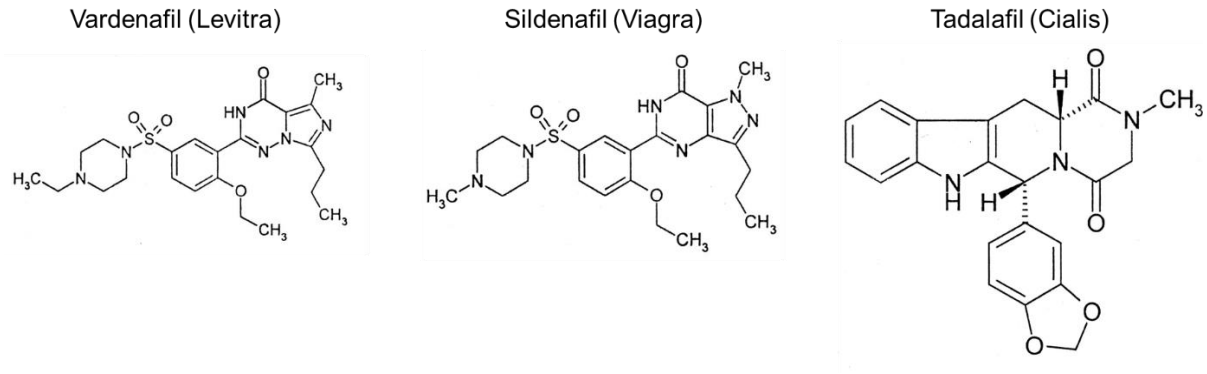

Figure 21. Molecular structures of PDE5 inhibitors in clinical practice (Images adapted from Wikipedia)

Inhibitors had been developed in the pharmaceutical industry to disrupt these enzymes and their subsequent actions. Currently, there are 3 PDE5 inhibitors (PDE5i) (sildenafil, tadalafil and vardenafil) in the market that have been used in various conditions (Figure 21)[248]. These medications currently used in clinical practice has been deemed safe and tolerated by patients. Side effects of the drugs include headaches (more than 10% of patients), flushing, dizziness, vomiting, dyspepsia, myalgia, nasal congestion, visual disturbances[249]. The action of the inhibitors include interaction between metal ions mediated through water, are involved with hydrogen bonding with the saddle of the Q pocket, and interact with the hydrophobic residues that line the cavity of the active site[248].

1.4.3 Current clinical usage of PDE5i

Erectile Dysfunction & Benign Prostatic Hyperplasia

PDE5 inhibitors have been licenced to be used in the UK for several conditions, one of which is treatment of erectile dysfunction. These inhibitors increase intracellular cGMP which in turn activates protein kinase G (PKG) and affects nitric oxide signalling, thereby causing smooth muscle relaxation and consequently, allowing for penile erection during sexual stimulation. PDE5i are normally taken as a single dose 30-60 minutes before sexual activity, with dosages varying between 10-20mg for vardenafil, 25-100mg for sildenafil, and 10-20mg for tadalafil. In addition, tadalafil is licensed to be taken for benign prostatic hyperplasia at 5mg once a day[249].

Pulmonary Arterial Hypertension

Pulmonary arterial hypertension occurs when there is increased pulmonary artery pressure (greater than 25 mmHg), and can be caused by a number of reasons, such as left sided heart disease, lung disease, chronic pulmonary emboli, and sarcoidosis, amongst others. As PDE5 is highly expressed in the smooth muscle cells of the lung vasculature, PDE5i are potent pulmonary vasodilators which increases pulmonary blood flow and inhibit vascular remodelling. Its mechanisms of action are through the cGMP-NO signalling pathway as well as natriuretic peptide-cGMP pathway[250]. Currently, sildenafil and tadalafil are licensed for use in the UK, and dosages vary from 20mg thrice daily for sildenafil or 40mg once daily for tadalafil [249].

Cardiovascular disease

PDE5 in present in vascular smooth muscle and in human heart tissue. In rabbits with ischaemia/reperfusion injury, sildenafil had decreased infarct size and maintained cardiac output, as it reduced aortic pressure through vasodilation and lowering arterial resistance. In humans who have experienced a myocardial infarction, treatment with PDE5i such as sildenafil or tadalafil improved their cardiac functional capacity and decreased the likelihood of heart failure worsening, as the right ventricular pressure is lessened. If taken long-term, cardiac hypertrophy may be reversed, as it reduces chronic pressure overload[247].

Diabetes & neurological disease

Diabetic patients more often have serum hyperglycaemia, which is associated with an increase in tissue inflammation, endothelial dysfunction and oxidative stress in the myocardium. Treatment with 50mg sildenafil daily for a month improved endothelial function and decreased albuminuria. When treating with tadalafil, it also suppresses production of reactive oxygen species (ROS)[247]. Lastly, studies have shown that tadalafil treatment for diabetic mice decreases TNF-α and interleukin (IL)-1β, and increases IL-10 which is an anti-inflammatory cytokine[251].

Raynaud's phenomenon

There has been a number of trials that have used PDE5i to treat Raynaud’s phenomenon, which is associated with systemic sclerosis and can lead to digital ulceration. A meta-analysis demonstrated that treatment with PDE5i for at least a month was effective in decreasing the frequency, duration and severity of attacks. There was also improved pain scores and a reduction in disability[252].

1.4.4 Mechanisms of action of PDE5 inhibitors

PDE5i have an effect on multiple pathways. The action of PDE5 enzymes is to hydrolyse cGMP to inactive 5'GMP. When blocked by a PDE5i, the concentration of cGMP increases in the body, which phosphorylates PKG and activates the enzyme, which in turn, activates a cascade of pathways that regulate a number of physiological functions such as alterations in vascular tone, smooth muscle relaxation, changes in endothelial permeability, and cell proliferation and differentiation[229 247 253]. It decreases serum calcium levels through stimulation of K^+-Ca^+ channels to effect smooth muscle relaxation[247]. It also induces caspase-dependent apoptosis in CLL cells[254]. Li *et al* and Das *et al* had found that PDE5i tended to reduce β-catenin levels, which downregulated cyclin D1 and survivin, which resulted in increased apoptosis[247 255].

Conversely, it can reduce ROS production, which decreased cell death[247]. The cascade also produces cytokines which affected cell proliferation and differentiation[251]. On a stromal basis, PDE5i enhanced NO/cGMP signalling and decreased proliferation of prostatic stromal cells[229]. It also affected the RhoA/ROCK pathway to regulate myofibroblast contraction[228]. Lastly, these inhibitors can also block the efflux functions of ABC transporters within the cell, which can be of use in chemotherapeutic treatments[256 232 257] (Figure 22).

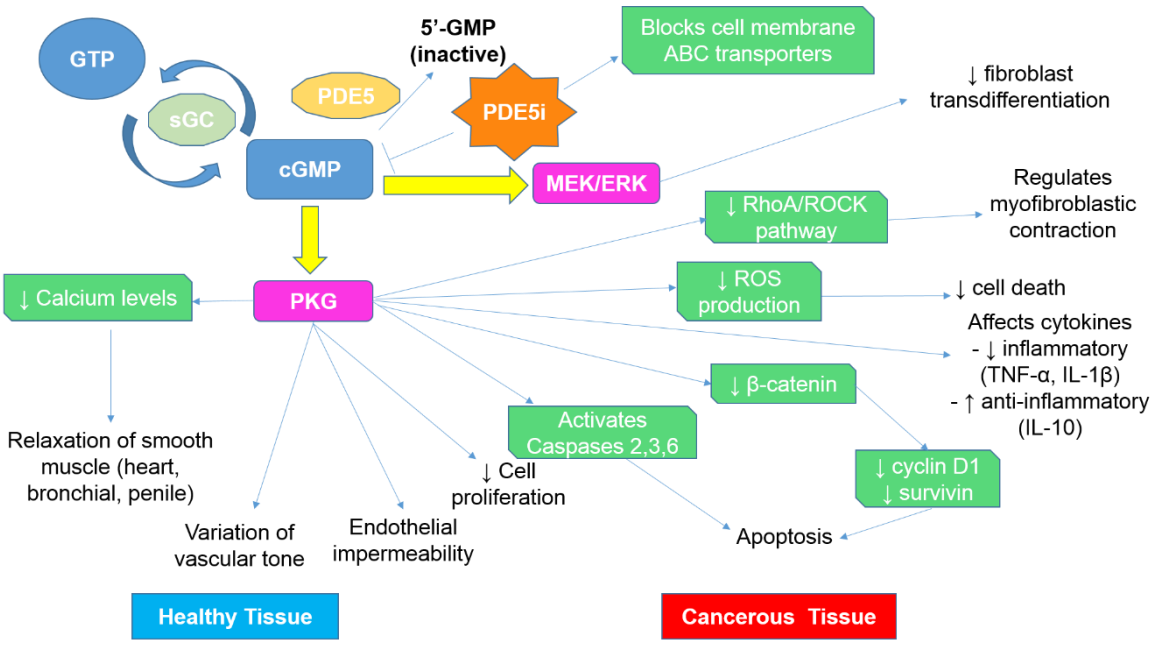

Figure 22. Multiple pathways of PDE5 inhibitor

1.4.5 PDE5 as a therapeutic target in cancer

It was reported that there is increased PDE5 expression in human carcinomas of the colon, thyroid, bladder, breast, prostate, pancreas, skin and lung, compared with normal tissues[247]. As such, it is believed that usage of PDE5i can be beneficial in the treatment of cancer for patients.

In the prostate, PDE5i were initially used to prevent and treat benign prostatic enlargement (BPH)[229]. Zenzmaier *et al* demonstrated that PDE5 was predominantly expressed in the prostatic stromal compartment, and that prostatic fibroblasts were induced by TGFβ1 to transdifferentiate to myofibroblasts. This induction of transdifferentiation can also be effected by nicotinamide adenine dinucleotide phosphate oxidase (NOX4) via the ROS signalling pathway[229]. NOX enzymes in humans reduce oxygen to hydrogen peroxide and are involved host defence or as signalling molecules[258]. However, PDE5 inhibition via the PKG and MEK/ERK pathways, decreased proliferation and transdifferentiation of prostatic stromal cells[229]. The transdifferentiation can also be reversed via the PI3K/AKT pathway when AKT is inactivated by phosphates[228].

High expression of PDE5 was noted in all human HNSCC cell lines. When treated with PDE5i, the cells became less viable and apoptosis was induced[243]. Phase II trials using PDE5i (Tadalafil) in HNSCC patients demonstrated inhibition of myeloid-derived suppressor cells and increased tumour-infiltrating cytotoxic T-cells, thus promoting anti-tumour immunity[244]. In thyroid cancer, high levels of PDE5 were found expressed in the tumour cells, compared with normal cells. It was found that PDE5i decreased cellular proliferation and migration of thyroid cancer cells[239]. This effect was also seen in colon cancer, where suppression of tumour cell growth was seen with PDE5i, thought to be via the β-catenin pathway[241].

In patients undergoing chemotherapy, PDE5i appeared to augment the effect of chemotherapy[247]. Through interactions with various agents, more ROS was generated, and there was increased autophagy and death receptor signalling, thereby potentiating pancreatic and bladder cancer cell death[247 254]. Moreover, PDE5i boosted the uptake of chemotherapy agents such as doxorubicin, gemcitabine or carboplatin into pancreatic and lung cancer cells[242 254]. In addition, PDE5i can affect the ABC transport channel function, such that an increase in cGMP concentrations intracellularly initiates a cascade of actions, as well as inhibiting the efflux functions in cancer cells, so that drugs such as paclitaxel or vinca alkaloids act to increase cancer cell sensitivity, both of which lead to apoptosis[253 256].

All these show that PDE5 is a potential target in cancer treatment, especially if it involves chemotherapy. Little is currently known in the literature about the expression of PDE5 in the

oesophagus. Cowie (2018) had demonstrated that PDE5 was expressed in both normal and oesophageal adenocarcinoma tissue, predominantly in the stromal compartment, while there was no expression in the normal or cancerous epithelial cells. As such, PDE5i can potentially be used in oesophageal cancer to sensitise cancer cells prior to chemotherapy treatment.

1.5 Aims of the Study

Response to chemotherapy for majority of patients with oesophageal adenocarcinoma treated with curative intent is low and poses a major clinical problem, as that is the mainstay of treatment prior to surgery. If pre-operative cytotoxic therapy has minimal effect for non-responsive patients, it has the risk of delaying surgery for this group of patients, who might subsequently have disease too advanced to cure. The tumour microenvironment has been proven to be crucial in numerous hallmarks of cancer, with cancer-associated fibroblasts (CAFs) being the biggest and one of the important components of the stroma. A prospective way forward could be to utilize CAFs and examine drugs that could potentially sensitize cancer cells to make them more susceptible to chemotherapy. This might enable them to respond sufficiently to cytotoxics and allow for improved outcomes for this group of patients.

The aim of this thesis is to investigate if CAFs influence chemoresistance in OAC, looking at chemotherapy response as a representation of chemoresistance.

The specific aims of the study were to:

- To determine if CAFs can promote chemoresistance in OAC

- To investigate if PDE5 inhibitors can increase sensitivity of OAC to chemotherapy

- To potentially understand the mechanisms by which PDE5 inhibitors can increase chemosensitivity

- To investigate the relationship between biomarkers specific to CAFs that are involved in chemoresistance and survival outcomes in OAC patients

Chapter 2 Materials and Methods

2.1 Tissue culture

2.1.1 General principles of cell culture

Cell culture is a technique that enables the proliferation of animal or human cells which has been grown in a nutrient medium for an extended period of time. It allows cells to be manipulated if required and provides a ready supply of DNA, RNA and proteins.

Routine cell culture was carried out in a laminar flow hood. All tissue culture reagents and media were stored in sterile containers at 4°C. Prior to use, media and reagents were placed in a water bath at 37°C. Cells were grown in a humidified environment of 5-10% CO_2 in incubators maintained at 37°C.

2.1.2 Oesophageal adenocarcinoma cell lines and growth requirements

Table 7. Oesophageal adenocarcinoma cell lines used in this study

Cell Lines	Origin
OE33	Adenocarcinoma of the lower oesophagus (Barrett's metaplasia), 73 year old female, Pathological stage IIA (UICC), poorly differentiated. Obtained from European Collection of Authenticated Cell Collections (ECACC).
FLO1	Distal oesophageal adenocarcinoma, 68 year old Caucasian male in 1991. Obtained from European Collection of Authenticated Cell Collections (ECACC).
MFD1	Distal oesophageal adenocarcinoma, 55 year old Caucasian male, who had neoadjuvant chemotherapy (Epirubicin, Oxaliplatin, and Capecitabine) and surgery. pT4N3(15/26)M0, Mandard score TRG 5. No Barrett's oesophagus. Patient died 7 months after surgery from recurrent disease. In-house cell line directly isolated from patient EN199-12.

Table 7 details the OAC cell lines that I had used for my experiments. All cell lines were maintained in logarithmic growth in a humidified cell incubator (HERA Cell, Heraeus) at 37°C with 5% CO_2 for OE33, and 10% CO_2 for FLO1 and MFD1 cells. Complete growth medium of Roswell Park Memorial Institute 1640 medium (RPMI) supplemented with 10%

w/v heat inactivated foetal calf serum (FCS), 2.0mM L-glutamine, 50IU/ml of penicillin (100 U/ml) and 50µg/ml of streptomycin was used for the culture of OE33 cells. Dulbecco's modified eagle medium (DMEM) supplemented with 10% w/v heat inactivated foetal calf serum (FCS), 2.0mM glutamine, and 50IU/ml of penicillin and 50µg/ml streptomycin was used for the culture of FLO-1 cells and MFD1 cells.

2.1.3 Primary fibroblast culture and growth requirements

Tissue from resected specimens of patients undergoing oesophageal cancer surgery at University Southampton Hospitals NHS Trust (UHSFT) were taken after obtaining written, informed consent. Appropriate ethical approval was received from the Southampton and South West Hampshire Research and Ethics Committee (REC09/H0504/66). The tissue was harvested and transported in serum-containing DMEM. To isolate fibroblasts, the tissue was cut into 2mm pieces and a single piece was placed in the centre of a six-well plate and placed in an incubator for a number of weeks. The explants were cultured in serum-containing DMEM.

Fibroblast cell lines used in this study were normal (NOF) and cancer-associated fibroblasts (CAFs) 612, 662 and 669 that had originated from cancer patients. Appendix A reports the demographics and clinical details of these patients that the fibroblast cell lines had originated from. They were grown in a humidified cell incubator at 37°C in 10% CO_2. Complete growth medium of Dulbecco's modified eagle medium (DMEM) supplemented with 10% w/v heat-inactivated foetal calf serum (FCS), 2.0mM glutamine, and 50I.U./ml of penicillin and 50µg/ml streptomycin was used for the culture of fibroblast cells lines.

NOFs and CAFs were extracted from the same patients using the outgrowth method, as described in the paragraph above. NOFs were taken from oesophageal tissue at least 10cm from the tumour. Demographic data of matched pairs of NOFs and CAFs used in this study are summarized in Appendix A.

2.1.4 Routine cell culture

Cells were grown as adherent monolayers in sterile cell culture flasks (25cm^2, 75cm^2 or 175 cm^2 Corning®) in a humidified incubator (5-10% CO_2) at 37°C, and media was changed to feed cells every 3-4 days until 80-90% confluence was achieved, usually 1-2 times a week. Cells were then passaged at a ratio of 1:4 to 1:8 depending on growth rate. Existing medium

was first aspirated, and the cell layer was then rinsed once with warmed PBS to remove remaining media and aspirated. Warmed trypsin (0.05% trypsin (w/v)/5mM EDTA, Invitrogen) was added and swirled around the flask to coat all cells, then left in the incubator for 5 mins at 37°C. Once the cells had detached from the plastic surface, an equal volume of serum-containing media was added to inactivate the trypsin and inhibit enzyme reaction. Aliquots of cell suspension was then added to new tissue culture flasks containing fresh serum-containing medium.

2.1.5 Production of conditioned media from CAFs and vardenafil-treated CAFs

Matched pairs of cancer-associated fibroblasts (CAFs) and normal oesophageal fibroblasts (NOFs) were used in the experiments. Both were plated in 6 well plates (100,000 cells/well) and left to adhere for 24 hours in 2ml of DMEM. After this time period, media was removed, cells were washed with PBS and aspirated, then 2ml of DMEM per well was added and left for 48 hours to produce conditioned media. Conditioned media was then collected, centrifuged at 1,000rpm for 5 mins and the supernatant is put into a new 50ml Falcon tube to be used immediately.

50μM of vardenafil was added to a 6-well plate, left to evaporate in the tissue culture hood, which was then dissolved with 1ml of PBS. It was then added to 1.5ml of DMEM containing 100,000 fibroblasts per well in a 6-well plate for 72 hours. The same steps were performed with methanol, which was used as a vehicle control. Media was then removed, fibroblasts washed with PBS, and fresh media replaced and left for 48 hours to produce conditioned media from vardenafil-treated fibroblasts (vCM).

Conditioned media (CM) was then collected and clarified by centrifugation at 1000 rpm for 5 mins. Fibroblasts adherent to the plate were counted and the concentration of CM normalised by the addition of serum-containing DMEM. Centrifugation allowed for the removal of debris and immediate usage of the CM reduced the likelihood of degradation of the fibroblast secreted fraction.

2.1.6 Storage and recovery of liquid nitrogen stocks

2.1.6.1 Cryopreservation of cells

Cells growing in log phase growth were added to a 15ml tube (BD Falcon) after trypsinization and centrifuged at 1,000rpm for 5 mins. The supernatant was removed and discarded. The remaining cell pellet was then re-suspended in foetal calf serum (FCS) containing 10% DMSO (Sigma-Aldrich®). One ml of cell suspension was pipetted into cryotubes in an insulated polycarbonate freezing container ("Mr Frosty", Nalgene®), and placed in the -80°C freezer overnight, before being transferred to -196°C liquid nitrogen for long-term storage.

2.1.6.2 Thawing cell stocks

Vials removed from liquid nitrogen were placed at room temperature for 5-10 mins. After thawing completely, the contents of the vial was pipetted into 15ml tubes (BD Falcon) containing 5ml of warmed serum-containing medium and centrifuged at 1,000 rpm for 5 mins. The supernatant was discarded and the cell pellet was re-suspended in complete growth medium and transferred to a cell culture flask (25cm^2 Corning®) containing fresh medium. Once it is confluent (usually after 24 hours), it is then trypsinized and transferred to a bigger cell culture flask (75cm^2 Corning®), and subsequently to a large flask (175cm^2 Corning®), usually after 48-72 hours. Cells retrieved from long-term storage were routinely cultured for 1-2 weeks before being used in experiments.

2.1.7 Cell counting

After cells have been centrifuged for 5 mins at 1000 rpm, 21 degree Celsius, the supernatant is aspirated, and the cell pellet is re-suspended in 1ml of media. A coverslip was placed on the middle of the haemocytometer (BLAU BRAND, Neubauer, Germany). 20µl was placed on the haemocytometer by allowing a drop held at the end of the tip to be taken under the coverslip by capillary action. The haemocytometer was then placed on the stage of the microscope, and the grids were located. A 1 mm^2 area (a quadrant) was then counted to give between 50 and 500 cells/mm - if there were too many cells the sample was diluted. Cells were counted in a total of four different quadrants, added together and divided by 4, then multiplied by 10,000. This gives the number of cells per ml.

2.2 Antibodies and reagents

Antibodies and reagents (including inhibitors) used in this study are detailed in Appendix B.

2.3 Analysis of cellular proteins

2.3.1 Western blotting

2.3.1.1 Cell lysis

Cells were washed once with warmed PBS and trypsinized at 37°C for 5 mins. An equal volume of serum-containing medium was added to quench the trypsin. The cell suspension was then transferred to a 15ml BD Falcon and centrifuged at 1,000rpm for 5 mins at 4°C. The supernatant was aspirated and the cell pellet was re-suspended in 1ml of PBS in a micro-centrifuge tube, then centrifuged at 80,000G for 4 mins at 4°C. The supernatant was aspirated off and the tubes kept on ice to reduce protein degradation.

20-50µL (depending on size of cell pellet) of Radio-immunoprecipitation assay (RIPA) buffer and 5µL of protease inhibitor (dilution 1:100, Calbiochem, Darnstadt, Germany) was added to each cell pellet, the mixture was vortexed for 10-15s, and the tubes were left on ice for 20 mins. It is then centrifuged at 80,000G for 5 mins at 4°C. The supernatant was then transferred to a new microcentrifuge tube and stored at -20°C for future use.

2.3.1.2 Estimation of protein concentration

Protein concentration was determined by using the Bio-Rad Protein Assay Dye Reagent Concentrate (Bio-Rad Laboratories Ltd, Munchen, Germany) according to the manufacturer's instructions. This is a colourimetric assay based on the method by Bradford (Bradford 1976 ref), where it is based on a colour change of Coomassie brilliant blue G-250 dye, of which the dye binds to primarily basic (particularly arginine) and amino acid residues. A blue colour develops, which is read on a spectrophotometer at an absorbance of 595nm. Bovine serum albumin [(BSA), Sigma-Aldrich®] protein standards were set up at protein concentrations of 0, 125, 250, 500, 750, 1500, 2000, 4000 and 5000µg/ml.

250µl of BioRad assay, prepared in a dilution fraction of 1:5 with deionized water, is pipetted into a 96-well plate. 1µl of protein lysate is mixed into the assay (in triplicate), and the plate was read at 590nm absorbance on the Varioskan® Flash (Thermo Fisher Scientific, Finland). The concentration of the unknown proteins was then quantified against the standard curve using Microsoft Excel.

2.3.1.3 Sodium dodecyl sulphate polyacrylamide gel electrophoresis (SDS-PAGE)

Proteins are separated using a 1.5mm thick polyacrylamide gel mounted on a vertical gel electrophoresis system. Separating gels are prepared according to the desired percentage of acrylamide gel required (Appendix C). The gel was poured into the gel cassette and covered with deionized water to eliminate the air interface, and left to set for 30 mins. The excess water is then poured away, and a stacking gel is then pipetted onto the separating gel, a 10- or 15-well comb was inserted and left to set for another 30 mins.

The gel was placed in the electrophoresis tank and the chamber filled with running buffer (Appendix C). Lysate samples were prepared by diluting it with 15µl of loading dye/DTT (ratio 1:10), heating it at 95°C for 5 mins, the contents were then vortexed and placed on ice. Samples were loaded in the polyacrylamide gels together with a reference ladder (Broad Range Marker, sc-2361, Santa Cruz), using capillary disposable pipette tips. Electrophoresis was performed at 180-200V, 400mA in running buffer for 50-60 minutes, until the dye reached the bottom of the gel, indicating that there was sufficient protein migration. The gel was then removed and equilibrated in transfer buffer (Appendix C).

2.3.1.4 Immunoblotting

The gel was then transferred to a nitrocellulose blotting membrane (Whatman plc, Kent, UK), and sandwiched between 2 chromatography filter papers and sponges, compressed in a Bio-Rad transfer cassette, and immersed in approximately 500ml of transfer buffer. Proteins were transferred onto the membrane at 100V, 400mA for 90-120 mins. After protein transfer had been completed, the membrane was placed into a 50ml BD Falcon tube and blocked with 5ml of 5% fat-free milk (Appendix C), to block non-specific proteins, at room temperature for 1 hour on an automatic roller for gentle agitation.

The blot was washed 3 times with 5ml of PBS/Tween (Appendix C) for 5 mins each time. Depending on the primary antibody, the blot was then incubated with the primary antibody at the desired concentration in blocking solution overnight at 4°C on an automatic roller, for signal amplification. The next morning, the blot was washed 3 times again, 5 mins each time, with 5ml of PBS/Tween before incubation with the appropriate secondary horseradish peroxidase-labelled (HRP) antibody (Appendix B) for 1 hour at room temperature on an automatic roller. The blot was washed again 3 times (5 mins each) with PBS/Tween and bound antibody was detected using chemiluminesence (SuperSignal™ West Pico, Thermo Fisher Scientific Inc., Rockford, USA) or enhanced chemiluminesence (SuperSignal™ West Femto, Thermo Fisher Scientific Inc., Rockford, USA), with images being collected by a CCD camera (ChemiDoc-it™ Imaging System, UVP, USA), using the UVP Software

Program. Blots were probed using HSC-70 (Appendix B) as a loading control. Subsequent re-probing of membrane for other proteins required the blot to be washed with 5ml of stripping buffer, 5-10mins at room temperature, before being washed twice with 5ml of deionised water, 5 mins at room temperature, then thrice with 5ml of PBS/Tween, 5 mins each time, before incubation with another primary antibody. Exposure of blots were then quantified by open access densitometry software Image J (National Institute of Health, USA).

2.3.2 Flow cytometry (FACS analysis)

Fluorescence-activated cell staining (FACS) is a fast, objective, quantitative method to sort cells based on the specific light scattering and fluorescent characteristics of each cell. Light is scattered in a forward or sideways direction when it hits cells. Forward scatter (FSC) is proportional to the surface area or size of the cell, while side scatter (SSC) is related to the granular content of the cell. Although every cell is different, FSC and SSC will be similar between cell types, therefore cell types of interest can be selected through gating, so as to allow further analysis of the gated population. The range over which a fluorescent compound can be excited is termed its absorption spectrum. Occasionally, there can be spillover from one channel into another, causing falsely positive identified signals. To adjust for this occurrence, compensation, which is a procedure that isolates the signal from one particular channel from other channels, is performed prior to a set of experiments. After experiments are performed, the data is analysed with FlowJo® (Version 10, USA).

Flow cytometry was performed on mixed populations of CAFs/epithelial cells and spheroids after various drug treatments. Media was aspirated out of each well and 100µl trypsin was added to each well and left in the incubator at 37°C for 5-10 minutes. All the spheroids with the same treatment were pipetted into a FACS tube and washed with 1ml of FACS buffer at 4°C for 5 mins at 1500 rpm. The excess FACS buffer was tipped out and the cells were re-suspended in 100µl FACS buffer. Antibody was added to the solution at a 1 in 40 concentration, and left at room temperature for 20-30 mins in the dark. Control samples were labelled with IgG class-matched isotype (BD Biosciences™) (Appendix B), which acted as the negative control. Unlabelled controls (7AAD) used primary dye, and unstained cells were used as the negative control for these. Cells were then washed with 1ml of FACS buffer and spun at 1,500rpm for 5 mins at 4°C. The excess was tipped out and the cells were re-suspended in 200µl of FACS buffer. Labelled cells were scanned with the BD FACS Canto™II cytometer (BD Biosciences™), and the results were subsequently analysed using

FACSDiva software (BD Biosciences™). With each cell line, the same settings were used for each experiment.

CD90 antibody was used to label fibroblasts, to be visualized on the red fluorescence channel with the allophycocyanin (APC) fluorochrome, at excitation laser line 633nm. EpCam antibody was used to label MFD1 epithelial cells, to be visualized on the green fluorescence channel with the fluorescein isothiocyanate (FITC) fluorochrome, at excitation laser line at 488nm. 7-aminoactinomycin D (7AAD) staining solution is a highly fluorescent dye for identification of non-viable cells. It binds to DNA and therefore is excluded from intact cells, and when excited by the 488nm excitation laser light, 7AAD fluorescence is detected in the far red range of the spectrum (650nm long-pass filter), and is visualized on PerCP-Cy5.5 fluorochrome. Fixable Viability Dye eFluor®506 was used to irreversibly label dead cells, to be visualized on the Marina Blue fluorescence channel, at excitation laser line 405nm up to 506nm.

2.4 Dose-response curves

2.4.1 Production of conditioned media

Conditioned media for these assays was produced by plating 100,000 fibroblasts in each well of a 6-well plate, topped up with 2ml of normal media in each well. They were left overnight and media was replaced and left for a further 48 hours. This was then aspirated from the plates, spun down with 1,000rpm at 21 degrees for 5 mins, and placed into 15ml fresh tubes (BD Falcon).

48 hours into plating the fibroblasts, 1000 MFD1 cells were added to each well of a 96-well plate with 100µl of normal media and left to adhere overnight. The media was removed and cells were washed with PBS once. Normal and conditioned media containing chemotherapy agents, made to a total of 100µl, was added to each well and left for 4 days.

All drug concentrations were tested in triplicate, with the drug being diluted in media in a separate 96-well plate to obtain 2X the top concentration, eg. 1/50 dilution (1/100 final dilution). Serial dilutions were then carried out to obtain the desired concentrations for each drug. 50µl of each dilution was then added in triplicate to the cells already plated in 50µl in a 96-well plate the day before.

2.4.2 Cell Proliferation assay

Cell viability was assessed by a colourimetric method using the CellTitre96® Aqueous Non-Radioactive Cell Proliferation Assay (Promega, Southampton, UK). The assay consists of solutions containing a tetrazolium compound, MTS [3-(4,5-dimethylthiazol-2-yl)-5-(3-carboxymethoxyphenyl)-2-(4-sulfophenyl)-2H-tetrazolium], and an electron coupling reagent PMS (phenazine methosulfate). Mitochondrial dehydrogenase cleaves the tetrazolium rings of thiazolyl blue tetrazolium bromide (MTT, Sigma) to form dark blue formazan product that is soluble in tissue culture medium. The level of formazan product of which absorbance is at 490nm is directly proportional to the number of viable cells. Both were combined and divided into 1ml aliquots in an unlighted tissue culture hood before being stored at -20°C.

According to the manufacturer's instructions of a dilution factor of 1:6, 2ml of the aliquots, was added to 10ml of normal media (RPMI) and 100 µl of this mixture was added to each well of a 96-well plate, using a multi-channel pipette, after media was aspirated out from each well. The plate was left in the 5% CO_2 incubator at 37°C for 2 hours, and the plate was read with Varioskan® Flash (Thermo Fisher Scientific, Finland) at an absorbance of 490nm.

2.4.3 IC50s

IC50, otherwise known as the half maximal inhibitory concentration, is the concentration of drug required to reduce response by 50%.

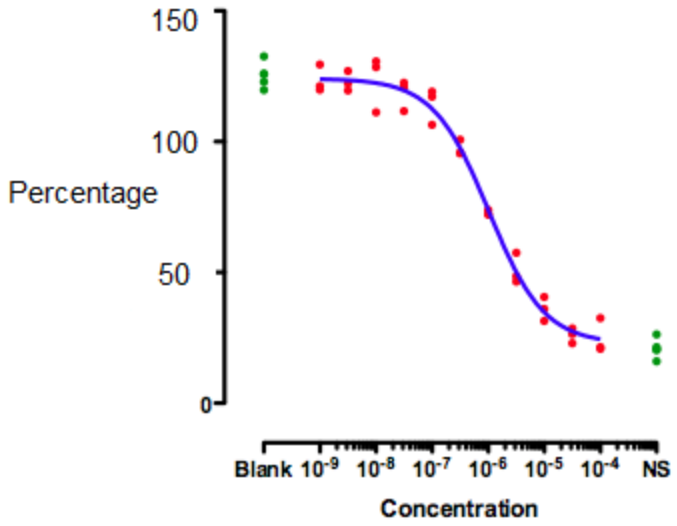

Figure 23. Example of IC50 dose-response curve

The values from the plate reader were entered into Excel. Deductions of values from wells without any cells were made from the original data, and then calculated as a percentage. For example, the growth inhibition in treated cells was expressed as a percentage of the untreated cells (control). The resulting data was then transferred into GraphPad PRISM (PRISM 7 for Windows, GraphPad Software Inc, San Diego, California) and IC50 curves were generated by the programme. After performing a number of repeat experiments, IC50s were obtained for each chemotherapy agent clinically used to treat oesophageal adenocarcinoma. These were then averaged out and plotted into histograms as standard error of means (SEM).

2.5 Colony Growth Assays

The clonogenic cell survival assay determines the ability of a cell to proliferate indefinitely, thereby retaining its reproductive ability to form a large colony or a clone. It was described in the 1950s for the study of radiation effects. Cells from an actively growing stock culture in monolayer are prepared in a suspension by the use of trypsin, which causes the cells to detach from the substratum. The number of cells per millilitre in this suspension is then counted using a haemocytometer. From this stock culture, 500 cells are seeded into a dish, and the dish is incubated for about 2 weeks. Each single cell divides many times and forms a colony that is easily visible with the naked eye, especially if it is fixed and stained. All the cells that make up the colony are the progeny of a single cell. Sometime there are less colonies than expected, because of suboptimal growth medium, errors in counting the number of cells initially plated, and the loss of cells by trypsinization and general handling.

2.5.1 Plating of cells

500 MFD1 cells were plated in each well of a 6-well plate with 2ml of normal media and left overnight to adhere. Media was then removed, and replaced with either normal media, CAF-conditioned media (CAF-CM) or conditioned media from vardenafil-treated CAFs (vCM), in duplicate, in the presence or absence of chemotherapy agents. The conditioned medium from CAFs and vardenafil-treated CAFs had been treated with 50μM Vardenafil/Methanol for 72 hours prior to change of media and the supernatant collected by centrifugation at 1,000rpm for 5mins before being used on colony growth assays. The fibroblasts were then counted and the supernatant diluted with normal media for normalization of media according to concentration of CAFs and vardenafil-treated CAFs.

Conditioned medium was placed for the first three days, then replaced after 3 days with normal media. After 12 days, all media was removed, the wells were washed with PBS, and placed in 500µl of 100% methanol and left on ice for 5 mins to fix cells.

2.5.2 Staining of cells

After fixing the cells with methanol on ice, the methanol was removed, and the wells were washed again with PBS. 100µl of 10% crystal violet was pipetted into each of the six plates, and is left on ice for 10 mins. The stained plates were then rinsed with sterile water (the used stain is collected in a bottle dedicated to spent stain) until all the plates had been stained. The plates were then left to air-dry overnight.

The following day, the colonies in each dish were viewed under a microscope. A cluster of blue-staining cells is considered a colony if it comprised at least 25 cells. The colonies were counted manually and the mean calculated. They were also imaged with the 3UV™ Transilluminator machine (GelDoc-It™ Imaging Systems, UVP, USA), using the UVP Visionworks LS Image Acquisition & Analysis Software, with exposure time of 252-554ms to obtain optimal images.

In addition, the crystal violet was dissolved in 200µl of 100% methanol in each well and 50µl of the dissolved solution is plated in triplicate in a 96-well plate and read with the Varioskan® Flash at an absorbance of 590nm to give a quantitative analysis. It is calculated as a percentage of survival of untreated cells in normal media, which acted as controls, and plotted using histograms on GraphPAD PRISM.

2.6 Spheroids

Three-dimensional (3D) culture systems are of increasing interest in cancer research since tissue architecture and the extracellular matrix (ECM) significantly influence tumour cell responses to microenvironmental signals. 3D cultures reflect better the in vivo tumour microenvironment in terms of cellular heterogeneity, nutrient and oxygen gradients, cell-cell interactions, matrix deposition and gene expression profiles.

Tumour spheroids are heterogeneous cellular aggregates that, when greater than 500µM diameter, are frequently characterized by hypoxic regions and necrotic centres.

3-dimensional spheroid co-culture assay was developed to investigate the impact of stromal cells on the epithelial cancer cells. Typical two-dimensional assays do not account for the

presence of extracellular matrix that is present around the stromal and tumour cells in vivo and therefore cellular behaviours within these cultures may be non-physiological. This spheroid assay was developed to attempt to replicate more closely the environment that is present around the oesophageal cancer stromal and tumour cells in actual tumours.

2.6.1 Composition & Treatment of spheroids

A total volume of 20,000 cells in 100µL was used to form spheroids in each well - 20,000 MFD1 cells, 20,000 fibroblasts, or 15,000 MFD1 cells and 5,000 CAFs were used in each well to create spheroids. These cells were left for 24 hours in ultra-low attachment (ULA)/low adherent 96-well plates (Corning®) to form spheroids.

They were initially treated with individual chemotherapy agents (Cisplatin, Carboplatin or 5FU) in 100µL making a total volume for 200µl. PBS was used as control for the untreated spheroids. The plates were left for 4 days in the 10% CO_2 incubator, after which the media was meticulously aspirated off and replaced in 100µl of combined MTS reagent per well and left in the 10% CO2 incubator for 4 hours. It was then read on the Varioskan® Flash machine at an absorbance of 490nm. The results were tabulated on Microsoft Excel and input into GraphPAD PRISM to determine the percentage of metabolically active cells.

Corresponding plates were also done for flow cytometry (FACS analysis) simultaneously, as per section 2.3.2, to determine the proportion of each cell type which were not viable.

2.6.2 Spheroids treated with chemotherapy and PDE5 inhibitors

To investigate the effect of PDE5 inhibitors on spheroids, the spheroids were plated and left for 24 hours, pre-treated with 100µM of vardenafil in 50µl of media, with methanol as vehicle control. Appropriate amounts of vardenafil and methanol were each placed in a well of a 6-well plate and allowed to evaporate in a tissue culture hood. The substrate in the well was then dissolved in PBS, and 50µl aliquots were placed in each relevant well of the 96-well spheroid plate. 24 hours after the first treatment of vardenafil, the spheroids were treated with individual chemotherapy agents (in the presence or absence of 100µM vardenafil or Methanol) in 50µl aliquots, making a total volume of 200µl per well.

After treatment for 4 days, media is meticulously and carefully aspirated out of each well, making sure spheroids are not aspirated out. Combined MTS reagent was placed in each well to determine cell viability. The plate was then incubated for 4 hours in the 10% CO2 incubator before being read with the Varioskan® Flash plate reader at an absorbance of 490nm. This was correlated with flow cytometry of similar corresponding plates.

2.7 PCR

2.7.1 RNA extraction, isolation and purification

Total RNA was extracted using an RNeasy Mini Kit (Qiagen Catalogue number 74104, Manchester, UK). The RNeasy procedure uses a highly denaturing guanidine-thiocyanate containing buffer on lysed and homogenized samples to inactivate RNases, then combines it with selective binding properties of a silica-based membrane using microspin technology, in the presence of ethanol as an appropriate binding condition. The sample is applied to an RNeasy Mini spin column where the total RNA binds to the silica membrane and contaminants are washed away, which in turn ensures purification of intact RNA.

Total RNA was extracted from cells in solution which have been centrifuged at 1,000 rpm for 5 mins with the supernatant discarded, or from cell pellets previously stored at -80°C. The cell pellets, totalling approximately 3-4x10^6 cells, were incubated at 37°C in a water bath until completely thawed. Cells were then disrupted by adding 350µL RLT buffer (high salt content) to the tissue culture plate, after the addition of 10µL of β-mercaptoethanol for further ribonuclease inhibition. The lysate was homogenized using the 3D Sonicator for 30s. The homogenized lysate was then transferred to a gDNA spin column, centrifuged for 30s at 8,000G (10,000rpm). The column was discarded and the flow-through was preserved, where 350µl 70% ethanol was added and mixed with pipetting. Up to 700µl of the lysate was then transferred to a RNeasy spin column and centrifuged at maximum speed (13,300 rpm) for 15s at room temperature to allow binding of RNA to the silica column. Flow through was discarded and 700µl RW1 buffer was then added to wash the column, and the centrifugation step was repeated. Next the column was washed with 500µl RPE buffer twice, centrifugation was repeated and flow-through was discarded. The column was then transferred to a new 1.5ml collection tube and the RNA was eluted with 30µl of RNAase-free water onto the RNeasy silica gel membrane. The tube was closed and centrifuged for 1 minute at 8,000G (10,000rpm). RNA was then quantified and stored at -80°C in aliquots.

2.7.2 Nucleic acid quantification

mRNA and cDNA quantification was performed using a Nanodrop 1000 Spectrophotometer (Thermo Scientific, UK)

1µl of deionized water was pipetted onto the pedestal and used as a reference marker to calibrate the spectrophotometer. It was then wiped clean with soft tissue. 1µl of DNA or

RNA was used for each sample reading, and the pedestal was cleaned thoroughly between samples. DNA and RNA samples were quantified in ng/µl, with 260/230 and 260/280 ratios being recorded to determine DNA and RNA quality respectively. DNA samples were considered to be satisfactory when the 260/280 ratios (absorbance of nucleic acid/absorbance of protein) were 1.8-2.0. RNA samples were considered to be satisfactory when the 260/230 ratios (absorbance of nucleic acid/absorbance of salts, solvents and protein) were 1.8 – 2.2. For cDNA samples, the 260/280 ratio of 1.8-2.2 was considered to be satisfactory.

RNA samples were then frozen at -80°C and cDNA stored at -20°C, ready for use as RT-PCR templates.

2.7.3 Reverse transcriptase polymer chain rOACtion (PCR) for cDNA synthesis

Template complementary DNA or copy DNA (cDNA) was obtained by reverse transcription of 1µg of RNA using a High Capacity cDNA Reverse Transcription Kit (Applied Biosystems). Reverse transcription PCR was done on 1µg of total RNA with incubations performed in a Techne Flexigene Thermal Cycler (Cole-Parmer, Staffordshire, UK). A short sequence of deoxy-thymine nucleotides [Oligo (dT)] is tagged as a complementary primer to the poly-A tail and provides a free 3'-OH end that can be extended by reverse transcription.

1 µl of Oligo $(dT)_{12-18}$ (500 µg/ml), 1µg of RNA and 14µL of nuclease-free water, and 1 µl of dNTP mix (10 mM mix of dGTP, dTTP, dCTP, dATP) were added to a 0.2 ml nuclease free microcentrifuge tube. The mixture was heated to 70ºC for 5 mins then quickly chilled on ice. This rOACtion denatures and incubates the RNA with the Oligo (dT) primer and as the mixtures are chilled, the primer anneals to the RNA.

10µl of RT Mastermix was added to the sample. The mastermix was made up of 5µl Buffer, 1.25µl 10mM dNTP mix, 0.625µl RNasin enzyme, 1µl M-MLV enzyme, and 2.125µl of water. The contents were mixed gently and incubated at 42ºC for 60 mins, to enable the reverse transcription reaction. It was then incubated at 95°C for 5 mins to inactivate the reaction, and held at 4°C. 75µl nuclease-free water was added to cDNA to make a total volume of 100µl, and this first-strand cDNA template was stored at -20°C.

2.7.4 Taqman quantitative real-time PCR (qRT-PCR)

QRT-PCR is a technique to quantify a specific sequence in cDNA so as to quantify gene expression as it is amplified by PCR in real time. The Taqman system uses a primer and probe complementary to the gene of interest. The oligonucleotide probe is labelled with a fluorescent reporter label on the 5' end and a quencher molecule on the 3' end. While the probe is intact, the proximity of the quencher dye greatly reduces the fluorescence emitted by the reporter dye. During polymerisation the probe anneals downstream from one of the primer sites and as this is extended by Taq DNA polymerase, the reporter dye is cleaved. The cleavage of the reporter dye separates the reporter dye from the quencher dye and increases the reporter dye signal. The cleavage also removes the probe from the target strand allowing primer extension to continue. The quencher is cleaved from the probe by the exonuclease activity of the polymerase when the chosen cDNA is copied during the PCR cycle, allowing an increase in fluorescent signal. The change in fluorescence is directly proportional to the number of copies of cDNA present and is measured at each cycle of the PCR. Each PCR cycle allows primer annealing and primer extension with cleavage of further reporter dyes.

Reactions are quantified by the point in time during cycling when the fluorescence exceeds a given threshold. A Ct value is generated and refers to the number of cycles needed to generate a defined amount of fluorescence during the linear phase of PCR. Thus a high Ct value indicates less expression of the gene of interest. SYBR© Green I Assay was used, which is a fluorescent dye that binds to all double-stranded DNA. As a DNA fragment is cleaved, a decrease in fluorescent signal is observed at Tm (temperature required to separate 50% of double-stranded DNA). However, small differences in starting template may skew Ct values exponentially, therefore values are normalized to the levels of a control gene, eg. glyceraldehyde-3-phosphate dehydrogenase (GAPDH) or beta actin (β-actin), which is expressed in equal amounts in all cells, so that it corrects for any variation in the original amount of total mRNA.

To establish the levels of phosphodiesterase 5 (PDE5) cDNA, α-SMA cDNA or control gene GAPDH cDNA in cells, qRT-PCR was performed with the AB7500 Real-Time PCR System (Applied Biosystems, Thermo Fisher Scientific, Finland) and the results analysed according to the standard curve method. Log cDNA concentration was plotted against Ct values for known amounts of cDNA (Universal Human Reference RNA, Stratagene, UK) and the equation of this standard curve used to calculate the amount of PDE5, α-SMA or GAPDH cDNA present in cells. C values represent the cycle number when the fluorescence of a sample increases above baseline fluorescence. The reaction then enters log phase, which signifies the quantity of the PCR product (fluorescence), and is directly proportional to the

input amount of cDNA. This is represented by the Ct value, which marks the number of cycles it took to reach this point.

Commercially available primers for PDE5A (Batch number: JN98217, Primer Design, Southampton, UK) and GAPDH (Batch number: JN98219, Primer Design, Southampton, UK) were used in the assessment of cDNA levels in cells (Appendix D). 5µl cDNA was suspended and made up to 50µl with nuclease free water and 50µl of Taqman universal PCR MasterMix (Catalogue number: PrecisionPLUS-LR-SY). The tubes were vortexed to ensure that the solutions were mixed and then centrifuged to eliminate bubbles. Each sample was loaded in triplicate into buckets and centrifuged for 1,200rpm for 1 min. The PCR plate was then sealed and loaded into the PCR machine.

The level of gene expression was compared between different cellular entities to endogenous controls using the delta delta Ct method.

$$\text{Target Gene Expression level/Fold change} = 2^{\Delta\Delta Ct}$$

$$2^{\Delta\Delta CT} = 2^{(\text{Ct of gene of interest (PDE5)} - \text{Ct of reference gene (GADPH)})_{\text{test sample}} - (\text{Ct of gene of interest} - \text{Ct of reference gene})_{\text{control sample}}}$$

2.8 Tissue Microarrays (TMA)

2.8.1 Database collection and refinement

A list of all oesophageal tissue stored in the Tissue Bank was obtained. Ethics approval was received from the Southampton and South West Hampshire Research and Ethics Committee (REC09/H0504/66). Rudimentary data existed on the list, and it served as a starting point in identifying all available oesophageal tissue within the Tissue Bank, and was updated meticulously by going through each label and updating it with patients' demographics, clinico-pathological and survival details. Clinico-pathological details consist of gender, performance status, body mass index, smoking status, stage at diagnosis, type of therapy, post-operative staging, TNM score and tumour regression grade (TRG) as a reflection of pathological response to chemotherapy, a system developed by Mandard *et al*[115]. Overall survival was measured from date of surgery to date of death or date of last follow-up, in the case of survivors. Recurrence was defined as time from operation to development of local, nodal or distant metastasis, whichever occurred first.

This list was cross-referenced with the upper gastrointestinal (UGI) database, which is a prospective database for all UGI resections that have been carried out at University

Hospitals Southampton (UHSFT) from 2005 onwards. The database was secured on an encrypted server with suitable back up facilities to ensure data was not lost.

The cohort of patients selected for the TMA are those who had undergone oesophageal resections from 2010-2015. They were chosen as this represented a modern series of oesophagogastric cancer patients who had undergone surgery only or neoadjuvant chemotherapy/chemoradiotherapy and surgery, which is the gold standard of treatment for curative oesophageal surgery currently in the world. All details were acquired from eQuest, UHSFT's results reporting system. The original pathology report was then acquired and subsequently pseudo-anonymized. This allowed the H&E slides to be located in the pathological archives of UHSFT.

The consistency of the data was checked in a number of ways - within data fields, clinico-pathological characteristics, mean, median, range and outlying data. The validity of the clinical data was checked by analysing its ability to produce known associations between clinic-pathological characteristics and survival.

2.8.2 Retrieval of slides and tissue blocks

Haematoxylin and eosin stained (H&E) slides from the cohort of patients selected were retrieved from the Histopathology Department at UHS as well as the Tissue Bank, together with their corresponding paraffin blocks. Blocks and slides sent away for trial purposes were requested back from those centres by the Tissue Bank. If H&E slides were not available, a re-cut of the slide was done from the original paraffin block.

2.8.3 Marking of slides

These H&E slides, which represent sections from multiple levels of resected tumour and lymph nodes, were reviewed by Consultant Histopathologist, Dr Eleanor Jaynes, and were marked for tissue microarray cores. The areas are marked in triplicate for tumour, stroma, and positive lymph nodes. Stroma was defined as collagen and cellularity combined, and was scored on areas surrounding tumour islands and areas with no corresponding tumour were ignored.

Corresponding blocks were then retrieved from the pathology archives of UHSFT. The H&E slides were placed on the blocks to allow marked areas to be identified on the donor block to be cored.

2.8.4 Construction of TMA

TMADesigner®2 (Version 1.0.0.12, Alphelys, France) was used to design the TMA, allowing for specification of grids, spot size, spot spacing, automatic calculation of spot positions in microns. For my TMA, a punch size of 1000µm was used, with a spot spacing of 1000µm.

Using the MiniCore®3 (Mitogen, Harpenden, UK), a core, 1mm in diameter and 3mm in length, is made into the recipient block. Triplicate cylindrical cores, of 1mm in diameter each, were physically extracted from the donor blocks of formalin fixed paraffin embedded tissue and transferred onto a new recipient paraffin block. This process is repeated until the TMA is finished. The TMA block is then placed in a 40 degrees oven overnight to assist in the wax adhering to the tissue cores, as it is helpful in reducing the number of cores lost when cutting sections for staining.

Figure 24. Tissue Arrayer Minicore®3 (ALPHELYS, France) for TMA creation

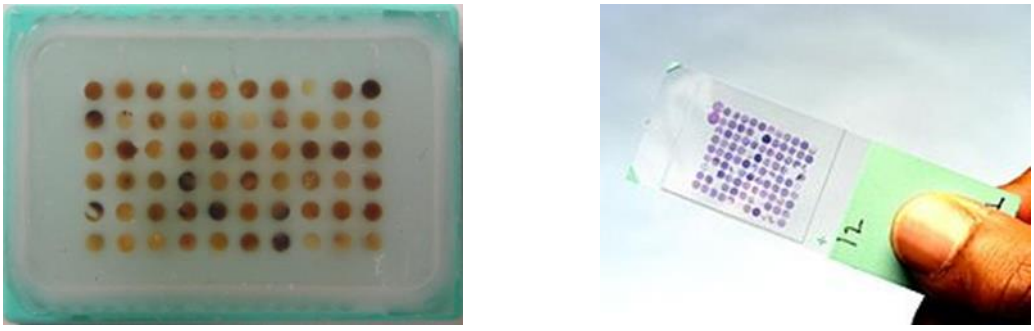

Figure 25. Appearance of TMA
Left - Appearance of TMA in paraffin. Right – Appearance after TMA has been cut with a microtome and stained with antibodies for immunohistochemistry.

TMAs were constructed for tumour, stroma and positive lymph nodes, which total 8 TMAs (3 tumour, 3 stroma, 2 lymph nodes).

A meticulous record of the positioning of the donor tissue was produced by the transfer of the pseudo-anonymized clinical data into the TMA designer® 3 software (Alphelys, France). Orientation spots were included to allow configuration of the TMA. Normal tissue from human kidney was included on the TMA to act as controls.

2.8.5 Biomarker selection

A biomarker is cellular, biochemical or molecular alterations that can be objectively measured and evaluated in biological media (eg. tissues, cells, fluids) as an indicator of normal biological processes, pathogenic processes or pharmacological responses to a therapeutic intervention. It can also be considered as key molecule or cellular events that link a specific environment exposure to a health outcome.

As such, biomarkers are used in combination to monitor and predict health states in individuals or across populations so that appropriate therapeutic intervention can be planned. The assessment of a typical biomarker in cancer helps in the development of therapies that can target the biomarker. This can minimize the risk of toxicity and reduce the cost of treatment.

Although biomarkers have advantages of objectivity and allowing precision of measurement, variability is a major concern. There are three aspects of measurement validity: 1) content validity, which shows the degree to which a biomarker reflects the biological phenomenon studied, 2) construct validity, which pertains to other relevant characteristics of the disease or trait, for example other biomarkers or disease manifestations, and 3) criterion validity, which shows the extent to which the biomarker correlates with the specific disease and is usually measured by sensitivity, specificity, and predictive power. Other factors which might impact on biomarker validity include measurement errors, differential bias (which tend to favour an association in either direction), cost, confounding factors that may later the measurement of the biomarker, and acceptability of the biomarker to the population being assessed.

These molecular targets have been selected for investigation based on results of a previous meta-analysis and systematic review of current evidence for clinically relevant prognostic biomarkers in oesophageal adenocarcinoma, and research interests of the laboratory team[259]. Areas of investigation were focused on interactions between tumour and surrounding micro-environment. These are explored in Chapter 5.

2.8.6 Immunohistochemistry

4 µm thick sections from the TMA were cut and mounted on positively charged SuperFrost (ThermoFisher Scientific) slides to aid in tissue adhesion. Slides were then dried at 60°C for approximately 20 minutes, which gets rid of excess wax.

Slides were labelled detailing the cohort, the antibody and concentration used, and length of incubation. Slides were then pre-treated with heat to 90°C for 20 minutes, before being rinsed in Envision™ FLEX Wash Buffer for 5-10 minutes. To prevent non-specific binding, blocking of endogenous peroxidase was performed at 20°C for 5 minutes. Most tissues will have endogenous peroxidase that will oxidise chromogen 3-diaminobenzidine (DAB), and lead to non-specific binding. DAB is oxidised by horseradish peroxidase to produce a brown substrate and signifies the antigen expression that can be visualised down the microscope. To block endogenous peroxidase activity, 300µl (per slides) of hydrogen peroxide was added at 20°C for 5 mins, prior to the antigen retrieval step.

After washing with wash buffer, 300µl of diluted antibody (Table 8) was then applied to the slides and incubated for 20 minutes. The slides were washed again and linker secondary rabbit antibody was applied for 15 minutes, so as to allow for greater dilutions of primary antibodies to be used whilst still achieving an interpretable level of staining. The slides were washed with wash buffer and HRP polymers were applied for 20 minutes. This polymer contained horseradish peroxidase conjugated to anti-Mouse/anti-Rabbit IgG attached to a sugar (dextran) backbone, and allows for visualization using DAB at a later time. The slides were then washed twice (5 minutes each) with substrate working solution, which has DAB chromogen in diluent, and that resulted in a brown precipitate localized around the polymer attached to the primary antibody. It was then rinsed with wash buffer counterstained with haematoxylin for 5 minutes, before being rinsed repeatedly to prevent the slides from drying out.

The staining was done with the Dako Autostainer, where all subsequent steps were automated on the equipment, except dehydration, clearing and mounting, so that there was standardisation and minimal variability between steps. Slides were removed from the machine and left in running water to blue the nuclei, then taken through an alcohol gradient to xylene by hand and mounted with pertex on a Leica coverslipper machine.

Table 8. List of antibodies used in IHC staining

Antibody	Supplier	FLEX Target Retrieval Solution (TRS)	Dilution
α-SMA	Dako	High	1:100
Periostin	Abcam	Low	1:500
Nestin	Abcam	Low	1:100

2.8.7 Scoring of TMA

Staining was scored by 2 surgeons, Professor Tim Underwood and Ms Clarisa Choh. Ideally, a pathologist would be beneficial in involvement of the scoring, however, they were unavailable during the specific period of time, therefore it was scored by 2 surgeons independently. Within each core, only representative relevant areas were scored under light microscopy. For immunohistochemical analysis of target molecules of interest, the staining intensity was scored on a scale of 1 to 3 (1=weak, <10% staining of area of interest; 2=moderate, 10-50% staining; 3=strong, over 50% staining). The TMA slides were also digitally scanned (Olympus dotSlide virtual microscopy system, University of Southampton) and images were saved in .tif files to aid in future clarification of scores if required.

As there were 3 cores for each sample, all cores were scored and averaged out to calculate the mean score. Methods of scoring the TMA cores included proportion of epithelial nuclei stained and the strength of the staining. For simplicity, the cores were scored only on the intensity of the stain.

2.9 Statistical analysis

Statistical analysis was performed using GraphPAD PRISM (Version 7 for Windows), Microsoft Excel (2013 edition), and IBM SPSS Statistics (Version 25).

P values

The *p* value is the statistical chance of a false positive occurring. By convention, the *p* value is set at <0.05, which means that the chance of a difference between groups occurring and being a false positive is less than 1 in 20. The null hypothesis occurs when no difference

exists between groups. When the null hypothesis is rejected because a true difference does not exist, a false positive has occurred, otherwise known as a type I error.

Analysis of clinico-pathological data of TMA patients

Clinico-pathological data from TMA patients were assumed not to have a normal distribution, so the data was represented with means and medians. Logistic regression was used to predict the probability that an event will occur, based on fitting the data to a logistic function. Multivariate analysis was performed to predict the probability of occurrence of an event by fitting data to a logistic function, and was used on associations of variables with an outcome.

Kaplan-Meier univariate survival analysis

Kaplan-Meier survival analysis was used to analyse the proportion of patients at risk of dying, which is calculated at regular time points, and is shown as percentage survival plotted against time as a curve. The curves were truncated at suitable time points based on the length of follow-up or patient death. This method is helpful as it allows analysis of incomplete data, for example, when patients are lost to follow up or when patients have died of the disease or other causes, and these patients are censored from subsequent analyses.

The Log rank test is used to determine if there is a statistical difference in survival between groups. This generates a total number of expected and observed deaths within groups using the life tables. This is then used to generate the log rank statistic, the *p* value for which is derived from referring to a chi-squared distribution table.

Cox proportional hazards model – multivariate survival analysis

Cox proportional hazards model, otherwise known as Cox's regression, is a form of multivariate analysis, and allows multiple variables to be simultaneously assessed to determine the size and interdependence of a relationship between variables.

The model generates a baseline survival curve and calculates the hazard ratio (HR) for a variable by measuring the effect of removing it and adding it to the model. Variables used in multivariate analysis include variables that are significant in univariate analysis. The size and interdependence of each variable's individual influence on overall and disease-free survival is determined. A HR of <1 means that an increase in the variable will predict an improved prognosis. A HR of >1 means that an increase in the variable, will predict a worse prognosis.

Parametric tests

Cells from the same cell line with difference passages were assumed to have normal distribution. Depending on the number of groups being analysed, a paired Student's t-test was used if there were 2 independent groups. If there are 3 or more groups, a one-way ANOVA test was used.

Chapter 3 Role of fibroblasts in tumour chemoresistance

3.1 Introduction & Aims

38% of patients with OG cancer are recommended a curative treatment plan. Of those, 31-43% of patients diagnosed with OAC have a curative treatment plan, usually consisting of neoadjuvant chemotherapy (NAC) and surgery, as NAC has been shown to increase survival by downstaging the primary tumour and lymph nodes[3]. Despite advancements in diagnosis, staging and treatment, survival rates are considerably lower than other solid cancers[5]. Despite the multitude of methods used to evaluate chemotherapy response, it has been demonstrated that response to chemotherapy is low at less than 40%[120].

The tumour microenvironment has been proven to be crucial in numerous hallmarks of cancer, with CAFs being the biggest and one of the important components of the stroma. Amongst other functions, they can secrete factors or be involved in cell-to-cell contact to influence OAC cells, such as to promote OAC tumour growth and cancer cell invasion[162]. Underwood & Hayden *et al* had also postulated that periostin, a CAF-secreted factor, was associated with chemoresistance in OAC, using FLO1 and OE33 cells[162].

OAC has a limited set of established cell lines, where there is minimal genomic information about the tumour of origin or how representative the cell lines are in relation to the primary cancer. Boonstra *et al* had undertaken a tremendous effort to verify all available 13 OAC cell lines and found that 3 cell lines actually originated from other tumour types[260]. The other 10 verified cell lines had no data for the matched primary tissue, only clinical information such as OE33 being derived in 1996 from a 73 year old female patient with stage IIa Barrett's cancer, while FLO1 was derived from a 68 year old Caucasian male with distal OAC. Beyond karyotyping and cell surface antigen phenotyping, it is unknown if the mutational burden of these cell lines was representative of the original tumour.

Therefore, in addition to OE33 and FLO1 cell lines in my experiments, I utilised a newly authenticated OAC cell line, MFD1, which has been proven to be stable over time and highly representative of OAC. This cell line had originated from a 55 year old Caucasian male with T3N1M0 OAC, who was treated with 3 cycles of neoadjuvant chemotherapy (Epirubicin, Oxaliplatin, Capecitabine), followed by oesophagectomy. Histopathological analysis of the specimen showed a ypT4N3 (15/26) M0 cancer with complete resection margins (R0), with no evidence of Barrett's oesophagus, and a Mandard score of TRG5. This reflected that the patient had an aggressive cancer and subsequently died 7 months after surgery from recurrent disease[245].

Genotyping of genomic DNA was performed on peripheral blood mononuclear cells (PBMC), tumour tissue and adjacent normal squamous epithelium, and two early passages of the MFD1 cell lines, as well as whole genome sequencing done from snap-frozen oesophageal tumour tissue and PBMC. MFD1 cells were also seeded and colonies were picked to identify mutations using Sanger sequencing. All these identified mutations in genes coding for ABCB1, DOCK2, SEMA5A and TP53, 2 of which are mutations common in OAC[261 262]. In vivo experiments revealed that MFD1 had the ability to form tumours in xenograft models that could respond to changes in the microenvironment[245].

The aim of this chapter is to investigate if CAFs can influence chemoresistance in OAC. This is first done by defining chemotherapy response in OAC cell lines, as a reflection of chemoresistance. Subsequent to that, conditioned media from CAFs was used to determine if CAFs have a role to play in affecting chemotherapy response.

3.2 Defining response to chemotherapy in oesophageal adenocarcinoma cell lines

There are various methods of defining response to chemotherapy. I have chosen to investigate the metabolic activity of cancer cells after treatment with chemotherapy, to determine its killing effect on the cells, as a representative of the cancer cell's response to chemotherapy.

Appendix E details a series of experiments to determine the appropriate time interval by which 50% of cancer cells die after treatment with chemotherapy. In essence, cells were plated for 24 hours, then treated with chemotherapy and left for 3 days, 5 days and 7 days, and were subsequently tested with MTT assays. It appeared that some of the dose-response curves on day 3 had not plateaued out, which meant that not all cells were killed completely by treatment. On the other hand, dose-response curves on days 5 and 7 had demonstrated a long plateau, which implied that majority of the cells were already dead, therefore did not require prolonged treatment. As such, 4 days was decided to be an optimum period for drug treatment. This was confirmed to be realistic and feasible with further experiments (Appendix E). Experiments were also performed to look at varying concentrations of chemotherapy drugs that could kill 50% of EAC cancer cell lines, and after several adjustments, the optimum concentrations were worked out to give a good range of drug concentrations, which were reproducible (Appendix F).

Figure 26 shows the results of my dose-response assays for 3 adenocarcinoma cell lines treated in normal media, with their corresponding IC50 chemotherapy drug dose. Those in normal media acted as controls for subsequent CAF-CM experiments.

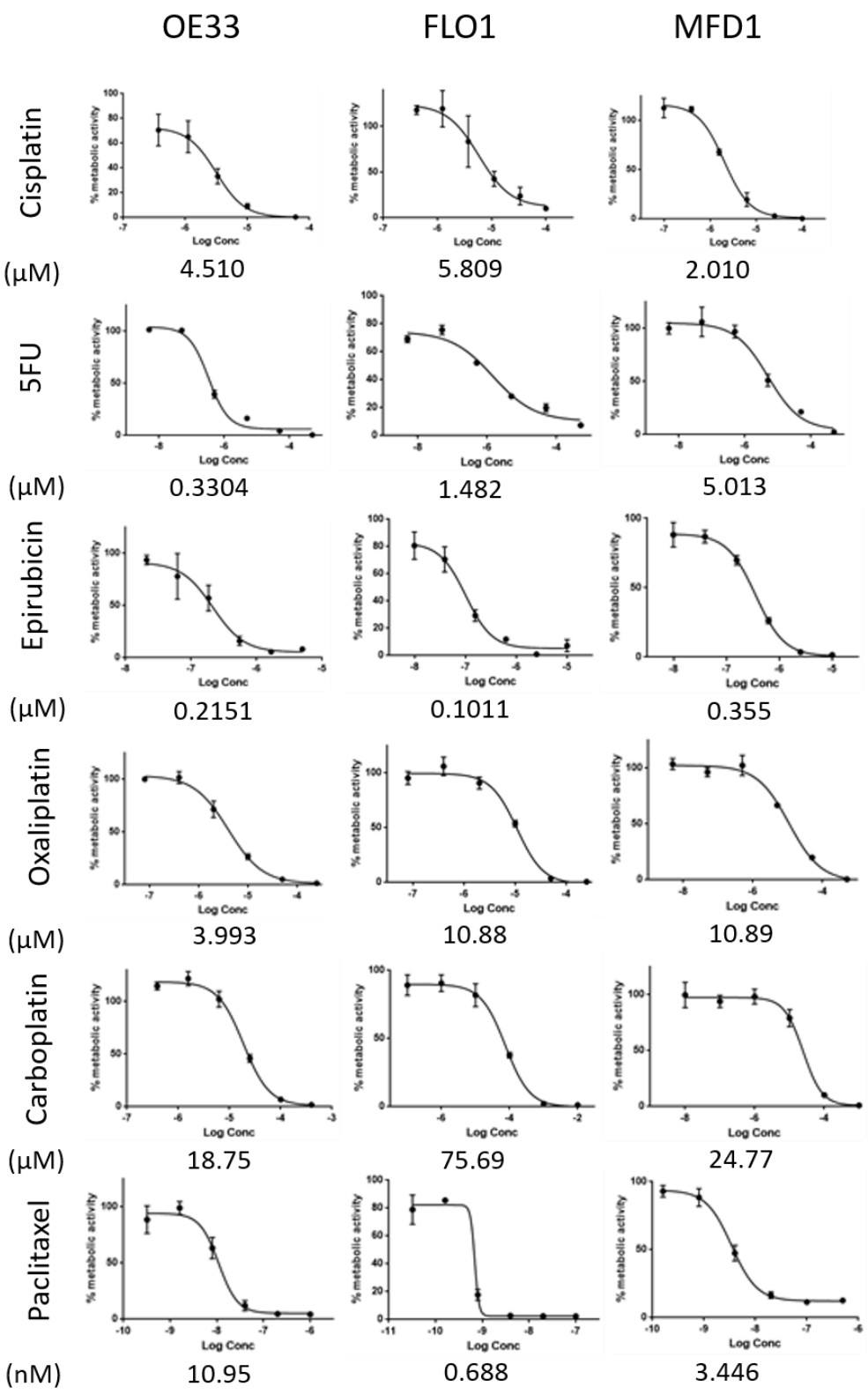

Figure 26. Representative dose-response curves of OAC cancer cells in normal media after chemotherapy treatment for 4 days.

IC50s were established for each cell line in normal media and acted as controls for subsequent experiments with CAF-conditioned medium

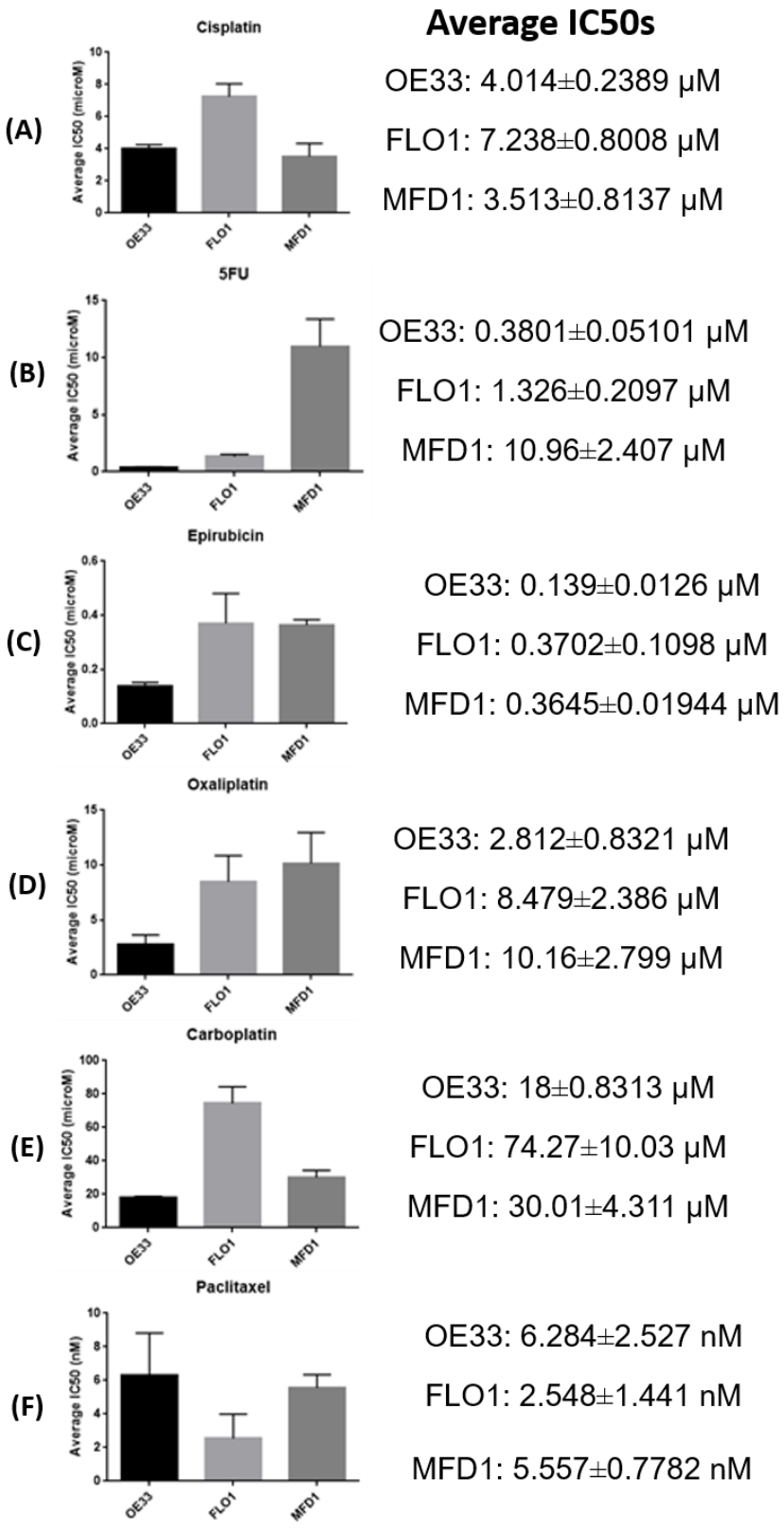

Figure 27. Histogram of average IC50s of individual OAC cell lines treated with chemotherapy drugs for 4 days.

This demonstrates that the FLO1 cell line appeared to be slightly resistant to the platinum compounds and epirubicin, while the MFD1 cell line appeared to be resistant to 5FU

Figure 27 shows a histogram of average IC50s after at least 4 repeats of each experiment per chemotherapy drug, all performed in normal media. It demonstrates that there is a slight resistance of the FLO1 cell line to platinum-based chemotherapy, mainly cisplatin and carboplatin. In addition, the MFD1 cell line appeared more resistant to 5FU treatment, compared to OE33 and FLO1 cell lines. OE33 appeared to be sensitive to 5FU, epirubicin, oxaliplatin and carboplatin, but resistant to paclitaxel, compared with the FLO1 and MFD1 cell lines.

I had expected the MFD1 cell line to be more resistant to epirubicin, 5FU and oxaliplatin, as this patient had received neoadjuvant EOX chemotherapy, yet had a Mandard TRG 5 tumour on resection, and had disease recurrence within the year. However it appeared to be resistant to 5FU only, and not the other 3.

This has to be contemplated with caution as further work needs to be done regarding how these concentrations correlate to plasma levels in patients, and whether it may potentially give side effects or be toxic for patients.

3.3 Additive effect of conditioned media on chemotherapy response

After establishment of IC50s of chemotherapy drugs on cells in normal media, the same experiments were carried out, but in CAF-conditioned medium to determine if CAFs would influence chemotherapy response.

The methodology is described in Chapter 2.4.1. These experiments were carried out on the MFD1 cell line, using medium obtained from 2 different CAFs. The MFD1 cell line was used because of the abundance of information we have on this cell line. NOFs were not used as my control media, as levels of secreted factors can be variable dependent on the passage of NOF cells, compared to normal media, which has been standardized with FCS, glutamine and antibiotics. In addition, I wanted to determine the effect of secreted factors from CAFs itself on chemotherapy response.

Figure 28 shows my results from experiments using conditioned medium from CAF612. In this set of experiments, more concentration of drug for platinum-based compounds is needed to kill 50% of cells in CAF-conditioned media, compared to normal media. There is very minimal shift of drug concentrations for epirubicin and 5FU. The increase of drug concentration for platinum-based compounds were less than 2 fold, which suggests that the secreted factors from CAFs could have added an element of chemoresistance in cancer cells. Log IC50s were calculated by the sum of squared F test where values of $p<0.05$ were considered to be statistically significant. Unfortunately, none were statistically significant.

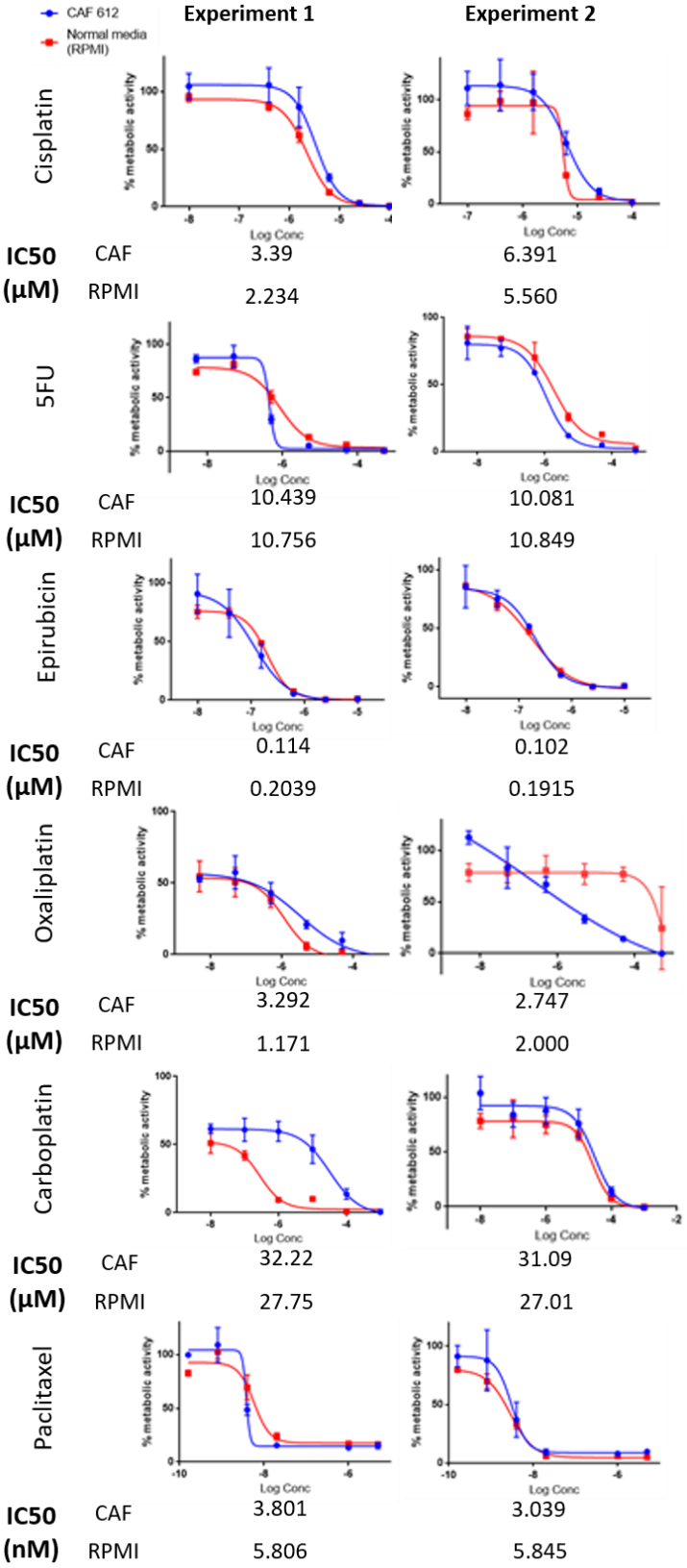

Figure 28. Dose-response curves of MFD1 cells for individual chemotherapy drugs after 4 days in culture in normal medium and CAF-conditioned medium from CAF612. It showed that platinum-based drugs had a higher IC50 in CAF-CM, compared to normal media

Subsequently, I used another CAF to investigate if this effect is true and reproducible.

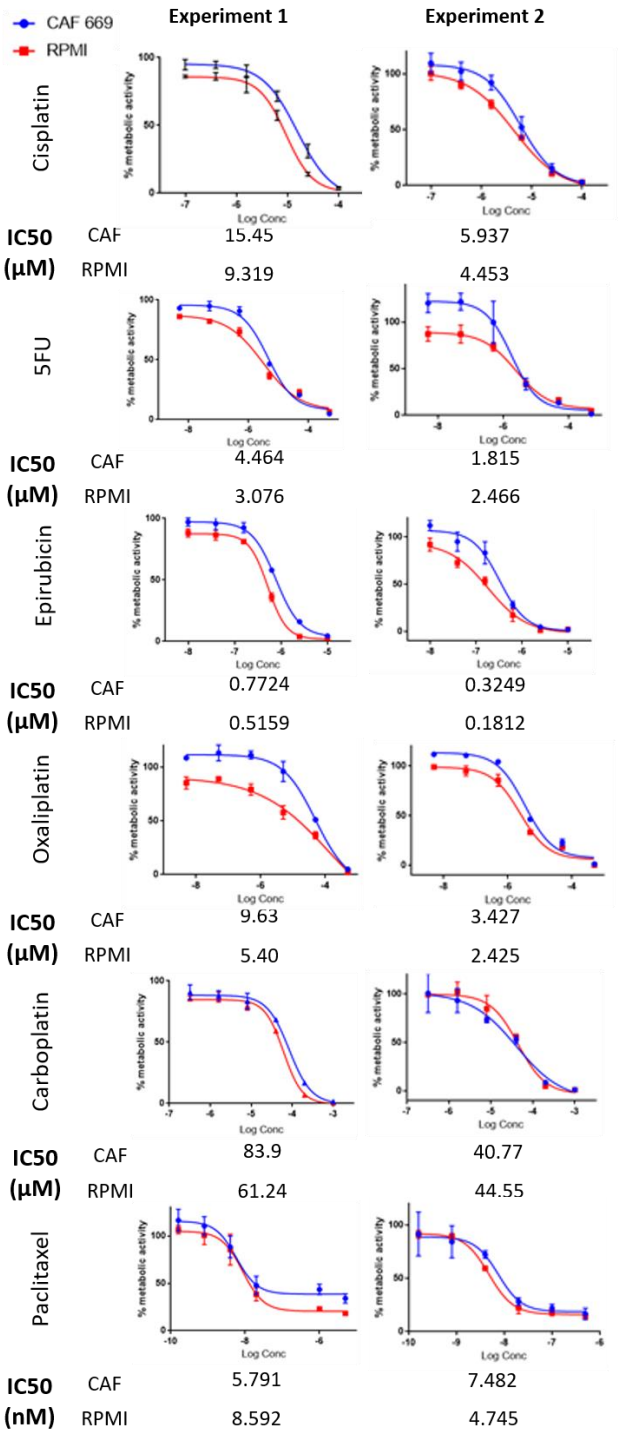

Figure 29. Dose-response curves of MFD1 cells for individual chemotherapy drugs after 4 days in culture in normal medium and CAF-conditioned medium from CAF669. A similar effect was seen with CAF-CM from CAF669 for cisplatin, oxaliplatin, epirubicin and paclitaxel

Figure 29 shows the results of my experiments using conditioned medium from CAF669. There is some data variability with different conditioned medium, with a higher drug concentration required to kill cells. This applied to 4 out of the 6 chemotherapy agents that was used, and it was not limited to platinum-based compounds only. Nevertheless, the fold change in drug concentration was less than 2 times for cisplatin, epirubicin and oxaliplatin.

In addition, this increase in drug concentration did not appear consistently with other chemotherapy drugs are used, for instance with 5FU, carboplatin and paclitaxel.

This may be due to the heterogeneity of CAFs, or the different passages of CAFs from which the conditioned media was derived, thereby influencing on the concentration of secreted factors in the media itself. As a result, it may have influenced the effect on the cancer cells. Using cell viability assays, I was looking at the cytotoxic effect on the cancer cells. I considered this method initially as it was economical, the assays were methodologically easy and quick to plate up, and automation could be used to quantify my results, and be highly reproducible. In addition, it can aid in the assessment of the interaction when looking at the mechanisms of action further down the line.

My results in the dose-response assays showed much variability. That was somewhat expected with 2 different CAFs which are heterogenous in nature. However, these were not consistent in the outcome. Further research into other methods of measuring proliferation has led me to consider colony formation assays, which tests cell survival and proliferation dependent on external stressors on cells[263]. These assays give information about survival after drug treatment, of which colonies can be counted manually and marked with a pen, or with an automated system. As such, I chose to perform colony growth assays, and counting the number of colonies formed. Methodology has been described in Chapter 2.5.

3.4 Colony growth assays in normal and conditioned medium

Appendix G details my optimization experiments of drug concentrations and quantification of colonies, which demonstrated that drug concentrations had to be adjusted with subtlety, so that there was a meaningful growth of colonies that could be managed with manual counting. Following on from that, the colonies were measured quantitatively by dissolving the crystal violet stain of the colonies and the optimal density was colourimetrically quantified it using the Varioskan® Flash machine. The values were then calculated as a percentage and plotted using histograms on GraphPAD PRISM, using untreated cells in normal media as my control.

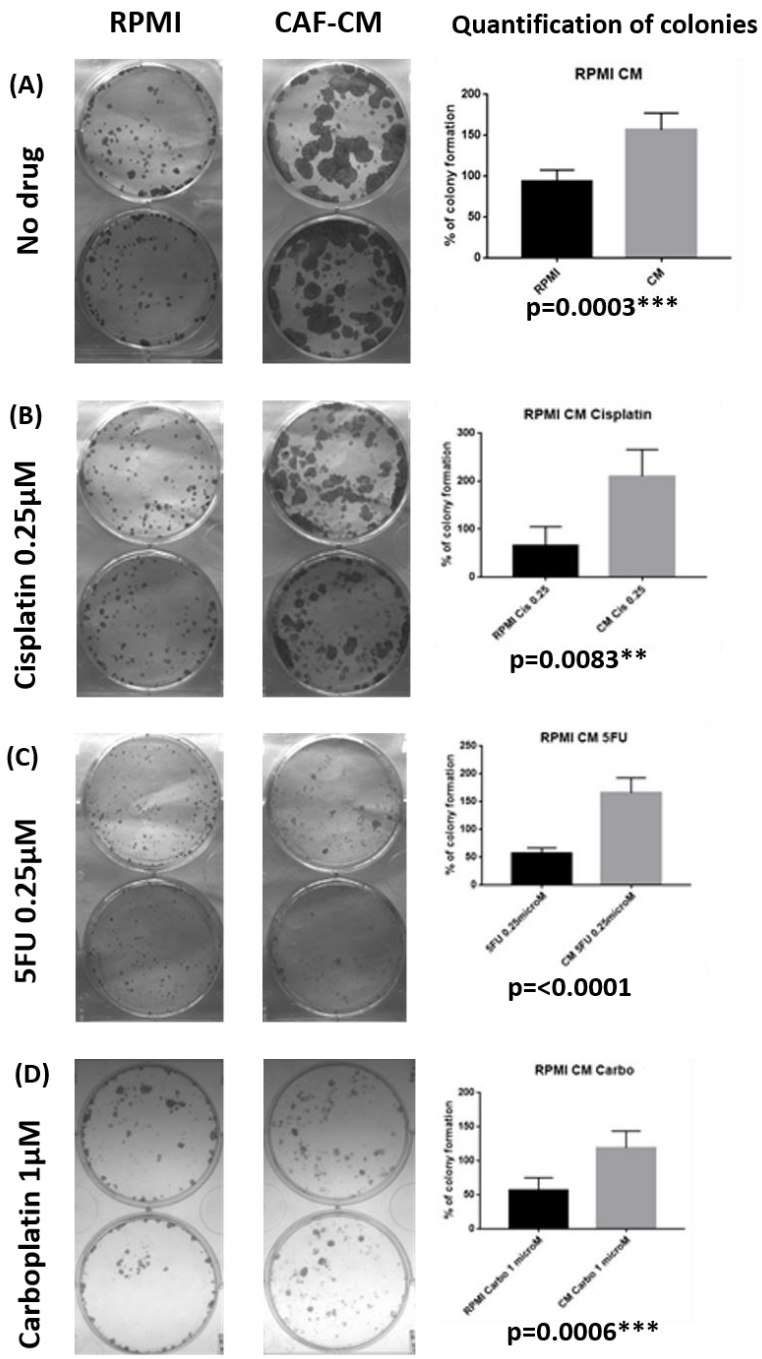

Figure 30. Representative colony growth assays (500cells/well) with 2ml of normal and CAF-CM, in the absence or presence of chemotherapy drugs.
(A) represent assays in the absence of chemotherapy drug and were my controls. (B)-(D) were normalized to RPMI in (A), which is why the quantification of colonies did not start at 100%, as there was already a killing effect in the presence of chemotherapy agents. Despite this, there was a significant proliferation of colonies, which also showed the cytostatic nature of the assay.

My colony growth assays had 500 cells seeded in each well of a 6-well plate with 2ml of media and left overnight to adhere. Media was then removed and replaced with either normal media (RPMI), CAF-conditioned media or conditioned media from vardenafil-treated CAFs. These were done in duplicate, and it was either in the absence or presence of

chemotherapy agents. The conditioned medium retrieved from CAFs and vardenafil-treated CAFs had been treated with Vardenafil/Methanol for 72 hours prior to change of media and the supernatant collected by centrifugation. The fibroblasts were counted and the supernatant diluted with normal media for normalization of media according to the concentration of CAFs and vardenafil-treated CAFs, before being used on the assays for colony growth. The CAF that was used to produce conditioned media was CAF 662.

Figure 30 demonstrates that OAC cancer cells had a significantly positive effect on colony growth when placed in CAF-conditioned media, compared with cells in normal media ($p=0.0003$). This effect was persistently seen in the presence of other chemotherapy agents.

This significant effect seen in colony growth assays, was not evident on my experiments using metabolic assays for cell proliferation. This may be explained by the fact that both my assays are measuring different aspects: the MTT assays give a snapshot view at a certain point in time (after 4 days of drug treatment) and measures the cytotoxic effect, while the colony growth assays assesses the longer term effects after initial drug treatment, as the cells are treated for a similar period of time, but then are left in normal media for 12 days before it is stained, dried and quantified. The latter is thereby a cytostatic assay instead. As such, this significant effect seen may very well reflect what occurs to cancer cells in humans.

However, one limitation is that it is a two-dimensional assay, and that can limit intercellular communication. Therefore I thought of utilizing a 3D culture to mimic the microenvironment.

3.5 Spheroids

I embarked on spheroid assays as it was a 3-dimensional system that allowed for co-culture of both CAFs and cancer cells, and somewhat replicates the microenvironment more physiologically, in terms of the cell-cell interactions and matrix deposition. This allowed me to investigate the effect of oesophageal CAFs on the epithelial cancer cells.

3.5.1 Appearance of spheroids

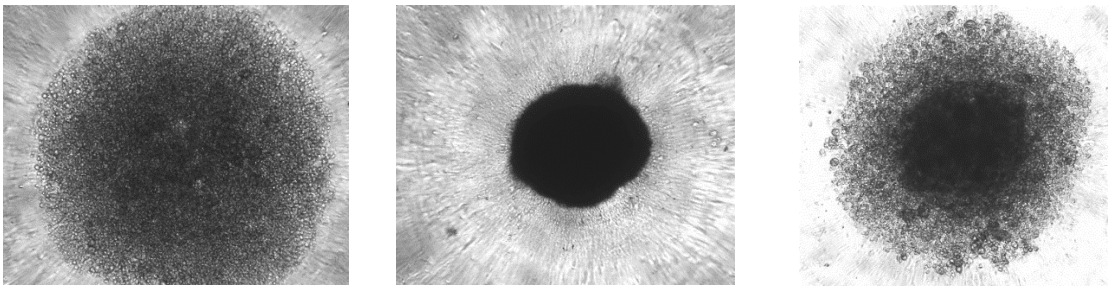

MFD1 CAF662 Co-culture of MFD/CAF662

Figure 31. Appearances of spheroids individually and in co-culture

When MFD1 cells were plated in spheroid plates, they appeared to be more spread out within the spheroid. Conversely, when CAFs alone (CAF662) were plated out, they seemed to create a denser spheroid. This may be due to the ECM proteins such as Type I collagen that are secreted by fibroblasts. This in turn creates a meshwork of proteins that increase density through intra- and intercellular interactions within the spheroids.

Appendix H demonstrates my optimization experiments for the appropriate number of cells to be used in each spheroid plate, and utilized the MTT cell proliferation assay to determine the metabolic activity for each type of spheroid. It was concluded that 20,000 cells in total were an appropriate number to be plated so as to give a good amount of metabolic activity for the MFD1 cells. When both types of cells were co-cultured together in a ratio of 3:1, there appeared to be a spheroid with a denser central core, which implied that this core may have consisted of the majority of CAFs (Figure 31).

3.5.2 Effect of spheroids

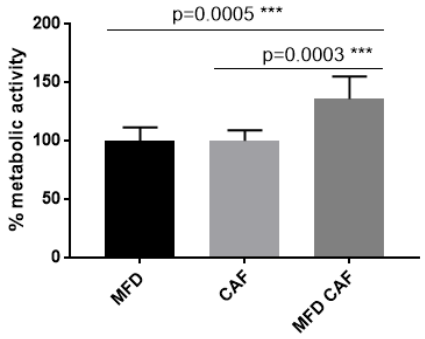

Figure 32. Histogram demonstrating metabolic activity of individual spheroids of cells, which was controlled for cell number.
There was enhanced metabolic activity to 135.5% of co-culture spheroids, which was significantly positive compared with MFD alone spheroids (p=0.0003*) or CAF alone spheroids (p=0.0005***)**

Looking at the metabolic activity of the individual spheroids, there was an increase in metabolic activity of the spheroids when in combination to 135.5%*** (p=0.0003) (Figure 32). This implied that when in co-culture, the cells appear to have a synergistic response in the combination spheroids (MFD CAF).

3.5.3 Effect of treatment on spheroids

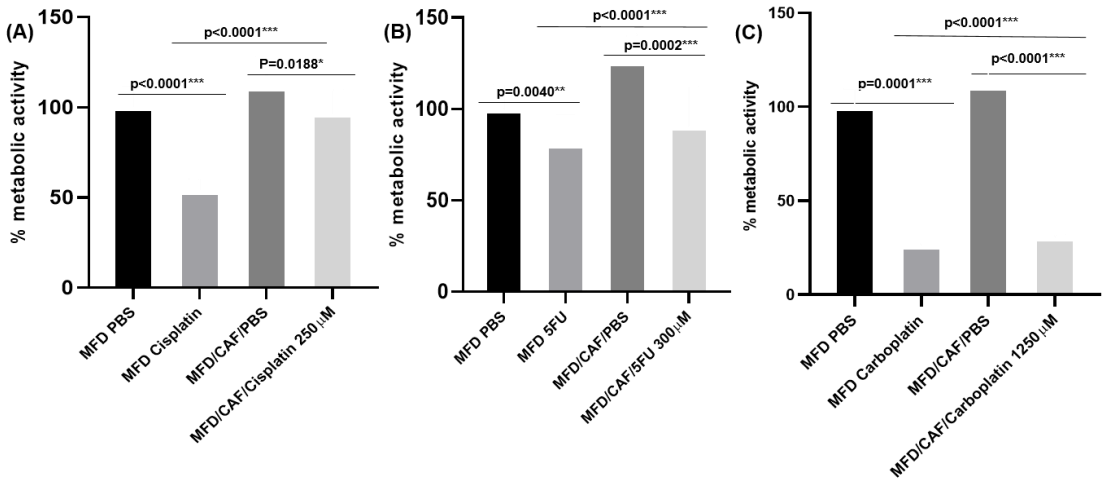

Figure 33. Representative histograms of spheroids treated with chemotherapy agents. The figure represent spheroid treatment (A) with cisplatin; (B) with 5FU; and (C) with carboplatin. All demonstrate results of a significant killing effect when MFD alone

spheroids were treated with a single chemotherapy agent. With co-cultured spheroids, the killing effect was still significant, despite being slightly diminished.

There was a significant result for MFD alone spheroids when treated with single chemotherapy agents (Figure 33). The results were similar with co-cultured (MFD/CAF) spheroids, when treated with different individual chemotherapy drugs. However, the killing effect was slightly diminished. Nevertheless, it was still statistically significant. This implied that the combination spheroids gave rise to more resistance, such that less cells in the spheroids were killed by chemotherapy.

3.6 Correlation with flow cytometry

Appendix I showed my optimization experiments of FACS analysis with fibroblasts and cancer cells.

EpCAM was delineated to be the antibody to identify MFD1 cancel cells as it occurs on basolateral cell surfaces of most epithelial carcinomas, and was demonstrated to have 86.88% positivity in the FITC fluorochrome channel. On the other hand, fibroblasts are heterogenous cells, and several markers such as platelet-derived growth factor alpha, or CD90 (Thy-1). CD90 is a cell surface glycoprotein that is expressed on human oesophageal fibroblasts and myofibroblasts, and my optimization experiments show that it was found to be a robust marker of CAFs, with 96.63% positivity in the APC fluorochrome channel. When dual-stained, less than 1% of either population stained for the counterpart stain.

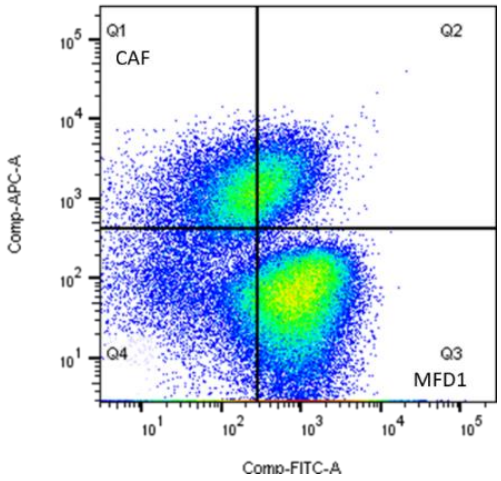

Figure 34. Dot scatter plot showing 2 distinct populations of cells of MFD1 cells and CAFs

Untreated co-cultured spheroids were put through FACS analysis, and 2 distinct populations are visible on dot scatter plots (Figure 34). EpCAM+ (MFD1) cells are in Q2 and Q3, while CD90+ (CAFs) cells are in Q1 and Q2.

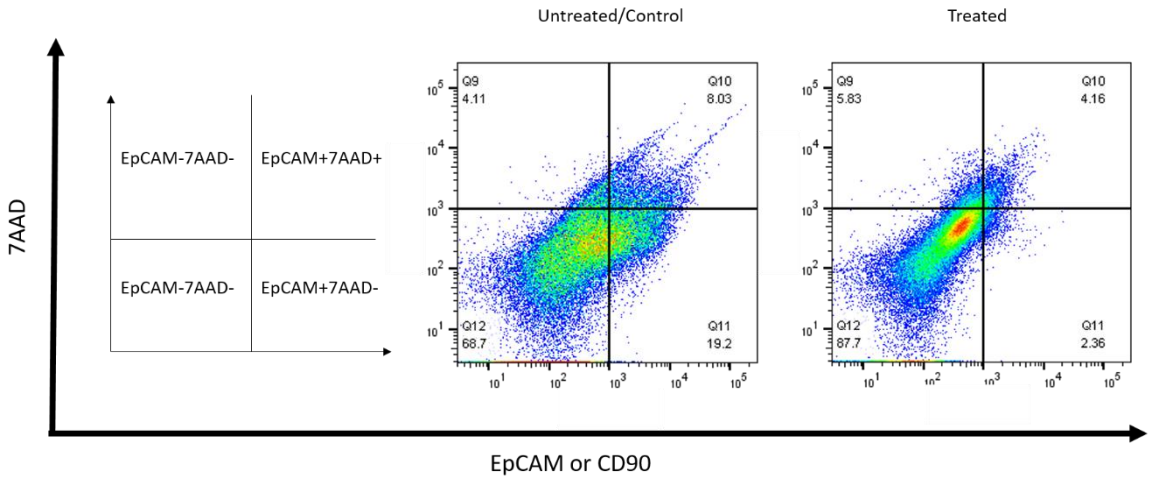

Figure 35. FACS dot plots demonstrating an example of proportions of CAFs or MFD1 cells identified after chemotherapy treatment using MFI

When plotted on a x- and y-axis, the fluorescence is read and quantified (Figure 35). The mean fluorescence intensity (MFI) is used to measure the shift in fluorescence intensity in a population of cells, and reflects an increase or decrease in expression of the marker. It is calculated by subtracting fluorescence from stain-positive cells from fluorescence from isotype cells, which was our control. 7AAD was used to determine cell viability for FACS analysis, and had positivity in the PerCP-Cy-5.5 fluorochrome channel.

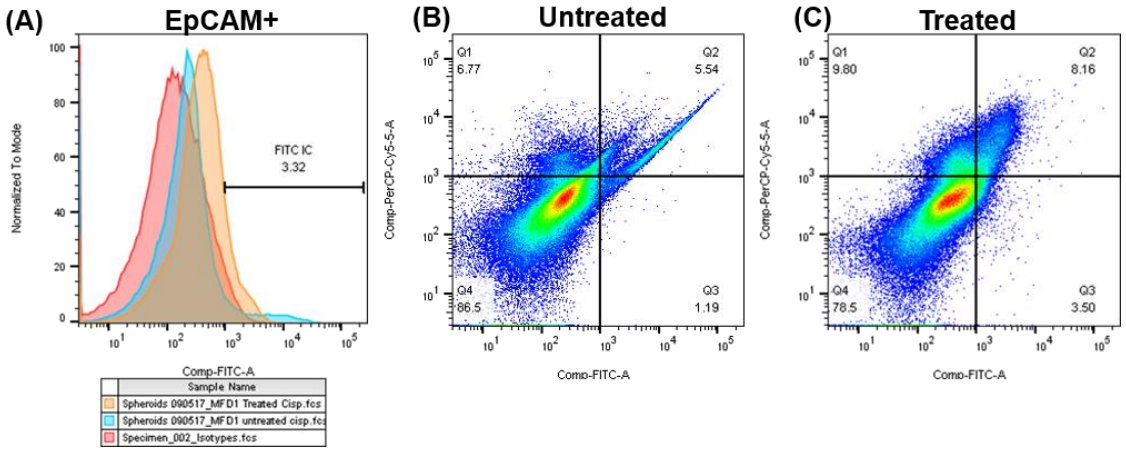

Figure 36. Histogram and dot scatter plots of cisplatin-treated MFD1 only spheroids. (A) shows a histogram plot of EpCAM+ cells gaining a right-shift of the curve with cisplatin treatment. (B) and (C) show a right-sided shift of the forward scatter, with a larger proportion staining for 7AAD and being non-viable cells after cisplatin treatment.

Figure 36 show a histogram plot of what occurs in an MFD1 only spheroids, before and after cisplatin treatment. There is a right-sided shift of cells becoming non-viable. When the MFI difference was calculated, it revealed an MFI difference of 8.38% in EpCAM+ cells after treatment, and 5.7% MFI difference in 7AAD+ cells (Figure 35). This included a small proportion of MFD1 cells in the spheroid which did not capture the antibody stain, possibly because they were non-viable to begin with.

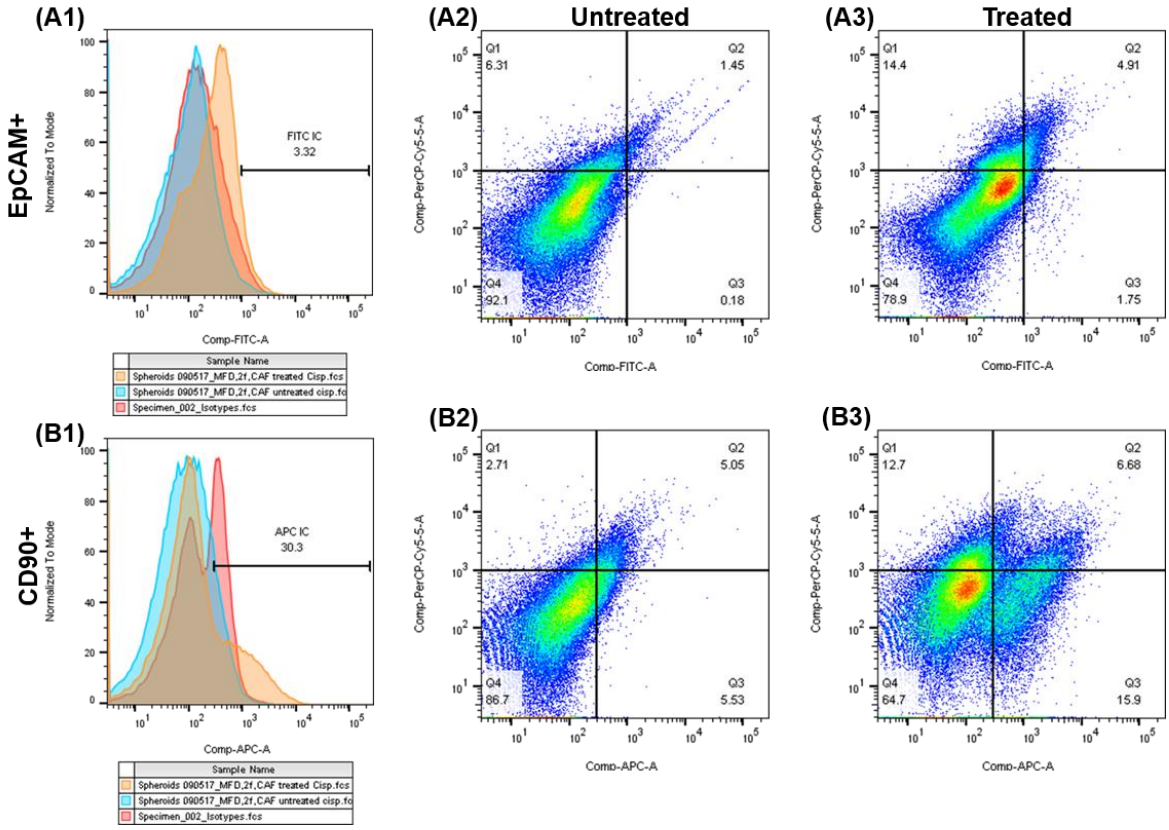

Figure 37. Histogram and dot scatter plots of co-cultured spheroids before and after 250μM cisplatin treatment

A1 shows a right shift with cisplatin treatment, which corresponds with a right-sided shift of the dot-scatter plot for EpCAM+ cells. Although B1 demonstrates that there was minimal shift of CD90+ cells on histogram plot with cisplatin treatment, B2 and B3 revealed that there is still a right-sided shift on dot scatter plot, implying that there is cell death of CAFs within the co-culture with cisplatin treatment

In untreated co-cultured spheroids (n=4), an MFI difference of 3.33% was demonstrated for EpCAM+ cells after treatment. Initially, 8.12% of untreated cells stained for 7AAD, which increased to 20.1% after treatment. Conversely, the MFI difference for CD90+ cells was 6% after treatment. 2.12% of non-viable cells after treatment presumably consisted of both CAFs and cancer cells (Figure 37). The initial small proportion of cells that stained for CD90 was probably due to the central core of CAFs being surrounded by cancer cells, and therefore the CD90 stain was unable to penetrate completely through to the core, until some

of the MFD cells in the spheroid became non-viable after treatment, thereby allowing the stain to penetrate through to some CAFs after treatment.

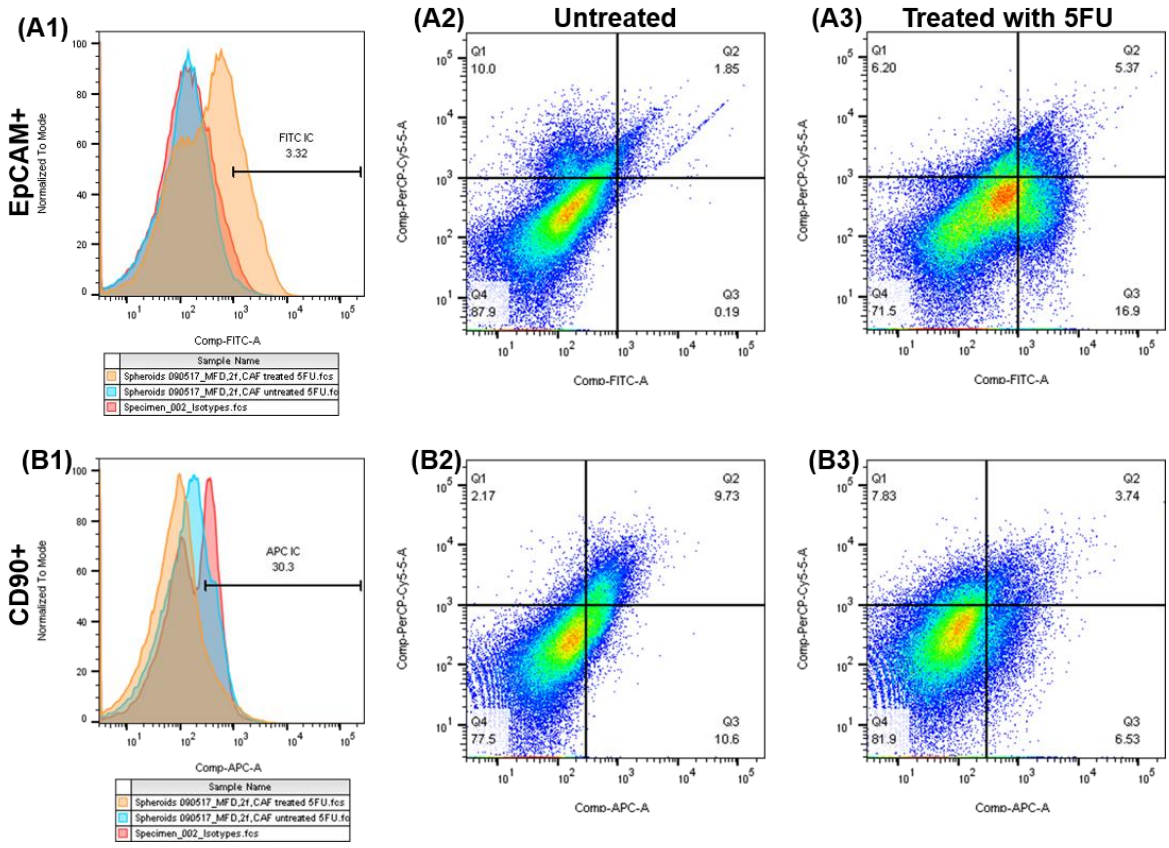

Figure 38. Histogram and dot scatter plots of co-cultured spheroids before and after 300µM 5FU treatment

A similar effect was seen in co-cultured spheroids treated with 5FU (n=4). Untreated co-cultured spheroids demonstrated an MFI difference of 18.9% for EpCAM positivity after 5FU treatment, and an MFI difference for CD90 positivity of 10% after treatment. The MFI for 7AAD showed a difference of 1.5% (Figure 38).

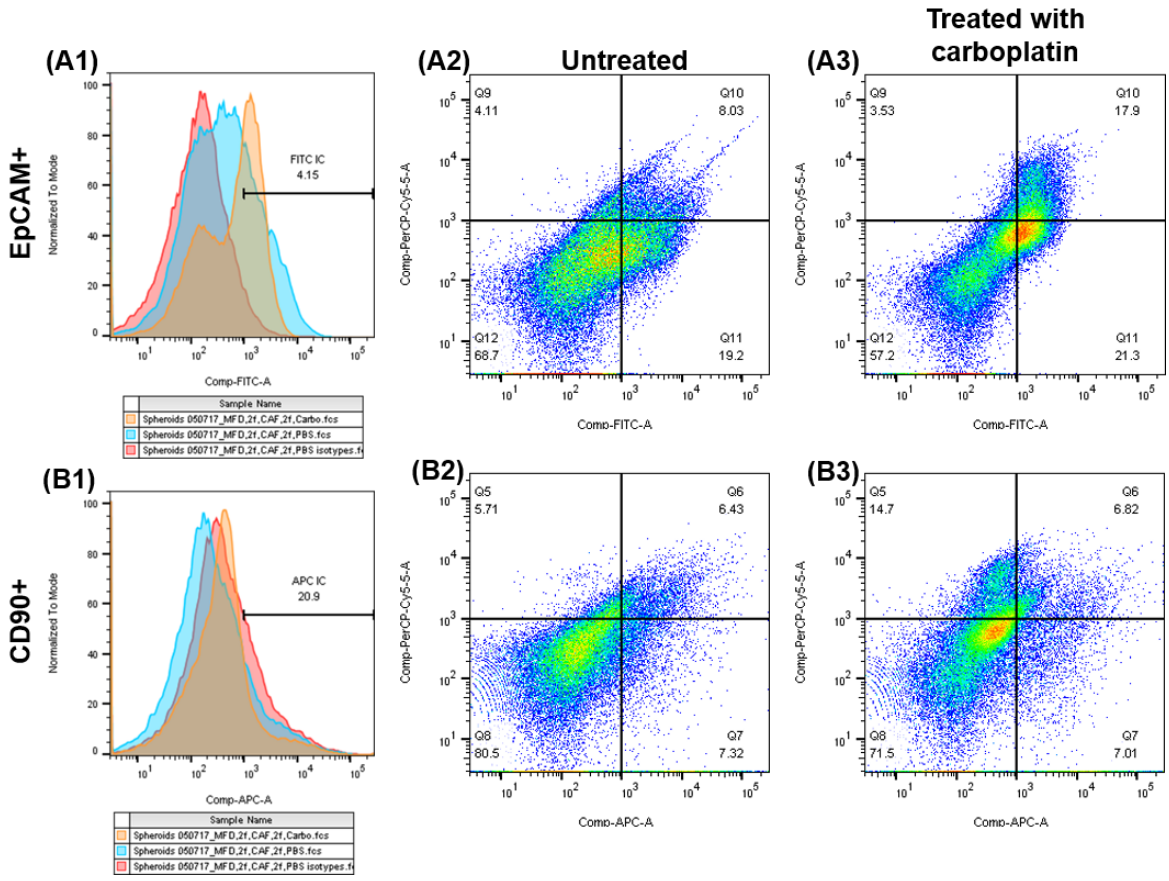

Figure 39. Histogram and dot scatter plots of co-cultured spheroids before and after 1250μM carboplatin treatment

Similarly, looking at experiments involving carboplatin (n=3), the MFI for EpCAM+ cells increased from 23.05% to 35.05%, while the CD90+ cells decreased by 0.1% after treatment. 7AAD showed an MFI difference of 10% (Figure 39). This suggested that perhaps the MFD1 cells were not completely killed by carboplatin, thereby allowing for more antibody to be taken up by cells partially injured by chemotherapy treatment.

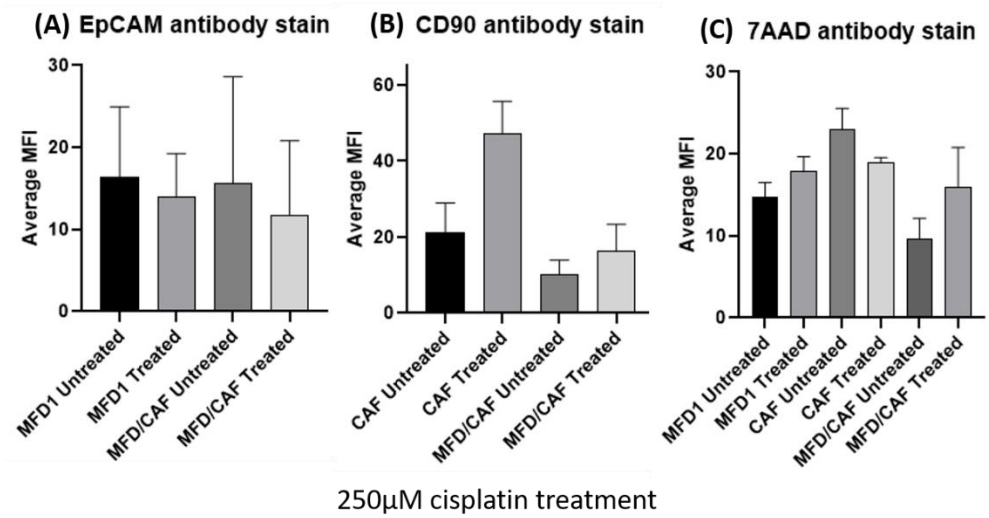

Figure 40. Histogram of average MFI after 250µM cisplatin treatment
(A) denotes spheroids made of MFD1- only versus MFD1/CAF co-cultures, and demonstrates a non-significant drop in MFI for EpCAM+ cells. Conversely, (B) showed a significant increase of MFI in CAF-only spheroids, which indicated that there was significant uptake of the CD90 stain after treatment (p=0.0490*). This increase was not significant in co-cultures. (C) shows an expected increase in MFI after treatment, for MFD1-only spheroids and their co-cultures, but it was not reflected in CAF-only spheroids.

Figure 40 show histograms that represent differences in MFI after cisplatin treatment (n=4).

MFI, as expected, had dropped after treatment for spheroids containing MFD1-only or co-cultures (A), with corresponding increases in MFI for non-viable cells, represented by 7AAD staining (C). Interestingly, there was an increase in MFI for CAF-only spheroids (represented by CD90 antibody stain) after cisplatin treatment (B). This may be hypothesized by cisplatin treatment breaking extracellular interactions that bind CAFs densely together, thereby causing the spheroid to open up slightly, which in turn allowed the CD90 antibody stain to be taken up by more CAFs. However, the drug concentration may not have been sufficient enough to cause significant cell death. This seemed to be reflected in (C) which demonstrated a decrease in 7AAD staining for CAF-only spheroids, which suggested that fewer cells died with treatment. Therefore the increase in average MFI for non-viable cells (C) in MFD1/CAF spheroids may be attributed to the action of cisplatin treatment on mostly MFD1 cells, though it was not significant.

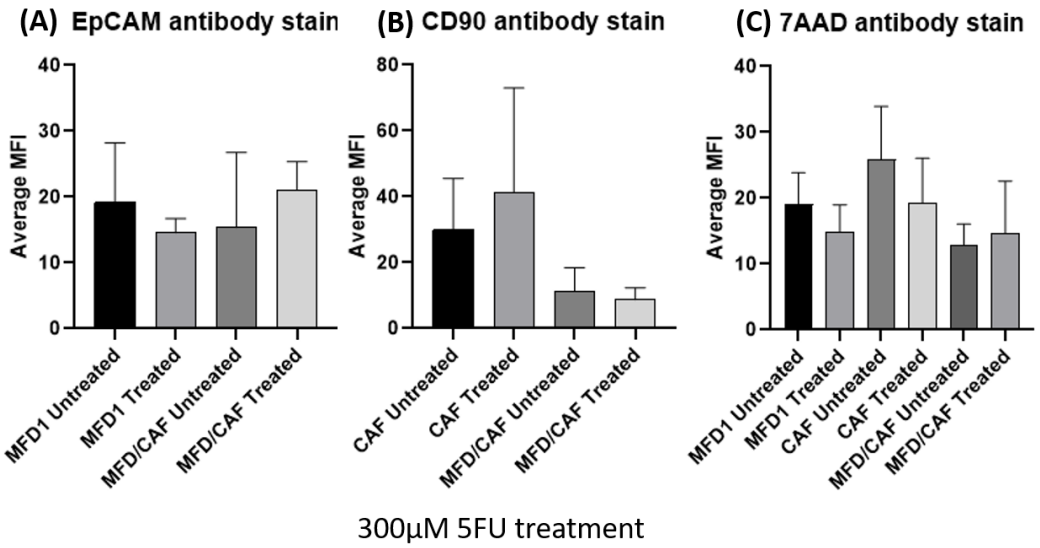

Figure 41. Histogram of average MFI after 300µM 5FU treatment

Figure 41 demonstrate the changes in MFI after 300µM 5FU treatment (n=4).

Looking at MFD1-only spheroids (A), MFI appeared to decrease for EpCAM+ cells with 5FU treatment, thereby implying that they were somewhat sensitive to this chemotherapy agent. However, in co-culture combination, there was a non-significant MFI increase when these spheroids were treated. This corresponded with a decrease in MFI in 7AAD+ cells in MFD1-only spheroids, and a slight MFI increase in co-cultured spheroids. This implied that although the MFD1 cells appeared to be less sensitive to treatment, with fewer cells dying (C). When combined with CAFs in the co-cultures, there was a rise in MFI in EpCAM+ staining, reflecting an element of resistance to treatment, but corresponded instead to a slight rise in MFI in cells staining for 7AAD, presumably because more CAFs had died with treatment and stained positive for 7AAD.

On the other hand, CAF-only spheroids had an MFI increase and took up more CD90 stain after treatment (B). This was perhaps because the interactions between these cells became disrupted and more cells were able to take up the antibody stain. However, in the co-cultured spheroids, less CD90 stain was taken up, compared to the CAF-only spheroids. Consequently, there appeared to be a corresponding MFI decrease with treatment for the CAF-only spheroids in terms of CD90 staining.

These findings suggested that 5FU treatment did not appear to have much effect on the MFD1-only spheroids, and implied that a resistance might be conferred on spheroids only when in co-culture. Alternatively, it should be considered that the treatment dose was not sufficiently high enough to be cytotoxic for cells, which may also explain the results.

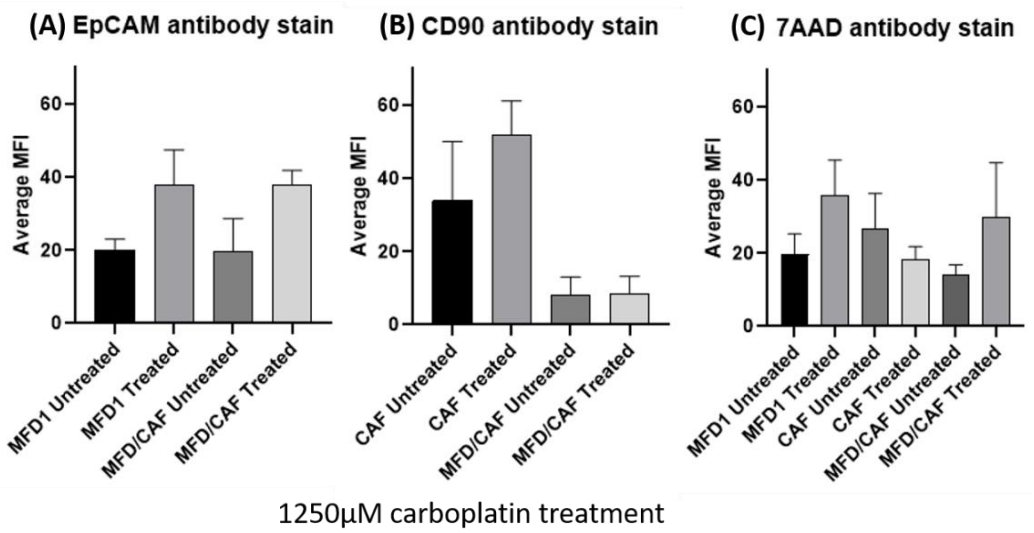

Figure 42. Histogram of average MFI after 1250µM carboplatin treatment.

Figure 42 demonstrate the MFI changes after 1250µM carboplatin treatment (n=4).

There was significant uptake of EpCAM staining after carboplatin treatment in both MFD1-only (p=0.0355*) and MFD/CAF (p=0.0328*) spheroids (A). This corresponded to a rise in MFI in both the MFD1-only and co-cultured spheroids, indicating that there was a good amount of cell death, but it was not statistically significant.

As seen with Figures 40 and 41, there was uptake of CD90 staining in the CAF-only spheroids after treatment (B). Although there was an increased uptake of CD90 stain for the CAF-only spheroids, when combined with MFD1 in co-culture, it appeared that the CD90 stain was not taken up very well, reflecting the drop in MFI (untreated). This may be explained by the structure of spheroids and location of CAFs within the spheroids (central). Even when the co-culture spheroids were treated, there was negligible uptake of CD90 stain. In addition, there was a drop in MFI for 7AAD staining for the CAF-only spheroids, indicating that chemotherapy treatment did not have much effect on CAFs (C).

These results demonstrate that this treatment had an effect on cell death, which could be mostly attributed to the killing effect on the MFD1 cells, as there was negligible effects on the CAF-only spheroids with treatment. Moreover, the concentration of drug was sufficient enough to cause an observable quantity of cell death.

3.7 Discussion

This chapter has illustrated various methods to measure response to chemotherapy, with 3 different OAC cell lines. Out of the 3 oesophageal cell lines used, the MFD1 cell line was chosen for further experiments due to various reasons. This is because it was a cell line derived locally (an OAC patient operated on in Southampton), with evidence to show that it was similar to the tissue of origin[245]. In addition, the cell line was found to be highly representative of the invasive OAC phenotype, it was stable over time and it retained the ability to form tumours in xenograft models that respond to microenvironmental stimuli. Whole genome sequencing was performed on this cell line, which identified several somatic acquired mutations such as ABCB1, DOCK2, TP53, and SEMA5A. TP53 mutations has been extensively documented in OAC, with recent genomic studies reporting a high mutation rate for TP53 of up to 70%, thereby suggesting that MFD1 is representative of OAC cancers[41 42 45]. In addition, other mutations such as ABCB1 may be potentially implicated in chemoresistance[246 256 264]. Therefore considerations have been made to use it as a starting point to determine if it was a factor that influenced chemoresistance in my experiments. If so, a mechanism of action could be further worked on with experiments involving efflux assays.

On the other hand, other cell lines such as FLO1 or OE33 are historic cell lines that were derived from patients with distal OAC or Barrett's cancer, where some karyotyping and cell surface antigen phenotyping were performed, but with no analysis of the primary tumour. Therefore it is not clear if the mutational burden in these cell lines were representative of the primary tumour of origin. It is also uncertain that it would retain similar characteristic morphological features with increasing passages of the cell lines[265]. Due to these reasons, it was deemed sensible to focus my experiments on the MFD1 cell line. Moreover, MFD1 have never been used in OAC spheroid experiments before, therefore I considered it a novel way to generate spheroids.

Ways of measuring response to chemotherapy treatment involved dose-response assays, colony growth assays and the use of spheroids. Different CAFs used in the form of conditioned medium had given rise to variable results in dose-response assays. The MFD1 cell line appeared more resistant to 5FU treatment, compared to OE33 or FLO1 cell lines, which was to be expected, especially when the cell line was derived from a patient whose tumour had poor histological response (Mandard TRG 5) despite receiving neoadjuvant EOX chemotherapy, evidenced by disease recurrence within the year. When conditioned medium from different CAFs were used, there was some variability with drug concentrations needed to kill cells. However, it eluded to a hint of reduced chemosensitivity when CAFs were involved, especially with cisplatin treatment. Nevertheless, the variability may be due to the heterogeneity of CAFs, or even the different passages of CAFs, which can influence

the concentration of secreted factors in the media that most likely have an effect on the cancer cells.

I then utilized colony growth assays as it would give information about cell survival after drug treatment, via colonies that could be manually counted or with an automated system. I have demonstrated strong evidence that when placed in CAF-conditioned media without drug treatment, OAC cancer cells had a significantly positive effect on colony growth. This effect was also seen in the presence of other chemotherapy agents. This difference in results from my experiments with metabolic assays can be explained by the fact that both assays are measuring different elements: the MTT or cell-proliferation assays measure the cytotoxic effect at a certain point in time, while the colony growth assays assess the cytostatic effect and look at the long term effects after treatment. The latter therefore may reflect what occurs to cancer cells in humans after treatment, on a cellular level. My results on this aspect reinforced my hypothesis that CAFs do play an important role in chemoresistance in OAC.

Following on from these experiments, spheroids were used as a surrogate for a 3D model to mimic the tumour microenvironment. My results show that the metabolic activity was significantly increased with co-cultured with CAFs. This effect persisted in the presence of chemotherapy agents, with less effective killing of OAC cells.

Flow cytometry was also performed on the spheroids to determine the effects of treatment on the cell types based on the fluorescent characteristics of each cell type, and if it correlated with my cell viability experiments. There appeared to be a right-sided shift of forward and side scatter on the dot scatter plots for MFD1-only spheroids after treatment. This was quantified with an increase in MFI of cells staining with the 7AAD stain which represented non-viable cells. This in turn indicated that MFD1 cells were susceptible to drug treatment. This effect was also evident in co-cultured spheroids in the presence of chemotherapy agents, with non-significant MFI differences seen after treatment. These differences were more noticeable in the platinum-based compounds.

Interestingly, the structure of CAF-only spheroids were denser than the MFD-only spheroids. The CAF-only spheroids appear to take up more CD90 antibody stain after treatment. This perhaps can be due to disruption of extracellular interactions between these cells, leading to breaking open of the dense spheroids and allowing more cells to take up the stain. Even with co-cultured spheroids, the proportion of cells staining for CD90 was small, and I hypothesized that it may be attributed to the central core of CAFs being surrounded by cancer cells, which did not permit the CD90 stain to penetrate completely through to the core of the spheroids, until drug treatment, which eventually disrupted the structure and allowed more stain to penetrate through to the CAFs. One way to prove this

hypothesis would be to attach fluorescent markers to both the MFD1 cells and CAFs before placing them in spheroid plates, both in the absence and presence of drug treatment. These can then be imaged with the Transilluminator machine or an appropriate programme to prove the locations of cells within the spheroid structure.

Refocusing on the MFD/CAF spheroids, flow cytometry indicated an MFI rise in 7AAD+ cells after treatment, which is likely to be due to the action of chemotherapy on mostly MFD1 cells, rather than CAFs. In particularly, co-cultured spheroids appeared to have an MFI rise in EpCAM+ cells after 5FU treatment, compared to MFD-only spheroids, which imply that there may be an element of resistance to this drug. These results may also be because the treatment dose was not high enough to kill a sufficient amount of cells.

All these results have to be considered with caution, as further work needs to be done regarding how these drug concentrations correlate to plasma levels in patients, and the potential side effects or toxicity it can cause to patients. It would be essential to identify the location of both cells in the spheroid structure with fluorescent markers. It would then be informative regarding what occurs in the spheroid after drug treatment. It would also be worth repeating flow cytometry of the untreated and treated spheroids with different concentration of drugs to determine the effective concentration that disrupts the spheroid structure and if it can correlate to non-toxic drug levels in human plasma. Another aspect to consider is the secreted factors in the conditioned media, which has proven to have a positive effect on cancer cells in some of my dose response assays, and more evident in my colony growth assays. The media would need to be fractionated, and the different components identified, together with their proportions and presumed functions, and how it can influence the sensitivity on the cancer cells.

3.8 Summary

This chapter has shown that CAFs appear to increase chemoresistance of OAC cells, to some extent. This may be due to a combination of secreted factors within the CAF-conditioned medium and direct cell-to-cell interactions within spheroids.

Chapter 4 Action of PDE5 inhibitors on oesophageal cancer and fibroblast cells

4.1 Introduction & Aims

PDE5 inhibitors (PDE5i) have been used in the clinical setting for many years in the treatment of various benign conditions, more commonly in erectile dysfunction and pulmonary arterial hypertension[250]. However, in recent times, there has been literature published repurposing these drugs for cancer, as these drugs are already known to be safe, effective and well-tolerated in the clinical setting. In addition, a number of human carcinomas such as colon, thyroid, bladder, breast, prostate, lung, skin and pancreas cancers are discovered to overexpress PDE5, compared to normal or surrounding non-cancerous tissue[230 236 247]. Therefore it is potentially of high therapeutic value in cancer, as patients may be able to undergo precision oncological therapy if they have an overexpression of PDE5.

Unsurprisingly, this exciting discovery of PDE5 expression in cancers has generated clinical trials using PDE5 inhibitors. A recent Phase II trial in head and neck squamous cancer demonstrated that PDE5 inhibitors can reverse tumour-specific immune suppression, through inhibition of myeloid-derived suppressor cells[244]. To date, 12 further trials have been registered exploring the effects of PDE5 inhibitors on a range of conditions, such as pancreatic cancer, abdominal cancer, gliomas or brain metastases, HNSCC, multiple myeloma, lymphatic malformations and myelodysplastic syndrome[266].

In particular, Zenzmaier *et al* had demonstrated that PDE5 inhibitors reduced fibroblast proliferation and reverted fibroblast-to-myofibroblast transdifferentiation in prostatic stromal cells, which highlighted the potential of PDE5i to target the stromal compartment[228 229]. More recently, Catalano *et al* found that CAFs treated with PDE5i diminished cancer cell proliferation, invasiveness and controlled tumour-stromal interactions, and that overexpression of PDE5 in breast cancer cells had correlated to shorter overall survival[230].

These studies suggest that PDE5 is a viable oncological target to explore, and their actions may be due to disruption of tumour-stroma interactions. To date, there is minimal information in the published literature on PDE5 and the use of its inhibitors in oesophageal cancer, let alone its effect on CAFs. Cowie had characterised PDE5 expression in oesophageal CAFs and NOFs, and had determined that PDE5i had an effect on oesophageal CAFs when TGFβ-dependent transdifferentiation of fibroblasts to CAFs was knocked down[267].

Combining this knowledge together with my results in Chapter 3, which demonstrated an increase in chemoresistance of OAC cells by CAFs, the aim of this chapter was to investigate the effect of PDE5i on chemoresistance. This was done by looking at the effect of conditioned medium from CAFs that had been pre-treated with PDE5i, using dose-response assays and colony growth assays. Vardenafil was used due to its effect on prostatic fibroblast transdifferentiation[228]. Spheroid assays were also used to investigate if direct contact with CAFs will potentiate any sensitivity effect if it were present.

If this was indeed the case, PDE5i could be used to affect the response of oesophageal cancer cells and make them more sensitive to chemotherapy. This could potentially be beneficial to numerous patients in both the neoadjuvant and palliative settings, to debulk tumours or relieve obstructive symptoms respectively.

4.2 PDE5 expression in OAC cell lines and primary fibroblasts

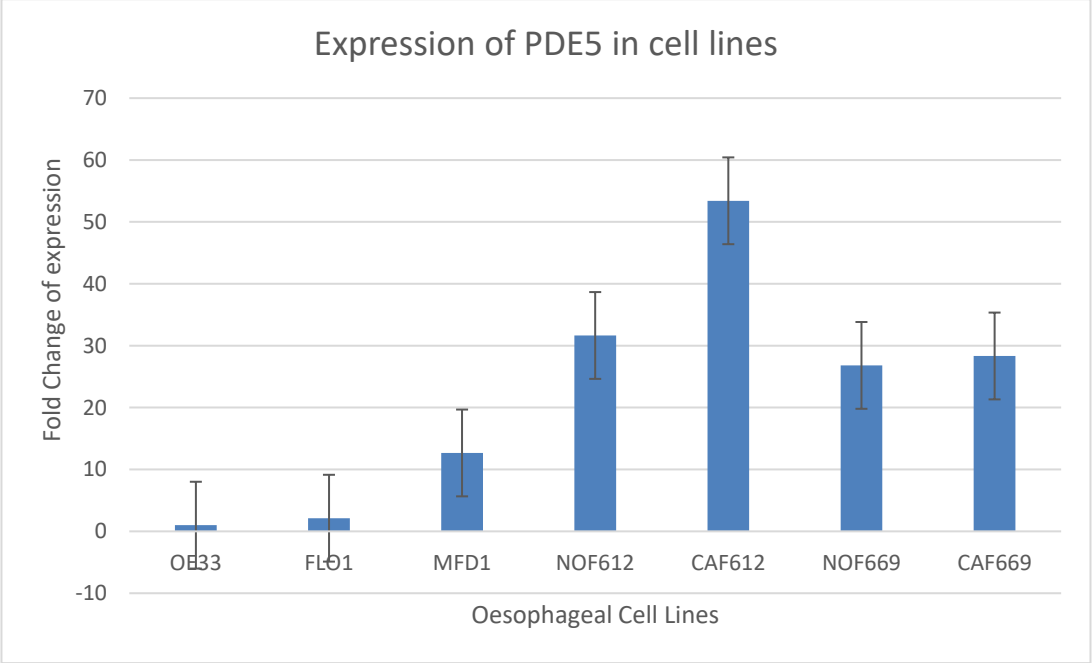

Figure 43. Representative graph tabulating expression of PDE5 in cancer cell lines and primary fibroblasts

Using qRT-PCR, I determined that primary fibroblasts expressed more PDE5 than cancer cell lines (n=3) (Figure 43). Using OE33 as the denominator for fold change, my results demonstrated that FLO1 had a 2-fold increase of PDE5, while MFD1 had a 12-fold increase of PDE5. Interestingly, all fibroblasts cell lines had a 30-50 fold increase of PDE5 expression: NOF 612 - 31-fold increase, CAF 612 - 53-fold increase, NOF669 - 27-fold

increase, CAF669 - 28-fold increase. This confirmed that there is a high expression of PDE5 in CAFs compared to epithelial cells in OAC.

4.3 Effect of PDE5i-treated conditioned medium on IC50s

The drug Vardenafil arrived dissolved in Methanol from the manufacturer, therefore our vehicle used was methanol. As per my previous results, only MFD1 cells were used in these experiments.

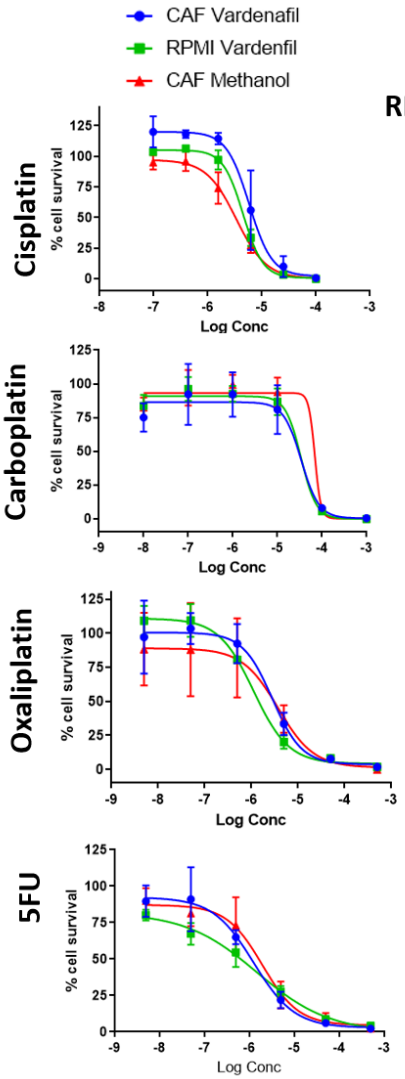

	IC50 (µM)		
	RPMI Vardenafil	CAF Vardenafil	CAF Methanol
Cisplatin	4.491	5.822	3.382
Carboplatin	33.80	34.31	69.07
Oxaliplatin	1.121	2.803	3.725
5FU	1.487	1.243	1.953

Figure 44. Representative dose-response assays of MFD1 cells in CAF-conditioned media (CAF Methanol) and vardenafil-treated CAF-conditioned media (CAF Vardenafil). RPMI Vardenafil was used as my control

These dose-response assays showed that in regardless of normal or CAF-conditioned medium, there were no differences in the concentration of drug required to kill 50% of cells, when the media contained vardenafil. On the other hand, without vardenafil treatment, there appeared to be an increased resistance of the cells to carboplatin, oxaliplatin and 5FU in the CAF-conditioned medium, thereby requiring more drug concentration to kill the same proportion of cells (Figure 44).

4.4 Effect of PDE5i-treated conditioned medium on colony growth assays

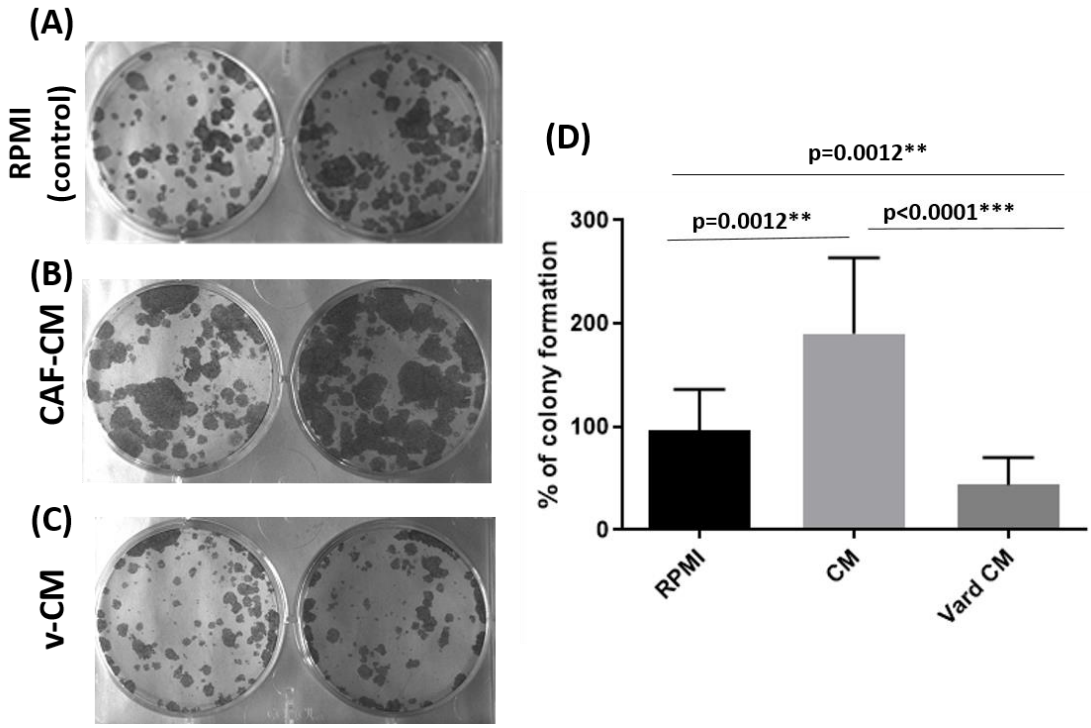

Figure 45. Representative colony growth assays cultivated, in duplication, in various media simultaneously in the absence of chemotherapy.
(A) show colony growth in normal media, RPMI, which acted as my control
(B) demonstrate increased colony growth in CAF-conditioned media (CAF-CM)
(C) demonstrate that cancer cells when cultured in vardenafil-treated conditioned media (vCM) resulted in a significant drop in colony growth
(D) show a histogram of colonies quantified in RPMI (control), CAF-CM and vCM. As seen previously, there was a significant colony growth when in CAF-CM, and a colony growth was significantly diminished when vardenafil-treated CM was used

Figure 45 shows my results of colony growth in different media in the absence of drug therapy. Five hundred MFD1 cells were plated per well and left in the individual media for 12 days (n=3). My results demonstrated that colony growth was significantly augmented in CAF-CM, while colony growth in vardenafil-treated conditioned media (vCM) was

significantly diminished, more so than those cultured in normal media (RPMI), which acted as my control.

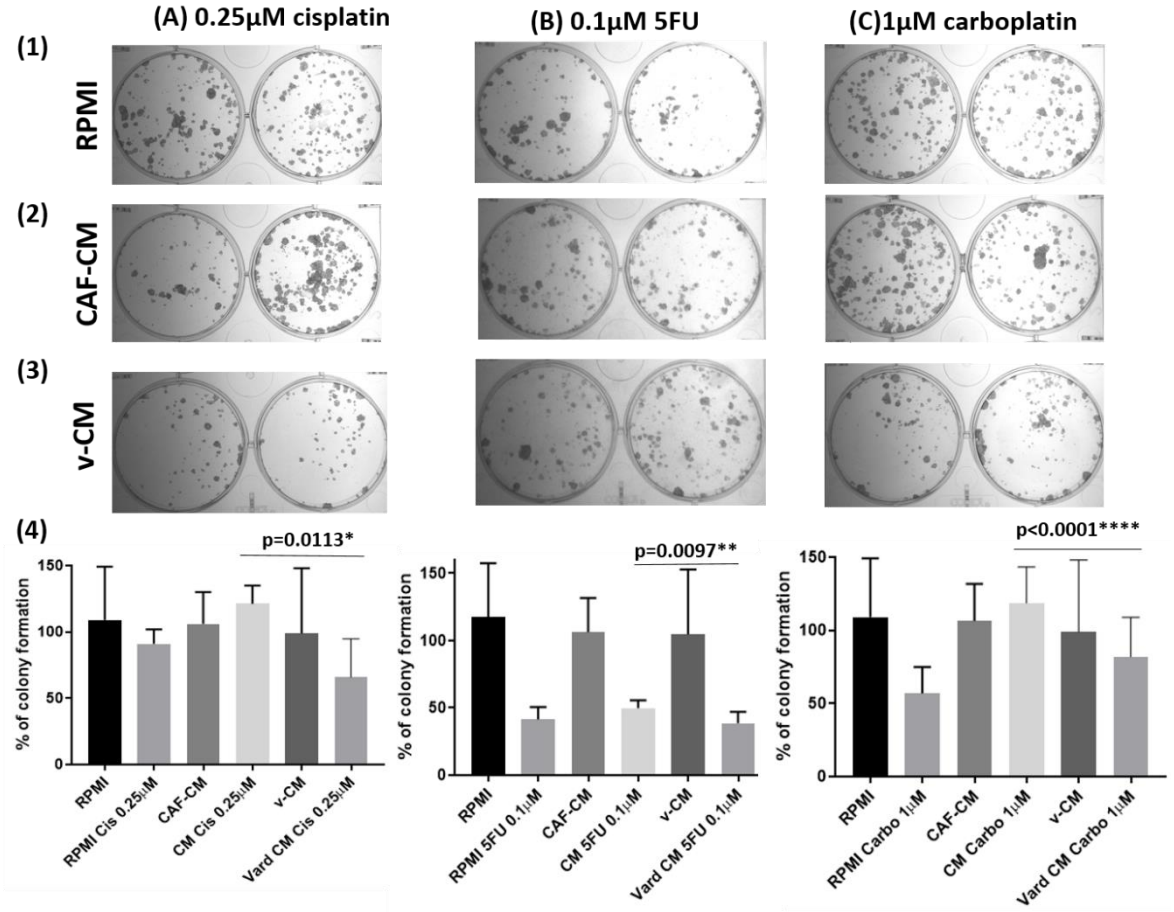

Figure 46. Representative colony growth assays in normal media, CAF-CM (from CAF662) and vCM in the presence of drug therapy.
Rows 1, 2 and 3 show colony growth in RPMI, CAF-CM and vardenafil-treated conditioned medium respectively, while columns A, B and C demonstrate cisplatin, 5FU or carboplatin treatment. Each of these assays show that there is a significant drop in colony growth when vardenafil-treated CM was used, compared with CAF-CM. Row 4 illustrates the histograms of the colony growth when quantified. The negative controls were labelled RPMI, CAF-CM and vCM.

After several optimizations of chemotherapy drug dosing in vardenafil-treated CAF-CM (Appendix G), Figure 46 demonstrated that vardenafil-treated conditioned media made the colonies more susceptible to the drug treatment, resulting in fewer colonies when it was quantified (n=4).

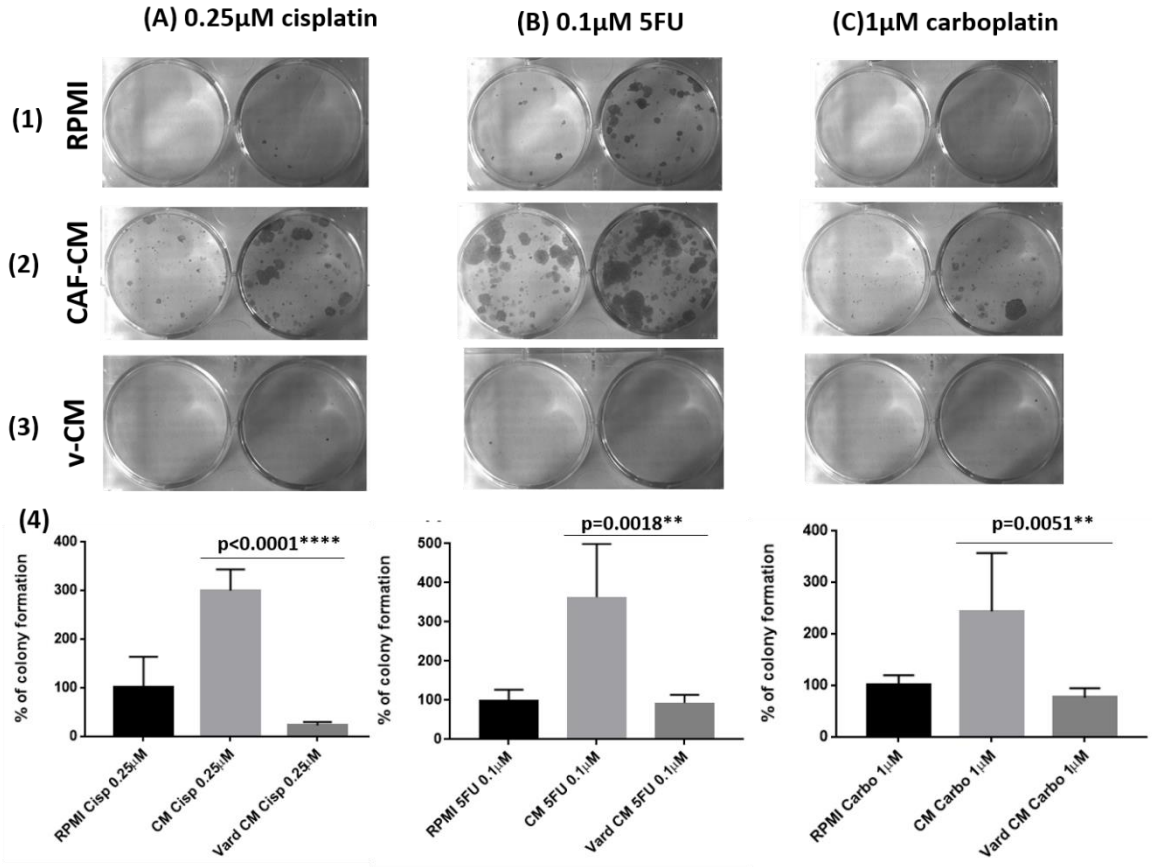

Figure 47. Representative colony growth assays in normal media, CAF-CM (CAF669), and vCM in the presence of cisplatin, 5FU and carboplatin drug treatments.
Similar to earlier experiments with CM from CAF662, there was a significant decrease in colony growth when vardenafil-treated CM was used on MFD1 cells in the presence of drug treatment

These experiments were subsequently repeated (n=4) using CAF-CM from CAF669 to determine its reproducibility, which showed similar results to the earlier experiments using CM from CAF662, whereby there was a significant drop in colony growth when vardenafil-treated-CM was used on MFD1 cells (Figure 47). There was a visual difference in colony growth patterns when different CAFs were used to generate the conditioned media – this could be accounted for by the heterogeneity of the CAFs. Nevertheless, the factors within the conditioned media was sufficient to cause a significant change regardless of the different CAFs.

4.5 Effect of PDE5i treatment on α-SMA expression in fibroblast cell lines

Further to work done in qRT-PCR, I sought to investigate the effect of PDE5i treatment on cellular proteins in fibroblast cell lines, namely using α-SMA expression. This is because it was found to be important in the survival outcome of oesophageal cancers[162]. As such, Western blotting was performed for PDE5 and α-SMA expression in cancer cell lines and primary fibroblasts (n=8).

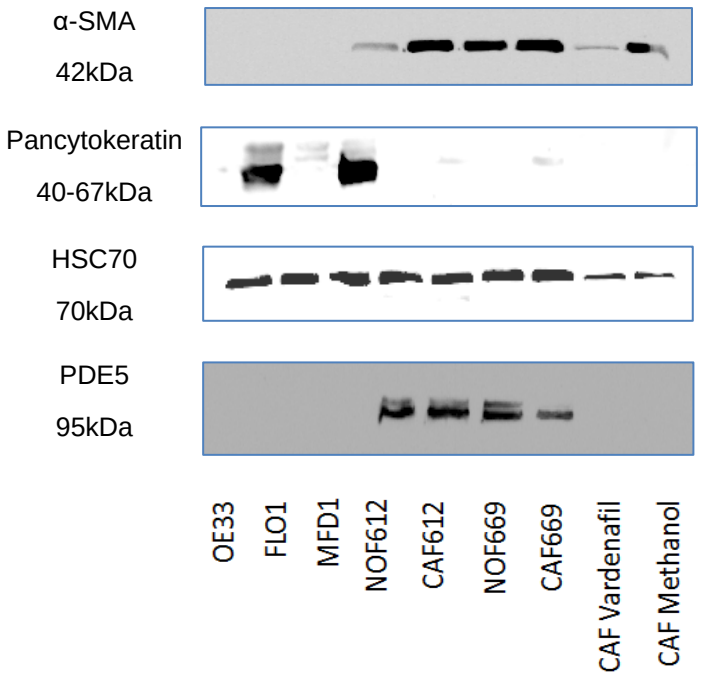

Figure 48. Immunoblot of PDE5 and α-SMA expressions in cancer cell lines and primary fibroblasts

Immunoblot analysis showed some PDE5 expression in NOFs and CAFs, but negligible in the cancer cell lines. Similarly, there was strong protein expression of α-SMA in NOFs and CAFs, but none in the cancer cell lines (Figure 48).

Furthermore, CAFS, when treated with vardenafil, appeared to produce less protein expression of α-SMA, compared to my control (CAF Methanol). This implied that PDE5i such as vardenafil may appear to partially reverse the CAF phenotype, such that less α-SMA is expressed on the cellular protein level.

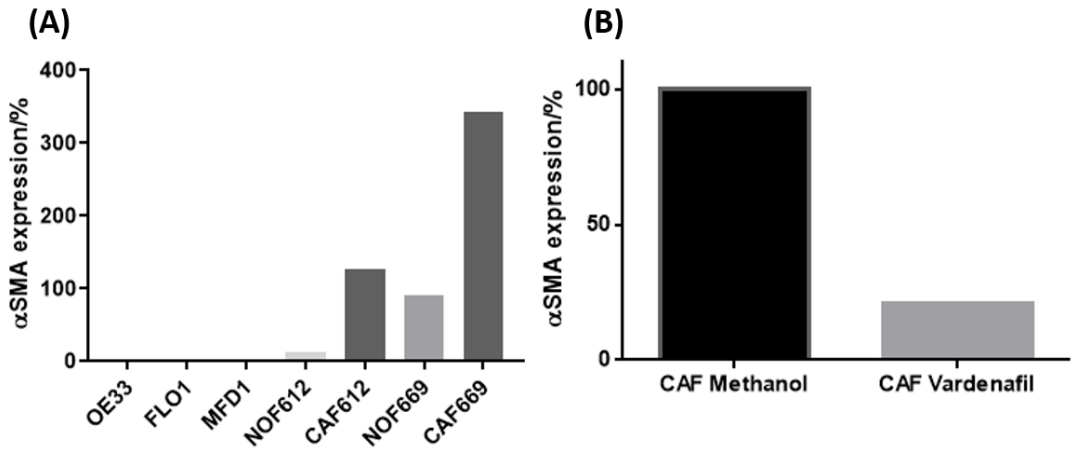

Figure 49. Histograms denoting the percentage of α-SMA expression of (A) oesophageal epithelial and fibroblast cell lines, and (B) CAFs, before and after PDE5i treatment, on cellular protein level

Figure 49 demonstrates my findings when the western blot is quantified using open access densitometry software ImageJ (Chapter 2.3.1.4), which was used to compare the density or intensity of bands on a western blot. Once the blot was scanned and saved in a digital format (.tif or .jpg), the file was opened in the ImageJ software, and converted to a grayscale image. The images were selected in sequence, then organised in a profile plot, where the peaks in the profile plot corresponded to the dark banks in the original image. Higher peaks represented darker bands. Wider peaks represented bands that cover a wider size range on the original blot. Each peak was highlighted and sized, then expressed as a percentage of the total size of all the highlighted peaks.

Having previously chosen the peak for my standard, the percent value for each peak is divided by the percent value for the standard, to give the relative density of each peak. In other words, the standard will have a relative density of 1, and the rest of the values are a measure of the relative density of other peaks, in comparison to the standard. These results were then moved into GraphPad PRISM program to create histograms, as seen in Figure 49.

Quantification of the immunoblot demonstrated that fibroblast cell lines, both NOFs and CAFs express more α-SMA than epithelial cancer cells (A). Not surprisingly, CAFs expressed much more α-SMA than their counterparts (NOFs), presumably because CAFs are activated myofibroblasts, therefore it was expected that they express more α-SMA than NOFs. (B) demonstrated a dramatic decrease of 89% in α-SMA expression when CAFs were treated with vardenafil, compared to their controls in methanol. This may be attributed to the knowledge that PDE5i can de-differentiate the CAF phenotype[228], therefore it was expected that there would be a drop in α-SMA expression when PDE5i was instituted.

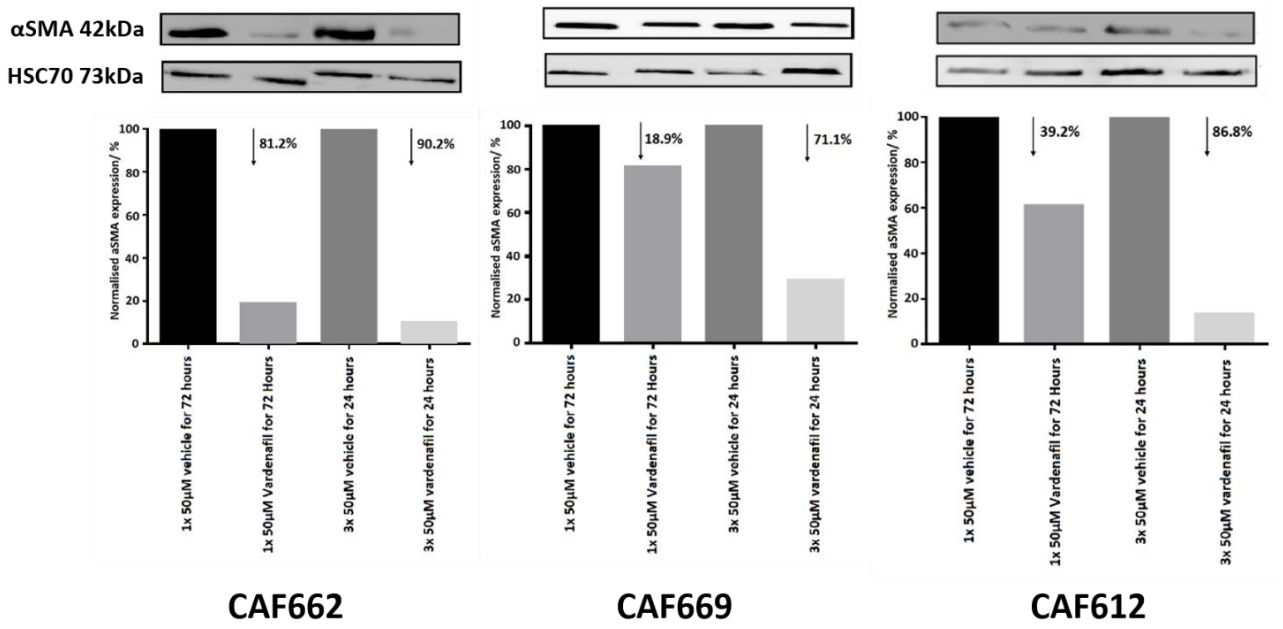

Figure 50. Immunoblot of α-SMA expression of CAF662, 669, 612 following vardenafil treatment 1x72 hours or 3x24 hours
They demonstrate a reduction of α-SMA for after both once-only and daily PDE5i treatment for 3 days

Vardenafil has a half-life of 18 hours in a human and is usually given as a once daily dose to maintain a therapeutic level. Therefore a comparison was made with CAFs treated with vardenafil for 72 hours, against CAFs treated with vardenafil every 24 hours for 3 days. Expectedly, even with different CAFs, there was a decrease in α-SMA in all 3 CAFs after treatment of vardenafil, more so with the daily treatment (Figure 50).

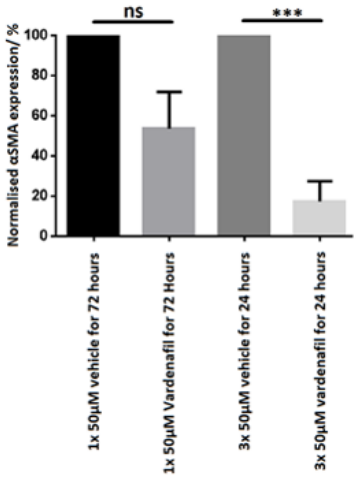

Figure 51. Combined results of CAFs treated with vardenafil showing a significant α-SMA reduction (p<0.001*)**

Interestingly, when results for all 3 CAFs were combined, there was a non-significant decrease of α-SMA (46.4%) (p=0.064), compared with treatment of the same dose of vardenafil every 24 hours for 3 days, where there was a significant drop of α-SMA of 82.7% (p<0.001***) (Figure 51).

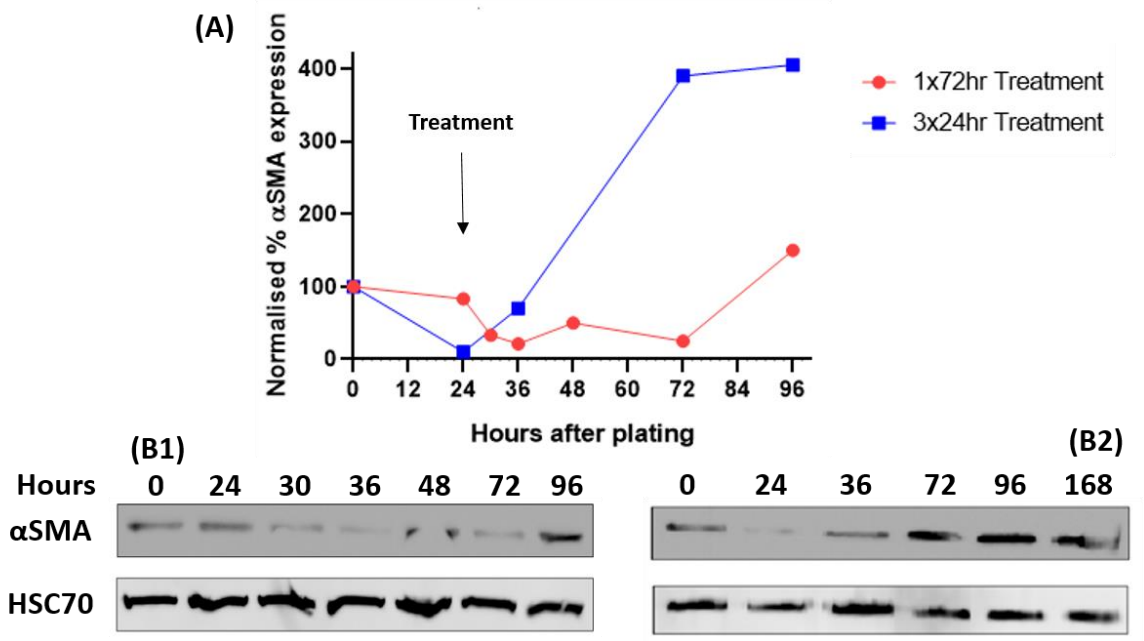

Figure 52. (A) Time course of CAF treated with vardenafil for 1x72 hours (red) and 3x24 hours (blue). B1 and B2 show immunoblots of CAF treated with vardenafil 1x72 hours (B1) and 3x24 hours (B2)

To investigate what occurred during and after treatment of CAFs, a time-course was performed on CAF 662 treated with 50μM vardenafil, and samples were taken at varying time points measuring α-SMA by immunoblotting. My findings showed that there was an initial drop, followed by a rebound increase in α-SMA. This effect was sustained regardless of treatment for 72 hours or once every 24 hours (Figure 52A). However, the increase in α-SMA appeared to be potentiated to a large extent with daily doses of vardenafil. Therefore in my subsequent experiments, spheroids were pre-treated once every 24 hours for 72 hours to maintain PDE5i activity on CAFs and minimise any drop of activity.

4.6. Effect of PDE5i on spheroid assays

We initially had to determine if vardenafil had any effect on cancer cells in spheroids in the first place. As such, we pre-treated both MFD1 spheroids and co-cultured spheroids with vardenafil or methanol (control) and analysed their metabolic activity.

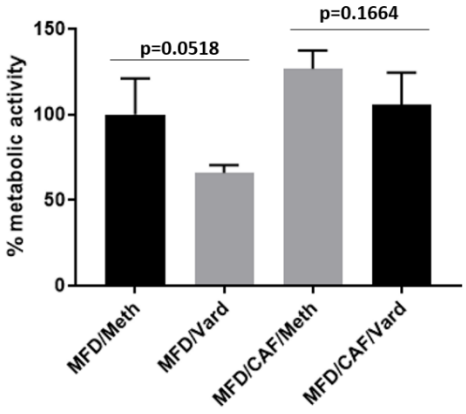

Figure 53. Representative histogram of pre-treated co-culture spheroids showing a non-significant decrease in metabolic activity with PDE5i treatment

Figure 53 show my findings when MFD1 only and co-culture (MFD/CAF) spheroids were pre-treated with either methanol (control) or vardenafil (n=15). Methanol was used as the control, as vardenafil from the manufacturer arrived as being dissolved in methanol.

My findings demonstrated that in the absence of drug therapy, there was a drop in metabolic activity for the MFD-only spheroids to 66%, though not significant (p=0.0518). Looking at the MFD/CAF spheroids, there was higher metabolic activity with my control (MFD/CAF/Meth) compared to the MFD-only spheroids, which was diminished non-significantly when the spheroids were pre-treated with vardenafil (p=0.1664). Interestingly, there was a drop in metabolic activity for the MFD-only spheroids. I did not expect PDE5 inhibition to have any noticeable effect on the MFD-only spheroids. However, observing in qRT-PCR that MFD1 cells expressed 10-fold more PDE5 than other epithelial cell lines such as OE33 or FLO1, it was not surprising that vardenafil had some effect on the MFD1 cells. Also, as expected, when MFD1 and CAFs were combined in co-culture, these spheroids achieved an enhanced metabolic activity, that was diminished with vardenafil treatment. This suggested that PDE5 inhibition could potentially have a negative effect on both MFD1 and CAFs, and implied that it may be useful in the 3D model, as a reflection of the TME.

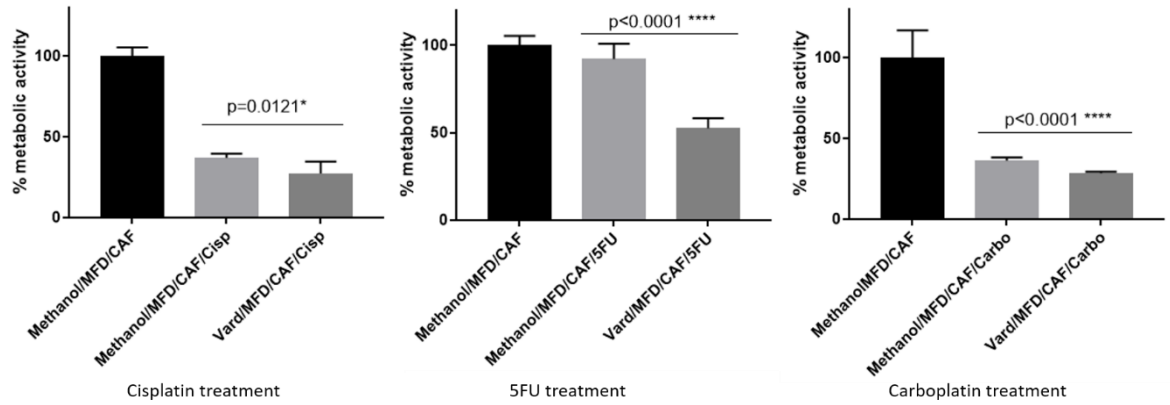

Figure 54. Representative histograms of pre-treated spheroids in the presence of chemotherapy. Methanol/MFD/CAF was my negative control

Subsequently, with chemotherapy treatment, there was significant evidence of chemoresistance of the pre-treated spheroids (n=5) (Figure 54). Although 5FU treatment did not decrease the metabolic activity of the pre-treated spheroid by much, compared with platinum compounds, the PDE5i pre-treatment still appeared to sensitise the MFD1 cells, such that 5FU had a major significant effect in decreasing the metabolic activity of the OAC cells. A similar effect was seen with cisplatin or carboplatin treatment.

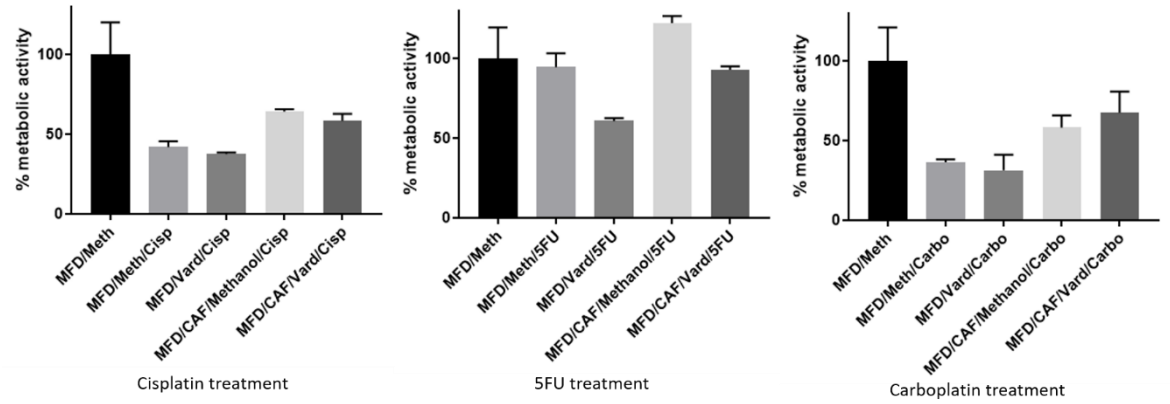

Figure 55. Comparison of MFD spheroids and co-culture (MFD/CAF) spheroids to demonstrate the sensitising effect of vardenafil, in the presence of chemotherapy

Using a different CAF, I examined lone MFD spheroids which were pre-treated with PDE5i (n=3). My findings showed decreased metabolic activity after chemotherapy for all 3 agents (Figure 55). However, when spheroids are co-cultured and then pre-treated, there appeared to be diminished metabolic activity for cisplatin and 5FU treatment, but not for carboplatin treatment. This variability in results might be explained by the heterogenous nature of the different CAFs used in the spheroids.

4.7 Correlation with flow cytometry

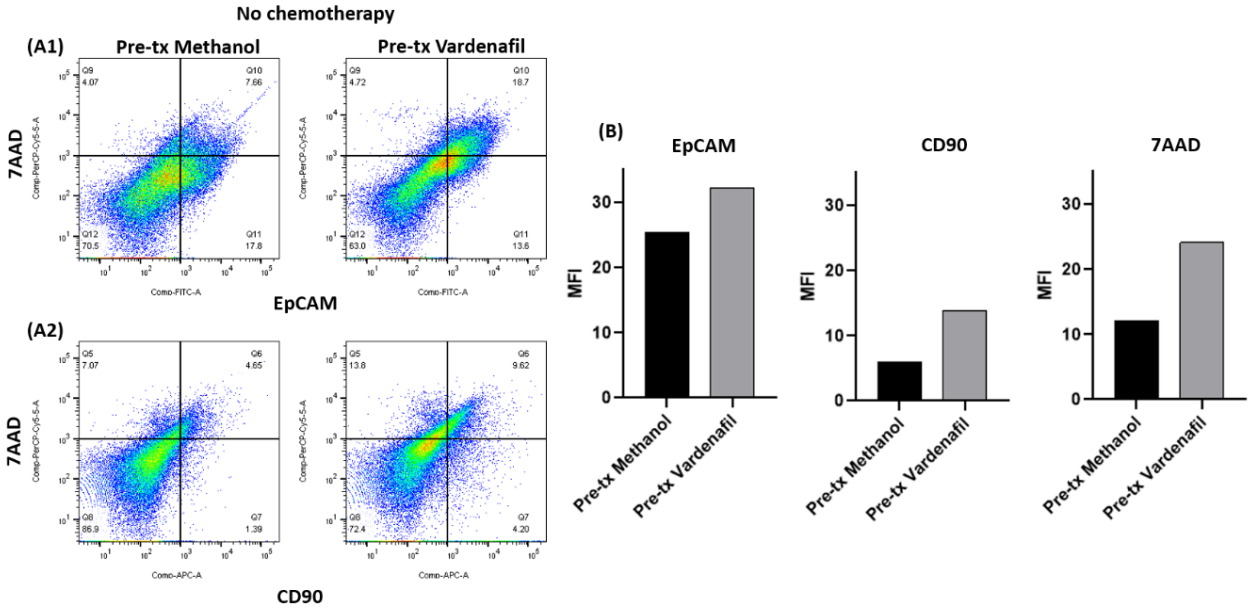

Figure 56. A1 and A2 show dot scatter plots of the effect of a higher MFI in spheroids pre-treated with vardenafil, compared to that of methanol, on EpCAM+ and CD90+ cells, in the absence of drug therapy (B) demonstrate the histograms of MFI for the EpCAM+, CD90+ and 7AAD+ cells

Looking at the FACS analysis of pre-treated spheroids in the absence of chemotherapy, the spheroids pre-treated with vardenafil appeared to generate a higher MFI, compared to pre-treated methanol, which were my controls (Figure 56). In addition, they coincided with a rise in 7AAD+ cells in spheroids in pre-treated vardenafil. Further information was gleamed from the dot-scatter plots in Q10 (top right) of Figure 56 (A1) – there appeared to be more EpCAM+ cells in the FITC fluorochrome channel (which represent the MFD1 cells which were EpCAM+) that was also stained with 7AAD. Similarly, there was an increase in CD90+ cells in spheroids pre-treated with vardenafil that also stained with 7AAD+ (Figure 56, A2. Q6 in top right of dot-scatter plots). These observations led to the conclusion that both methanol and vardenafil had effects in making cells non-viable, which seemed more noticeable with vardenafil.

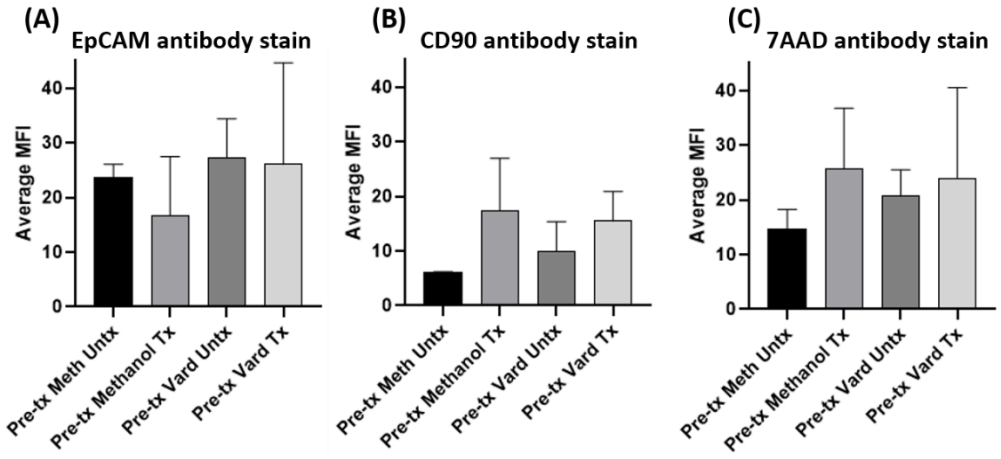

Figure 57. Histograms of average MFI changes before and after 250μM cisplatin treatment.
My negative controls were classified as pre-treated methanol untreated.

Examining the FACS analysis of pre-treated spheroids that were subsequently treated with cisplatin, there was a non-significant drop in MFI after cisplatin treatment (Figure 57A), denoting that treatment has acted on these cells and made them non-viable. This corresponded with the cells staining positively for 7AAD, with a right-sided shift on their corresponding dot-scatter plot, implying that the cells that had died could be attributed to MFD1 cells (Figure 57C).

Interestingly, spheroids pre-treated with methanol had a lower average MFI before treatment, compared to those pre-treated with vardenafil. Perhaps vardenafil has made both the MFD1 cells and CAFs in the spheroids more sensitive in obtaining the antibody stain before any drug treatment.

Similarly, the CD90+ cells seem to load up the antibody stain more easily when pre-treated with vardenafil, compared with methanol (Figure 57B). After cisplatin treatment, there is an increase in average MFI, signifying that more CAFs have taken up the CD90 antibody stain and are still viable, with minimal shift seen on their dot-scatter plot, therefore not reflecting a greater increase in 7AAD+ cells (Figure 57C). They may still be survivable due to the concentration of drug not sufficient enough to kill the CAFs by the time it reached the CAFs in the central core.

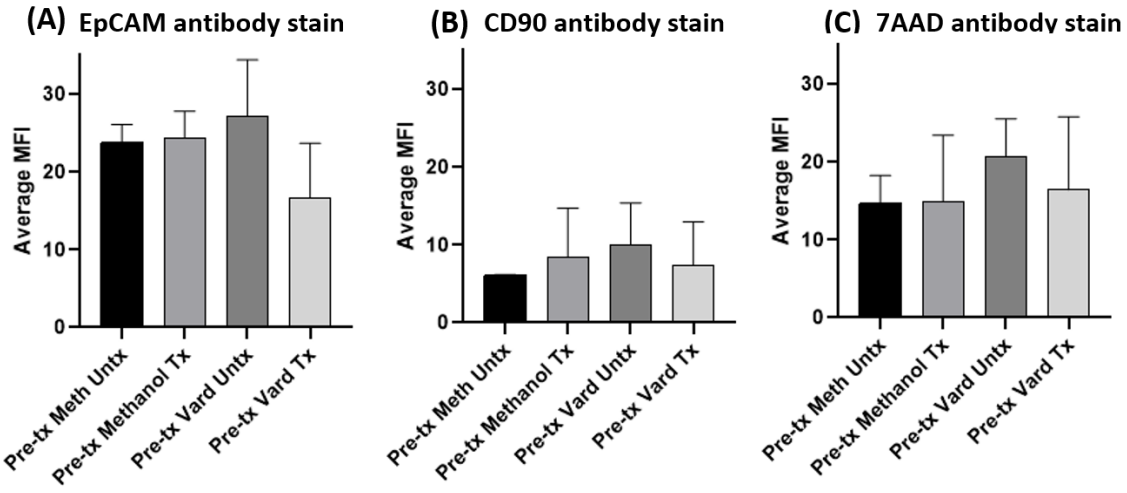

Figure 58. Histograms for average MFI changes before and after 300μM 5FU treatment

Conversely, with 5FU treatment, there was minimal uptake of the EpCAM antibody stain with 5FU treatment in the pre-treated methanol spheroids, implying that they were resistant to drug treatment (Figure 58A). This was reflected in the similarities of cells taking up the 7AAD antibody stain (Figure 58C), and to CD90+ cells, in both types of pre-treatment (Figure 58B).

Interestingly, as shown in Figure 58A, there was a sizeable but non-significant drop of MFI in EpCAM+ cells when treated with cisplatin in the spheroids pre-treated with vardenafil, with a small decrease in MFI in CD90+ cells. This seemed to suggest that vardenafil has made a proportion of the pre-treated vardenafil spheroids sensitive to the drug treatment, where vardenafil may have worked on MFD1 cells and to a lesser extent, CAFs too. However, the effect was not as substantial as I had expected. Perhaps this may have been because a smaller amount of drug had reached the CAFs, thought to be centrally located. Therefore, compared with spheroids pre-treated with methanol, there was only a slight sensitivity of the CAFs to 5FU treatment which was not significant.

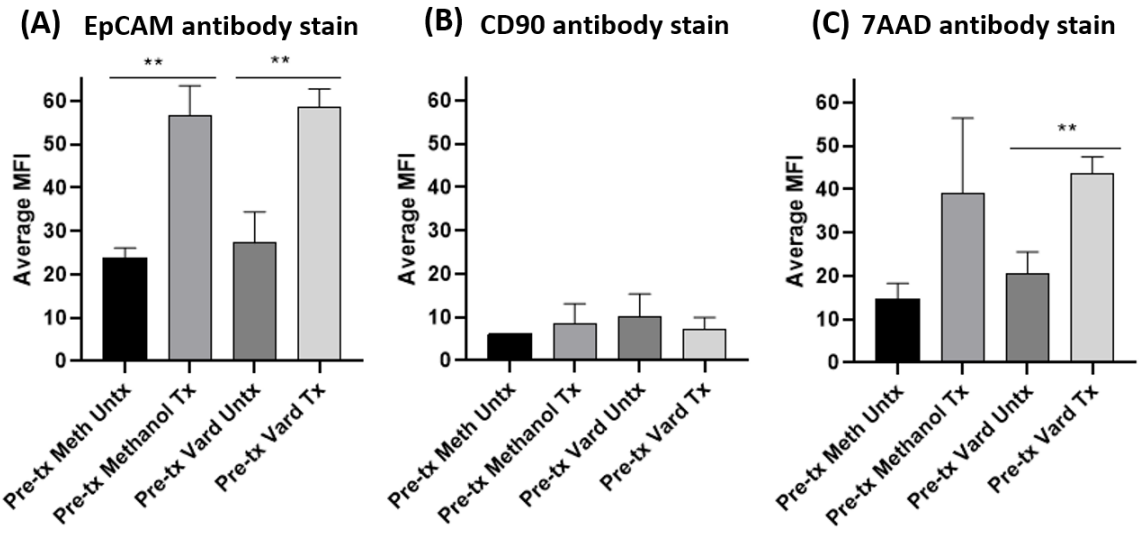

Figure 59. Histograms of average MFI changes before and after 1250μM carboplatin treatment

On the other hand, there was a significant rise in average MFI with carboplatin treatment in both pre-treated methanol (p=0.0082) and pre-treated vardenafil (p=0.0078) spheroids. This corresponded with a rise in MFI in 7AAD+ cells for both types of spheroids, with a significant result for the pre-treated vardenafil spheroids treated with carboplatin (p=0.01). This suggested that carboplatin treatment had a significant effect in acting on both types of spheroids, however mainly on the MFD1 cells, judging from the rise in EpCAM positivity, with no difference in CD90 positivity, which represents CAFs. This has led me to question if MFD1 cells were more sensitive to platinum compounds after pre-treatment with vardenafil, evidenced by an increase in MFI (Figure 59A and 59C). Alternatively, my drug dose of carboplatin may have been high enough to cause a noticeable effect on cells such that they were able to uptake sufficient antibody staining

Conversely, there was no difference in drug treatment on CAFs, thought there was a slight MFI drop in the pre-treated vardenafil spheroids after carboplatin treatment. This may be attributed to vardenafil acting on the CAFs and making those cells slightly sensitive to drug treatment such that carboplatin acted on them and made them non-viable (Figure 59B).

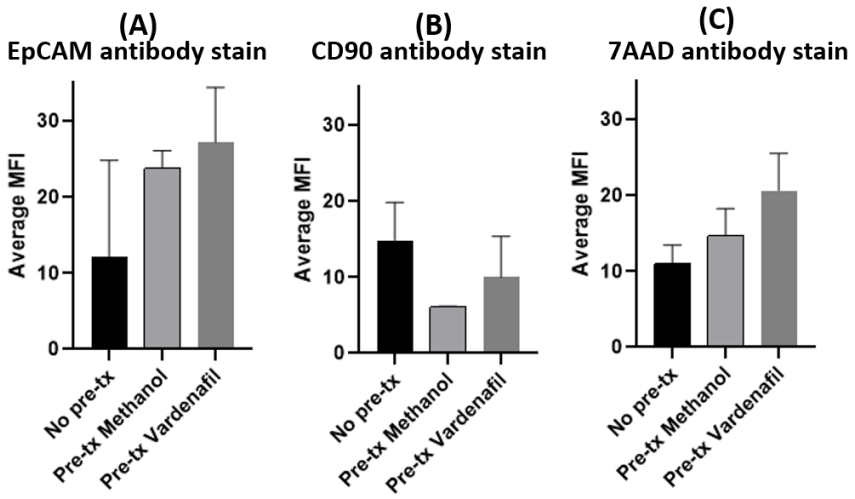

Figure 60. Histograms demonstrating effects of methanol and vardenafil on average MFI of spheroids

Thinking back about the effect of methanol on either type of cells, I subsequently plated the spheroids with media with no pre-treatment, and found that without pre-treatment, there was a lower MFI for EpCAM+ and 7AAD+ cells. The higher level of MFI increased non-significantly with pre-treatment of both methanol and vardenafil, which corresponded to a similar increase in 7AAD+ cells (Figure 60A and C). This appeared to suggest that both methanol and vardenafil alone had an effect on the MFD1 cells. We know from Chapter 4.2 that MFD1 contains a small proportion of PDE5, and therefore the pre-treatment may have acted on the MFD1 cells in the spheroids and made them less viable. On the other hand, the spheroids pre-treated with methanol or vardenafil achieved a lower starting MFI in CD90+ cells in the absence of chemotherapy, indicating that even with pre-treatment, there was more resistance of the spheroids to take up antibody stain, signifying that pre-treatment may have tightened the central core of CAFs, and did not allow for stain to be penetrate or be taken up by the cells in the central region.

4.8 Discussion

This chapter has demonstrated that there was high PDE5 expression in fibroblasts by qRT-PCR, which appeared consistent on a cellular protein level, and that it was more pronounced in CAFs than NOFs or epithelial cancer cells. From published literature, PDE5 expression is reported to occur in solid carcinomas of the head and neck, thyroid and GI tract[239 241 242 244]. In particular, PDE5 was found to be highly expressed in CAFs present in prostate and breast cancers[228 230 267], but it has not been reported in the published literature for oesophageal cancer so far. My results have shown that PDE5 is present in oesophageal

adenocarcinoma, particularly in fibroblasts, but is more pronounced in CAFs, and that there was no expression in cancer cells.

CAFs are proven to be important components of the tumour microenvironment, and have an important role in cancer progression, in terms of growth, invasiveness and chemoresistance, as described in Chapter 1.3. My results demonstrated a high PDE5 expression that was consistent in various CAFs despite its diversity, and it had corresponded to a strong α-SMA expression in CAFs and NOFs, but not in epithelial cells on qRT-PCR and immunoblot. When CAFs were treated with vardenafil, protein expression of α-SMA in CAFs was diminished. This suggested that PDE5 inhibition partially deactivates CAFs, such that there was less protein expression of α-SMA.

Moreover this drop in α-SMA was effectively sustained with a once-daily vardenafil treatment, compared with vardenafil treatment every 3 days. CAFs treated with a once-daily dose had a significant drop of 82.7% in α-SMA expression, while those with a 72-hour dose had a 46.4% decrease in α-SMA expression. This suggested that it might be a better option to have a once-daily dose to achieve a sustainable effect once the treatment is used in the clinical setting.

A positive effect was seen in my colony growth assays in the absence of chemotherapy, with a significant increase of colony growth when in CAF-CM, while those in vardenafil-treated CM were diminished. This positive finding was reproducible with CM from another CAF, which reflects that despite the heterogeneity of CAF, it can still produce a similar effect. This proved that there are factors within the conditioned medium that increase colony growth.

In the presence of chemotherapy, this positive finding was not found to be significant in dose-response assays. MFD1 cells were slightly more resistant to carboplatin, oxaliplatin and 5FU, requiring a higher drug concentration (non-significant) to kill 50% of cells when in CAF-CM, compared to CM from vardenafil-treated CAFs. The effect of sensitisation of the epithelial cancer cells, thought to be attributable to factors secreted by CAFs, appeared to be more obvious in cytostatic (colony growth) assays rather than cytotoxic (dose-response) assays.

In the absence of chemotherapy, MFD-only spheroids had a lower metabolic activity, while MFD/CAF co-cultured spheroids had an enhanced basal metabolic activity, which was diminished with vardenafil treatment. This indicated that PDE5 inhibition could have a useful effect on the co-culture, by action on both types of cells, to reduce the augmented metabolic activity when CAFs are present. The PDE5i may also have acted on the MFD1 cells, as it appeared that these cells had expressed some PDE5, compared to other epithelial cell lines. This is relevant as my experiments were performed in a 3D model, as a reflection of

the TME. Further experiments could be considered to replace the MFD1 cells with other epithelial OAC cell lines to determine if it would give a reproducible result.

In the presence of chemotherapy, the PDE5i pre-treatment appeared to sensitise the MFD1 cells, and there was evidence of chemoresistance of the pre-treated spheroids for both MFD-only and co-cultured spheroids, especially with platinum compound treatment. There was a variability in results, which could be due to the diverse nature of the different CAFs used in the spheroids.

With regards to the flow cytometry results, methanol and vardenafil appeared to have some initial effect on co-cultured spheroids, compared with untreated spheroids, in the absence of chemotherapy. Pre-treatment with either drug increased their MFI in EpCAM+ cells, which corresponded to a similar increase in 7AAD+ cells. Pre-treatment may have had an effect more on the MFD1 cells and made them less viable. Comparing my controls of pre-treated methanol spheroids against the pre-treated vardenafil spheroids, the former generated a higher MFI, which coincided with a rise in 7AAD+ and CD90+ cells. It highlighted that pre-treatment may have had effects on both types of cells, but was more pronounced with vardenafil treatment.

When the pre-treated spheroids were treated with chemotherapy, there was a non-significant MFI decrease in EpCAM+ cells in pre-treated vardenafil spheroids, more so in platinum compounds than 5FU, which implied that pre-treatment had sensitised a proportion of cells, and those subsequently got killed by drug therapy, with a corresponding rise in 7AAD+ cells. There did not appear to have much change to the uptake of CD90 antibody stain. One hypothesis is that the concentric cores that spheroids form appeared to be very dense and did not allow secreted factors from the conditioned medium to act on the cells within the core of the spheroid, due to tightly connected cell-cell interactions. With vardenafil pre-treatment, the spheroidal core may have opened up partially, thereby permitting the drug to penetrate through the spheroid, sensitise the cells in the spheroid and allow more cell death to occur. This occurrence may be due to disruption of cell-cell interactions within the spheroid. However, this remains to be investigated.

Further work could also be carried out to determine the location of CAFs and MFD1 cells within the spheroid, using fluorescent markers, in the absences and presence of drug therapy. That will then provide information on what occurs to the cells with drug treatment, and whether drug does penetrate to the central core to achieve an effect on CAFs. Work should also be carried out on the secreted factors within the conditioned medium, to discover the factors present, classify them appropriately, and then focus on investigating a plausible mechanism of action.

4.9 Summary

This chapter has demonstrated that PDE5 was highly expressed in oesophageal adenocarcinoma CAFs, compared to epithelial cells, and that it corresponded with α-SMA that is reflective of CAFs. My results proved an augmented effect in colony growth, which was diminished with conditioned medium from vardenafil-treated CAFs. I demonstrated that once-daily PDE5i treatment was more optimal than a dose every 3 days, to sustain a level effect. Lastly, the spheroid assays appeared to suggest that vardenafil could have some effect on sensitizing cancer cells to chemotherapy, particularly with platinum-based agents, through its effect on CAFs, both via conditioned media or in direct contact, though more work needs to be done to validate these results.

Chapter 5 Tissue Microarray

5.1 Introduction & Aims

So far, my results have demonstrated that CAFs can affect colony growth and dose-responses, and that the chemoresistant effect is ameliorated, to an extent, by PDE5i treatment with vardenafil. My results in chapter 4 also proved that there was high expression of PDE5 in oesophageal CAFs, which was also associated with a high α-SMA expression. However, I had not determined the specific mechanisms PDE5i utilize to influence chemoresistance due to time limitations. Instead, I had sought to examine biomarkers specific to CAFs that might be involved in chemoresistance, and to investigate their relation to survival outcomes in OAC patients.

To date, a meta-analysis looking at IHC biomarkers in OAC had identified 6 markers with prognostic significance, including COX2, CD3, CD8, p53, EGFR and HER2[259]. However, there has been minimal literature about biomarkers in oesophageal CAFs. Alpha-SMA is a strong surrogate marker for CAFs, and a strong relationship between α-SMA and survival outcome had been shown in oral squamous cell carcinoma, with overall and disease-free 5-year survival rates being significantly lower for patients with α-SMA positive CAFs who had been treated with 5FU chemoradiotherapy[195]. Matsuoka *et al* also showed that presence of α-SMA positive CAFs was linked with a higher pT-stage and pN-stage, thus implying a poorer prognosis[195]. This important relationship was further investigated in OAC, which found that high α-SMA expression was common in the OAC stroma and that this group of 183 OAC patients had a significantly poorer overall survival of 48.14 months, compared with patients with a-SMA negative stroma whose mean survival was 78.66 months[162].

Looking at the wider picture of oesophageal cancer, Kwon investigated the gene expression profile of OSCC tissue and found that periostin (POSTN) was one of the 13 genes which were upregulated by more than 70%, and that it was strongly expressed in fibroblasts with IHC[268]. Periostin is an important TGFβ-induced matricellular protein that is secreted by CAFs, and can function as an adhesion molecule promoting cell motility or interact with other ECM proteins[269 270]. It can also act as a ligand for αV/β3 and αV/β5 integrins to support cancer cell migration or become resistant to apoptosis by activation of the PI3K/AKT signalling pathway[162 269]. Saadi *et al* determined 12 dysregulated genes in BO patients, which included α-SMA, FAP, IL6 and periostin[270]. Underwood *et al* also looked at a publicly available OAC microarray dataset and identified POSTN as an important ECM protein in OAC that was located in blood vessel walls in normal oesophageal mucosa, but was localized to the stromal-cancer cell interface in OAC. Moreover, high expression of POSTN

corresponded with areas of high α-SMA expression and were associated with a significantly poor survival of 46.8 months, compared to patients with minimal POSTN staining with a mean survival time of 76.45 months, and they had a shorter time to recurrence[162].

Interestingly, nestin has been shown to play a significant role in drug resistance, specifically dependent on P-glycoprotein involvement[271]. Nestin is a class VI intermediate filament protein that is predominantly expressed in neural stem cells and musculoskeletal cells like vascular smooth muscle cells. It was initially found to be highly expressed in GISTs[272], and had also been detected in solid cancers such as pancreas, breast, prostate, thyroid and gastric cancers[273]. Nestin has been described to aid in cell proliferation and disassembly of vimentin filaments during mitosis[274]. It has also been reported to be involved in the process of invasion, metastasis, and angiogenesis, especially when it was found to be highly expressed in vascular endothelial cells in metastatic cancer lesions and in pancreatitis and vascular malformations[273]. Poorer survival outcomes were noted in lung cancer patients that had positive nestin expression in cancer cells.

Pertaining to oesophageal cancer, nestin was detected in more than half of cases with dysplastic Barrett's oesophageal mucosa, and this important finding was postulated that it could be a marker for malignant transformation in BO[275]. When investigated in OSCC tumour cells, it was found to be highly expressed in cell lines and specimens, and related to cancer cell proliferation and a poorer prognosis, with shorter overall and disease-free survival[276 277]. When investigated in OAC patients, nestin was found to be an important up-regulated protein in proteomic analysis[278]. IHC staining of the TME revealed that nestin staining was confined to CAFs, vasculature and smooth muscle cells, and their presence was correlated with poor overall survival for 34 patients[278]. Interestingly, out of their cohort of 189 patients, only 34 patients (18%) had positive staining for nestin in the stroma, which implied that it may work as a distinct biomarker that is associated with poor prognosis.

Therefore, my aim was to examine the presence of PDE5, α-SMA, periostin and nestin in tumour tissue, stroma and lymph node tissue, and if it showed any relation to survival outcomes. This was done through IHC staining, and has been performed for the largest cohort of OAC patients to date. IHC staining was utilized as it was one of the more sensible ways to assess protein expression in solid cancers, as it is standardised and can be focused on specific areas and a variety of biomarkers could be tested[259]. This will inform on future studies, so as to investigate the effect of the presence of these biomarkers in cancer progression and chemoresistance of OAC, and provide starting information for other solid cancers.

5.2 Construction of clinico-pathological OAC database & description of TMA creation and scoring methodology

Due to minimal information available from the Tissue Bank, I went through all available data in the Tissue Bank and identified all available oesophageal tissue from 2009 onwards. The list was also updated with patients' demographics, clinic-pathological information, including type of therapy, post-operative histological staging, and survival outcomes. The Tissue Bank patient list was then cross-referenced with the prospectively-collected UGI resectional database, which included oesophageal operations at UHS from 2000 onwards, and a final list of patients from 2010-2015 with OAC resected and suitable for TMA analysis was created (Figure 61). Follow-up was recorded until end of 2016. Further methodology is described in Chapter 2.8.

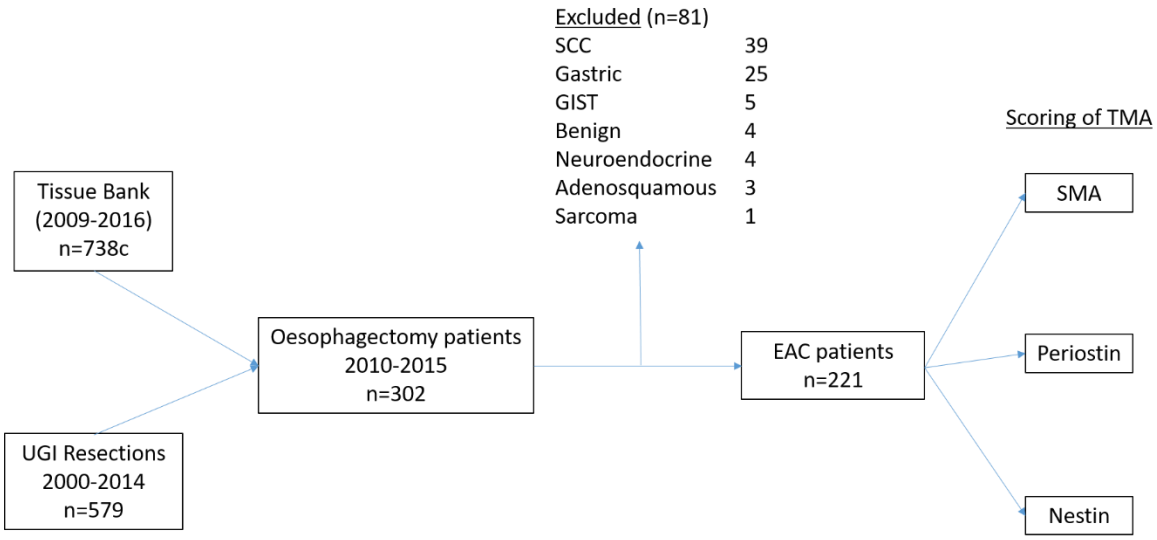

Figure 61. Flowchart demonstrating acquisition of OAC patients for TMA scoring

Haematoxylin and eosin stained (H&E) slides from this cohort of patients were retrieved from the Histopathology Department at UHS, together with their paraffin blocks. The H&E slides were marked in triplicate for tumour, stroma, and positive lymph nodes, by Dr E Jaynes (Consultant Histopathologist). These were then placed on corresponding blocks to allow identified areas cored and inserted on the donor block. The TMAs were then created in triplicate, and a meticulous record of the positioning of the donor tissue was documented. Sections were cut from the TMA and mounted on positively charged SuperFrost slides, and automated staining was performed with various antibodies applied to each slide for TMA cores. Scoring was then instituted.

Different methods have been described in scoring TMAs, based on the staining intensity or the proportion of epithelial nuclei stained. Evaluation of IHC results is usually reported by a standardised semi-quantitative approach of calculating the H-score (histochemical score), which takes into account different staining intensities as well as the factor intensity to the percentage of positive cells, and gives a range between 0-300[279]. A discriminatory threshold can be decided, then the sample can be considered positive or negative based on that threshold.

TMA scoring should ideally be performed by different pathologists, and at different time points, so as to minimise inter- and intra-observer variability. Scoring can performed either manually by pathologists, or be automated. However, due to limitations of time and resources, scoring of my TMA was done by 2 surgeons, performed at different time periods. Using light microscopy, each core was scored on proportion of staining in the relevant areas. For simplicity, intensity of the stain was disregarded during the scoring process.

Table 9. Demographics and clinico-pathological variables for overall OAC patient cohort

Overall, n=221	Mean	Median	n	%
Age (years)	68.72	69.70		
Overall Survival (months)	30.39	24.89		
Gender	Male	189	85.5%	
	Female	32	14.5%	
Treatment Modality	Chemotherapy	150	67.9%	
	Chemonaive	71	32.1%	
Performance status	0	70	31.7%	
	1	84	38.0%	
	2	12	5.4%	
	Unknown	55	24.9%	
BMI	<25	21	9.5%	
	25-29.9	27	12.2%	
	30-34.9	19	8.6%	
	>35	6	2.7%	
	Unknown	148	67.0%	
T-stage	T0	5	2.3%	
	T1	6	2.7%	
	T2	58	26.2%	
	T3	130	58.8%	
	T4	22	10.0%	
N-stage	N0	69	31.2%	
	N1	144	65.2%	
	N2	8	3.6%	

Table 9 reports the demographic and clinico-pathological details of the overall OAC patient group. The median age was 69.7 years, with males predominantly affected. Similar proportions of patients have WHO performance status 0 or 1 (able to carry out normal activity or light work). Just under a quarter have a BMI more than 25, which is interesting as obesity was a recently discovered risk factor for OAC, as described in Chapter 1. Unfortunately, BMI was not available for more than half of the population being studied, therefore it was not considered in our variables. Majority (58.8%) of this group have been staged as T3, with a large proportion (65.2%) having an N1 nodal status. Median follow-up time was 24.59 (95% CI 20.25-28.57) months.

This group was then separated into chemonaive patients and patients who underwent neoadjuvant chemotherapy to determine if there were any differences between the groups.

Table 10. Demographics of patients that proceeded straight to surgery

Chemonaive, n=71	Mean	Median	n	%
Age (years)	73.47	77.07		
Overall Survival (months)	28.82	22.95		
Gender	Male	57		80.3%
	Female	14		19.7%
T-stage	T0	4		5.6%
	T1	5		7.1%
	T2	30		42.3%
	T3	29		40.8%
	T4	3		4.2%
N-stage	N0	35		49.3%
	N1	34		47.9%
	N2	2		2.8%

Table 10 details the demographic data of patients who underwent surgery alone. This group of patients appeared to be older, with a median age of 77.07 years, with a slightly shorter overall survival time of 22.95 months. As expected, the group consisted of predominantly males, with similarly proportions of people with T-stage (T2/3) and N-stage (N0/1).

Usually, straight to surgery management is reserved for patients with stages 1 or occasionally 2A (T1-3 N0). Strangely, there was a sizeable proportion of node-positive patients, and even some patients with T_4 tumours, that proceeded straight to surgery. This was quite bizarre, as usually these patients would have been offered NAC to downstage their disease before surgery, but perhaps these patients had chosen to exercise their choice of treatment to be surgery first, and then have adjuvant treatment post-operatively if it was deemed necessary. Alternatively, they might have been understaged prior to surgery. Taking into account that treatment options were evolving during the period of the population

group being studied (2010-2015), it might account for the shorter survival time due to the poorer prognosis of these patients.

Table 11. Demographics of patients that had neoadjuvant therapy prior to surgery

Overall, n=150	Mean	Median	n	%
Age (years)	66.47	67.80		
Overall Survival (months)	31.14	26.42		
Gender	Male	132		88.0%
	Female	18		12.0%
T-stage	T0	1		0.7%
	T1	1		0.7%
	T2	28		18.7%
	T3	101		67.3%
	T4	19		12.6%
N-stage	N0	34		22.7%
	N1	110		73.3%
	N2	6		4.0%
Tumour Regression Stage (TRG)	TRG1	15		10.0%
	TRG2	33		22.0%
	TRG3	17		11.3%
	TRG4	39		26.0%
	TRG5	43		28.7%
	Unknown	3		2.0%

Focusing on the group of patients that had neoadjuvant treatment involving chemotherapy, this group accounted for two-thirds of the overall group. This predominantly-male cohort had a similar median age of 67.8 years, with an overall survival time of 26.42 months.

Majority of patients in this group had T3N1 disease. 69.3% of patients had demonstrable signs of local pathological tumour regression (TRG 1-4). Interestingly, despite having chemotherapy, this subgroup only had 32% of patients who were considered responders to neoadjuvant therapy (TRG1 or TRG2) in these histopathological specimens, while 54.7% of patients had minimal or no response (TRG4 or TRG5). This reiterates the concept that OAC appears similar to pancreatic cancer, being partially resistant to neoadjuvant chemotherapy treatment. If we are able to target this subgroup of patients to make them more responsive to chemotherapy, that could help to downstage the disease, improve R0 resections and prolong overall survival times.

Moving forward, I will be exploring the expression of PDE5, α-SMA, periostin, and nestin in my cohort of patients and examine their relation to survival outcomes. I had chosen these biomarkers to investigate as they were reflective of CAFs (α-SMA and periostin) based on Underwood et al's publications, as well as their relation to drug resistance (PDE5 and nestin). My hypothesis was that tissue positive for each biomarker was associated with poorer survival.

5.3 Expression of PDE5

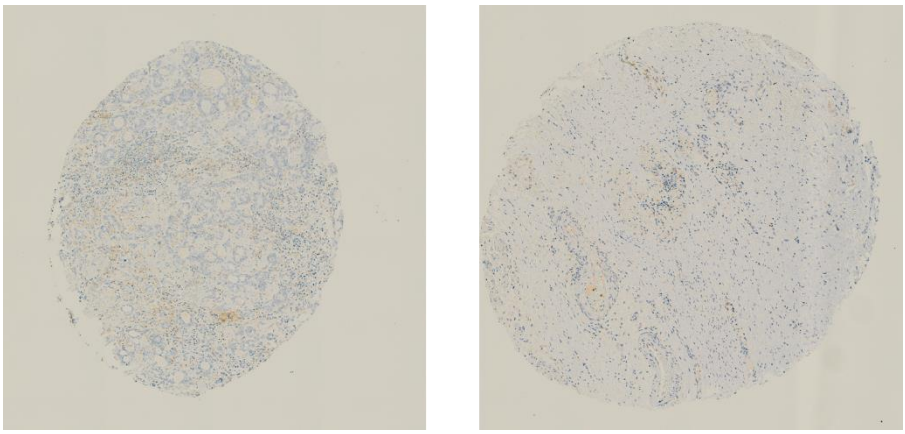

Figure 62. IHC staining for PDE5 antibody, Santa-Cruz, 1:500 dilution

As PDE5 had been proven to be present in the stroma, I had performed a trial of IHC staining of tumour stroma with a PDE5 antibody from, Santa Cruz, which I had used for my western blotting experiments, with a range of dilutions ranging from 1:100 to 1:500, as advised by the manufacturer (Appendix B). Unfortunately, the stain was not taken up adequately, despite changing dilutions or using newly-bought vials of antibody. I was also unable to obtain antibodies produced by other manufacturers such as Abcam or ThermoFisher within the expected time frame, therefore this has been put on hold.

Future work can be done to optimise IHC staining of PDE5 on my TMA. Once that has been carried out, it can be used on another cohort of patients to validate the potential for PDE5 to act as a biomarker.

5.4 Expression of α-SMA and association with survival/prognosis

Alpha-SMA is expressed mostly in CAFs, which are large spindle-shaped cells that react with the α-SMA antibody. Using IHC, I examined the proportion of staining for α-SMA positive cells in the TMAs of tumour, stroma and lymph node tissue for OAC patients. Stain

appeared to be taken up by blood vessels, cell membranes and within cytoplasm of stromal cells.

For each specimen, a score was assigned based on the amount of positive staining present in the cancer cells, stroma and lymph node tissue. Scores were allocated for proportion of staining – 1 for less than 10% of staining, and was considered to be α-SMA negative. Scores 2 and 3 were allocated for 10-50% staining and greater than 50% respectively. If there was insufficient or no tissue prepared in the TMA, the core was excluded from the scoring, and labelled as not applicable.

Tumour TMA

For the tumour TMA, 182 cores in triplicate were scored out of 221, with a capture rate of 82.4%.

Table 12. Clinico-pathological features of α-SMA staining of tumour TMA

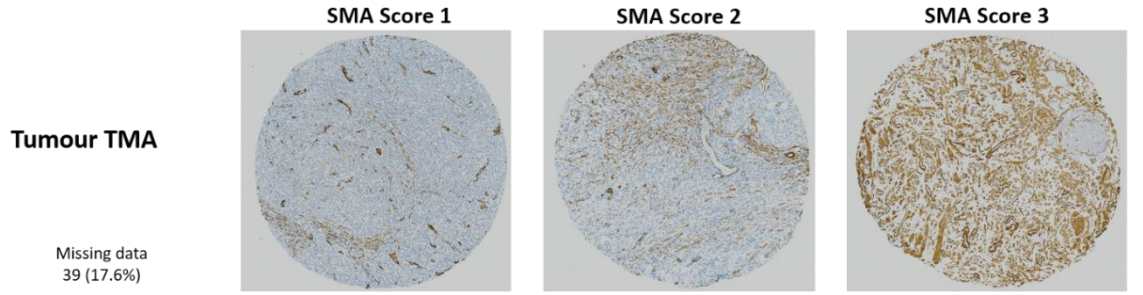

		SMA Score 1	SMA Score 2	SMA Score 3
n (% of total stained)		19 (10.4%)	87 (47.8%)	76 (41.8%)
Median Age (years)		73	70	70
Gender		15 male, 4 female	78 male, 9 female	65 male, 11 female
pT-stage	T0-1	8	21	15
	T2	4	12	6
	T3	5	48	44
	T4	2	6	11
pN-stage	N0	10	44	26
	N1	4	19	18
	N2+	5	24	32
Treatment	Surgery only	7	31	27
	Chemotherapy	12	56	49
Tumour Regression Grade	TRG1	12	1	0
	TRG2	1	15	10
	TRG3	2	3	7
	TRG4	2	19	13
	TRG5	5	18	19

Table 12 details the demographics and pathological features of the 3 groups with α-SMA staining. All 3 groups had predominantly males and similar median ages. Majority (89.6%) of the groups who scored 2 and 3 had a pathological stage of T3 and nodal positive, who underwent NAC. A large proportion of those who had NAC and scored 2 (71%) and 3 (80%) were considered non-responders (TRG 3-5). Interestingly, in the group with SMA score 1, 12 out of 19 patients had T0-2 disease and just over 50% were nodal negative. Not surprisingly, it corresponded to 68.4% of patients classed as having responsive disease (TRG 1 or 2).

Kaplan-Meier survival analysis was performed on these groups. A log-ranked test was used to determine the relation between α-SMA staining of tumour and survival, with p-values less than 0.05 considered to be statistically significant.

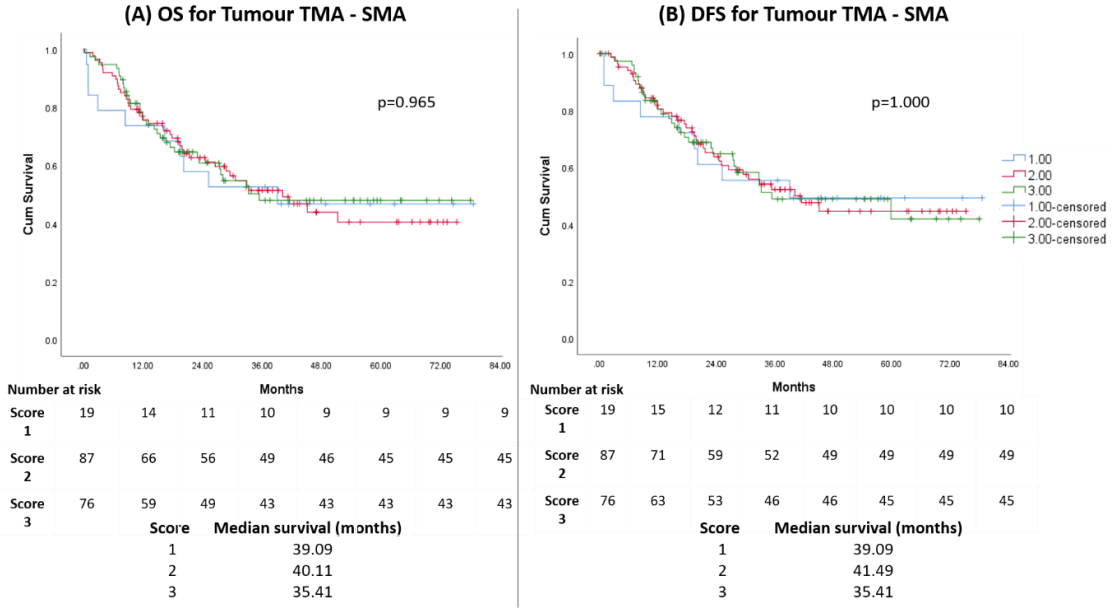

Figure 63. Kaplan-Meier curves showing overall survival (A) and disease-free survival (B) for tumour tissue stained with α-SMA

Figure 63 illustrate the median survival times for all 3 groups, and the numbers at risk. These demonstrate that there were no differences in overall and disease-free survival amongst the 3 groups on statistical analysis.

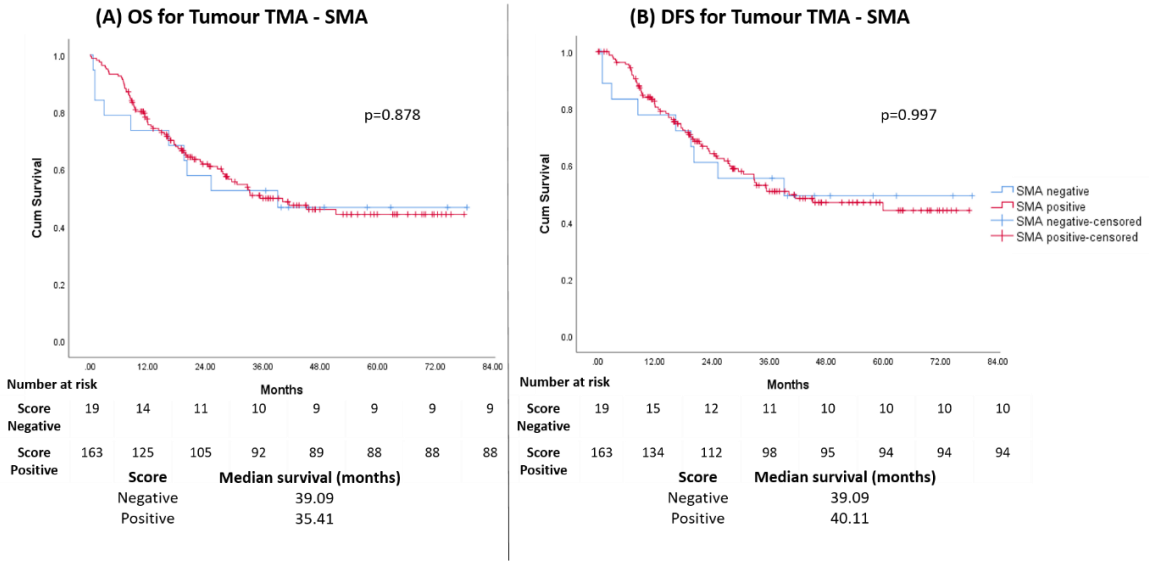

Figure 64. Kaplan-Meier survival curves for overall (A) and disease-free (B) survival of tumour with α-SMA staining grouped into negative and positive groups

Even when the groups were re-classified into α-SMA negative (score 1) or positive (scores 2 and 3), no differences were found in overall or disease-free survival (Figure 64).

Stromal TMA

Table 13. Clinico-pathological features of stromal TMA with α-SMA staining

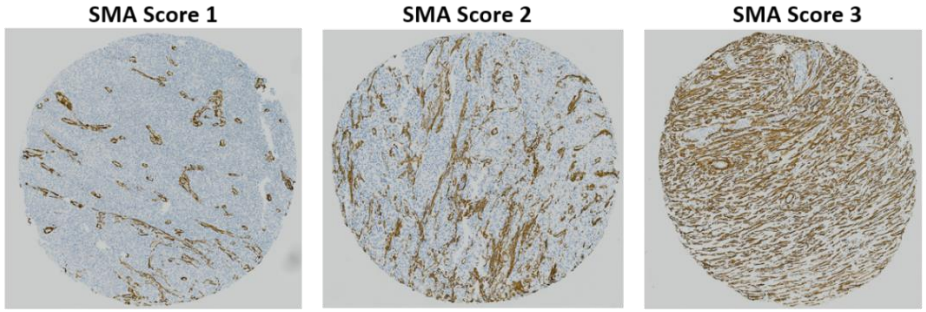

		SMA Score 1	SMA Score 2	SMA Score 3
n (% of total stained)		20 (12.8%)	69 (44.2%)	67 (42.9%)
Median Age (years)		71	69	69
Gender		19 male, 1 female	59 male, 10 female	58 male, 9 female
pT-stage	T0-1	7	16	7
	T2	2	13	7
	T3	10	35	41
	T4	1	5	12
pN-stage	N0	7	33	23
	N1	7	15	13
	N2+	6	21	31
Treatment	Surgery only	6	21	23
	Chemotherapy	14	48	44
Tumour Regression Grade	TRG1	0	2	1
	TRG2	4	9	6
	TRG3	1	8	4
	TRG4	4	14	15
	TRG5	5	15	18

The stromal TMA had a capture rate of 70.6%, with 156 cores scored.

Table 13 details the pathological features of the 3 groups with α-SMA staining of the stromal TMA. All 3 groups had similar median ages. Those with T3 pathology accounted for more than 50% in each group, and over 50% in each group were positive for nodal burden. Over two-thirds had NAC prior to surgery, and yet, similar proportions in each group had TRG 3-5, which were considered non-responders to treatment.

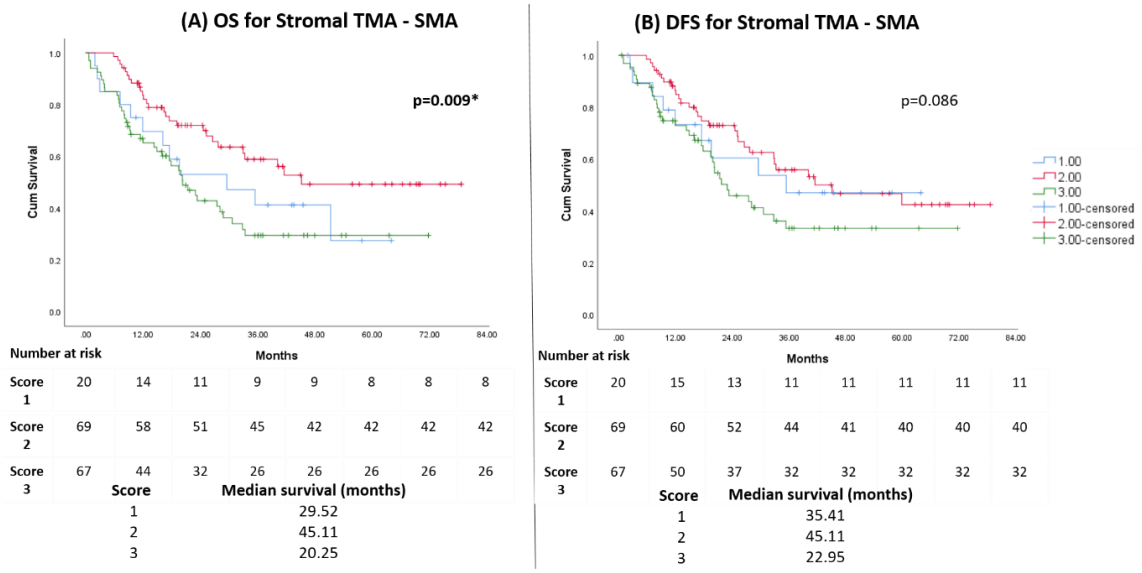

Figure 65. Kaplan-Meier curves showing overall (A) and disease-free (B) survival of stroma that was stained for α-SMA

Figure 65 illustrate the OS and DFS survival curves for the stromal TMA and the numbers at risk. It appeared that there was poorer survival if >50% of the stroma stained with α-SMA, compared to those who stained 10-50% of the stroma. However, Figure 65B seemed to suggest that there might be a disease-free survival advantage if <50% of the stroma was stained with α-SMA. Overall, there was a significant difference in overall survival if <50% of the stroma stained with α-SMA, and no significant difference in disease-free survival.

I then proceeded to examine if presence of α-SMA in the stroma (rather than the proportion) had an effect on the survival outcome.

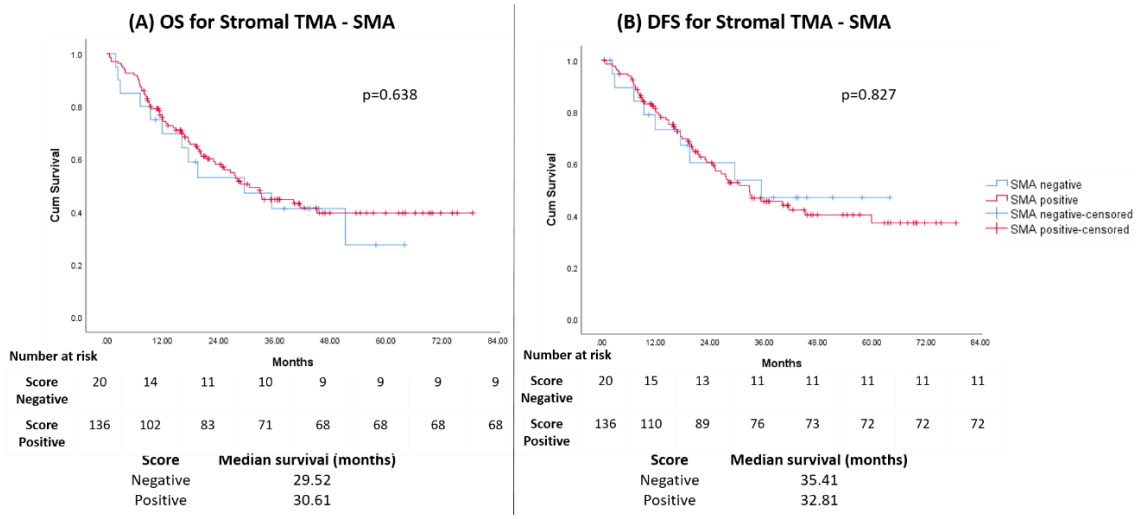

Figure 66. Kaplan-Meier curves of overall (A) and disease-free (B) survival of stroma stained with α-SMA grouped into negative and positive groups

Figure 66 showed no survival differences in the absence or presence of α-SMA in the stroma. This was slightly strange, as it did not correspond with Underwood *et al*'s publication

which reported that both moderate-high expression of α-SMA correlated with a lower overall survival after surgery[162]. This disparity may be due to subjective scoring of the cores. We will consider if NAC was a factor affecting the survival outcomes, in our analysis later in Chapter 5.7.

Lymph Node TMA

For the LN TMA, only those with positive pN-stage were selected to be in the TMA, as I wanted to investigate if there were any particular findings for patients with nodal burden. There were 108 patients who were node-negative, and 113 patients who were node-positive. Out of the latter, 97 out of the 113 were scored, resulting in a capture rate of 85.8%.

Table 14. Clinico-pathological features of α-SMA staining of lymph node (LN) TMA

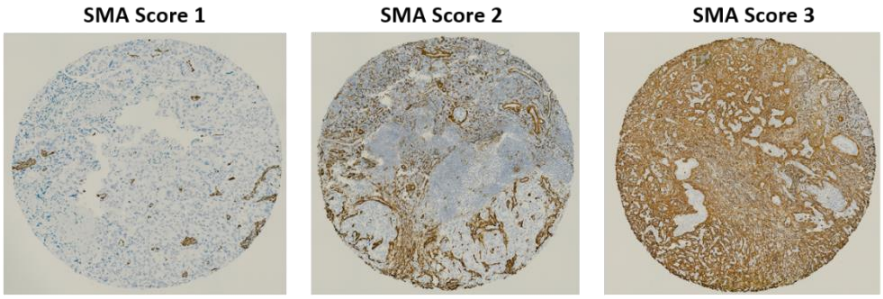

		SMA Score 1	SMA Score 2	SMA Score 3
n (% of total stained)		14 (14.4%)	34 (35.1%)	49 (50.5%)
Median Age (years)		70	69	70
Gender		12 male, 2 female	32 male, 2 female	42 male, 7 female
pT-stage	T0-1	3	3	1
	T2	0	5	2
	T3	9	21	36
	T4	2	5	10
pN-stage	N1	10	12	14
	N2	2	15	18
	N3	2	7	17
Treatment	Surgery only	4	12	23
	Chemotherapy	10	22	26
Tumour Regression Grade	TRG1	1	2	1
	TRG2	2	2	1
	TRG3	2	2	1
	TRG4	4	7	5
	TRG5	1	9	18

Table 14 provides the pathological features of the 3 groups with α-SMA staining for the LN TMA. In this group of patients with positive nodal burden, majority (>50%) of them had at least T3 tumour pathology. In the group with α-SMA staining score 3, there were equal proportions of people who had either surgery only or who had NAC prior to surgery. All groups had similar median ages, with no differences in pathological staging between the groups. Groups scoring 2 and 3 were noted to have a higher TRG status, with at least 50% of patients were considered non-responders (TRG3-5).

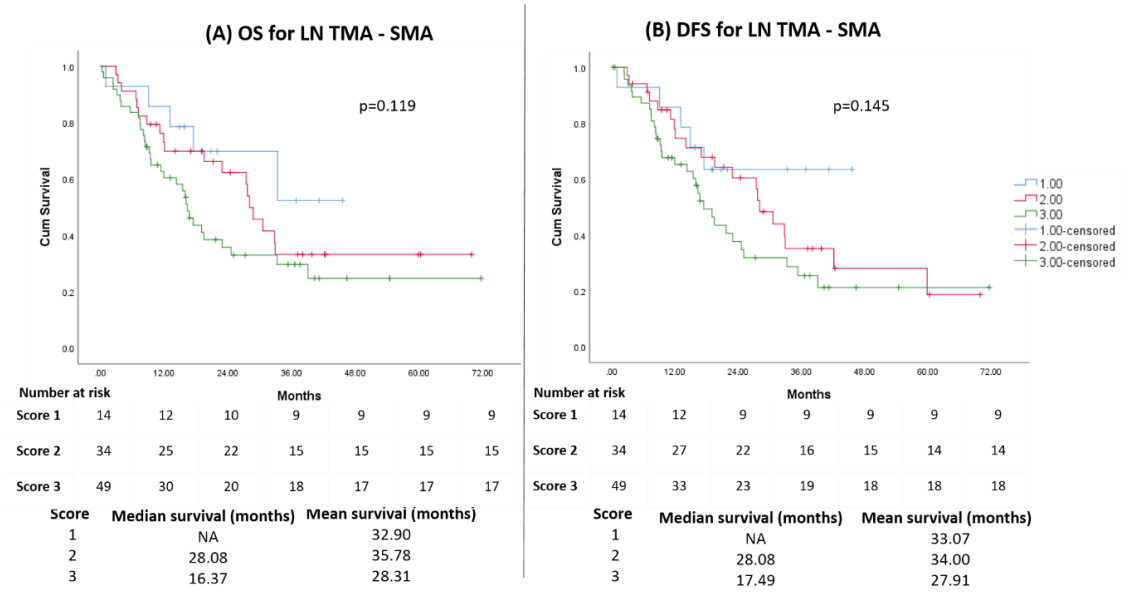

Figure 67. Kaplan-Meier curves of overall (A) and disease-free (B) survival of positive LNs that stained for α-SMA

As for the TMA from positive lymph nodes, there appeared to be a lower median survival with increasing expression of α-SMA, however median survival was not able to be calculated for those scoring 1 (<10% α-SMA staining) (Figure 67), as it had not reached cumulative survival of 0.5 yet. However, this implied that patients with positive lymph nodes upon resection may improve their survival if their CAFs could be reverted, so that α-SMA could be downregulated.

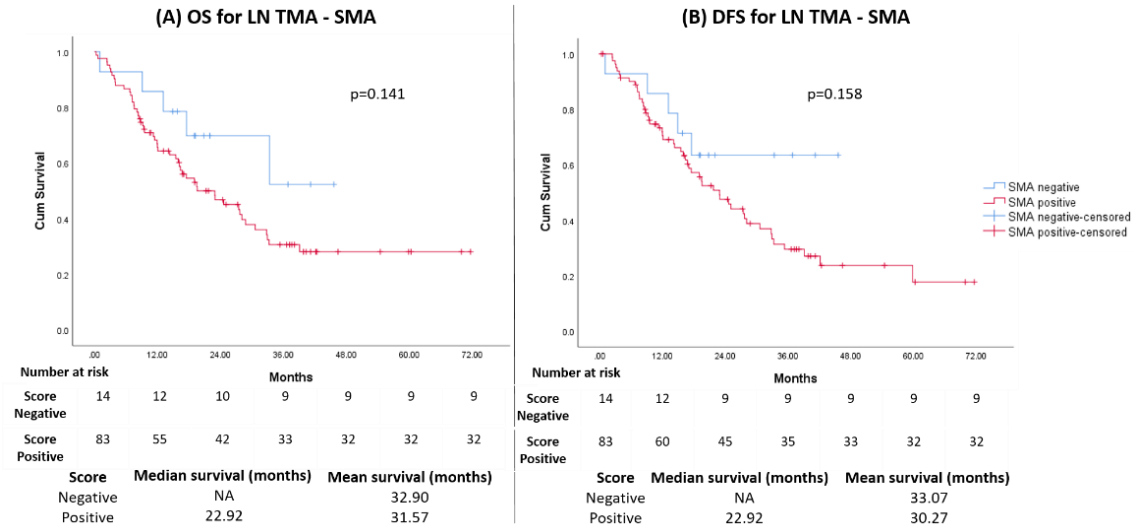

Figure 68. Kaplan-Meier survival curves for overall (A) and disease-free (B) survival for LNs segregated into negative or positive α-SMA staining

When scores 2 and 3 were combined into an α-SMA positive group, the results showed a trend, with this group tending to a poorer median survival than that of the α-SMA negative group. However, it did not show any significant difference in OS or DFS, probably because a median survival could not be calculated for the α-SMA negative group (Figure 68).

5.5 Expression of Periostin

Similarly for periostin, according to the proportion of staining in the core, each specimen was allocated a score: 1 – less than 10% of staining, and considered to the POSTN-negative; 2 – 10-50% staining, and 3 – greater than 50% staining visualized, and both scores were considered to be POSTN-positive. The specimen was excluded from scoring if there was inadequate tissue in the TMA. Stain appeared to be taken up by cell membranes of tumour cells, blood vessel walls and within cytoplasm of stromal cells.

Tumour TMA

Table 15. Clinico-pathological features of periostin staining of tumour TMA

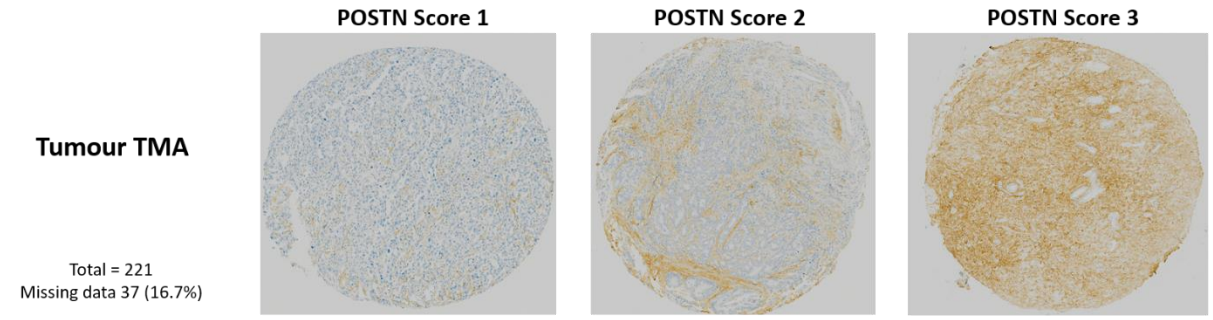

n (% of total stained)		59 (32.1%)	82 (44.6%)	43 (23.4%)
Median Age (years)		71	71	68
Gender		50 male, 9 female	71 male, 11 female	39 male, 4 female
pT-stage	**T0-1**	24	16	4
	T2	9	12	2
	T3	22	46	30
	T4	4	8	7
pN-stage	**N0**	40	30	12
	N1	12	19	10
	N2+	7	33	21
Treatment	**Surgery only**	24	29	12
	Chemotherapy	35	53	31
Tumour Regression Grade	**TRG1**	1	1	1
	TRG2	9	9	8
	TRG3	4	5	4
	TRG4	13	12	10
	TRG5	8	26	8

Table 15 illustrate the clinico-pathological demographics of the groups scoring 1-3 for periostin staining of tumour. The capture rate of this TMA stained was 83.3%, with 184 cores stained.

The median age for those scoring 3 was slightly younger at 68 years, compared with 71 years in the groups scoring either 1 or 2. For patients in the group scoring 1 on periostin staining, similar proportions had T0/1 or T3 pathological staging, and 68% of this group was node negative, while for those scoring 2 and 3, majority of them had T3 pathology, and had positive nodal burden. As expected, at least 60% in each group had NAC prior to surgery, and yet greater than 70% of patients in each of the 3 groups had poor non-responder TRG status 3-5.

I looked at this in relation to the survival outcomes and Figures 69-70 demonstrate my findings.

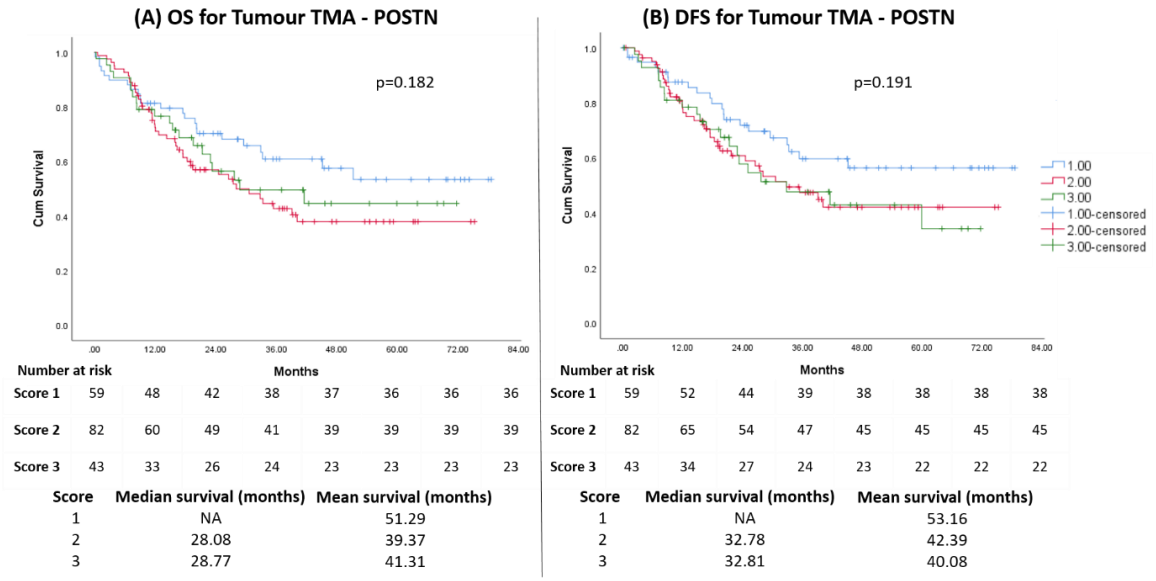

Figure 69. Kaplan-Meier survival curves of tumour TMAs with POSTN staining for overall (A) and disease-free (B) survival

Figure 69 show no significant differences in survival outcomes for periostin staining of tumour TMA. However, the higher median survival for those scoring 1 on periostin staining could not be calculated as it had not reached a cumulative survival of 0.5 yet.

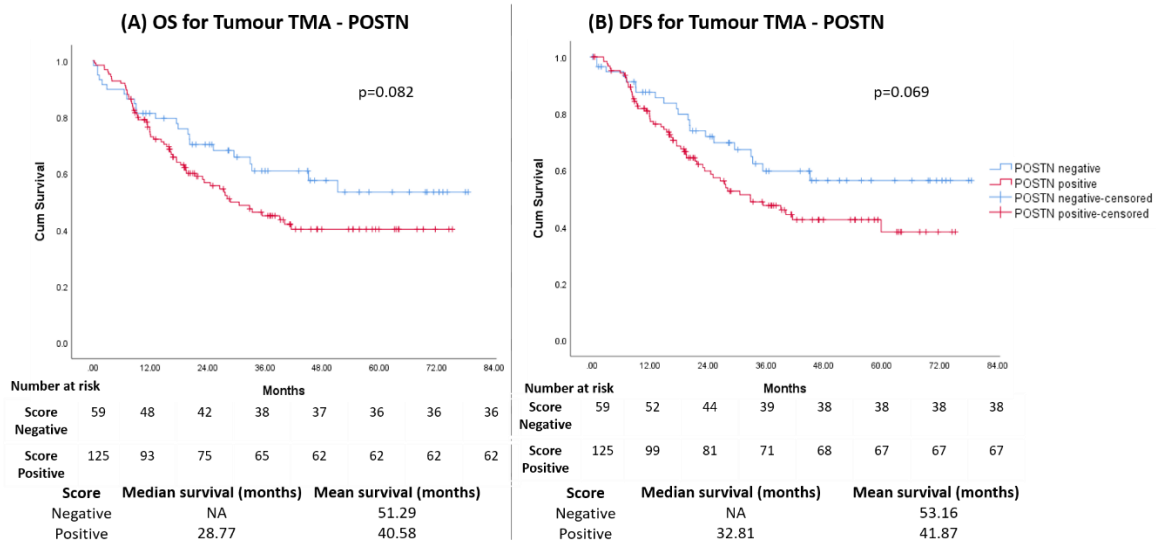

Figure 70. Kaplan-Meier curves for overall (A) and disease-free (B) survival in tumour TMA stained with periostin and grouped into negative or positive groups

When the groups were re-classified into negative (score 1) or positive (scores 2&3) for periostin, it appeared that there was a survival advantage in both OS and DFS if they were negative for periostin (<10% staining by proportion), though the survival differences were not significant (Figure 70).

Stromal TMA

Table 16. Clinico-pathological features of periostin staining of stromal TMA

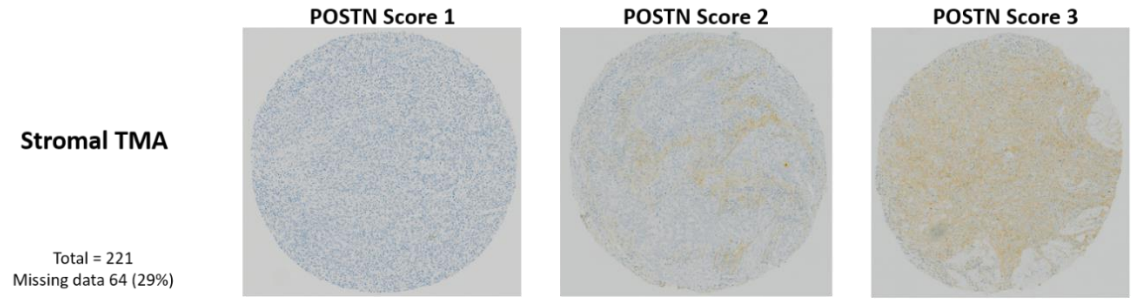

n (% of total stained)		51 (32.5%)	49 (31.2%)	57 (36.3%)
Median Age (years)		68	72	70
Gender		43 male, 8 female	42 male, 7 female	52 male, 5 female
pT-stage	**T0-1**	15	6	9
	T2	8	9	5
	T3	21	32	34
	T4	7	2	9
pN-stage	**N0**	22	22	19
	N1	13	10	13
	N2+	16	17	25
Treatment	**Surgery only**	11	16	23
	Chemotherapy	40	33	34
Tumour Regression Grade	**TRG1**	1	1	2
	TRG2	9	4	6
	TRG3	4	6	3
	TRG4	14	7	12
	TRG5	12	15	11

Table 16 illustrate the clinico-pathological features of the 3 groups with stromal periostin staining. The capture rate of staining for the stromal TMA was 71%, with 157 cores stained and scored.

The median age in all 3 groups were similar, between 68-72 years. Those in the group scoring 1 had 45% of patients with early disease (T0-T2), while those scoring 2 and 3 had a larger proportion of patients in each group with more advanced disease (T3 N1+ pathology). Despite the majority of patients (>60%) in each group undergoing NAC prior to surgery, at least approximately two-thirds of these patients have high non-responder TRG status (TRG 3-5).

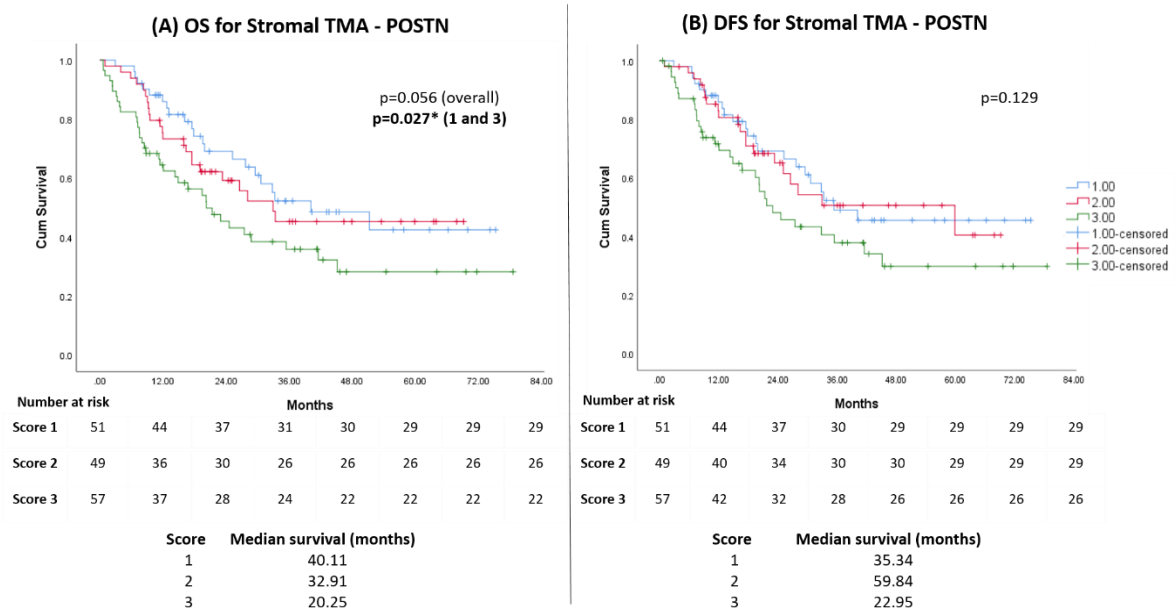

Figure 71. Kaplan-Meier survival curves of stromal TMAs with POSTN staining for overall (A) and disease-free (B) survival

Kaplan-Meier survival analysis indicated that overall survival was low at 20.25 months if over 50% of stroma had periostin staining. This was significant if compared with patients who had less than 10% of their stroma stained with periostin, where median survival was 40.11 months. However, when all 3 groups were analysed together, an association was seen but OS was not statistically significantly (p=0.056) (Figure 71A). Similarly, there were no significant differences in disease-free survival (figure 71B).

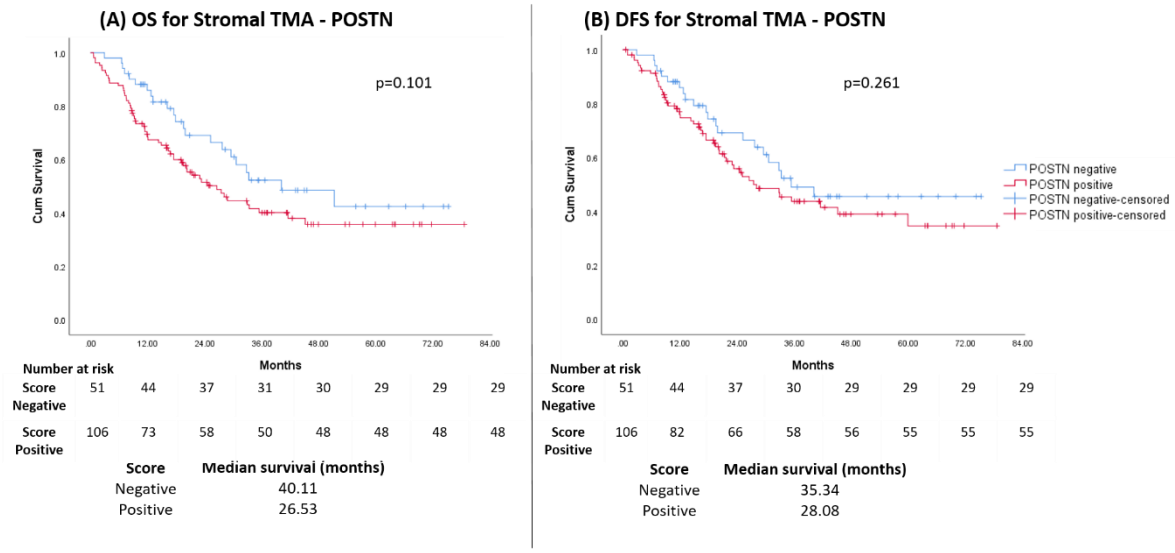

Figure 72. Kaplan-Meier curves for overall (A) and disease-free (B) survival in stromal TMA stained with periostin and grouped into negative or positive groups

When segregated into negative (score 1) vs positive (scores 2&3) periostin groups, although OS and DFS were lower for the POSTN-positive group, the survival outcomes were not significantly different (Figure 72).

Lymph Node TMA

Table 17. Clinico-pathological features of periostin staining of LN TMA

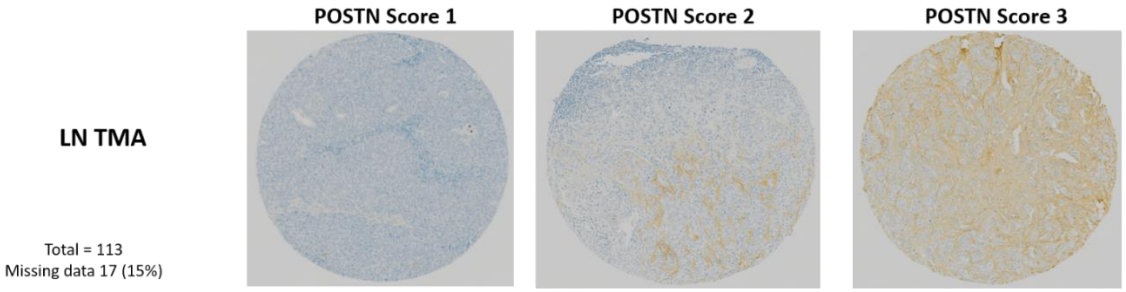

n (% of total stained)		54 (56.3%)	27 (28.1%)	15 (15.6%)
Median Age (years)		69	69	71
Gender		48 male, 6 female	24 male, 3 female	13 male, 2 female
pT-stage	T0-1	6	1	0
	T2	4	2	1
	T3	33	20	12
	T4	11	4	2
pN-stage	N1	21	12	3
	N2	17	10	8
	N3	16	5	4
Treatment	Surgery only	20	12	6
	Chemotherapy	34	15	9
Tumour Regression Grade	TRG1	3	1	0
	TRG2	4	1	0
	TRG3	1	4	0
	TRG4	12	3	1
	TRG5	14	6	8

Out of 113 patients with positive LNs, 85% of the TMA, with 96 cores successfully stained with periostin.

The demographics for all 3 groups were similar, together with their tumour pathology. Majority in each group had advanced disease of T3 or T4 status, which was expected in these patients who had positive LNs. Oddly, more than 37% of patients in each group underwent surgery only, and it was not consistent with those staged with early (T0-2) disease). Even for those who underwent NAC, more than 69% of them had a higher non-responsive TRG status. Perhaps these patients were understaged prior to surgery, which resulted in them having surgery first, or they may have had aggressive disease, which resulted in a positive nodal burden that was resistance to chemotherapy downstaging.

Interestingly, 56.3% of the positive LNs were scored into the first group, with minimal periostin staining, compared with the other 2 groups combined. This is a curious finding, as I had expected most of the positive LNs to have scored 2 or 3 with periostin staining, on the assumption that these patients already had a poorer prognosis with presence of nodal burden. However, this may not be the case and further survival analysis was performed on this TMA stained with periostin.

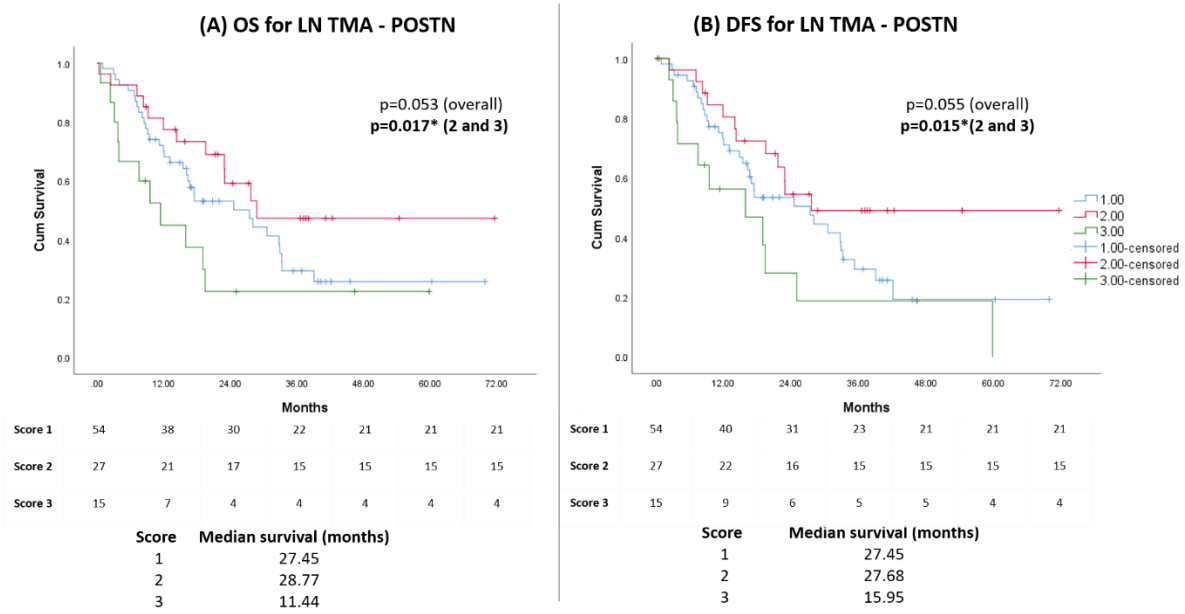

Figure 73. Kaplan-Meier survival curves of LN TMA with POSTN staining for overall (A) and disease-free (B) survival

Figure 73 demonstrate that there was a significant difference in OS and DFS between >50% periostin staining (score 3; median survival 11.44 months) and 10-50% periostin staining (score 2; median survival 27.45 months). However, when all 3 groups were analysed, there was a trend, but no significant differences in OS or DFS for periostin staining in positive LNs.

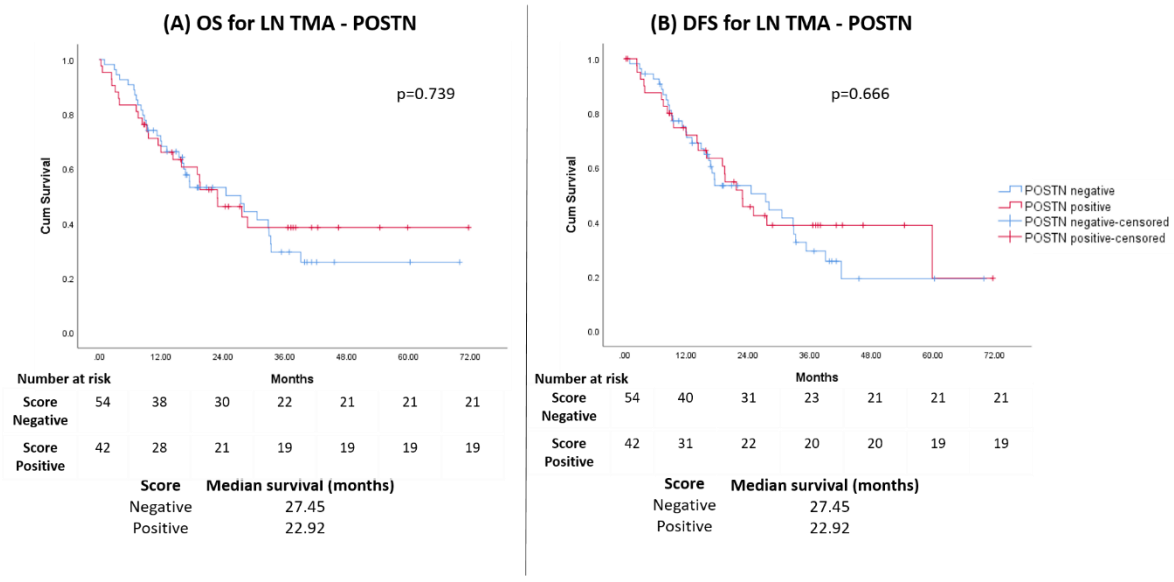

Figure 74. Kaplan-Meier curves for overall (A) and disease-free (B) survival in stromal TMA stained with periostin and grouped into negative or positive groups

On the other hand, when the 3 groups were separated into negative (score 1) or positive (scores 2&3) periostin staining, there was no differences seen in OS or DFS (Figure 74).

5.6 Expression of Nestin

Likewise, nestin coring was based on the proportion of the TMA stained: 1 for less than 10% staining, which was considered to be nestin-negative. Score 2 was assigned for those with 10-50% staining, and score 3 was apportioned to more than 50% staining, both of which was deemed to be nestin-positive. Staining was judged to be taken up by CAFs, blood vessels and smooth muscle cells.

Tumour TMA

Table 18. Clinico-pathological features of nestin staining of tumour TMA

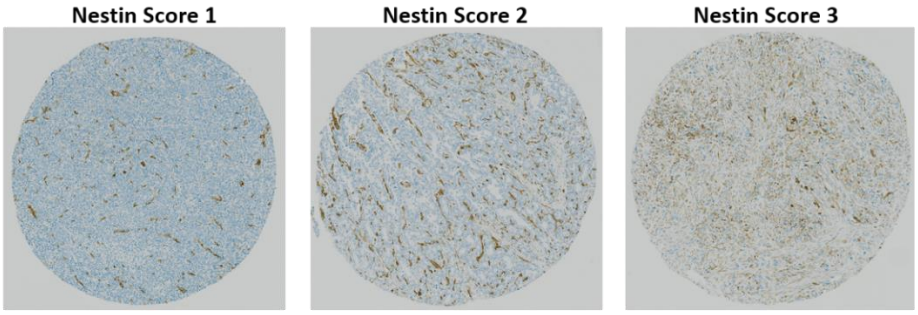

n (% of total stained)		91 (49.4%)	85 (46.2%)	8 (4.3%)
Median Age (years)		70	70	74
Gender		74 male, 17 female	79 male, 6 female	7 male, 1 female
pT-stage	**T0-1**	21	22	1
	T2	6	13	3
	T3	54	42	3
	T4	10	8	4
pN-stage	**N0**	38	39	4
	N1	22	17	3
	N2+	31	29	1
Treatment	**Surgery only**	33	29	3
	Chemotherapy	58	56	5
Tumour Regression Grade	**TRG1**	2	1	0
	TRG2	14	12	0
	TRG3	7	6	0
	TRG4	17	16	2
	TRG5	18	21	3

Table 18 illustrate the demographics and clinico-pathological data for patients scoring 1-3 with regards to nestin staining of tumour. There was an 83.3% capture rate with nestin staining and scoring.

All 3 groups have similar median age, with those scoring 3 having a slightly older median age of 74. Approximately two-thirds of each group had undergone NAC prior to surgery. Nevertheless, more than 50% of those scoring 1 or 2 had T3 tumour pathology, and equal proportions of N0 or N2+ pathology. Two-thirds of patients in these same groups were scored with TRG3-5, and stratified as non-responders.

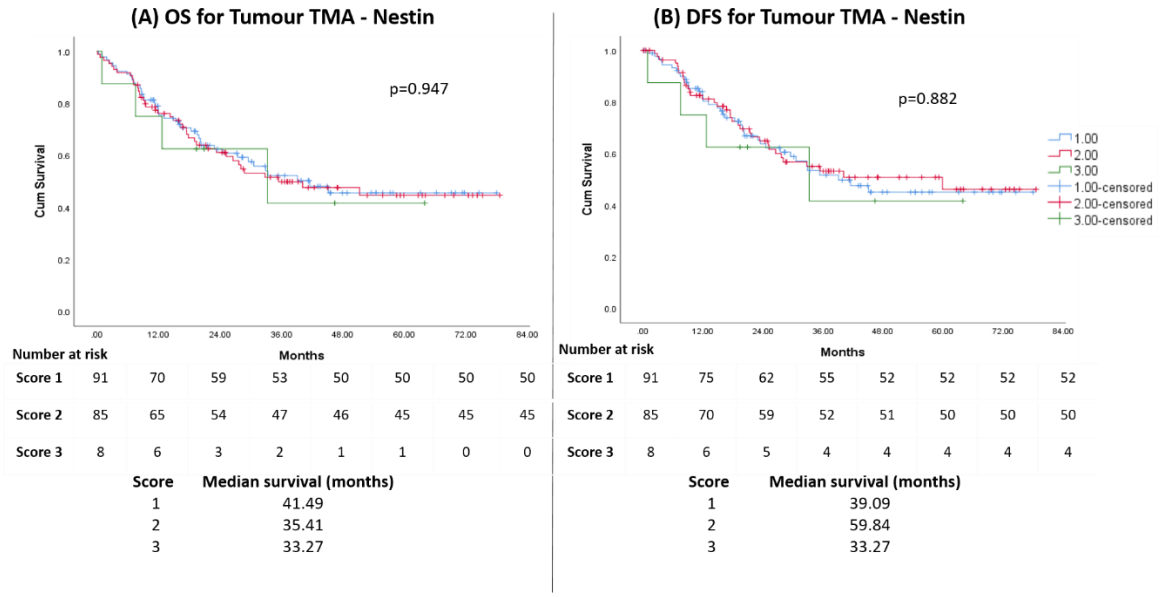

Figure 75. Kaplan-Meier survival curves of tumour TMA with nestin staining for overall (A) and disease-free (B) survival

Figure 75 demonstrate that there was no significant differences in OS or DFS in tumour stained with nestin.

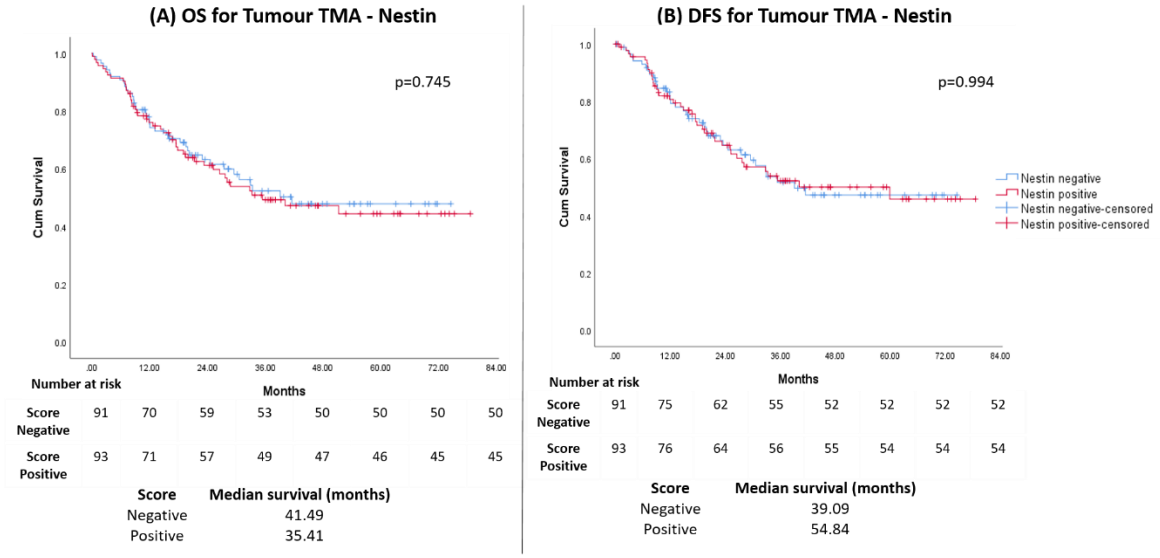

Figure 76. Kaplan-Meier curves for overall (A) and disease-free (B) survival in tumour TMA stained with nestin and grouped into negative or positive groups

Even when grouped into negative (score 1) or positive (scores 2&3) staining for nestin, there was no difference in OS or DFS (Figure 76).

Stromal TMA

Table 19. Clinico-pathological features of nestin staining of stromal TMA

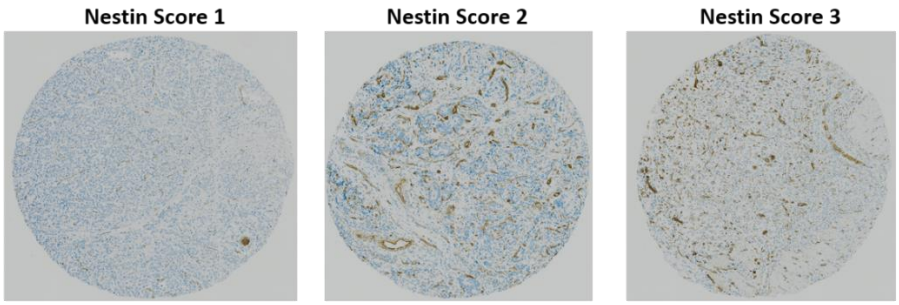

		Nestin Score 1	Nestin Score 2	Nestin Score 3
n (% of total stained)		110 (70.1%)	45 (28.7%)	2 (1.3%)
Median Age (years)		69	71	66
Gender		95 male, 15 female	41 male, 4 female	1 male 1 female
pT-stage	T0-1	19	9	2
	T2	15	8	0
	T3	60	26	0
	T4	16	2	0
pN-stage	N0	42	19	2
	N1	28	7	0
	N2+	40	19	0
Treatment	Surgery only	32	18	0
	Chemotherapy	78	27	2
Tumour Regression Grade	TRG1	4	0	0
	TRG2	15	3	1
	TRG3	10	3	0
	TRG4	25	8	0
	TRG5	24	13	1

Table 19 illustrate the demographics and clinico-pathological data for stroma stained with nestin, which were scored 1-3, dependent on proportion with nestin staining. There was a capture rate of 71%, with 157 cores adequately stained and scored.

70.1% of patients had less than 10% of stroma stained with nestin. Just over 50% of this group had T3 tumour pathology, with equal proportions either being nodal negative, or being nodal positive with N2 status. Over two-thirds of this group had NAC prior to surgery, and yet, 53% had poor TRG 3-5 status. Similarly in the group scoring 2, demographics and T- and N-stage were comparable. Including treatment modalities and TRG status. On the other hand, the 2 people in scoring 3 for nestin staining, appeared to have early disease (T0-1N0), underwent NAC and 1 patient had a TRG-responsive status (TRG2), while the other had TRG-nonresponder status (TRG5).

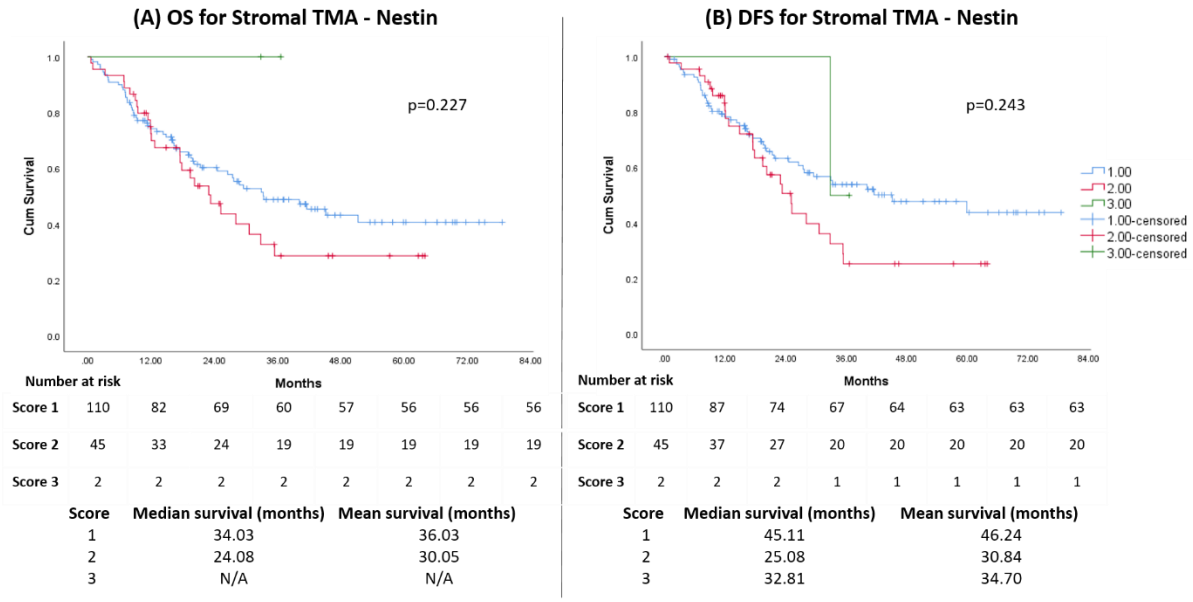

Figure 77. Kaplan-Meier survival curves of stromal TMA with nestin staining for overall (A) and disease-free (B) survival

Figure 77 illustrate the OS and DFS for stroma stained with nestin, together with the number at risk below the graphs. Although there was a drop of median OS times from 34.03 months to 24.08 months when nestin staining increased to greater than 10%, it was not statistically significant. Similarly, for DFS, there was a decrease in median survival times between groups scoring 1 and 2, but it was not significant. The median survival time for the group scoring 3 was based on 2 patients, which would have skewed the data. Therefore, I re-grouped them into negative or positive for nestin (Figure 78).

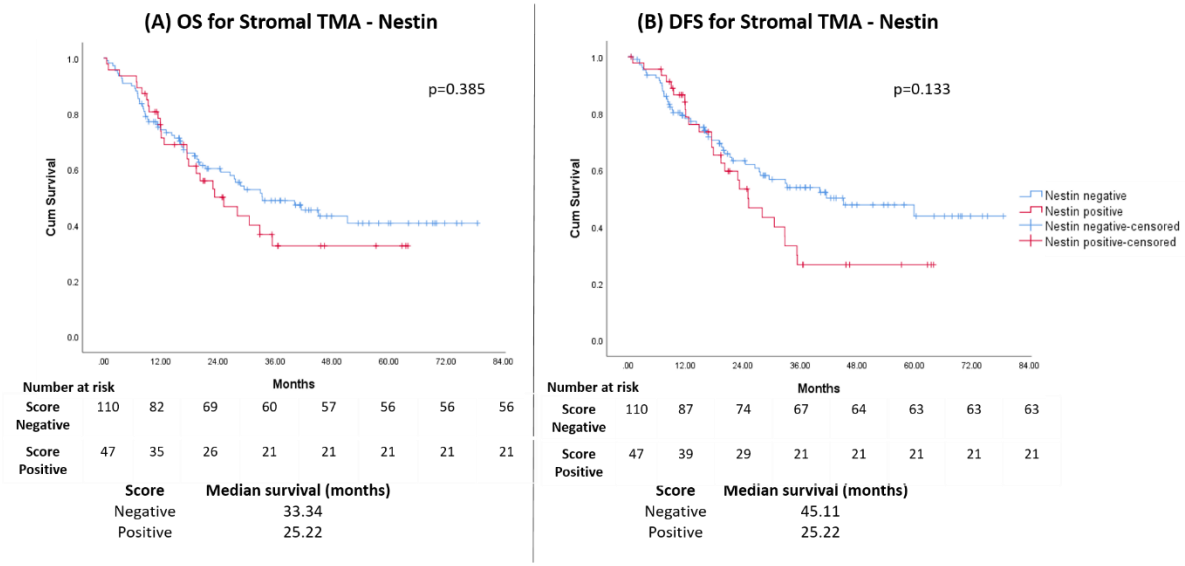

Figure 78. Kaplan-Meier curves for overall (A) and disease-free (B) survival in stromal TMA stained with nestin and grouped into negative or positive groups

When grouped into negative or positively-stained stroma with nestin, there were still no significant differences in survival outcome (Figure 78).

Lymph Node TMA

Table 20. Clinico-pathological features of nestin staining of LN TMA

LN TMA

Total = 113
Missing data 17 (15%)

Nestin Score 1

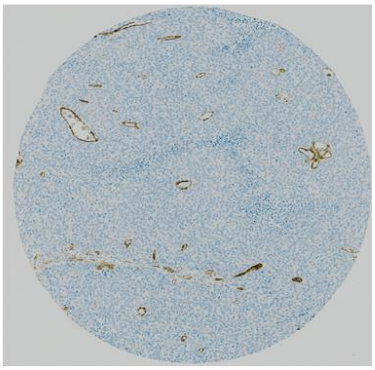

Nestin Score 2

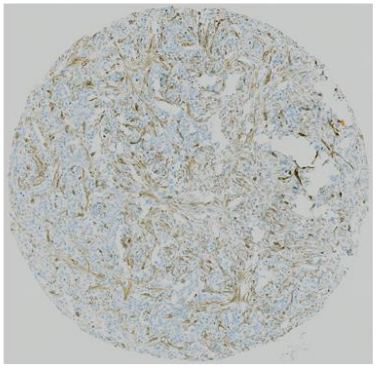

n (% of total stained)		81 (84.4%)	15 (15.6%)
Median Age (years)		70	69
Gender		70 male, 11 female	15 male, 0 female
pT-stage	**T0-1** **T2** **T3** **T4**	6 7 53 15	1 0 12 2
pN-stage	**N1** **N2** **N3**	30 29 22	6 6 3
Treatment	**Surgery only** **Chemotherapy**	31 50	7 8
Tumour Regression Grade	**TRG1** **TRG2** **TRG3** **TRG4** **TRG5**	4 4 4 15 23	0 1 1 1 5

Table 20 illustrate the demographics and clinico-pathological features of the patients in the LN TMA who were either negative (<10% of staining) or positive (>10% of staining). Out of the 113 positive LNs in the TMA, 96 were scored, resulting in an 85% capture rate.

84.4% of patients had less than 10% of their TMA stained with nestin. Majority of them had T3 or T4 disease, with high nodal burden. Out of the 60% of patients in this group who underwent NAC, 84% had non-responsive disease, based on their TRG scores. It is intriguing to discover that 40% of these patients went straight to surgery, of which it could be explained with 13 of the patients who had early disease (T0-T2). However, the other 17 patients would have had advanced disease, and so could have undergone the NAC and surgery pathway. Perhaps in these 17 patients, their disease pre-operatively were understaged, or patients chose to have surgery first and defer chemotherapy till later.

On the other hand, 15.6% of patients made up for those who were considered positively stained for nestin. 93% had advanced disease (T3/T4), and equal proportions underwent

NAC and surgery or surgery alone. 88% of patients who underwent NAC had TRG 3-5 status, which accounted for a high proportion of non-responsive disease.

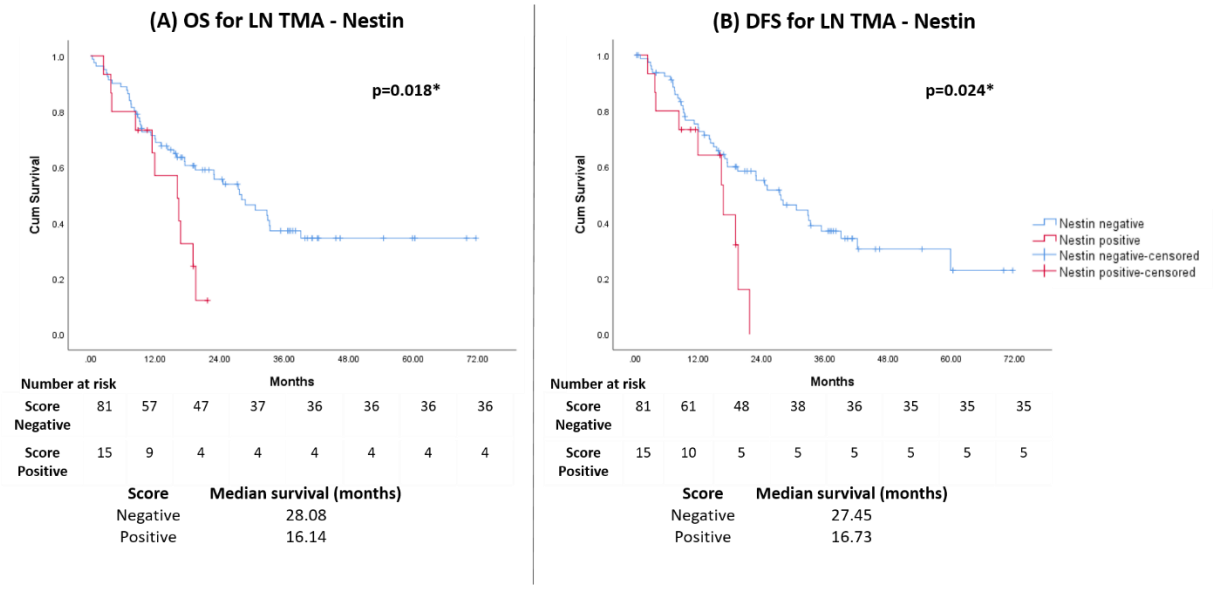

Figure 79. Kaplan-Meier curves for overall (A) and disease-free (B) survival in LN TMA stained with nestin and grouped into negative or positive groups

Figure 79 demonstrate that there were significant differences in OS and DFS in the LN TMA. This implied that presence of nestin in LNs conveyed a poorer prognosis and lower survival for death (16.14 months) or recurrence (16.73 months).

5.7 Relationship of variables with survival outcome

To streamline the variables to be compared, the antibody stains have been grouped into 2 groups of either being stain-negative or stain-positive for variable analysis.

Table 21. Univariate and multivariate analysis of patient and tumour factors with overall survival of OAC patients

Overall Survival		Mean 69.74 Median 70 (69-72)				Univariate Analysis			Multivariate Analysis		
				Months		Hazard	Confidence	Overall	Hazard	Confidence	Overall
Factors	Categories	n	%	Mean OS	Median OS	Ratio	Interval	p-value	Ratio	Interval	p-value
Age	Age>65	150	67.9	50.8	-	1		0.050*	0.606	0.349-1.051	0.074
	Age<65	71	32.1	42.91	28.08	0.657	0.431-1.003				
Gender	Male	189	85.5	47.08	45.11	1		0.306			
	Female	32	14.5	51.62	-	0.72	0.384-1.351				
Treatment Modality	Chemotherapy	148	67	51.87	-	1		0.021*			NA
	Chemonaive	73	33	40.12	62.91	0.618	0.410-0.931				
TRG	1	15	10.1	73.72	-	1		0.000*	1.393	1.047-1.853	0.023*
	2	34	23	63.38	-	0.067	0.009-0.494				
	3	17	11.5	47.53	25.22	0.189	0.078-0.459				
	4	39	26.4	51.5	-	0.512	0.222-1.177				
	5	43	29.1	34.04	17.85	0.416	0.217-0.796				
pT-stage	1	68	30.8	68.14	-	1		0.0000*	1.399	0.938-2.088	0.1
	2	25	11.3	53.37	-	0.085	0.038-0.190				
	3	107	48.4	35.84	27.45	0.215	0.090-0.517				
	4	21	9.5	21.25	7.5	0.468	0.261-0.841				
pN-stage	0	108	48.9	61.41	-	1		0.000*	1.483	1.131-1.943	0.004*
	1	46	20.8	44.19	51.22	0.0149	0.084-0.264				
	2	39	17.6	26.99	19.56	0.326	0.177-0.602				
	3	28	12.7	18.86	12.07	0.654	0.370-1.153				
α-SMA	SMA Tumour -	19	10.4	44.05	39.09	1		0.878			
	SMA Tumour +	163	89.6	44.9	35.41	0.95	0.490-1.840				
	SMA Stroma -	20	12.8	33.23	29.52	1		0.638			
	SMA Stroma +	136	87.2	41.94	30.61	0.863	0.0466-1.596				
	SMA LN -	14	14.4	32.9	-	1		0.141			
	SMA LN +	83	85.6	31.57	22.92	1.967	0.785-4.933				
Periostin	POSTN Tumour -	59	32.1	51.29	-	1		0.082			
	POSTN Tumour +	125	67.9	40.58	28.77	1.525	0.944-2.461				
	POSTN Stroma -	51	32.5	45.49	40.11	1		0.101			
	POSTN Stroma +	106	67.5	38.58	26.53	1.505	0.921-2.459				
	POSTN LN -	54	56.3	31.46	27.45	1		0.739			
	POSTN LN +	42	43.7	35.6	22.92	0.913	0.536-1.556				
Nestin	Nestin Tumour -	91	49.5	44.58	41.49	1		0.745			
	Nestin Tumour +	93	50.5	44.82	35.41	1.075	0.696-1.659				
	Nestin Stroma -	110	70.1	43.12	33.34	1		0.385			
	Nestin Stroma +	47	29.9	32.56	25.22	1.231	0.770-1.969				
	Nestin LN -	81	84.4	35.76	28.08	1		0.018*	Not included		
	Nestin LN +	15	15.6	13.74	16.14	2.253	1.131-4.488				

Table 21 illustrate the univariate and multivariate analysis of associated patient and tumour factors with overall survival. On univariate analysis, factors such as age greater than 65, use of chemotherapy, pT-stage, pN-stage and TRG status were significant. No statistical differences were found with gender or staining of any tissue with α-SMA, periostin or nestin. Multivariate analysis of these variables demonstrated that TRG status and nodal positivity was statistically significant, which suggested that these factors were of prognostic importance in overall survival.

Although nestin staining of LNs gave a significant result on univariate analysis, it was excluded from this multivariate analysis as the staining and scoring was only done on patients who had positive cancerous LNs. This was done on the assumption that the positive LNs might be positively stained with α-SMA, periostin or nestin. This subpopulation will be analysed in the later part of this section.

Table 22. Univariate and multivariate analysis of patient and tumour factors with disease-free survival of OAC patients

Disease-Free Survival		Mean 69 Median 70 (69-72)				Univariate Analysis			Multivariate Analysis		
				Months		Hazard	Confidence	Overall p-	Hazard	Confidence	Overall
Factors	Categories	n	%	Mean OS	Median OS	Ratio	Interval	value	Ratio	Interval	p-value
Age	Age>65	150	67.9	52.45	32.81	1		0.047*	0.6	0.350-1.028	0.063
	Age<65	71	32.1	44.02	-	0.642	0.413-0.998				
Gender	Male	189	85.5	48.47	45.11	1		0.184			
	Female	32	14.5	54.63	-	0.629	0.315-1.255				
Treatment Modality	Chemotherapy	148	67	51.11	-	1		0.488			
	Chemonaive	73	33	46.17	42.15	0.854	0.546-1.335				
TRG	1	15	10.1	69.46	-	1		0.000*	1.308	0.995-1.718	0.054
	2	34	23	61.82	-	0.131	0.031-0.551				
	3	17	11.5	50.08	-	0.217	0.094-0.500				
	4	39	26.4	50.27	59.84	0.432	0.178-1.047				
	5	43	29.1	34.22	17.85	0.44	0.233-0.829				
pT-stage	1	68	30.8	68.14	-	1		0.000*	1.413	0.956-2.087	0.083
	2	25	11.3	59.91	-	0.088	0.039-0.202				
	3	107	48.4	37.53	27.45	0.199	0.078-0.509				
	4	21	9.5	22.45	11.21	0.465	0.248-0.871				
pN-stage	0	108	48.9	64.23	-	1		0.000*	1.517	1.165-1.975	0.002*
	1	46	44.19	43.94	42.15	0.122	0.066-0.224				
	2	39	26.99	27.37	22.92	0.336	0.180-0.628				
	3	28	18.86	20.97	14.3	0.663	0.369-1.194				
α-SMA	SMA Tumour -	19	10.4	46.46	39.09	1		0.997			
	SMA Tumour +	163	89.6	46.33	40.11	0.999	0.498-2.004				
	SMA Stroma -	20	12.8	38.64	35.41	1		0.827			
	SMA Stroma +	136	87.2	42.69	32.81	1.081	0.537-2.176				
	SMA LN -	14	14.4	33.07	-	1		0.158			
	SMA LN +	83	85.6	30.67	22.92	1.918	0.764-4.815				
Periostin	POSTN Tumour -	59	32.1	53.16	-	1		0.069			
	POSTN Tumour +	125	67.9	41.87	32.81	1.584	0.960-2.614				
	POSTN Stroma -	51	32.5	45.75	35.34	1		0.261			
	POSTN Stroma +	106	67.5	40.81	28.08	1.331	0.807-2.196				
	POSTN LN -	54	56.3	30.06	27.45	1		0.666			
	POSTN LN +	42	43.7	34.14	22.92	0.889	0.522-1.516				
Nestin	Nestin Tumour -	91	49.5	45.26	39.08	1		0.994			
	Nestin Tumour +	93	50.5	47.33	59.84	0.998	0.635-1.571				
	Nestin Stroma -	110	70.1	46.24	45.11	1		0.133			
	Nestin Stroma +	47	29.9	31.79	25.22	1.443	0.892-2.334				
	Nestin LN -	81	84.4	34.07	27.45	1		0.024*	Not included		
	Nestin LN +	15	15.6	14.52	16.73	2.241	1.092-4.599				

Table 22 tabulate the significance of patient and tumour factors for disease-free survival for my cohort of OAC patients. Factors such as age over 65, pT-stage, pN-stage and TRG statuses were statistically significant on univariate analysis for disease-free survival. No differences were found in gender, treatment modality, or antibody positivity in α-SMA or periostin or nestin (nestin in positive LNs were excluded).

Multivariate analysis found that nodal status was statistically significant. This indicated that positive nodal burden was considered to be an important factor in disease recurrence, as expected. Response to chemotherapy, based on the TRG status, and age over 65 were associated with, but not significant, for disease recurrence.

Table 23. Univariate and multivariate analysis of patient and tumour factors in overall survival of OAC patients with positive LNs

Overall Survival						Univariate Analysis			Multivariate Analysis		
				Months		Hazard	Confidence	Overall	Hazard	Confidence	Overall
Factors	Categories	n	%	Mean OS	Median OS	Ratio	Interval	p-value	Ratio	Interval	p-value
Age	Age>65	76	67.2	35.31	28.77	1		0.045*	0.597	0.291-1.225	0.159
	Age<65	37	32.7	24.53	13.12	0.601	0.363-0.995				
Gender	Male	101	89.4	33.15	23.31	1		0.497			
	Female	12	10.6	23.08	13.12	1.291	0.616-2.707				
Treatment Modality	Chemotherapy	70	61.9	36.67	27.45	1		0.089			
	Chemonaive	43	38.1	26.12	17.52	0.66	0.408-1.069				
TRG	1	4	5.7	NA	NA	1		0.003*	2.169	1.225-3.839	0.008*
	2	6	8.6			-	-				
	3	8	11.4			-	-				
	4	23	32.9			0.349	0.104-1.168				
	5	29	41.4			0.434	0.210-0.897				
pT-stage	1	9	8	41.48	-	1		0.001*	2.605	1.299-5.225	0.007*
	2	7	6.2	39.77	-	0.066	0.009-0.502				
	3	77	68.1	31.39	22.95	0.233	0.066-0.822				
	4	20	17.7	19.43	7.17	0.448	0.246-0.818				
pN-stage	1	46	40.7	44.19	51.22	1		0.001*	1.218	0.728-2.038	0.453
	2	39	34.5	26.99	19.56	0.328	0.178-0.604				
	3	28	24.8	18.86	12.07	0.658	0.373-1.162				
α-SMA	SMA Tumour -	10	8.8	18.46	8.45	1		0.178			
	SMA Tumour +	100	88.5	33.19	23.31	0.604	0.288-1.268				
	SMA Stroma -	15	13.3	25.16	17.52	1		0.53			
	SMA Stroma +	95	84.1	33.29	24.59	0.807	0.411-1.581				
	SMA LN -	14	12.4	32.9	-	1		0.141			
	SMA LN +	83	73.5	31.57	22.92	1.967	0.785-4.933				
Periostin	POSTN Tumour -	19	16.8	37.55	45.11	1		0.174			
	POSTN Tumour +	83	73.5	29.27	18.35	1.597	0.809-3.155				
	POSTN Stroma -	29	25.7	32.67	60.61	1		0.367			
	POSTN Stroma +	65	57.5	29.62	19.04	1.303	0.732-2.318				
	POSTN LN -	54	47.8	31.46	27.45	1		0.739			
	POSTN LN +	42	37.2	35.6	22.92	0.913	0.536-1.556				
Nestin	Nestin Tumour -	51	45.1	33.28	22.95	1		0.553			
	Nestin Tumour +	50	44.2	28.46	19.04	1.163	0.706-1.914				
	Nestin Stroma -	68	60.2	31.72	19.56	1		0.982			
	Nestin Stroma +	26	23	24.56	22.95	1.007	0.564-1.796				
	Nestin LN -	94	83.2	34.49	27.68	1		0.050*	4.224	1.667-10.704	0.002*
	Nestin LN +	17	15	18.34	16.14	1.873	0.990-3.544				

I was interested in patients with positive LNs, as that had not been examined before. Therefore, I focused on the subgroup of patients with positive LNs, Table 23 illustrate my findings for this subgroup.

In patients with lymph nodes positive for cancer, this subgroup had a median age of 70 years (range 27-86 years). It demonstrated that age over 65, response to chemotherapy (according to TRG status), pT-stage, pN-stage and nestin positivity in lymph nodes were significant in overall survival on univariate analysis. Multivariate analysis of the significant individual variables was carried out, and pT-stage, TRG status and nestin positivity in cancerous LNs were found to be important factors affecting overall survival.

Table 24. Univariate and multivariate analysis of patient and tumour factors in disease-free survival of OAC patients who are LN-positive

Disease-Free Survival						Univariate Analysis			Multivariate Analysis		
				Months		Hazard	Confidence	Overall p-	Hazard	Confidence	Overall
Factors	Categories	n	%	Mean OS	Median OS	Ratio	Interval	value	Ratio	Interval	p-value
Age	Age>65	76	67.2	35.55	27.68	1		0.067			
	Age<65	37	32.7	25.53	15.95	0.617	0.367-1.039				
Gender	Male	101	89.4	33.77	24.59	1		0.375			
	Female	12	10.6	22.56	14.1	1.397	0.665-2.937				
Treatment Modality	Chemotherapy	70	61.9	34.83	23.31	1		0.623			
	Chemonaive	43	38.1	30.15	25.08	0.881	0.531-1.462				
TRG	1	4	5.7	48.75	-	1		0.038*	1.382	0.925-2.064	0.074
	2	6	8.6	41.59	-	0.179	0.024-1.351				
	3	8	11.4	29.9	24.59	0.303	0.071-1.291				
	4	23	32.9	39.875	35.34	0.349	0.104-1.169				
	5	29	41.4	19.65	12.07	0.458	0.222-0.946				
pT-stage	1	9	8	35.48	-	1		0.014*	2.024	1.104-3.710	0.023*
	2	7	6.2	40.25	42.15	0.212	0.060-0.756				
	3	77	68.1	32.82	23.31	0.236	0.066-0.850				
	4	20	17.7	19.71	8.12	0.45	0.236-0.856				
pN-stage	1	46	40.7	43.94	42.15	1		0.002*	1.341	0.843-2.131	0.215
	2	39	34.5	27.37	22.92	0.345	0.185-0.645				
	3	28	24.8	20.97	14.3	0.673	0.374-1.211				
α-SMA	SMA Tumour -	10	8.8	20.44	16.37	1		0.268			
	SMA Tumour +	100	88.5	34.16	25.08	0.642	0.292-1.415				
	SMA Stroma -	15	13.3	27	19.56	1		0.845			
	SMA Stroma +	95	84.1	33.56	25.08	0.928	0.441-1.955				
	SMA LN -	14	12.4	33.07	-	1		0.158			
	SMA LN +	83	73.5	30.27	22.92	1.918	0.764-4.815				
Periostin	POSTN Tumour -	19	16.8	37.02	33.27	1		0.422			
	POSTN Tumour +	83	73.5	31.04	21.73	1.31	0.676-2.540				
	POSTN Stroma -	29	25.7	34.2	30.61	1		0.598			
	POSTN Stroma +	65	57.5	31.21	22.95	1.17	0.652-2.099				
	POSTN LN -	54	47.8	30.06	27.45	1		0.666			
	POSTN LN +	42	37.2	34.14	22.92	0.889	0.522-1.516				
Nestin	Nestin Tumour -	51	45.1	34.49	24.59	1		0.655			
	Nestin Tumour +	50	44.2	30.66	21.73	1.126	0.669-1.892				
	Nestin Stroma -	68	60.2	34.34	24.59	1		0.708			
	Nestin Stroma +	26	23	24.88	23.31	1.119	0.621-2.014				
	Nestin LN -	94	83.2	34.851	27.68	1		0.050*	3.278	1.347-7.794	0.009*
	Nestin LN +	17	15	17.44	16.73	1.897	0.976-3.685				

Table 24 detail my findings on disease-free survival of this subpopulation of node-positive patients after univariate and multivariate analysis had been carried out. TRG status, pT-stage, pN-stage, and nestin positivity in LNs were found to be significant on univariate analysis. Age over 65 was strongly associated with DFS, but it was not statistically significant.

When these factors were further investigated with multivariate analysis, T-stage and presence of nestin in LNs were found to be of significance in disease recurrence. Nestin positivity (HR 3.278) appeared to be a stronger predictor of disease recurrence, compared to pathological T-stage (HR 2.024). My analysis has provided evidence that nestin is an important independent biomarker that should be considered of prognostic significance, and predictive of death or disease recurrence in patients with positive nodal tissue.

5.8 Discussion

This chapter has highlighted that biomarkers are a valuable tool to provide prognostic information, and that it could be applied for use in OAC. Analysing my cohort of 221 OAC patients has revealed that nodal and tumour regression status were significant factors in overall survival, while nodal stage was found to be an important consideration in disease recurrence. Moreover, when the subgroup of patients with positive LNs were analysed, pathological T-stage, TRG status and nestin positivity in LNs were found to be significant variables for overall survival. T-stage and nestin positivity in LNs were also shown to be important factors for disease recurrence.

Although there was a median OS of 45.11 months in patients with 10-50% α-SMA in the stroma, compared with 20.25 months in those with more than 50% stromal α-SMA, there were no significant differences in survival outcomes of α-SMA in tumour, stromal or nodal tissue. Oddly, there appeared to be similar survival for α-SMA-positive stroma (median OS 30.61 months) compared with α-SMA-negative stroma (29.52 months). This is in contrast to a study conducted by Underwood *et al*, which reported that moderate/high expression of α-SMA correlated with poorer overall survival (79 vs 48 months) after oesophagectomy[162]. My analysis also found poorer OS and DFS if there was an increasing proportion of α-SMA in positive nodal tissue, but it was not significant.

Similar to Underwood ***et al's*** paper on a different cohort of OAC patients[162], who had reported a poorer survival outcome with stromal staining of periostin, my findings showed an association of lower survival outcome with positivity for periostin in tumour or stroma – overall survival (tumour not available; stroma 26.53 months) and DFS (tumour not available; stroma 28.08 months), though it was not significantly different. Median survival time could not be calculated for those scored as periostin negative for tumour tissue, because cumulative survival had not surpassed the 0.5 mark, which implied that this group of patients had a survival advantage. As for lymph nodes, my results did not show any survival differences in positive LNs stained with periostin.

Manousopoulou *et al* examined nestin in the stroma and found that nestin positivity correlated with a poor prognosis in OAC[278]. In my study, nestin staining in the tumour did not correlate with survival. Nestin positivity in stroma for my cohort of patients, on the other hand, correlated with a poorer overall survival of 25.22 months and a shorter time to recurrence, compared with those scored negative for nestin, though it was not statistically significant.

The most intriguing finding involved patients who had positive LNs for cancer. This group had 15% of patients positive for nestin and was found to have a devastatingly poor survival

outcome and were highly prone to disease recurrence. This is an interesting finding as there is currently only 1 publication in the literature about the association of nestin in lymph nodes[280]. This paper had shown that nestin had labelled bone marrow cells specifically with mesenchymal stem cell properties, and that these nestin-positive cells made up most stromal cells within the lymph nodes. This included endothelial cells and were also found within T-cells and around B-cells. It may be that these cells play an important role in tumour progression through their interactions within the TME. My results should be further explored by examination of patients with lymph nodes negative for cancer cells (N_0), to investigate the presence of nestin in this group, as well as its correlation to survival outcomes. If that link is proven, it would be important to consider the interactions within lymphoid tissue, and evaluate the involvement of other cells such as TILs, TAMs or dendritic cells.

Biomarkers cannot be discussed without the mention of the REMARK guidelines, which stand for reporting recommendation for tumour marker prognostic studies. Its aims were to encourage transparent and complete reporting, as well as standardization of the relevant information being reported to allow others to judge the usefulness of the data[281]. Table 25 provide details of the REMARK guidelines.

Table 25. Reporting recommendations for tumour marker prognostic studies (REMARK guidelines)

REMARK Guidelines		Description
Introduction		1. State the marker examined, the study objectives and any prespecified hypothesis
Materials and Methods	Patients	2. Describe the characteristics of the study patients, including their source and inclusion and exclusion criteria 3. Describe treatment received and how chosen
	Specimen characteristics	4. Describe type of biological material used (including control samples), and methods of presentation and storage
	Assay methods	5. Specify the assay method used and provide a detailed protocol, including specific reagents or kits used, quality control procedures, reproducibility assessments, quantitation methods, and scoring and reporting protocols. Specify whether and how assays were performed blinded to the study end point
	Study design	6. State the method of case selection, including whether prospective or retrospective and whether stratification or matching was employed. Specify the time period from which cases were taken, the end of the follow-up period, and the median follow-up time 7. Precisely define all clinical end points examined 8. List all candidate variables initially examined or considered for inclusion in models 9. Give rationale for sample size
	Statistical analysis methods	10. Specify all statistical methods, including details of any variable selection procedures and other model-building issues, how model assumptions were verified, and how missing data were handled 11. Clarify how marker values were handled in the analyses
Results	Data	12. Describe the flow of patients through the study, including the number of patients included in each stage of the analysis and reasons for dropout. Specifically, both overall and for each subgroup extensively examined report the number of patients and the number of events 13. Report distribution of basic demographic characteristics (at least age and sex), standard (disease-specific) prognostic variables, and tumour marker, including numbers of missing values
	Analysis and presentation	14. Show the relation of the marker to standard prognostic variables 15. Present univariate analyses showing the relation between the marker and outcome, with the estimated effect (hazard ratio and survival probability). Preferably provide similar analyses for all other variables being analysed. For the effect of a tumour marker on a time-to-event outcome, a Kaplan-Meier plot is recommended 16. For key multivariable analyses, report estimated effects (hazard ratio) with confidence intervals for the marker and, at least for the final model, all the other variables in the model 17. Among reported results, provide estimated effects with confidence intervals from an analysis in which the marker and standard prognostic variables are included, regardless of their significance 18. If done, report results of further investigations, such as checking assumptions, sensitivity analyses, internal validation.
Discussion		19. Interpret the results in the context of the prespecified hypothesis and other relevant studies; include a discussion of limitations of the study 20. Discuss implications for future research and clinic value

My work, by and large, had corresponded to the REMARK guidelines to a certain extent. The biomarkers to be examined were described, together with my hypothesis in relation to survival outcomes. Patient characteristics such as demographics, performance status, BMI and pretreatment T- and N-staging were reported together with the treatments received. Unfortunately, details about how patients were chosen for their treatment were not available. However, it was assumed to be according to national guidelines, depending on their staging profile. A detailed protocol was described in a stepwise fashion on the creation of the TMAs and how assay was used on the TMAs. Case selection was performed on all consecutive OAC patients on our prospectively-collected UGI database, together with identification of the time period of the cases and the end of the follow-up period, with median follow-up time reported at 24.59 months. Stratification was carried out during analysis of the data, to simplify categories into subgroups of patients negative or positive for α-SMA, periostin and nestin. In addition, age was also stratified into 2 groups above or below 65 years of age, according to data from AUGIS[5]. Clinical end-points were defined as overall and disease-free survival, and were examined, and statistical methods were described, together with univariate and key multivariate analysis reported with hazard ratios and confidence intervals. The flow of patients for the study was illustrated with a flowchart and the attrition rates for each antibody were detailed.

One point that has yet to be carried out is internal validation of the biomarkers. Ideally, this should be carried out using independent sample cohorts from multiple hospitals, with the study population being representative of the disease stage and prevalence, and should include power calculations to define the study size and certify statistical significance. This process allows for an unbiased evaluation of the performance of the biomarker. This can be achieved with the use of multicentre collaborations with centralized registries of clinical samples, such as the Oesophageal cancer clinical and molecular stratification (OCCAMS) study based in Cambridge, which is a network of clinical centres recruiting OAC patients for tissue collection with the aim of identifying clinical, demographics and molecular factors affecting disease progression in OAC.

Once validated with other independent cohorts, the biomarker could potentially be introduced into the clinical setting for use, with a view to customizing therapy. However, the clinical utility of these biomarkers is yet to be decided, as a biomarker for post-resection tissue, or as a diagnostic biomarker from specimens taken during initial diagnostic endoscopy. Ideally, biomarkers for diagnostic biopsies are preferably, as neoadjuvant treatment can be tailored to aggressively downstage the disease prior to surgery. Based on my results, periostin could potentially be used in diagnostic tumour tissue as a prognostic biomarker, as it had provided distinct median OS and DFS differences, even though it was not significant. The other biomarkers of α-SMA and nestin should otherwise be geared as

post-resection prognostic markers, as stroma can be examined in detail on post-resection specimens for these patients, and inform patients of the overall survival outcomes, as well as ascertain if further adjuvant treatment could be modified specifically for them. Moreover, if patients have positive nodal burden post-surgery, use of α-SMA, and in particular, nestin, would be beneficial in identifying this subgroup of patients for further personalised systemic therapy if they desire.

From my results, nodal staging has proved to be a pivotal criterion for OS and DFS for OAC patients. Therefore any method should be utilized to downstage patients with positive LNs to improve their survival outcomes and decrease their likelihood of disease recurrence. For patients found to have positive LNs after surgery, nestin could be used as a prognostic biomarker to identify patients who could potentially benefit from further adjuvant therapy to increase survival rates and slow disease recurrence.

5.9 Summary

For the whole cohort of patients, N-stage and TRG status were correlated with a significantly poorer overall survival, with N-stage being a crucial variable in a shorter time to disease recurrence. Periostin and α-SMA positivity in tumour, stroma or lymph nodes appeared to have no statistically significant associations with survival outcomes. Moreover, for patients with a positive nodal burden, nestin presence in stroma and particularly in positive lymph nodes, had resulted in lower survival outcomes, and would be a useful addition for those post-oesophagectomy, to identify those patients with a poorer prognosis and who might benefit from further individualised adjuvant treatment, in the form of CRT.

Chapter 6 Final Discussion and Future Work

6.1 Overview of the study

The main objectives of this study were to explore the effects of CAFs on chemoresistance in OAC, and to investigate if PDE5 inhibitors, a drug already used in the clinical setting, could modify chemosensitivity of OAC cells through their cancer-cell stroma interface. Furthermore, I examined the biomarkers specific to CAFs that are involved in drug resistance and their association with survival outcomes in OAC patients.

After illustrating several methods to measure response in chemotherapy in 3 OAC cell lines, the MFD1 cell line was chosen to assess tumour response to chemotherapy in 2D and 3D in vitro models. Assays in the form of dose-response, colony growth, and spheroids were utilized, with different CAFs, in the form of conditioned media or co-cultures, to examine their effects on MFD1 in the absence or presence of SOC chemotherapy agents.

I had demonstrated that CAFs play an important role in inducing some chemoresistance in MFD1, with positive colony growth of MFD1 cells using CAF-CM even in the presence of cytotoxic drugs, and higher drug doses were required for an effective killing effect of MFD1 cells. Metabolic activity of OAC cancer cells was increased when co-cultured with CAFs, and this effect persisted despite the presence of chemotherapy agents, which in turn generated less effective killing of MFD1 cells. This has led me to speculate that these effects seen are due to a combination of secreted factors from CAFs as well as direct interactions between cells.

CAFs have been proven to be crucial elements in the tumour microenvironment, as they impact on cancer growth, invasiveness and chemoresistance. Initially, the CAF phenotype was originally thought to be irreversible[282]. However, myofibroblasts was shown to be reversible, and this had the potential to hinder cancer progression as well as potentially improve chemotherapy response[228]. PDE5 inhibition was found to reverse activated fibroblasts (CAFs) in prostate stromal fibroblasts, and it is thought that this effect can be reflected in other solid cancers such as head and neck or gastrointestinal cancers. I have shown that PDE5 is present in OAC[228 229], with high expression in fibroblasts on qRT-PCR and the cellular protein level, with minimal/no expression in the cancer cells. This had corresponded to high α-SMA expression in CAFs and NOFs. Furthermore, PDE5 inhibition of CAFs had a substantial decrease of protein expression of α-SMA, which was sustained when treated on a daily basis, rather than treatment every 72 hours. This effect was demonstrated in the drop in colony growth and diminished metabolic activity within

spheroids when PDE5 inhibition was utilised, particularly when platinum compounds had been used for treatment. Moreover, lower drug doses were required to kill MFD1 cancer cells after PDE5i treatment, implying that the treatment had an effect on CAFs, either through its secreted factors or by direct contact, which may have made the cells more chemosensitive.

Establishing clinical utility of biomarker is fraught with challenges. My preliminary results of investigating survival outcomes of using α-SMA, periostin and nestin, based on IHC, show some promise. Nodal staging and TRG status from post-oesophagectomy specimens were important variables associated with a poorer overall survival. Expectedly, a higher nodal stage correlated significantly with shorter time to disease recurrence. For this cohort of patients with positive nodal burden, their T-stage, TRG status and nestin positivity in LNs impacted significantly on overall survival, while T-stage and nestin positivity in LNs were significant principal indicators for early disease recurrence and shorter survival times.

6.2 Discussion and suggestions for future work

Response to chemotherapy is a major problem in solid cancers, especially in OAC where the 5-year survival rate is 15% at best[3]. There has been some work reporting the importance of CAFs in drug resistance, but it was done mainly in OSCC[221-223 227], with little published in OAC. The aim of my project was to characterise the link between CAFs and drug resistance, and to establish preliminary data on PDE5i use for sensitising OAC cancer cells to chemotherapy. I also worked to ascertain if biomarkers specific to CAFs could be employed as prognostic tools to provide survival outcome data in OAC patients.

Using an array of assays has allowed me to demonstrate the heightened chemotherapy response with the presence of CAFs or their conditioned medium, in spite of the diversity of CAFs utilized. This strongly suggested that secreted factors present in the medium, and direct interaction of CAFs, had manipulated the cancer cells to become more resistant to chemotherapy. The next step would be to analyse the secretome and explore the factors present by fractioning the conditioned medium. The secretome could then be analysed by proteomics and genomics to identify components, which then can be classified and arranged in decreasing proportions. These factors would then be examined to clarify the factors which were particularly important in enabling this effect of chemoresistance, before focusing on investigating a plausible mechanism of action. It would be interesting to see if proteins associated with mTOR-4E/BP1 pathway were involved, like in pancreatic adenocarcinoma[123], or recently discovered IL-6 which was found to drive EMT transition and drug resistance in OAC[283].

An initial challenge in this project was the creation of OAC spheroids with its application in flow cytometry. After much optimization, co-cultured spheroids were generated and appeared to have a dense core. Correlating it with flow cytometry, it appeared that that the CD90 uptake was low, and implied that it may not have been able to penetrate to the core of the spheroids. Therefore, I had speculated that the core consisted of fibroblasts, and were surrounded by cancer cells that were held together by tight cell-cell connections, that CD90 could not penetrate. With PDE5i treatment, the dense core appeared to be less tightly-bound to the naked eye under the microscope, which I presumed may have allowed chemotherapy drug treatment to penetrate the spheroid, thus causing more cell death. This was on the hypothesis that CAFs became less activated or reverted with PDE5i treatment, thereby resulting in re-sensitisation of cancer cells via the disruption of cell-cell assembly or the reduction of secreted factors from CAFs.

To further enhance our understanding of OAC spheroids, co-cultured spheroids could be labelled with separate fluorescent markers and imaged with magnified views, which will inform us of the locations of cancer cells and fibroblasts within the spheroids. That may then provide an explanation why CD90 uptake was reduced in flow cytometry analysis. In addition, the imaging should also include spheroids treated with PDE5i, with measurement of spheroid sizes and real-time analysis of spheroids after treatment. This will facilitate further comprehension, and provide an avenue to pursue. It will be fascinating and important to establish mechanism of action, and determine specific pathways that are initiated in the process.

This lab-based aspect of my project has several limitations. I have predominantly focused on 1 OAC cell line due to the abundance of information we have from whole genome sequencing, namely somatic mutations such as ABCB1, DOCK2, TP53 and SEMA5A. I was inclined to explore the ABCB1 mutation, and apply drug efflux assays as a starting point to investigate if that pathway is a potential mechanism of action. Nevertheless, to ensure applicability to OAC, it would be prudent to repeat these experiments in other OAC cells lines and evaluate the presence of the chemoresistance effect. Moreover, it would be judicious to use a range of PDE5i concentrations to explore its efficacy and effectiveness so as to inform clinical trials in the future. Further work still needs to be done to correlate these concentrations to plasma drug levels in patients, and determine if it would cause potential side effects or toxicity to patients.

As a clinician, I believed that it would be beneficial to examine the survival outcomes using CAF-related biomarkers. This way, some prognostic statistics can be provided to patients after their resection, and adjuvant therapy may be tailored accordingly. Additionally, it would be advantageous if this information became applicable in the neoadjuvant setting so that

neoadjuvant treatment could be customized from the start, at point of diagnosis, and improve survival and possibly, quality of life for OAC patients.

For the microarray aspect of my project, my results encompassed a high uptake of antibody staining, which was highly encouraging and enabled me to carry out survival analysis and determine the importance of α-SMA, periostin and nestin in OAC. Nodal staging and tumour regression grade were found to be crucial factors for overall survival, with nodal staging being the chief variable for disease-free survival. Some of my results regarding α-SMA and periostin were in conflict with previous publications from the group, where presence of these markers had correlated with a poorer survival[162]. To mitigate these conflicting results, it would be worth validating my results on a different cohort of OAC patients, preferably in a multi-centre setting using a collaborative approach. In addition, it would be reasonable to standardize the method of scoring. Firstly, it would be more appropriate for different pathologists experienced in OAC reporting (rather than surgeons) to perform the scoring, ideally using a masked approach. Secondly, to ensure scoring consistency, a semi-quantitative approach by means of a histochemical score, which combines stain intensity with percentage of positive cells. Unfortunately, as this is based on manual and subjective visual assessment, there is a level of observer bias that could impact on reproducibility. Alternatively a quantitative approach with automated image analysis being applied is more rigorous and can increase robustness to the scoring, as it provides precision to the scoring process and results in a greater degree of objectivity and reproducibility. One of the few shortcomings of this approach is that it is dependent on the quality of the image, which is in turn based on a camera's resolution. Nevertheless, it allows for a high throughout processing in a timely fashion.

An exciting result of my project is that all 3 biomarkers are present in cancerous lymph nodes, but nestin has proven to be a significantly important predictive marker for overall survival and disease recurrence in this cohort of patients. This has strong prognostic implications for patients with positive nodal burden, and should be a group of patients to target with aggressive adjuvant therapy after surgery. It would be worth trying other antibody stains for PDE5 to evaluate if there was any association with survival outcomes.

An interesting finding that I have observed is that there was a proportion of patients staged with nodal disease that proceeded straight to surgery without neoadjuvant therapy, which would disadvantage the patients and result in a poorer survival outcome. Similarly, there were patients were more advanced disease (T4N1+) being treated with curative intent, where previously, these patients would have been deemed too frail or old or having disease too advanced to undertake treatment with curative intent. With multiple trials currently taking place to evaluate neoadjuvant therapy, radiotherapy is increasingly used for neoadjuvant management prior to surgery, which might influence the nodal staging, an important factor

in prognosis. There are also growing numbers of patients presenting with early disease, due to increased awareness from various cancer campaigns that grant more opportunities for these patients to undergo neoadjuvant treatment.

All these ever-changing advances in cancer management impact on survival. Consideration should also be given to carrying out clinical trials of PDE5i on OAC patients, primarily in the palliative setting in the first instance, as these patients might have a survival benefit from aggressive adjuvant therapy after sensitisation with PDE5i treatment. If that is successful and a survival advantage is observed, then PDE5i treatment could be progressed to the neoadjuvant setting.

6.3 Conclusion

My project has proven that CAFs have an important role in chemoresistance in oesophageal adenocarcinoma. This can be potentially reversed by PDE5i, which are already used in the current clinical setting, though more work needs to be done to verify and validate the results. Biomarkers such as nestin can be used by patients to provide prognostic information, especially for those with positive nodal burden. Further work can be carried out to guide their views on whether PDE5i treatment may be feasible in sensitising remaining cancer cells for further adjuvant therapy.

Appendix A

Demographic data of NOF and CAF matched pairs

Below are patient demographics from which primary fibroblasts were extracted and derived from:

	NOF/CAF 612	*NOF/CAF 662*	*NOF/CAF 669*
Gender	Female	Male	Female
Age at Diagnosis	59	67	71
Body Mass Index	28.3	25.4	33.8
Stage at Diagnosis	T2N0	T2N0	T2N0
Treatment	Surgery only	Neoadjuvant chemotherapy & surgery	Surgery only
Chemotherapy Regime	N/A	Epirubicin, oxaliplatin, 5-fluorouracil	N/A
Chemotherapy Completed	N/A	Yes	N/A
TRG	N/A	4	N/A
Stage at Resection	pT1 pN0 pM0	pT3 pN0 pM0	pT2 pN0 pM0
Resection status	R0 No lymphovascular invasion	R0 No lymphovascular invasion	R0 No lymphovascular invasion
Positive nodes	0/28	0/15	0/30
Recurrence	Disease free	Disease free	Disease free at death
Survival Status	Alive	Alive	Dead

**Data correct as of 6/9/2016*

Appendix B

Antibodies and reagents

All reagents and inhibitors were maintained at -20^{o}C for long-term storage.

Primary Antibodies

Primary antibody	**Species**	**Supplier**	**Catalog/ Ref no.**	**Lot number**	**Conc**	**IHC dilution**	**WB/FACS dilution**
HSC-70	Rabbit	Santa Cruz	SC33575	F1511	200µg/ml	N/A	1:1000
HSC-70	Mouse	Santa Cruz	SC7298	F0413	200µg/ml	N/A	1:1000
Cytokeratin	Mouse	Dako	M3515	00009650	136mg/L	N/A	1:500
Vimentin	Mouse	Dako	M7020	00066112	61mg/L	N/A	1:1000
α-SMA	Mouse	Dako	M0851	00089943 20019979	71mg/L	1:100	1:500
PDE5A	Rabbit	Santa-Cruz	SC32884	F1413 F2711	200µg/ml	1:50 1:500	1:1000
Periostin	Rabbit	Abcam	14041	GR296166-3	1µg/mµL	1:500	1:1000 1:10,000
HGF	Rabbit	Abcam	83760	GR303317-3	0.5mg/ml		1:1000
Nestin	Mouse	Abcam	22035	GR312885-1	1mg/ml	1:100	1:1000
MCT4	Rabbit	Santa Cruz	SC-50329 376140		200µg/ml 200µg/ml	1:50	1:200 1:100
APC anti human CD90		Biolegend	328114	B199831	100µg/ml		1:40

FITC anti human EPCAM		Biolegend	324204	B183991	50µg/ml		1:40
APC Isotype control IgG1		Biolegend	400122	B216781	200µg/ml		1:40
FITC Isotype control IgG2		Biolegend	400310	B194980	200µg/ml		1:40
Fixable Viability Dye eFluor® 506		Bioscience	65-0866-14	4300709			1µL per $1x10^6$ cells
7AAD Viability Staining Solution		Biolegend	420403	B226292 B208328	50µg/ml		5µL per $1x10^6$ cells

Secondary Antibodies

Secondary antibody	**Species**	**Supplier**	**Catalog/ Ref no.**	**Lot number**	**Conc**	**IHC/ dilution**	**WB/FACS dilution**
Polyclonal rabbit	Anti-mouse	Dako	P0260	00090941	1.3g/L		1:1000
Polyclonal swine	Anti-rabbit	Dako	P0217	00086784	1.3g/L		1:1000
Polyclonal rabbit	Anti-goat	Dako	P0449	00088534	0.55g/L		1:1000

Drug Reagents

Drug Reagent	Supplier	Diluent	Concentration
Vardenafil	Sigma	Methanol	1mg/ml
Cisplatin	Accord	Water	1mg/ml
5-fluorouracil	Accord	Water	50mg/ml
Carboplatin	Accord	Water	10mg/ml
Paclitaxel	Accord	Polyoxyl castor oil and anhydrous ethanol	6mg/ml
Oxaliplatin	Accord	Lactose monohydrate and water	5mg/ml
Epirubicin	Teva Hospitals	Water	2mg/ml

Appendix C

Media, solutions and buffers

Phosphate buffered saline (PBS), 10x

NaCl 80g

KCl 2.5g

Na2HPO4 2.5g

KH2PO4 2.5g

Made up to 1 litre with distilled water, titrated to pH 7.2 and autoclaved

Recipe for SDS-polyacrylamide gels

Separating Gel	Solution	10%	7%	Stacking Gel (for all)
	30% Acrylamide	6.6ml	4.7ml	1.4ml
	4X Tris HCl pH 8.8	5.0ml	5.0ml	2.5ml (4X Tris HCl pH 6.8)
	dH2O	8.3ml	10.2ml	6.0 ml
	10% AMPS	100 microL	100 microL	100 microL
	TEMED	15 microL	15 microL	15 microL

Running Buffer (10X)

Tris 30g

Glycine 144g

SDS 10g

Deionized water to 1 litre

Western blot running buffer

100ml 10X running buffer

900ml Deionized water

Western blot transfer buffer

100ml	10X running buffer
300ml	Ethanol
600ml	Deionized water

PBS/Tween (0.1%)

33ml	30X PBS
1ml	Tween 20
966ml	Water

Western blot blocking buffer

PBS/Tween	50ml
Marvel skimmed milk powder	2.5g

Appendix D

Primer sequences

Gene ID	Sequence	Batch number	Product size (bp)
PDE5A	F TGATCAGTGCCTGATGATCC R AATGGAGAGGCCACTGAGAA	JN98217	61
GAPDH	F CTCTTTCCAGTGTGGGGTGT R CTCTCTTTCGTTTGGTCATTTGATG	JN98219	84

Appendix E

Optimization of time-course for dose response assays

To determine the appropriate time interval by which 50% of cancer cells die after treatment with a chemotherapy agent, I performed a series of experiments with different time points to investigate this aim, with 2 OAC cell lines and a variety of standard-of-care (SOC) chemotherapy drugs used to treat OAC.

These tables are the results of my experiments.

OE33

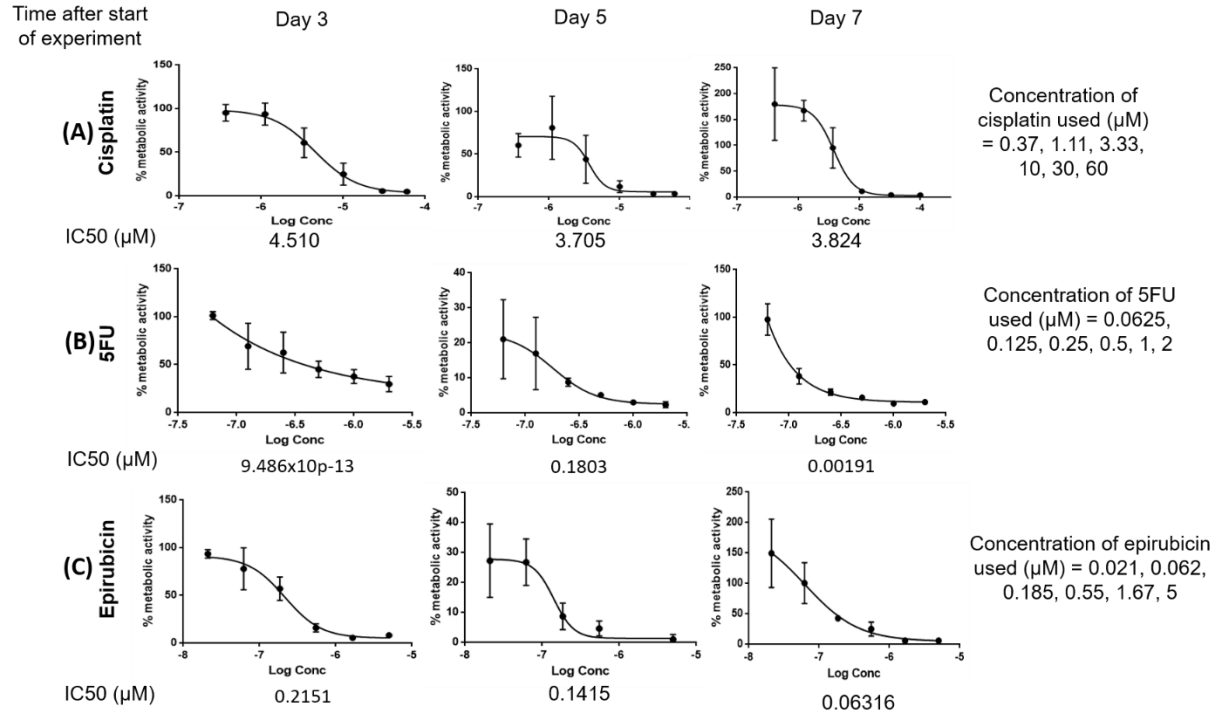

Figure 80. Time course of OE33 cell line treated with (A) cisplatin, (B) 5FU, (C) epirubicin

Figure 84 shows a time course of the OE33 cell line treated with SOC chemotherapy. Row A illustrates a representative dose-response curves after cisplatin treatment, with metabolic activity measured after day 3 of treatment, day 5 and day 7. The effect of chemotherapy on OAC cells was measured by metabolic activity, as a representation of proportion of cells killed by chemotherapy. Rows B and C show the time course after treatment with 5FU and epirubicin respectively. Overall, there was observable killing of OAC cells when treated with different concentration of drug. These are shown as sigmoid curves, which is representative of the IC50 curve.

FLO1

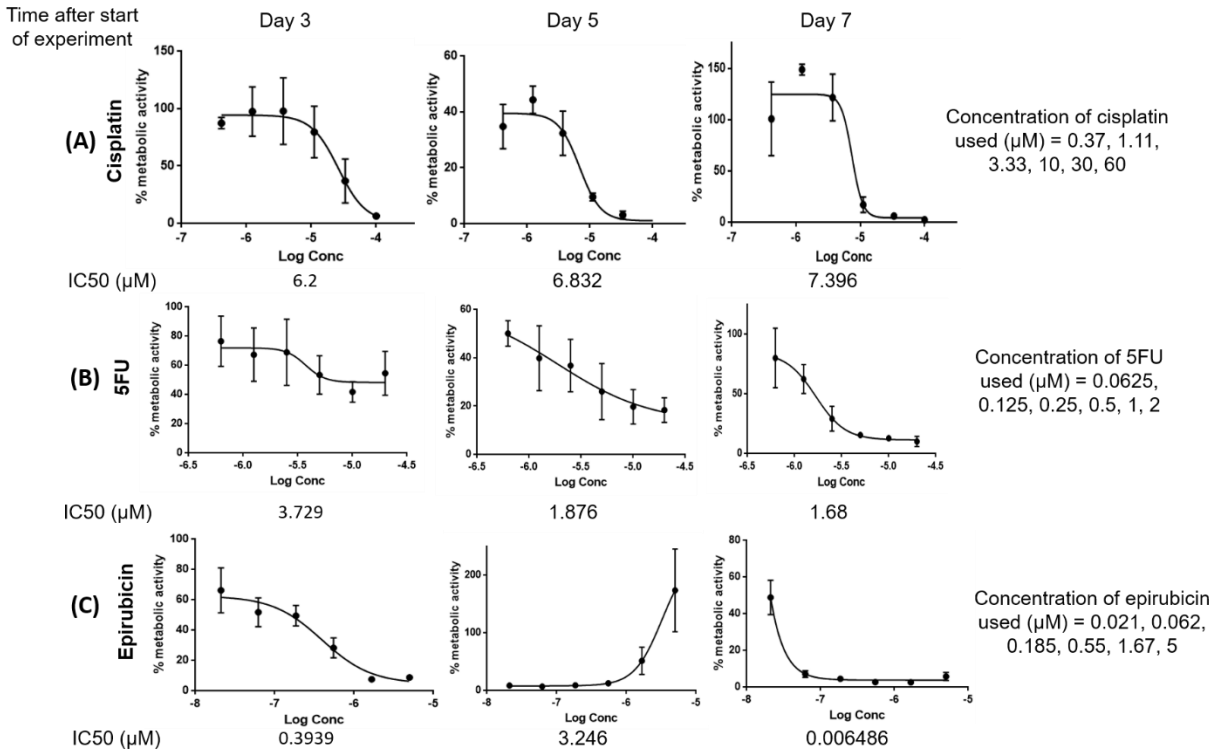

Figure 81. Time course of FLO1 cell line treated with (A) cisplatin, (B) 5FU, (C) epirubicin

Figure 85 shows representative dose-response results for the FLO1 cell line treated with SOC chemotherapy. For Day 3 curves, the lower end of some of the curves had started to plateau out, which meant that not all cells had been killed completely by the drug. However, graphs for day 5 and day 7 demonstrated a long plateau of the graph, which signified that the majority of cells were already dead, and leaving them treated with drug for a longer period of time did not make much difference. These experiments had helped me to decide that a time period of 4 days was the optimum time period to allow the drug to effectively treat the cells, while allowing for the logistics of carrying out the experiments of drug treatment and colourimetric detection.

Some of the curves had large error bars – This was because initially, when the drugs doses were calculated and titrated, I did not dose the drug in separate plates, but mixed it in the media with the cells, before taking out the calculated volume (eg. 4-fold) and pipetted it into the subsequent wells. In addition, doses were pipetted in the wrong direction for FLO1 cells that were treated with epirubicin for 5 days. Therefore when it was read on the plate reader and charted, the graph was in the opposite direction.

Confirmation of 4 days as appropriate time interval for treatment of cells

Cisplatin

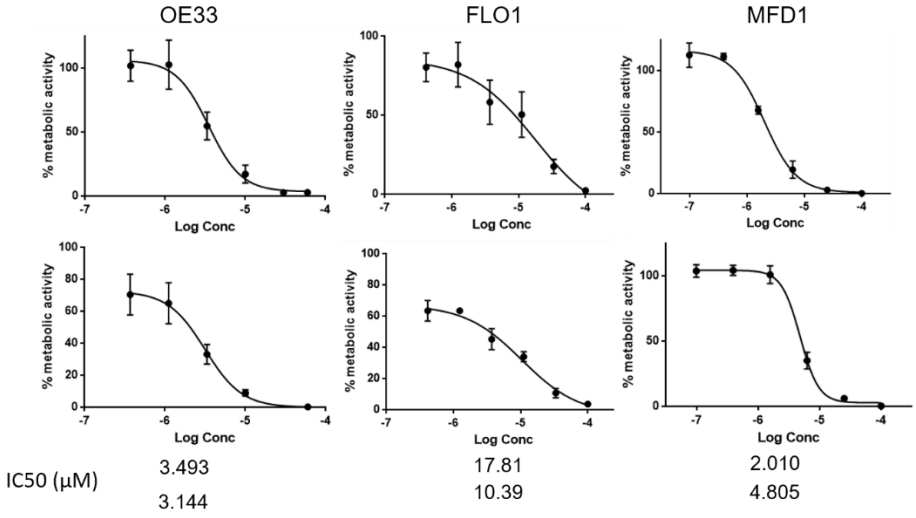

Figure 82. Dose-response assays of OAC cell lines treated with cisplatin for 4 days

I proceeded to perform dose-response assays to confirm that using a 4-day time course was appropriate. Figure 86 demonstrate representative dose-response curves for cisplatin treatment of OE33, FLO1 and MFD1, all of which are OAC cell lines. MFD1 is an in-house OAC cell line, which was used in my experiments as our group had extensive genomic information about this cell line and its origins. Figures 87-91 demonstrate representative dose-response curves for 5FU, epirubicin, oxaliplatin, carboplatin and paclitaxel treatment of OAC cell lines. These chemotherapy agents were chosen as they are commonly used for NAC treatment of OAC.

5FU

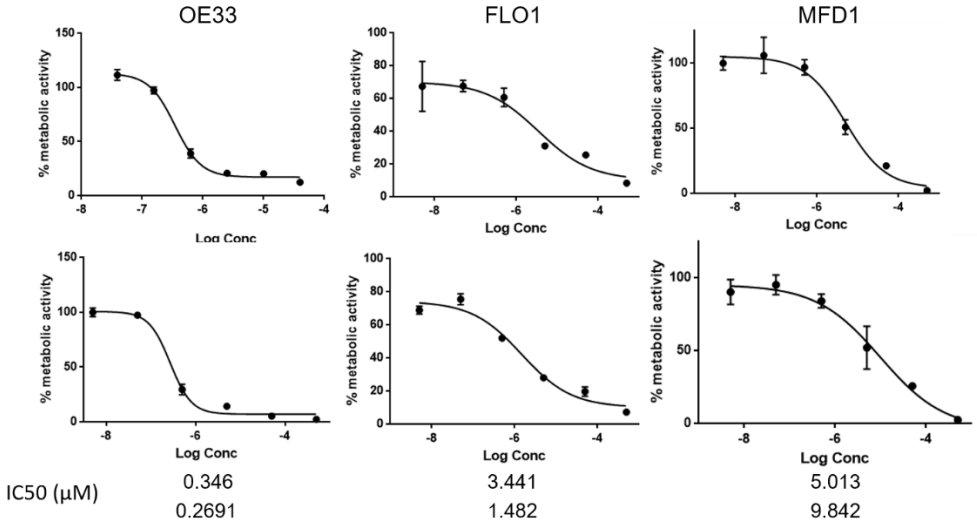

Figure 83. Dose-response assays for OAC cell lines treated with 5FU for 4 days

Epirubicin

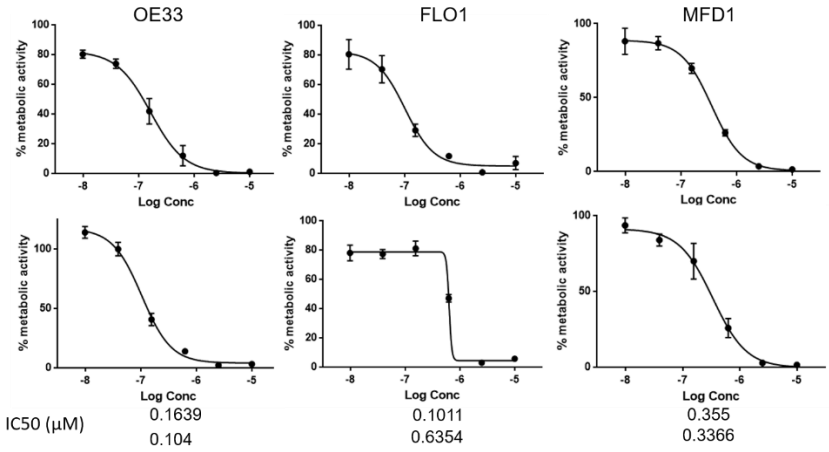

Figure 84. Dose-response assays of OAC cell lines treated with epirubicin for 4 days

Oxaliplatin

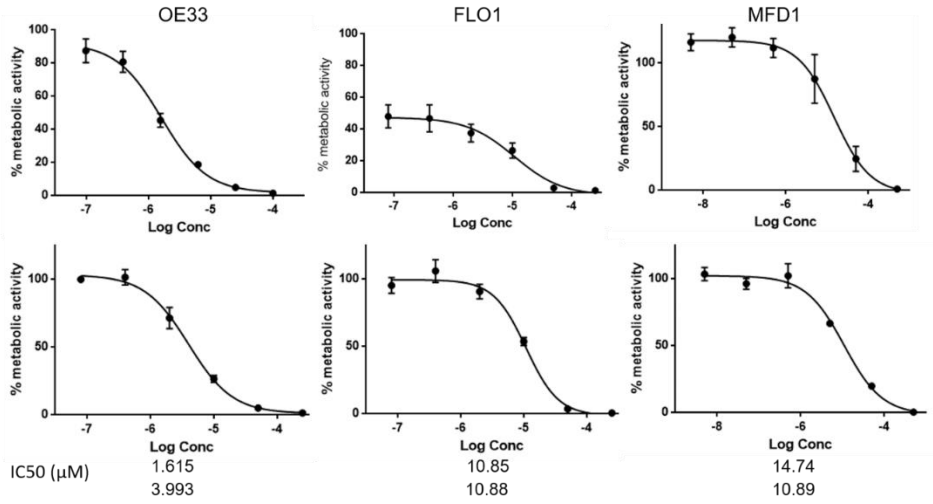

Figure 85. Dose-response assays with OAC cell lines treated with oxaliplatin for 4 days

Carboplatin

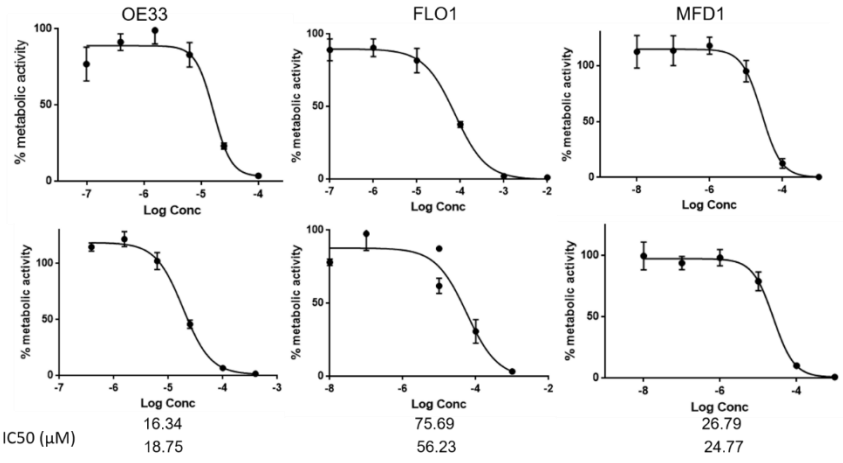

Figure 86. Dose-response assays of OAC cell lines treated with carboplatin for 4 days

Paclitaxel

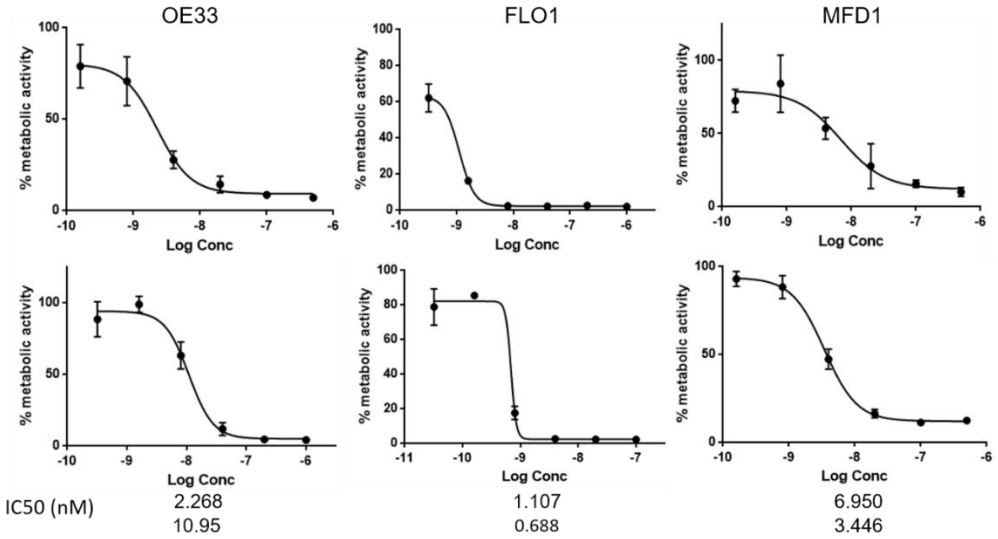

Figure 87. Dose-response assays of OAC cell lines treated with Paclitaxel for 4 days

In summary, the dose-response curves from figures from 87-91 demonstrate that treatment with chemotherapy for 4 days is the optimum time period for drugs to have a maximal effect on OAC cell lines.

Appendix F

Optimization of drug concentration for dose-response assays

Following on, to determine the appropriate concentrations of drugs needed to kill OAC cells, I performed experiments looking at varying concentrations of chemotherapy drugs that was appropriate to kill 50% of OAC cell lines (OE33, FLO1, MFD1).

The graphs below show my results.

OE33

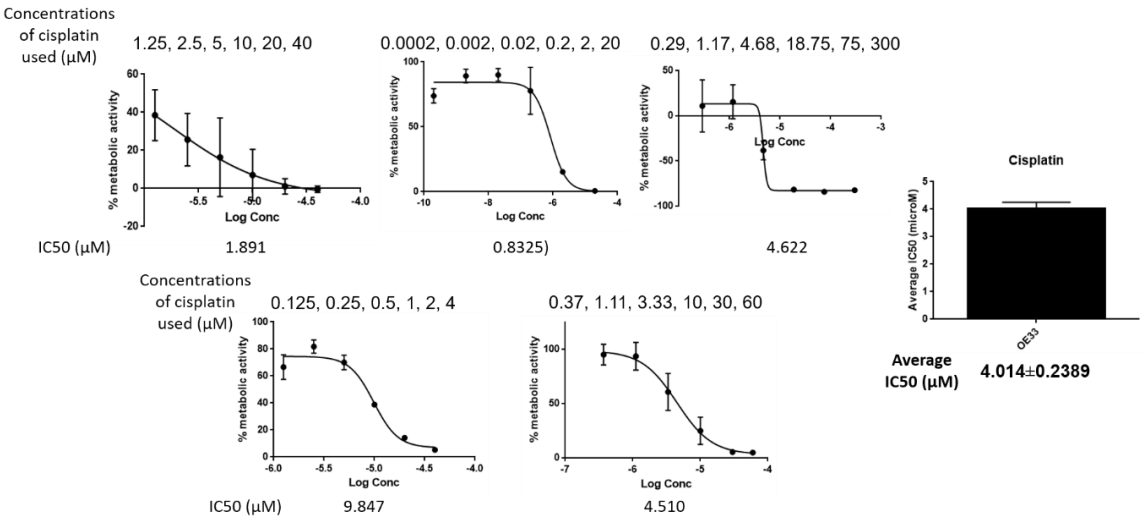

Figure 88. Concentrations of cisplatin used in OE33 dose-response assays

After the initial experiments, Figure 92 demonstrated that it was evident the doses of cisplatin were too high and killed too many cells at the start. Therefore after a number of dose adjustments, the optimum concentrations were worked out to give a good range of killing of cells, and the latest doses were repeated (n=7) to confirm reproducibility of IC50 curves.

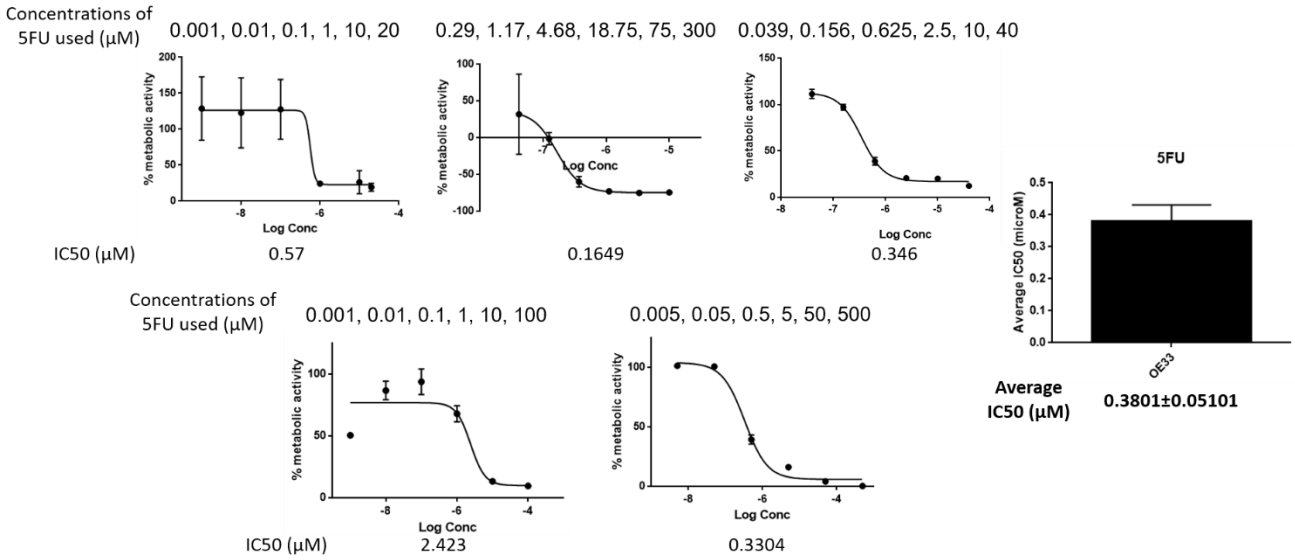

Figure 89. Concentrations of 5FU used in OE33 dose-response assays

After 7 changes of drug doses for 5FU, the optimum dose-response assay was performed and repeated (n=5) to confirm reproducibility (Figure 93).

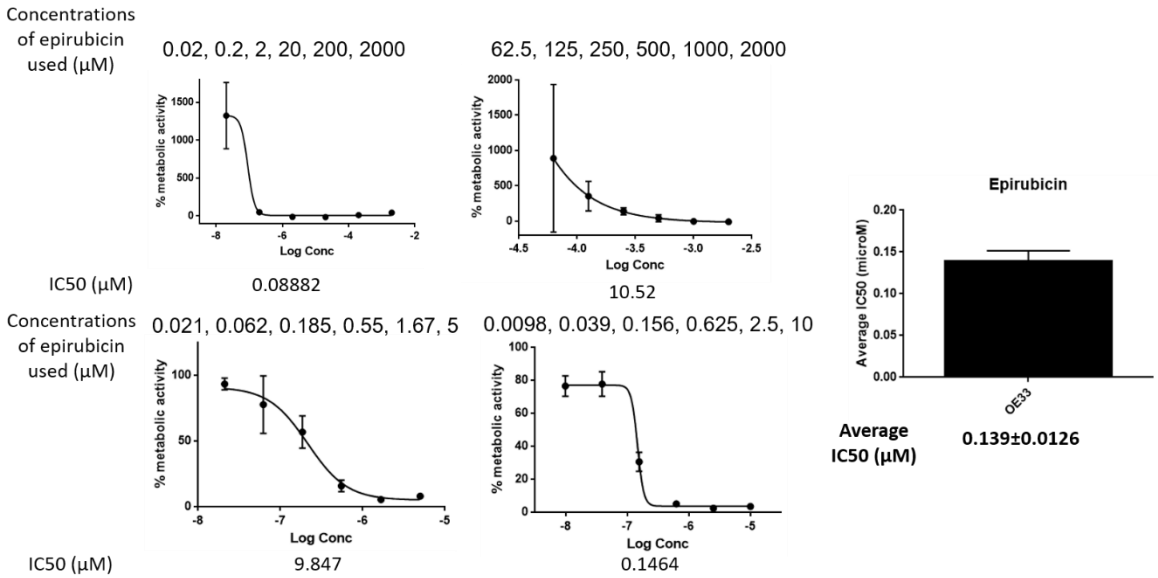

Figure 90. Concentrations of epirubicin used in OE33 dose-response assays

After 4 changes of drug dosing for epirubicin, the optimum dose-response assays were repeated (n=4) to confirm reproducibility (Figure 94).

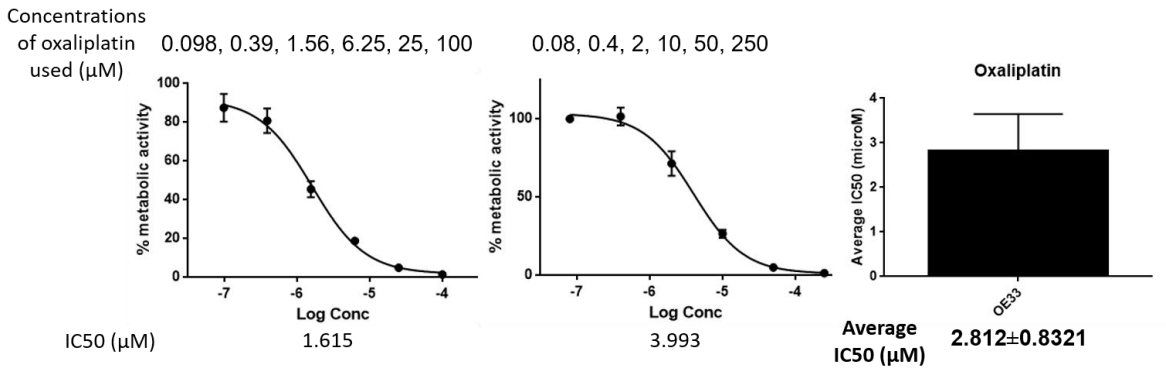

Figure 91. Concentrations of oxaliplatin used in OE33 dose-response assays

After 4 changes of drug dosing for oxaliplatin, the optimum dose-response assay was repeated (n=4) to confirm reproducibility (Figure 95).

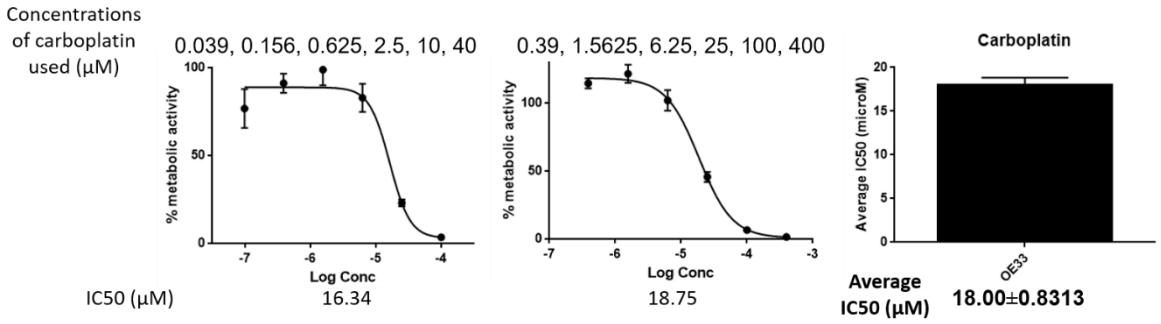

Figure 92. Concentrations of carboplatin used in OE33 dose-response assays

After 2 changes of drug dosing for carboplatin, the optimum dose-response assay was repeated (n=3) to confirm reproducibility (Figure 96).

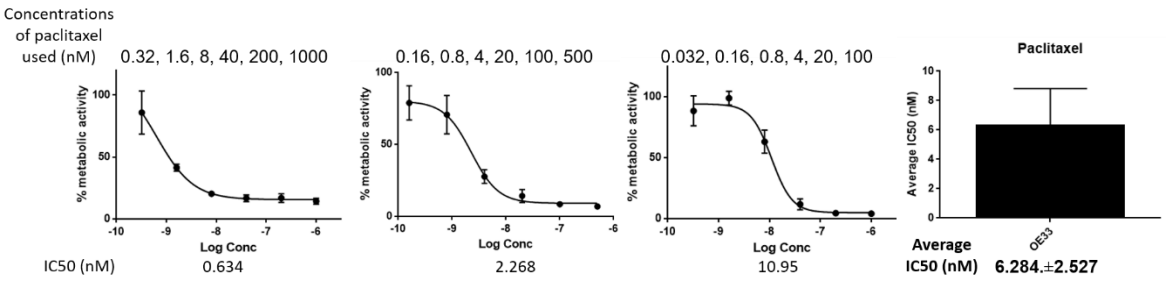

Figure 93. Concentrations of paclitaxel used in OE33 dose-response assays

After 3 changes of drug dosing for paclitaxel, the optimum dose-response assay was repeated (n=3) to confirm reproducibility (Figure 97).

FLO1

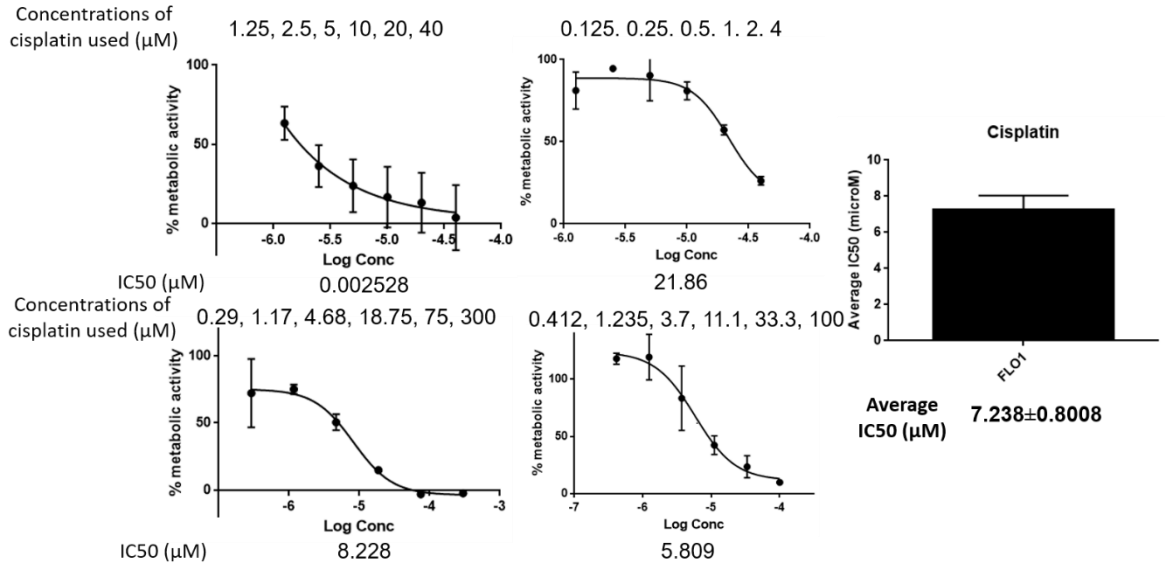

Figure 94. Concentrations of cisplatin used in FLO1 dose-response assays

After 4 changes of drug dosing for cisplatin in FLO1 cell lines, the optimum dose-response assay was repeated (n=6) to confirm reproducibility (Figure 98).

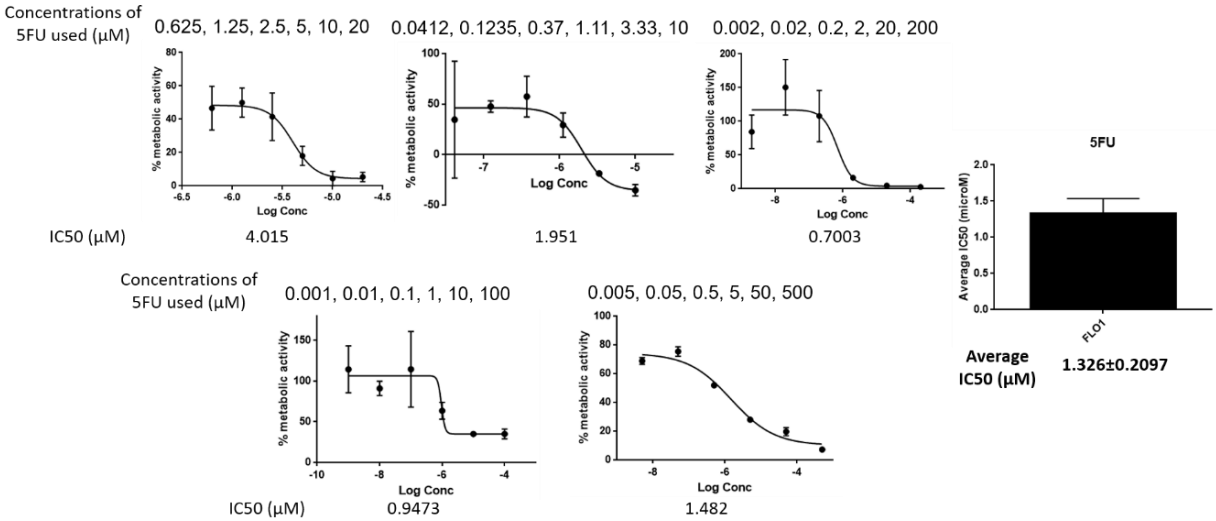

Figure 95. Concentrations of 5FU used in FLO1 dose-response assays

After 5 changes of drug dosing for 5FU in FLO1 cell lines, the optimum dose-response assay was repeated (n=6) to confirm reproducibility (Figure 99).

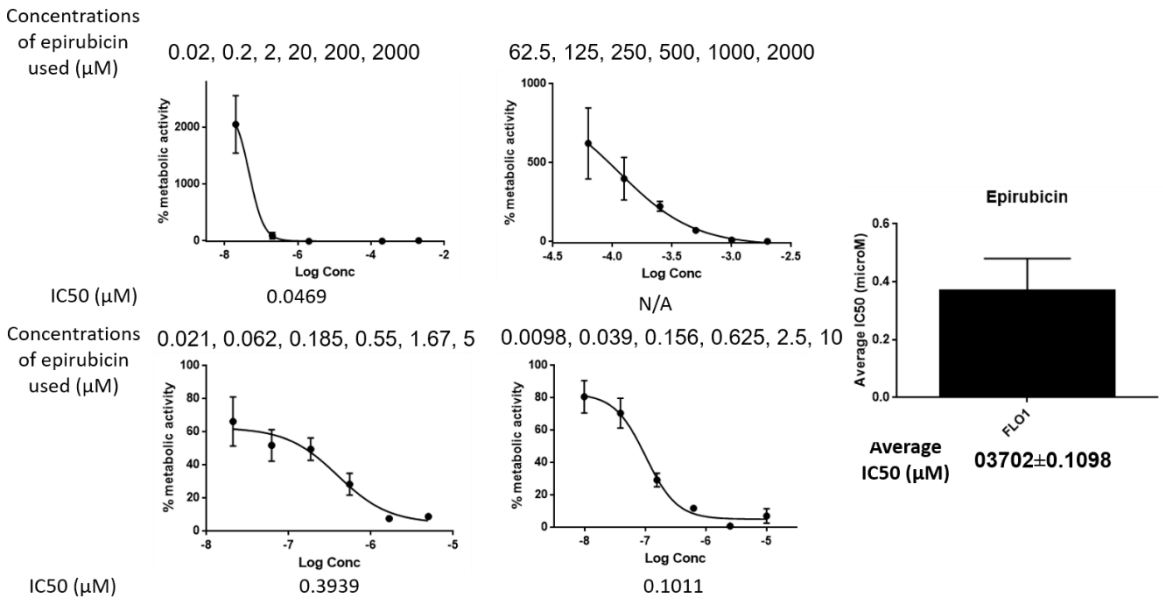

Figure 96. Concentrations of epirubicin used in FLO1 dose-response assays

After 4 changes of drug dosing for epirubicin in FLO1 cell lines, the optimum dose-response assay was repeated (n=5) to confirm reproducibility (Figure 100).

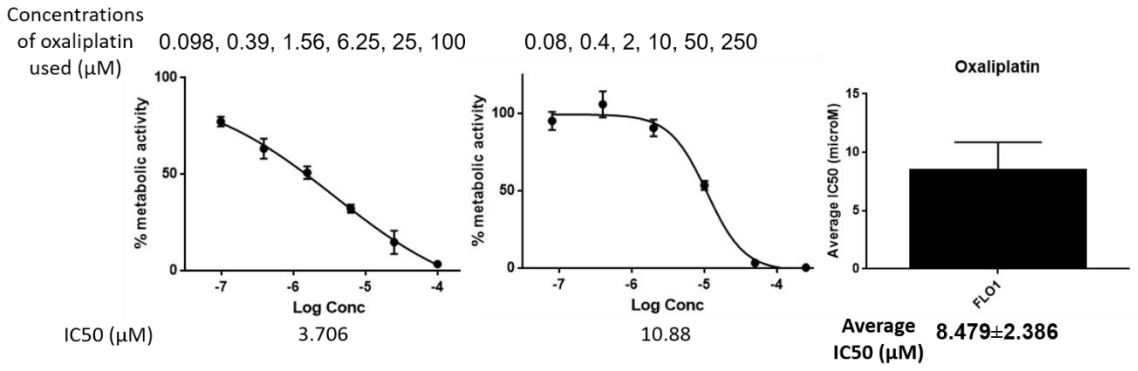

Figure 97. Concentrations of oxaliplatin used in FLO1 dose-response assays

After 2 changes of drug dosing for oxaliplatin in FLO1 cell lines, the optimum dose-response assay was repeated (n=3) to confirm reproducibility (Figure 101).

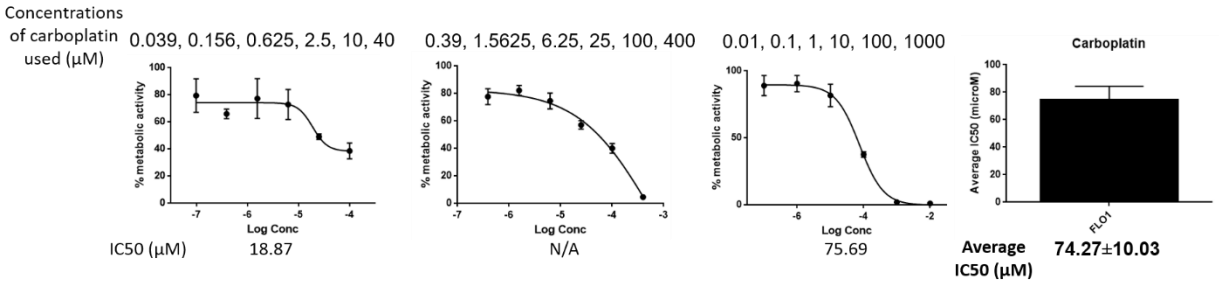

Figure 98. Concentrations of carboplatin used in FLO1 dose-response assays

After 3 changes of drug dosing for carboplatin in FLO1 cell lines, the optimum dose-response assay was repeated (n=3) to confirm reproducibility (Figure 102).

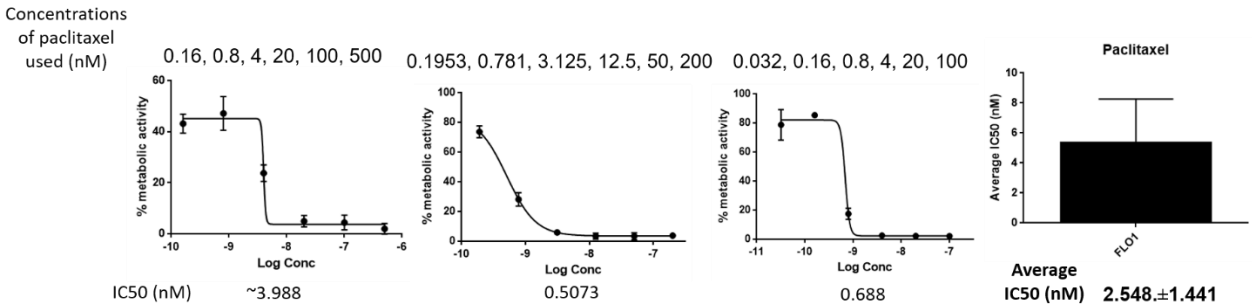

Figure 99. Concentrations of paclitaxel used in FLO1 dose-response assays

After 3 changes of drug dosing for paclitaxel in FLO1 cell lines, the optimum dose-response assay was repeated 3 times to confirm reproducibility (Figure 103).

MFD1

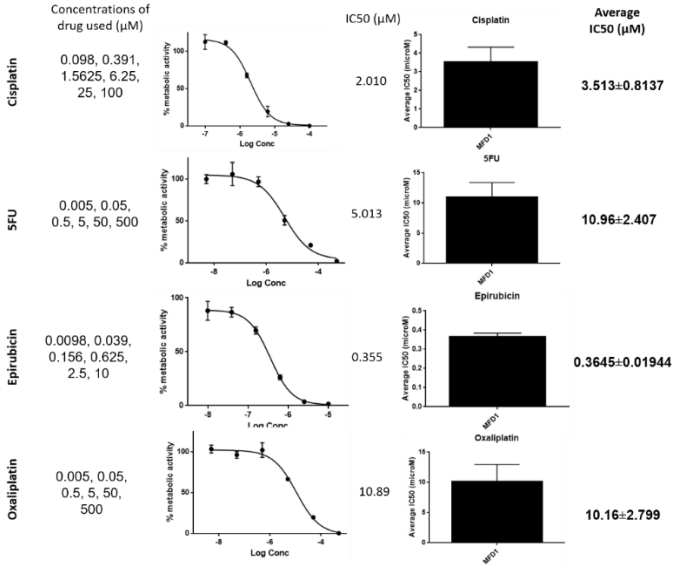

Figure 100. Concentrations of ECF used in representative MFD1 dose-response assays

In MFD1 cell lines, the optimum dose-response assay was repeated for cisplatin (n=3), 5FU (n=4), epirubicin (n=3) and oxaliplatin (n=4) to confirm reproducibility (Figure 104).

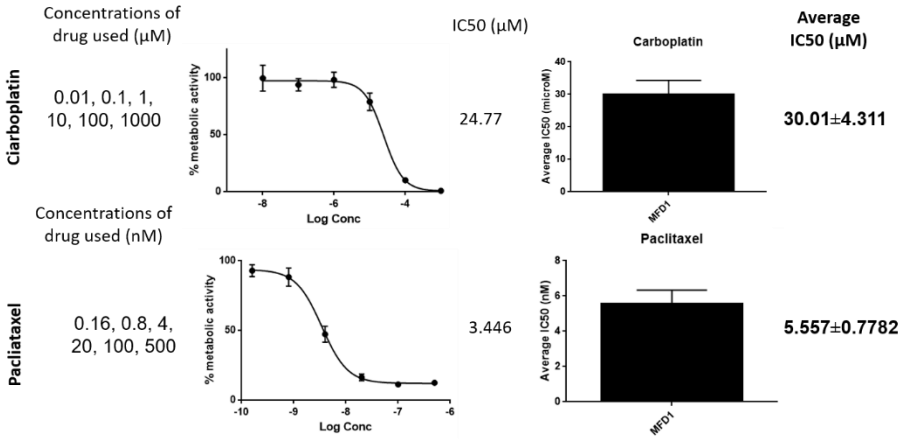

Figure 101. Concentrations of carboplatin and paclitaxel used in representative MFD1 dose-response assays

In MFD1 cell lines, the optimum dose-response assay was repeated for carboplatin (n=3) and paclitaxel (n=8) to confirm reproducibility (Figure 105). These were grouped together as they were used in the CROSS trial for neoadjuvant CRT prior to surgery.

Overall, my initial results showed that dosing of drugs was not sufficiently accurate, hence the bigger error bars. Once that was amended, my IC50 values had smaller error bars and appeared to be more accurate with less standard deviation.

Appendix G

Optimization of colony growth assays

Another way to determine the ability of MFD1 cells was to grow and form colonies, which I used as a way of measuring proliferation. These are my experiments showing the optimization of the concentrations of chemotherapy drugs for colony growth assays in 6-well plates, such that it was feasible to count individual colonies. To measure this quantitatively, the crystal violet stain of the colonies was dissolved and quantified colorimetrically using the Varioskan® Flash machine. The values were then calculated as a percentage and plotted using histograms on GraphPAD PRISM, using untreated cells in normal media as controls.

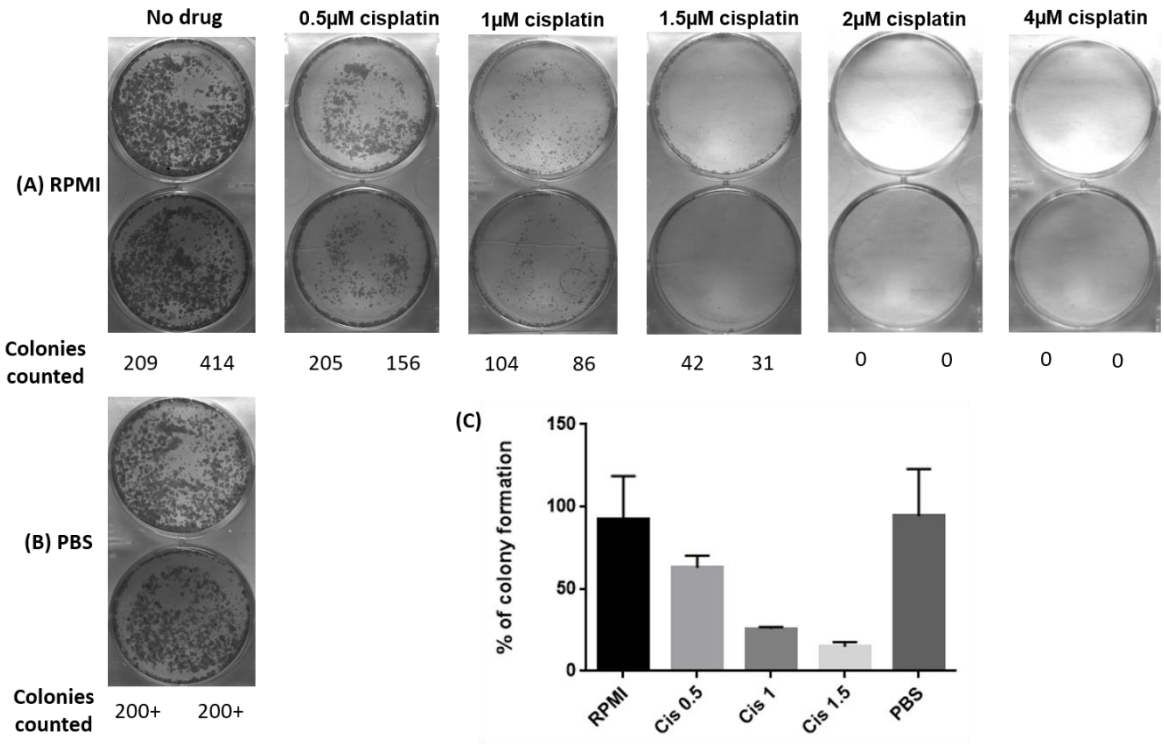

Figure 102. Seeding of 1000 cells per well (in duplication) in normal media in the presence or absence of Cisplatin treatment

Figure 106 shows the seeding of cells in each well in PBS and normal media (RPMI) in the absence and presence of cisplatin. As seen in Figure 106A, concentrations of 1.5-4μM cisplatin was demonstrated to be too high to allow colonies to form. Figure 106C show the quantification of the colonies, which illustrate that percentage of colonies drop as concentration of cisplatin treatment increased, as expected.

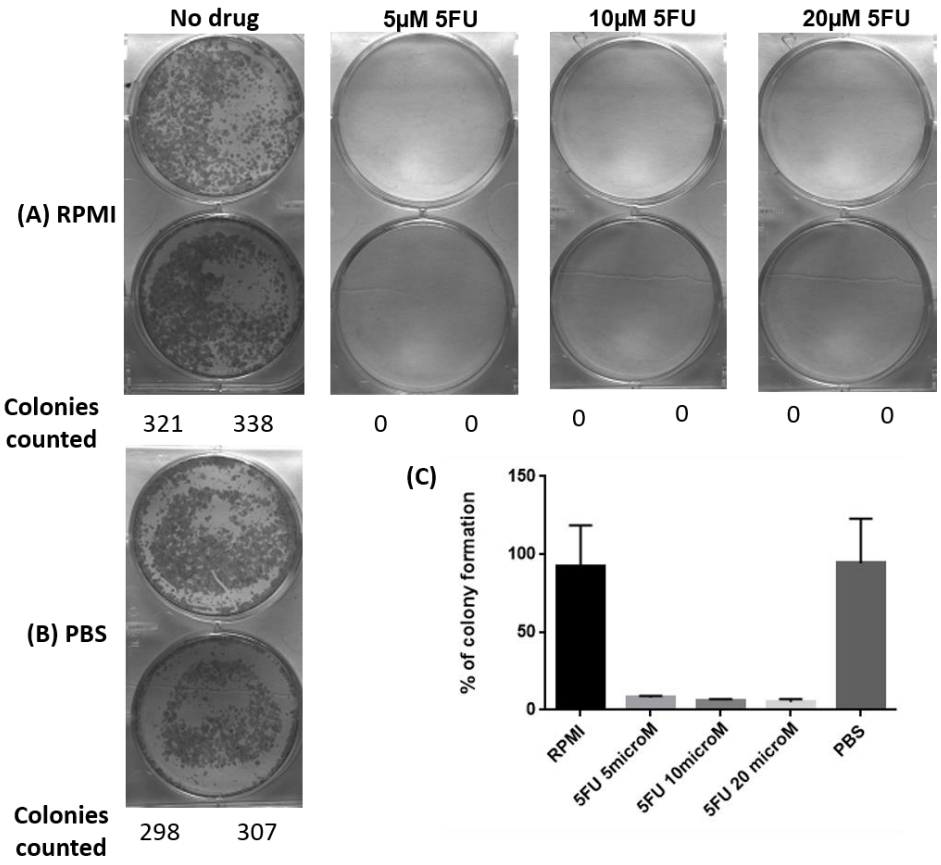

Figure 103. Seeding of 1000 cells per well in normal media in the presence or absence of 5FU treatment

Figure 107 show colony formation in the absence or presence of 5FU treatment. Figure 107A demonstrated that concentrations of 5-20μM 5FU were too high for colonies to grow, which was confirmed by quantification of the colonies formed, as illustrated in Figure 107C.

In addition, seeding 1000 cells per well resulted in colony numbers too challenging to count, in wells where there was an absence of chemotherapy. This could give rise to error when manually counting the colonies. Subsequently, the number of cells seeded was halved to 500 cells per well to counter the error and enable counting of colonies to be more manageable. I also lowered the concentration of drug, and used CAF-conditioned medium from 1 CAF (CAF662) to determine the effect of CAF-CM on the growth of colonies.

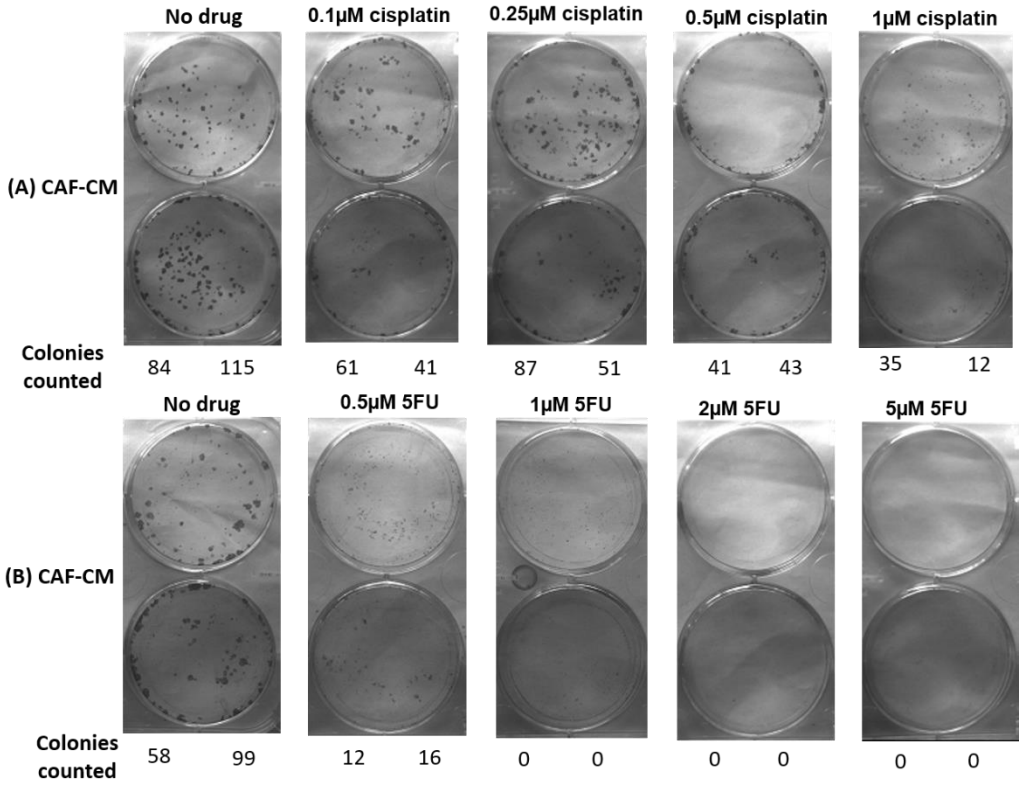

Figure 104. Seeding of 500 cells per well in CAF-conditioned media in the presence or absence of cisplatin/5FU treatment

Figure 108 demonstrate a series of experiments where 500 cells were seeded in each well, using CAF-conditioned media. From this experiment, counting of colonies was much more manageable. However, 0.5μM 5FU still seemed too high a concentration to allow meaningful growth of colonies (Figure 108B), so my next experiment was planned for even lower concentrations of 5FU. These 2 experiments in normal media and CAF-conditioned media were carried out in sequence, therefore various factors such as incubator temperature, plating of cells, etc. may affect the growth of colonies. Hence the next experiment containing both types of media was performed simultaneously to minimize this effect.

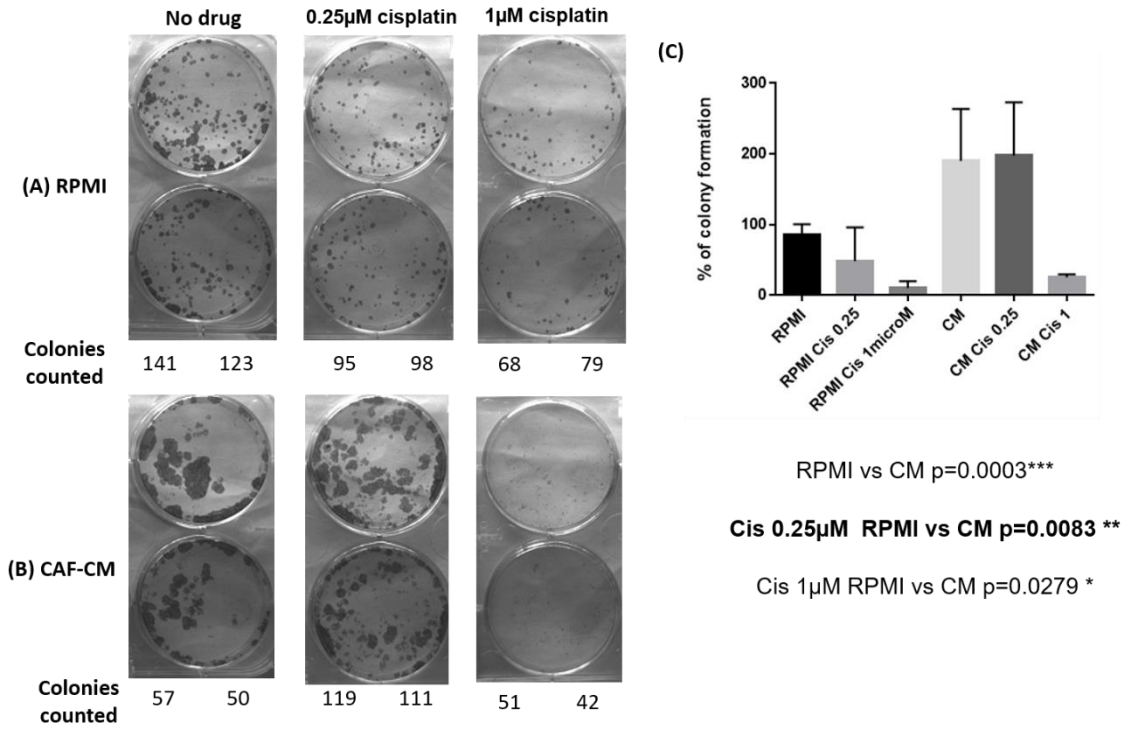

Figure 105. Comparing colonies in normal and CAF-conditioned media in the presence or absence of cisplatin treatment

Figure 109 show colony growth in normal (A) and CAF-CM (B) in the absence and presence of cisplatin. The experiments were repeated (n=3) and colony formation was quantified in Figure 109C. The counting of colonies in the CAF-CM media was challenging as the colonies were not separate but converging onto one another. Because of this, the number of colonies counted may not be reflected accurately. However, when the colonies were quantified, it showed that there was a significant difference in colony formation in CAF-CM, compared to normal media, which was also significantly reflected in the presence of different concentrations of cisplatin.

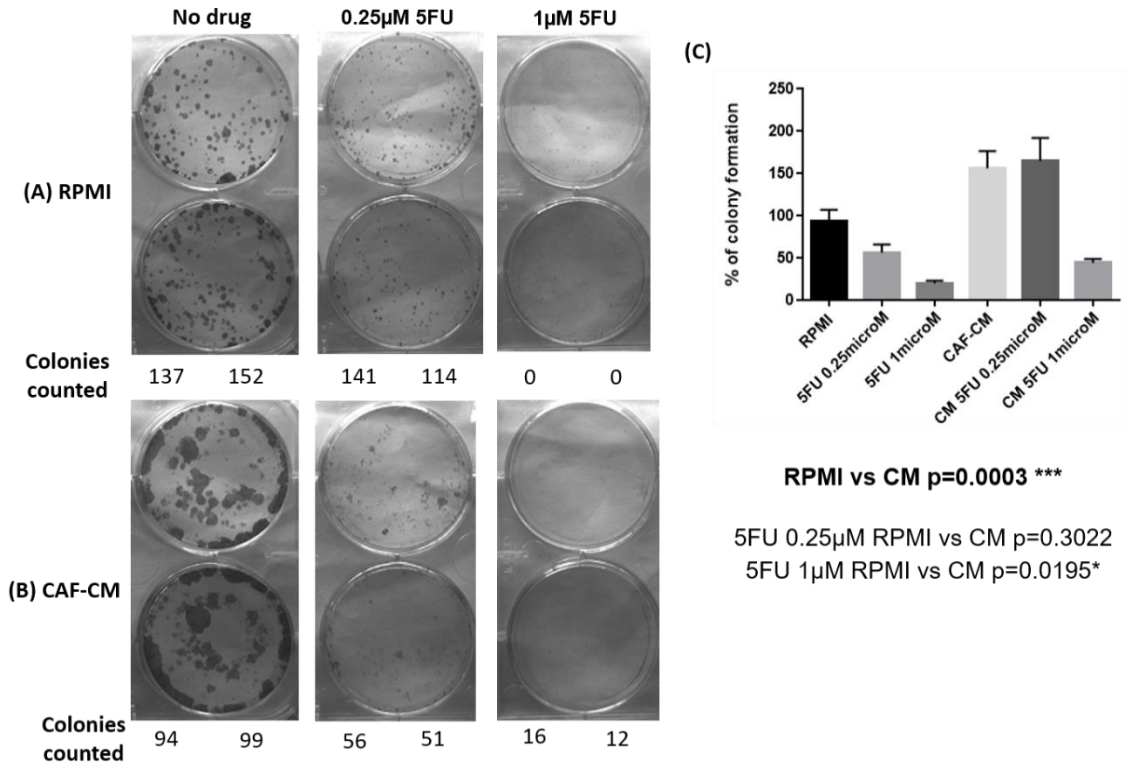

Figure 106. Comparing colonies in normal and CAF-conditioned media in the presence or absence of 5FU treatment

Figure 110 show colony growth in normal (A) and CAF-CM (B) in the absence and presence of 5FU. The experiments were repeated (n=3) and colony formation was quantified in Figure 110C. As previously, colony counting was challenging in CAF-CM, as the colonies were converging onto one another. In addition, the colonies that I had counted were much bigger in size, so that may skew the results of number of colonies counted.

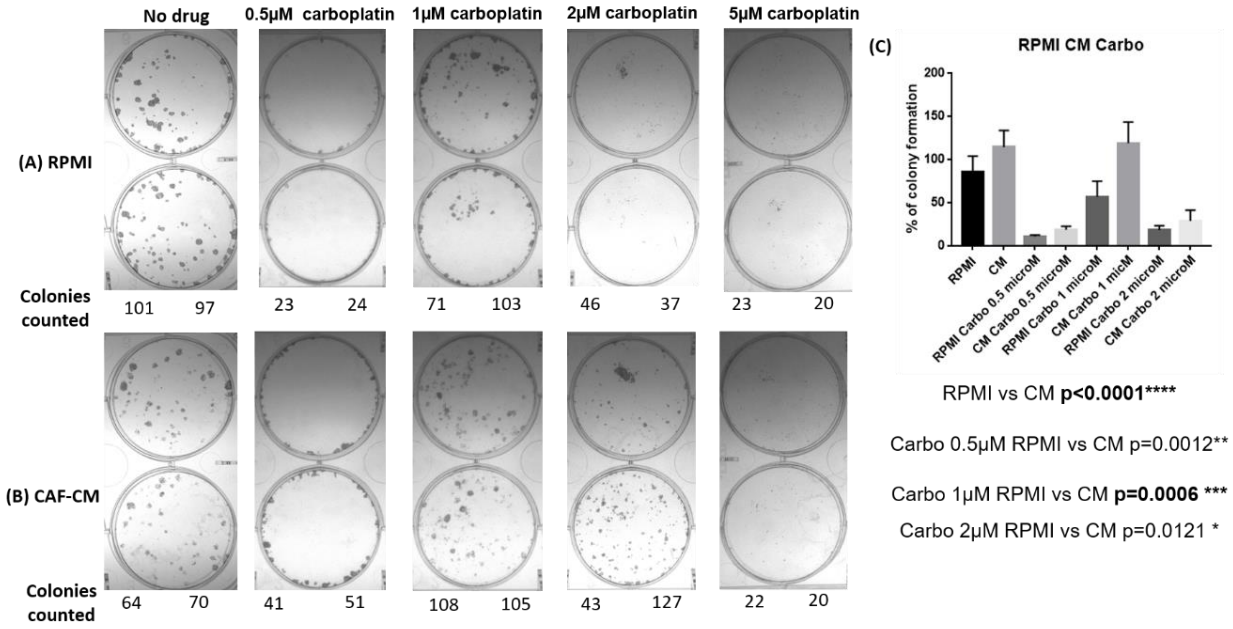

Figure 107. Colony growth assay in normal and CAF-CM in the presence or absence of carboplatin treatment

Figure 111 show colony growth in normal (A) and CAF-CM (B) in the absence and presence of carboplatin. Figure 111C show quantification of colony formation, which demonstrate a significant colony growth in the absence or presence of carboplatin treatment. Experiments were in the presence of 10 and 50μM carboplatin treatment, which did not show any colony growth (plates and graphs not shown), signifying that drug concentration was too high for any colony formation.

I then proceeded to optimize my experiments in vardenafil-treated CAF-conditioned medium (vCM) in the presence and absence of drug treatment.

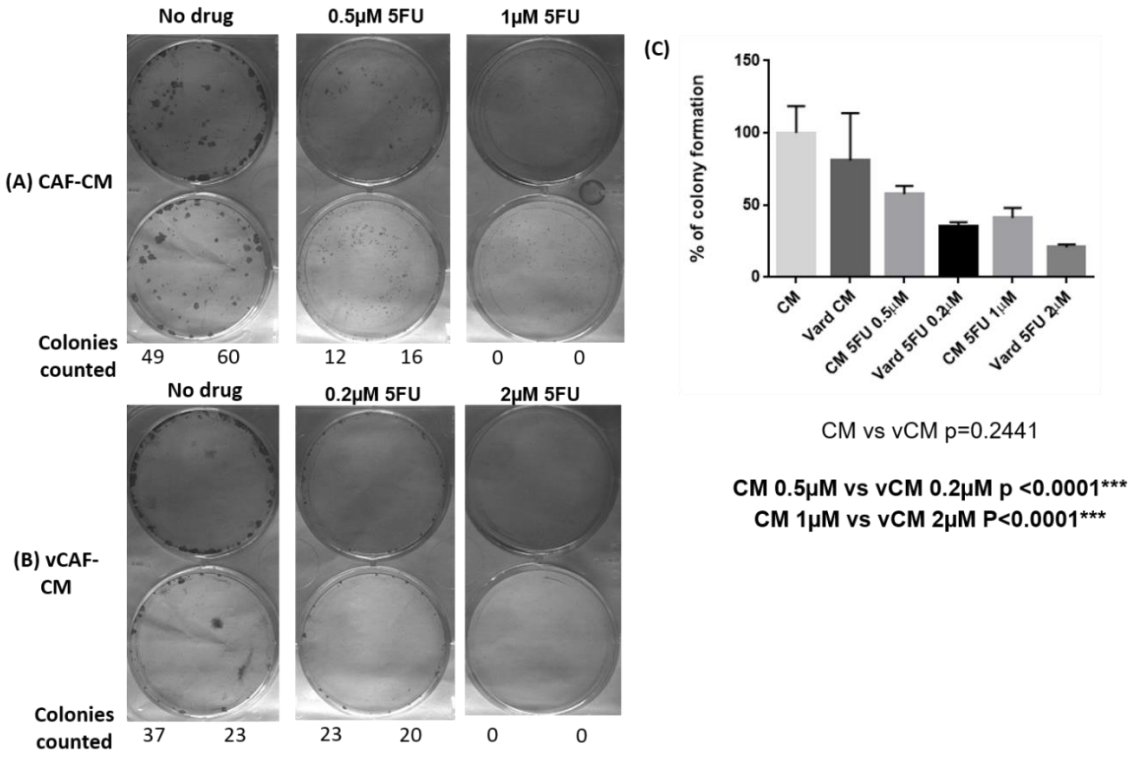

Figure 108. Colony growth assay in CAF-CM and vCM in the presence of 5FU treatment

Figure 112 showed that there is a significant drop of colony growth when cells are in vardenafil-treated CM, in the presence of 5FU chemotherapy treatment. There were no cells in cells seeded in vCAF-CM, in the presence of 0.5μM 5FU, therefore a lower concentration of 0.2μM 5FU was used instead, as shown in Figure 112B.

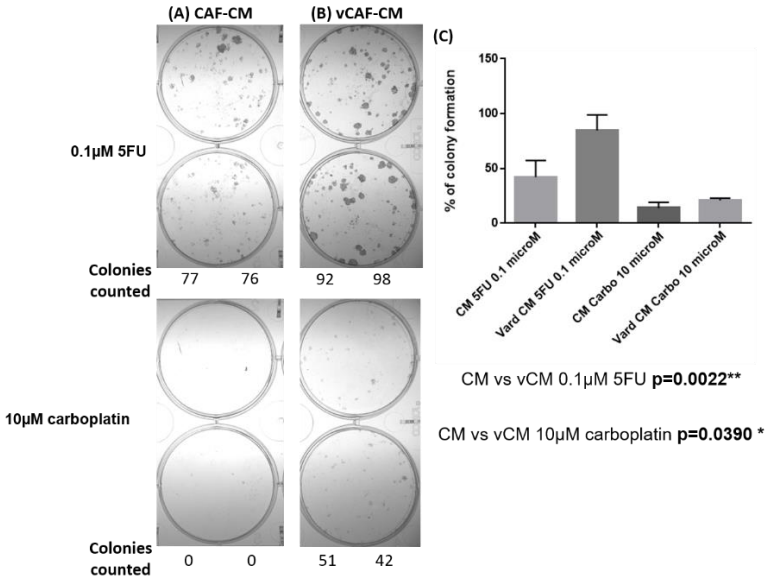

Figure 109. Colony growth assay in CAF-CM and vCM in the presence of 5FU and carboplatin treatments

When I repeated the experiment with a lower concentration of 5FU, and a higher concentration of carboplatin (Figure 113), these results showed a significant increase in colony growth in vardenafil-treated CM, more than those in CAF-CM for both drugs. However, there was too much cell killing with 10μM carboplatin such that there were no colonies evident in CAF-CM, therefore I repeated my experiments with an adjusted dose of carboplatin to establish my results more specifically.

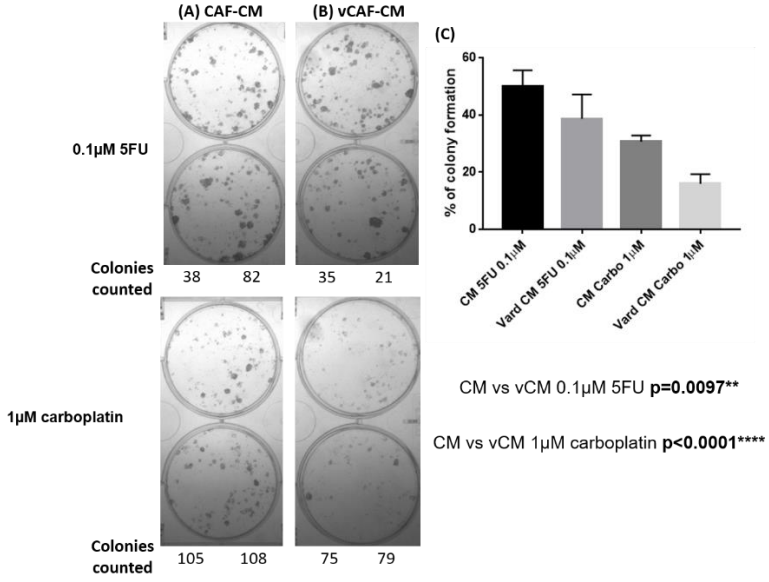

Figure 110. Colony growth assay in CAF-CM and vCM in the presence of 5FU and carboplatin treatments after adjustment of drug dosage

Figure 114 show colony formation in CAF-CM and vCM in the presence of 0.1μM 5FU and 1μM carboplatin treatment. It demonstrated that there was a significant decrease in colony growth when cells are grown in vCM, in the presence of chemotherapy treatment.

Appendix H

Optimization of spheroid assays

Spheroids have been increasingly used in experiments as it can mimic a more physiologically similar microenvironment. Literature was reviewed and it was decided to use 20,000 cells to form the spheroid assay and investigate if that amount of OAC cells or fibroblasts could survive in that volume. Below are my results.

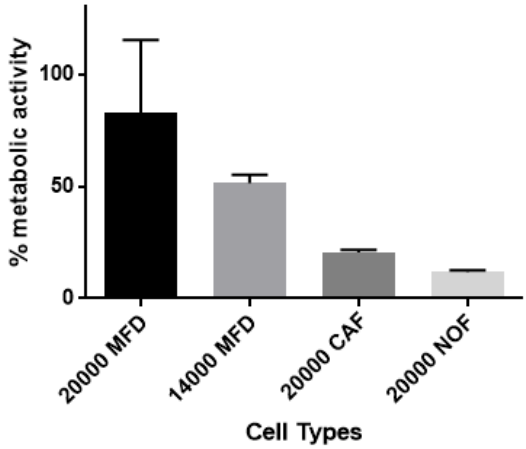

Figure 111. Metabolic activity of spheroids in various amounts cells

When we plated 20,000 MFD1 cells in spheroid plate assays and left them for 7 days, I found that in their spheroidal form, the MFD1 spheroid had 82.9% of metabolic activity (Figure 115). However, when the total number of MFD1 cells plated was decreased to 14,000 cells, there was less metabolic activity (51.4%). This could be due to the inability of the spheroids to form a sufficiently dense-enough structure for cell-cell interaction to enable survival of the cells. When plating fibroblasts alone, I had expected both to have decreased survival, due to the denser core that fibroblasts form. As expected, CAF669 had only 20.5% metabolic activity, while NOF669 had 11.8%.

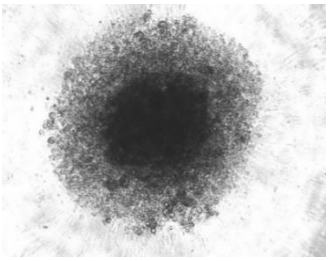

Figure 112. Co-culture spheroid of MFD and CAFs in 3:1 ratio

Based on my results, I decided to use 20,000 cells in total as it appeared to still have a good amount of metabolic activity for the MFD1 cells. Using a 3:1 ratio of cancer cells to fibroblasts, I plated 15,000 MFD1 cells with 5,000 CAFs or NOFs in a co-culture, which appeared to be morphologically sound (Figure 116). I then treated them with different concentrations of individual chemotherapy agents. Based on my previous IC50 results, I used a 25-50-fold increase in drug concentrations to determine if any effect is present.

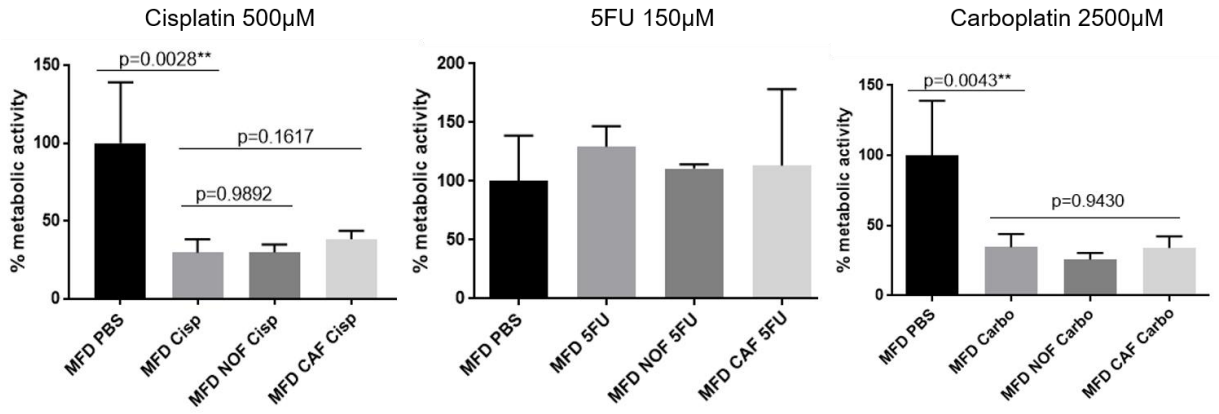

Figure 113. Histograms of spheroids in the absence and presence of chemotherapy agents

As expected with cisplatin treatment, majority of MFD1 spheroid have not survived, leaving 29.7% metabolic activity (Figure 117). A similar effect is seen with carboplatin treatment. However, it is the converse with 5FU treatment, with increased metabolic activity despite treatment. This led me to consider if this cell line is resistant to this antimetabolite, given that the patient from which this cell line originated from had EOX treatment.

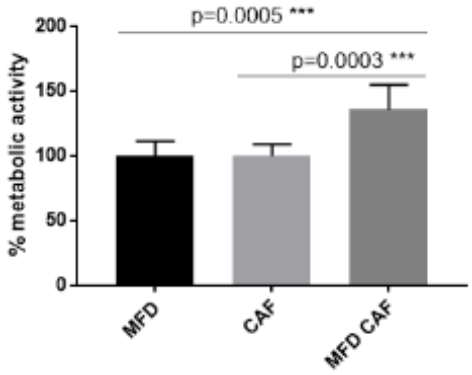

Figure 114. Histogram of spheroids in co-culture

As NOFs appeared to have negligible effects, I focused on CAFs, as my hypothesis is based on CAFs enhancing chemoresistance of OAC cells. In the absence of chemotherapy, there is significant evidence that CAFs confer chemoresistance to OAC cells (Figure 118).

Appendix I

Optimization of FACS analysis of fibroblasts and cancer cells

Flow cytometry is a method that establishes culture purity by evaluating cell surface expression of epithelial, endothelial or stromal cell markers. Cancer cells are epithelial cells which have certain surface markers for expression, such as cytokeratins, cell adhesion molecules such as E-cadherin, epithelium specific antigen (EpCAM), and cell surface proteins such as CA125. EpCAM was chosen to be the antibody to identify MFD1 cancer cells as it occurs on the basolateral cell surfaces of most epithelial cells and carcinomas, and is represented by the FITC fluorochrome channel.

On the other hand, fibroblasts are heterogenous, so there is no lone marker that will identify all fibroblasts. CD90 (Thy-1) is a cell surface glycoprotein that is expressed on human oesophageal fibroblasts and myofibroblasts[284]. As such, it was used to identify oesophageal fibroblast populations by FACS.

Gating for live cells was optimized with individual cell lines to ensure majority of live cells was encompassed. In addition, there was further gating for single cells (Figure 119).

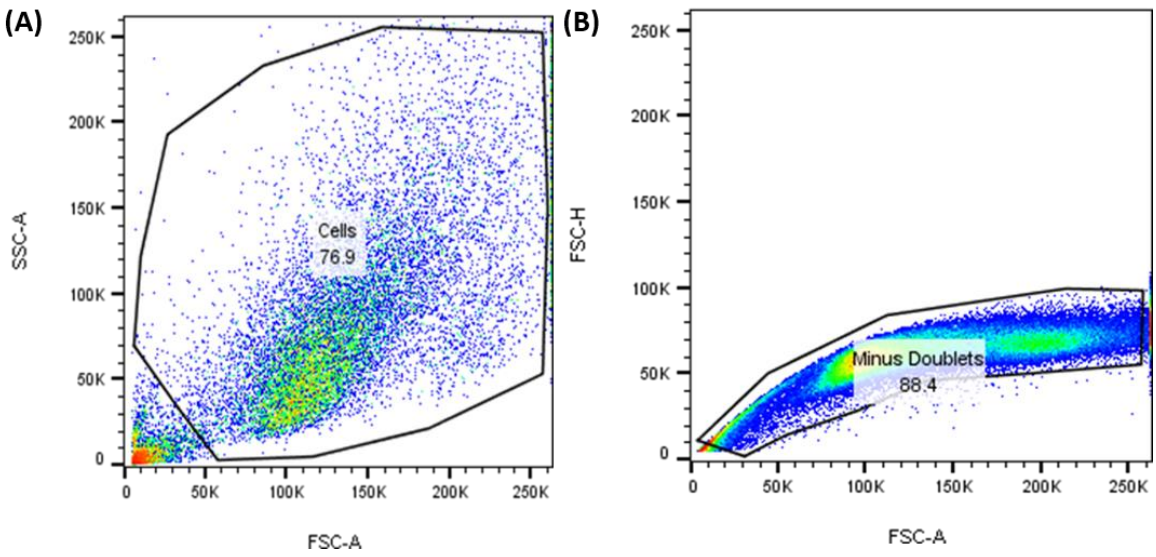

Figure 115. Scatter plots showing gating to exclude cell debris (A) and gating for single cells (B)

To determine if the individual cell lines would be stained with the antibody, several experiments (n=6) were carried out with the EpCAM and CD90 stains as well as their isotypes (Figure 120). It demonstrated that the individual cell lines were positive for their respective antibodies.

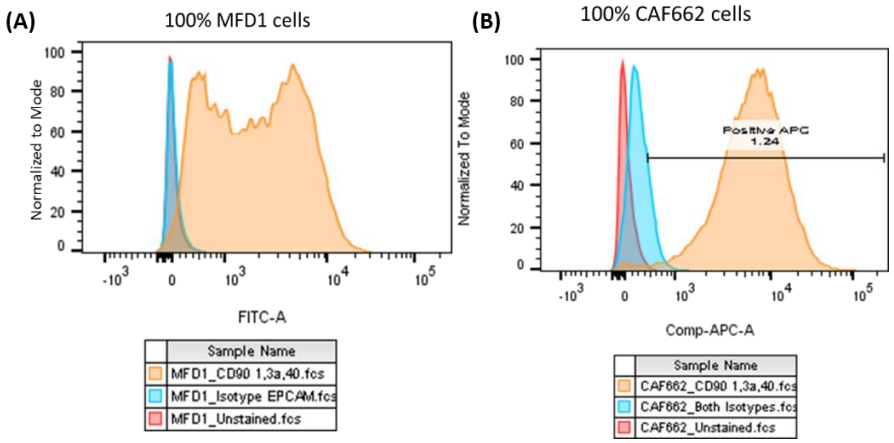

Figure 116. Histograms showing positivity of individual cell lines and the unstained mixture for (A) MFD1 cells in the FITC channel and (B) CAFs in the APC channel

To make certain that each cell population does not have positivity with the opposing stain, I dual-stained the MFD and CAF populations separately (n=3). It showed that neither of the cell populations dual-stained (Figure 121).

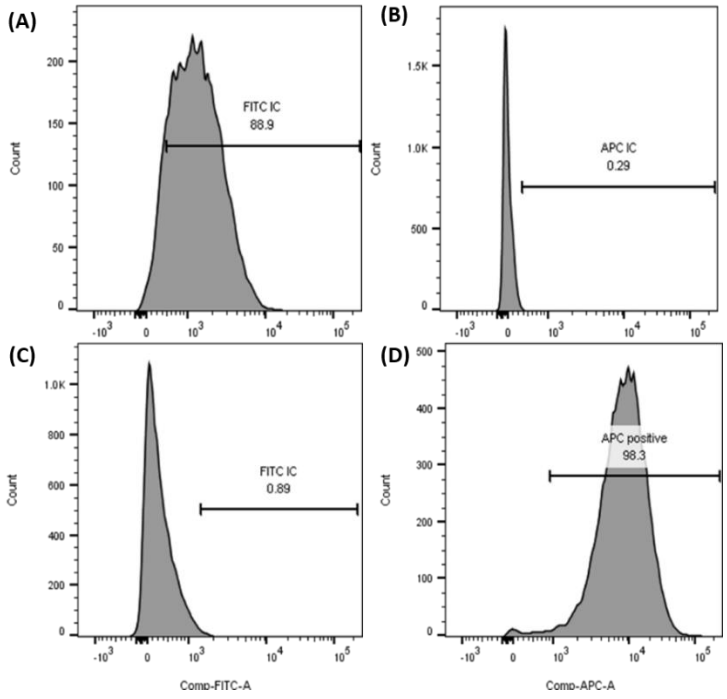

Figure 117. Histograms showing that MFD cells do not stain for CD90 (A and B) and CAFs do not stain for EpCAM (C and D)

When the cells were mixed together in a 3:1 ratio, FACS analysis was carried out to determine if the staining of both cell groups would be compromised. Figure 122 showed that there was no compromise of stains despite mixing of both cell populations (n=6), therefore I was confident that putting the spheroids through flow cytometry would be fruitful.

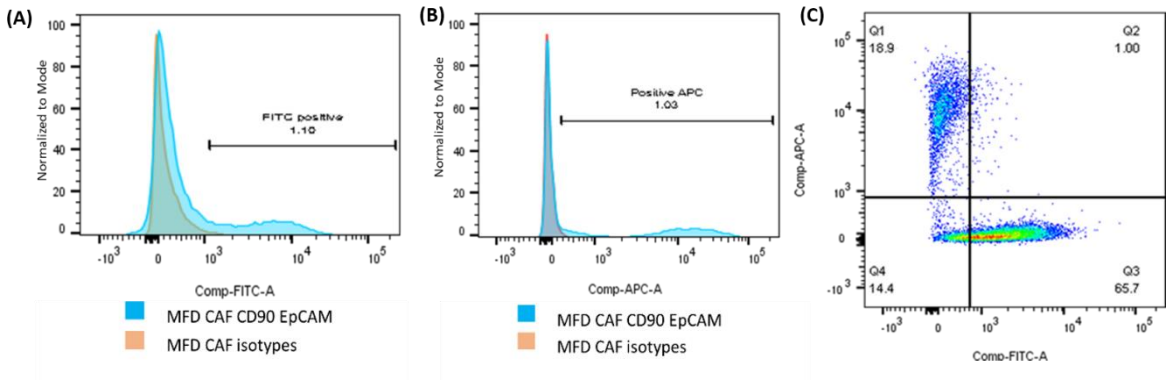

Figure 118. Histograms showing positive staining of MFD1 and CAF cells in FITC (A) and APC (B) channels. (C) show a dot scatter plot demonstrating 2 distinct populations of MFD and CAF cells

As I would be working with spheroids treated with chemotherapy agents, I needed to determine which antibodies were appropriate to stain non-viable cells. Initially, I used propidium iodide (PI) as it is excluded by viable cells but can penetrate cell membranes of dead or dying cells. However, after usage on untreated spheroids (co-culture of MFD and CAFs in 3:1 ratio), the FACS results showed that the majority of cells (74.3%) were not viable. Other cell viability stains gave variable results, with a small proportion (13.85%) of cells stained with Fixed Viability Dye (FVD) not being viable, while it appeared that there was no cell death with 7AAD (n=2) (Figure 123).

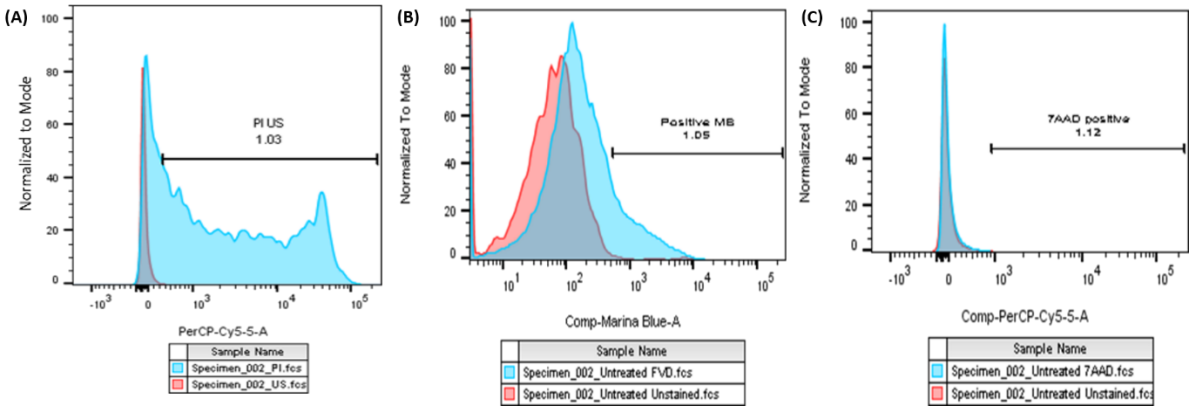

Figure 119. Histograms showing staining of non-viable cells using PI (A), FVD (B) and 7AAD (C)

Because of the variability of results, I went back to individual cell populations, treated MFD cells with dimethyl sulfoxide (DMSO), and carried out FACS analysis of the treated MFD cells with 7AAD (a new bottle was used). These showed that before treatment, 94.36% of cells were viable, and after treatment with DMSO, 65.46% of cells stained for 7AAD and were non-viable (n=2) (Figure 124). Therefore, it was decided to use 7AAD to determine cell viability for FACS analysis.

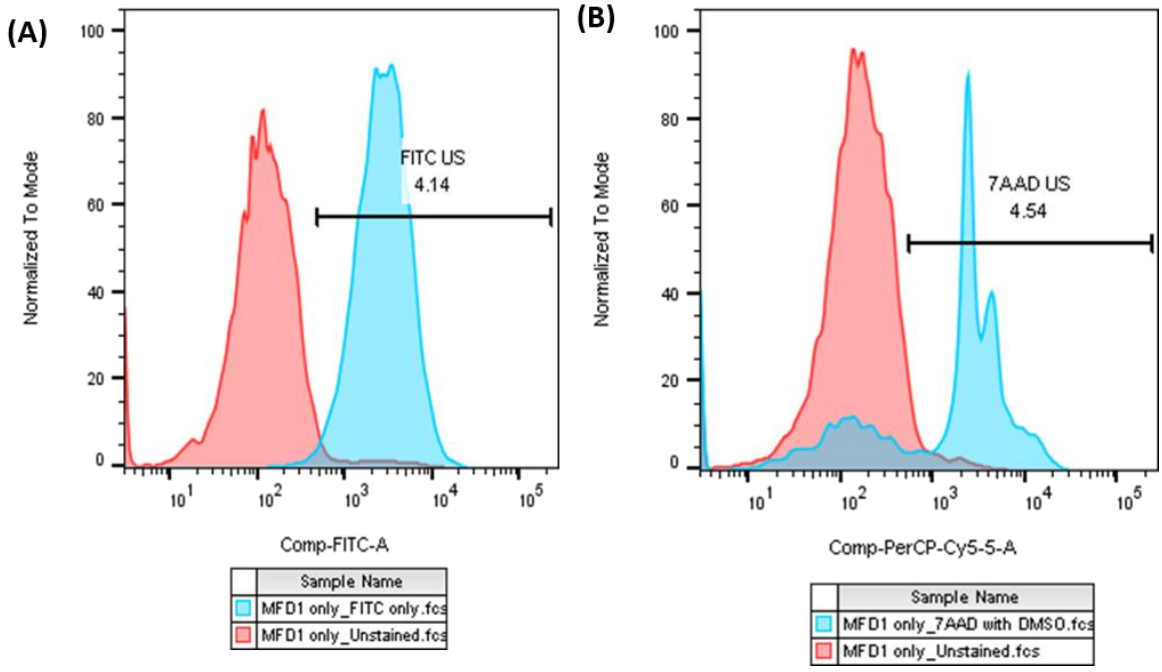

Figure 120. Histograms showing staining of MFD1 cells before (A) and after (B) DMSO treatment

Appendix J

Presentations and Publications

Publication

Edwin Garcia, Annette Hayden, Charles Birts, Edward Britton, Andrew Cowie, Karen Pickard, Massimiliano Mellone, **Clarisa Choh**, Mathieu Derouet, Patrick Duriez, Fergus Noble, Michael J White, John Primrose, Jonathan Strefford, Matthew Rose-Zerilli, Gareth J Thomas, Yeng Ang, Andrew D Sharrocks, Rebecca C. Fitzgerald, and Timothy Underwood.

Authentication and characterisation of a new oesophageal adenocarcinoma cell line: MFD1.

Scientific Reports 2016; **6**: 32417.

Poster Presentations

NCRI Cancer Conference, Liverpool, 2016

PDE5 Inhibitors Can Ameliorate Chemoresistance in Oesophageal Adenocarcinoma Caused by Cancer-Associated Fibroblasts

Clarisa TP Choh, AL Hayden, JP Blaydes, TJ Underwood

10th National Barretts Symposium, London, 2016

Cancer-Associated Fibroblasts Can Promote Chemoresistance in Oesophageal Adenocarcinoma In Vitro

Clarisa TP Choh, AL Hayden, JP Blaydes, TJ Underwood

10th National Barretts Symposium, London, 2016

Optimising PDE5 Inhibitor Induced Dedifferentiation of Cancer-Associated Fibroblasts

Ewan AG Kyle, Annette L Hayden, **Clarisa Choh**, Timothy Underwood

10th National Barretts Symposium, London, 2016

Optimising Chemoradiation Methodology for the Study of the Tumour Microenvironment in Oesophageal Adenocarcinoma

Ewan AG Kyle, Annette L Hayden, **Clarisa Choh**, Timothy Underwood

References

1. Arnold M, Soerjomataram I, Ferlay J, Forman D. Global incidence of oesophageal cancer by histological subtype in 2012. *Gut* 2015;64(3):381-87.

2. Rubenstein JH, Shaheen NJ. Epidemiology, Diagnosis, and Management of Esophageal Adenocarcinoma. *Gastroenterology* 2015;149(2):302-17.

3. Healthcare Quality Improvement Partnership Ltd, Association of Upper GI Surgeons of Great Britain & Ireland. National Oesophago-Gastric Cancer Audit 2019. 2019.

4. Lepage C, Rachet B, Jooste V, Faivre J, Coleman MP. Continuing rapid increase in esophageal adenocarcinoma in England and Wales. *American Journal of Gastroenterology* 2008;103(11):2694-9.

5. Healthcare Quality Improvement Partnership Ltd, Association of Upper GI Surgeons of Great Britain & Ireland. National Oesophago-gastric Cancer Audit 2016. 2016.

6. CRUK Oesophageal Cancer, UK CR. *About Oesophageal Cancer*. http://www.cancerresearchuk.org/about-cancer/oesophageal-cancer/about (accessed 12/06/2020).

7. Health Do. Chief Medical Officer Annual Report 2008, 2008.

8. Lagergren J, Smyth EC, Cunningham D, Lagergren P. Oesophageal cancer. *The Lancet* 2017;390(10110):2383-96.

9. Thurumurthy SG, Chaudry MA, Thurumurthy SSD, Mughal M. Oesophageal cancer: risks, prevention, and diagnosis. *British Medical Journal* 2019;366:I4373.

10. Hur C, Miller M, Kong CY, Dowling EC, Nattinger KJ, Dunn M, et al. Trends in oesophageal adenocarcinoma incidence and motality. *Cancer* 2013;119:1149-58.

11. Coleman HG, Xie SH, LLagergren J. The epidemiology of esophageal adenocarcinoma. *Gastroenterology* 2018;154(2):390-405.

12. Cook MB, Kamangar F, Whiteman DC, Freedman ND, Gammon MD, Bernstein L, et al. Cigarette smoking and adenocarcinomas of the esophagus and esophagogastric junction: a pooled analysis from the international BEACON consortium. *Journal of the National Cancer Institute* 2010;102:1344-53.

13. Whiteman DC, Sadeghi S, Pandeya N, Smithers BM, Gotley DC, Bain CJ, et al. Combined effects of obesity, acid reflux and smoking on the risk of adenocarcinomas of the oesophagus. *Gut* 2008;57:173-80.

14. Park J, Morley TS, Kim M, Clegg DJ, Scherer PE. Obesity and cancer - Mechanisms underlying tumour progression and recurrence. *Nature Reviews Endocrinology* 2014;10(8):455-65.

15. Hoyo C, Cook MB, Kamangar F, Freedman ND, Whiteman DC, Bernstein L, et al. Body mass index in relation to oesophageal and oesophagogastric junction adenocarcinomas: a pooled analysis from the Internatonal BEACON Consortium. *International Journal of Epidemiology* 2012;41:1706-18.

16. Singh S, Sharma AN, Murad MH, Buttar NS, El-Serag HB, Katzka DA, et al. Central Adiposity Is Associated With Increased Risk of Esophageal Inflammation, Metaplasia, and Adenocarcinoma: A Systematic Review and Meta-analysis. *Clinical Gastroenterology and Hepatology* 2013;11(11):1399-412.e7.

17. Pandolfino JE, El-Serag HB, Zhang Q, Shah N, Ghosh SK, Kahrilas PJ. Obesity: a challenge to esophagogastric junction integrity. *Gastroenterology* 2006;130(3):639-49.

18. Rubenstein JH, Taylor JB. Meta-analysis: the association of oesophageal adenocarcinoma with symptoms of gastro-oesophageal reflux. *Alimentary Pharmacology & Therapeutics* 2010;32(10):1222-7.

19. Rubenstein JH, Scheiman JM, Sadeghi S, Whiteman D, Inadomi JM. Esophageal adenocarcinoma incidence in individuals with gastroesophageal reflux: synthesis and estimates from population studies. *American Journal of Gastroenterology* 2011;106(2):254-60.

20. Today M. What's Wrong with Morrisey's Esophagus?, 2013.

21. Fitzgerald RC, di Pietro M, Ragunath K, Ang Y, Kang JY, Watson P, et al. British Society of Gastroenterology guidelines on the diagnosis and management of Barrett's oesophagus. *Gut* 2013;0:1-36.

22. Sharma P, Dent J, Armstrong D, Bergman JJGHM, Gossner L, Hoshihara Y, et al. The development and validation of an endoscopic grading system for Barrett's esophagus: the Prague C&M criteria *Gastroenterology* 2006;131:1392-99.

23. di Pietro M, Fitzgerald RC. Revised British Society of Gastroenterology recommendation on the diagnosis and management of Barrett's oesophagus with low-grade dysplasia. 2017;0:1-2.

24. Al-Kaspooles MF, Hill HC, Nava HR, Smith JL, Douglass HO, Gibbs JF. High-grade dysplasia within Barrett's esophagus: controversies regarding clinical opinons and approaches. *Annals of surgical oncology : the official journal of the Society of Surgical Oncology* 2002;9(3):222-27.

25. Tan MC, Mansour N, White DL, Sisson A, El-Serag HB, Thrift AP. Systematic review with meta-analysis: prevalence of prior and concurrent Barrett's oesophagus in oesophageal adenocarcinoma patients. *Alimentary Pharmacology & Therapeutics* 2020;52:20-36.

26. Desai TK, Krishnan K, Samala NR, Singh J, Cluley JD, Perla S, et al. The incidence of oesophageal adenocarcinoma in non-dysplastic Barrett's oesopahgus: a meta-analysis. *Gut* 2012;61(7):970-76.

27. Ross-Innes CS, BDebiram-Beecham I, O'Donovan M, Walker E, Varghese S, Lao-Sirieix P, et al. Evaluation of a minimally invasive cell sampling device couple with assessment of Trefoil factor 3 expression for diagnosing Barrett's esophagus: A multi-centre case-control study. *Plos Med* 2015;12(1):e1001780.

28. Januszewicz W, Tan WK, Lehovsky K, Debiram-Beecham I, Nuckcheddy T, Moist S, et al. Safety and acceptability of esophageal cytosponge cell collection device in a pooled analysis of data from individual patients. *Clinical Gastroenterology and Hepatology* 2019;17(4):647-56.

29. Offman J, Muldrew B, O'Donovan M, Debiram-Beecham I, Pesola F, Kaimi I, et al. Barrett's oESophagus Trial 3 (BEST3): Study protocol for a randomised controlled trial comparing the cytpsponge-TFF3 test with usual care to facilitate the diagnosis of oesophageal pre-cancer in primary care patients with chronic acid reflux. *BMC Cancer* 2018;18(1):784.

30. Singh S, Devanna S, Varayil JE, Murad MH, Iyer P. Physical activity is associated with reduced risk of esophageal cancer, particularly esophageal adenocarcinoma: A systematic review and meta-analysis. *BMC Gastroenterology* 2014;14:101.

31. Moore SC, Lee IM, Weiderpass E, Campbell PT, Sampson JN, Kitahara CM, et al. Association of leisure-time physical activity with risk of 26 types of cancer in 1.44 million adults. *JAMA - Journal of the American Medical Association* 2016;176(6):816-25.

32. Lagergren K, Lagergren J, Brusselaers. Hormone replacement therapy and oral contraceptives and risk of oesopahgeal adenocarcinoma: A systematic review and meta-analysis. *International Journal of Cancer* 2014;135:2183-90.

33. Brusselaers N, Maret-Ouda J, JKonings P, El-Serag HB, Lagergren J. Menopausal hormone therapy and the risk of esophageal and gastric cancer. *International Journal of Cancer Research and Prevention* 2017;140:1693-99.

34. Cronin-Fenton DP, Murray LJ, Whiteman DC, Cardwell C, Webb PM, Jordan SJ, et al. Reproductive and sex hormonal factors and oesophageal and gastric junction adenocarcinoma: a pooled analysis. *European Journal of Cancer* 2010;46(11):2067-76.

35. Xie F, Zhang Y, Zheng Q, Jin H, Wang F, Chen M, et al. Helicobacter pylori infection and esophageal cancer risk: An updated meta-analysis. *World Journal of Gastroenterology* 2013;19(36):6098-107.

36. Singh S, Garg SK, Singh PP, Iver PG, El-Serag HB. Acid-suppresive medications and risk of oesopahgeal adenocarcinoma in patients with Barrett's oesophagus: a systematic review and meta-analysis. *Gut* 2014;63:1229-37.

37. Liao LM, Vaughan TL, Corley DA, Cook MB, Casson AG, Kamangar F, et al. Nonsteroidal anti-inflammatory drug use reduces risk of adenocarcinomas of the esophagus and esophagogastric junction in a pooled analysis. *Gastroenterology* 2012;142:442-52.

38. Singh S, Singh AG, Singh PP, Murad MH, Iyer PG. Statins are associated with reduced risk of esophageal cancer, particularly in patients with Barrett's esophagus: a systematic review and meta-analysis. *Clinical Gastroenterology and Hepatology* 2013;11:620-29.

39. Nie S, Chen T, Yang X, Huai P, Luu M. Association of Helicobacter pylori infection with esophageal adenocarcinoma and squamous cell carcinoma: a meta-analysis. *Diseases of the esophagus : official journal of the International Society for Diseases of the Esophagus / I.S.D.E* 2014;27(7):645-53.

40. Jankowski JAZ, de Caestecker J, Love SB, Reilly G, Watson P, Sanders S, et al. Esomeprazole and aspirin in Barrett's oesophagus (AspECT): a randomised factorial trial. *The Lancet* 2018;392:400-08.

41. Dulak AM, Stojanov P, Peng S, Lawrence MS, Fox C, Stewart C, et al. Exome and whole-genome sequencing of esophageal adenocarcinoma identifies recurrent driver events and mutational complexity. *Nat Genet* 2013;45(5):478-86.

42. Weaver JM, Ross-Innes CS, Shannon N, Lynch AG, Forshew T, Barbera M, et al. Ordering of mutations in preinvasive disease stages of esophageal carcinogenesis. *Nat Genet* 2014;46(8):837-43.

43. Mourikis TP, Benedetti L, Foxall E, Temelkovski D, Nulsen J, Perner J, et al. Patient-specific cancer genes contribute to recurrently perturbed pathways and establish therapeutic vulnerabilities in esophageal adenocarcinoma. *Nature Communications* 2019;10:3101.

44. Noorani A, Bornschein J, Lynch AG, Secrier M, Achilleos A, Eldridge M, et al. A comparative analysis of whole genome sequencing of esophageal adenocarcinoma pre- and post-chemotherapy. *Genome Research* 2017;27:902-12.

45. Nones K, Waddell N, Wayte N, Patch A-M, Bailey P, Newell F, et al. Genomic catastrophes frequently arise in esophageal adenocarcinoma and drive tumorigenesis. *Nature Communications* 2014;5:5224.

46. Hardwick RH, Barham CP, Ozua P, Newcomb PV, Savage P, Powell R, et al. Immunohistochemical detection of p53 and c-erbB-2 in oesophageal carcinoma; no correlation with prognosis. *European Journal of Surgical Oncology* 1997;23(1):30-5.

47. Casson AG, Evans SC, Gillis A, Porter GA, Veugelers P, Darnton SJ, et al. Clinical implications of p53 tumor suppressor gene mutation and protein expression in esophageal adenocarcinomas: results of a ten-year prospective study. *Journal of Thoracic & Cardiovascular Surgery* 2003;125(5):1121-31.

48. Madani K, Zhao R, Lim HJ, Casson AG. Prognositic value of p53 mutations in oesophageal adenocarcinoma: final results of a 15-year prospective study. *European Journal of Cardiothoracic Surgery* 2010;37(6):1427-32.

49. Schneider PM, Stoeltzing O, Roth JA, Hoelscher AH, Wegerer S, Mizumoto S, et al. P53 mutational status improves estimation of prognosis in patients with curatively resected adenocarcinoma in Barrett's esophagus. *Clinical Cancer Research* 2000;6(8):3153-8.

50. Duhaylongsod FG, Gottfried MR, Iglehart JD, Vaughn AL, Wolfe WG. The significance of c-erb B-2 and p53 immunoreactivity in patients with adenocarcinoma of the esophagus. *Annals of Surgery* 1995;221(6):677-83; discussion 83-4.

51. Fisher OM, Lord SJ, Falkenback D, Clemons NJ, Eslick GD, Lord RV. The prognostic value of TP53 mutations in oesophageal adenocarcinoma: a systemic review and meta-analysis. *Gut* 2017;66:399-410.

52. Alexandrov LB, Nik-Zainal S, Wedge DC, Aparicio SAJR, Behjati S, Biankin AV, et al. Signatures of mutational processes in human cancer. *Nature* 2013;500(7463):415-21.

53. Kim SM, Park YY, Park ES, Cho JY, Izzo JG, Zhang D, et al. Prognostic biomarkers for esophageal adenocarcinoma identified by analysis of tumor transcriptome. *PLoS ONE [Electronic Resource]* 2010;5(11):e15074.

54. Secrier M, Li X, de Silva N, Eldridge MD, Contino G, Bornschein J, et al. Mutational signatures in esophageal adenocarcinoma define etiologically distinct subgroups with therapeutic relevance. *Nat Genet* 2016;48(10):1131-41.

55. Frankell AM, Jammula S, Li X, Contino G, Killcoyne S, Abbas S, et al. The landscape of selection in 551 esophageal adenocarcinomas defines genomic biomarkers for the clinic. *Nat Genet* 2019;51(3):506-16.

56. Bornschein J, Wernisch L, Secrier M, Miremadi A, Perner J, MacRae S, et al. Transcriptomic profiling reveals three molecular phenotypes of adenocarcinoma at the gasoesophageal junction. *International Journal of Cancer* 2019;145(12):3389-401.

57. Turkington RC, Knight LA, Balayney JK, Secrier M, Douglas R, Parkes EE, et al. Immune activation by DNA damage predicts response to chemotherapy and survival in oesophageal adenocarcinoma. *Gut* 2019;68(11):1918-27.

58. Sawas T, Killcoyne S, Iyer PG, Wang KK, Smyrk TC, Kisiel JB, et al. Identification of prognostic phenotypes of esophageal adenocarcinoma in two independent cohorts. *Gastroenterology Clinics of North America* 2018;155(6):1720-28.

59. Jammula S, Katz-Summercorn AC, Li X, Linossi C, Smyth EC, Killcoyne S, et al. Identification of subtypes of Barrett's esophagus and esophageal adenocarcinoma based on DNA methylation profiles and integration of transcriptome and genome data. *Gastroenterology Clinics of North America* 2020;158:1682-97.

60. (NICE) NIfHaCE, Suspected cancer: recognition and referral [NICE. *Gastrointestinal tract (upper) cancers - recognition and referral*. https://cks.nice.org.uk/gastrointestinal-tract-upper-cancers-recognition-and-referral#!scenario (accessed 19/6/20).

61. Hwang JJ, Iyer RV, Salo JC. *Cancer Management, Esophageal Cancer*. http://www.cancernetwork.com/cancer-management/esophageal/page/0/3 (accessed 13/07/2017).

62. Rodriguez D, Jones N. *Understand the Progression of Esophageal Cancer*. http://www.everydayhealth.com/esophageal-cancer/progression-of-esophageal-cancer.aspx (accessed 13/07/17).

63. Healthcare Quality Improvement Partnership Ltd, Association of Upper GI Surgeons of Great Britain & Ireland. National Oesophago-Gastric Cancer Audit 2015. 2015.

64. Blazeby JM, Farndon JR, Donovan J, Alderson D. A prospective longitudinal study examining the quality of life of patients with esophageal carcinoma. *Cancer* 2000;88(8):1781-7.

65. Jacobs M, Macefield RC, Elbers RG, Sitnikova K, Korfage IJ, Smets EMA, et al. Meta-analysis shows clinically relevant and long-lasting deterioration in health-related quality of life after esophageal cancer surgery. *Qual Life Research* 2014;23:1155-76.

66. Schandl A, Lagergren J, Johar A, Lagergren P. Health-related quality of life 10 years after oesophageal cancer surgery. *European Journal of Cancer & Clinical Oncology* 2016;69:43-50.

67. Cunningham D, Allum WH, Stenning SP, Thompson JN, Van de Velde CJ, Nicolson M, et al. Perioperative chemotherapy versus surgery alone for resectable gastroesophageal cancer. *New England Journal of Medicine* 2006;355(1):11-20.

68. Allum WH, Stenning SP, Bancewicz J, Clark PI, Langley RE. Long-term results of a randomized trial of surgery with or without preoperative chemotherapy in esophageal cancer. *Journal of Clinical Oncology* 2009;27(30):5062-67.

69. Sjoquist KM, Burmeister BH, Smithers BM, Zalcberg JR, Simes RJ, Barbour A, et al. Survival after neoadjuvant chemotherapy or chemoradiotherapy for resectable oesophageal carcinoma: An updated meta-analysis. *The Lancet Oncology* 2011;12(7):681-92.

70. Korst RJ, Kansler AL, Port JL, Lee PC, Kerem Y, Altorki NK. Downstaging of T or N Predicts Long-Term Survival After Preoperative Chemotherapy and Radical Resection for Esophageal Carcinoma. *Annals of Thoracic Surgery* 2006;82(2):480-85.

71. Langer R, Ott K, Feith M, Lordick F, Siewert JR, Becker K. Prognostic significance of histopathological tumor regression after neoadjuvant chemotherapy in esophageal adenocarcinomas. *Modern Pathology* 2009;22(12):1555-63.

72. Bollschweiler E, Holscher AH, Metzger R, Besch S, Monig SP, Baldus SE, et al. Prognostic significance of a new grading system of lymph node morphology after neoadjuvant radiochemotherapy for esophageal cancer. *Annals of Thoracic Surgery* 2011;92(6):2020-27.

73. Kelsen DP, Ginsberg R, Pajak TF, Sheahan DG, Gunderson L, Mortimer J, et al. Chemotherapy followed by surgery compared with surgery alone for localized esophageal cancer. *New England Journal of Medicine* 1998;339(27):1979-84.

74. Matsuyama J, Doki Y, Yasuda T, al. E. The effect of neoadjuvant chemotherapy on lymph node micrometastases in squamous cell carcinomas of the thoracic esophagus. . *Surgery (United Kingdom)* 2007;141(5):570-80.

75. Kelsen DP, Winter KA, Gunderson LL, Mortimer J, Estes NC, Haller DG, et al. Long-term results of RTOG trial 8911 (USA intergroup 113): A random assignment trial comparison of chemotherapy followed by surgery compared with surgery alone for esophageal cancer. *Journal of Clinical Oncology* 2007;25(24):3719-25.

76. Ychou M, Boige V, Pignon JP, Conroy T, Bouche O, Lebreton G, et al. Perioperative chemotherapy compared with surgery alone for resectable gastroesophageal adenocarcinoma: An FNCLCC and FFCD multicenter phase III trial. *Journal of Clinical Oncology* 2011;29(13):1715-21.

77. Alderson D, Langley RE, Nankivell MG, Blazeby JM, Griffin M, Crellin A, et al. Neoadjuvant chemotherapy for resectable oesophageal and junctional adenocarcinoma: Results from the UK Medical Research Council randomised OEO5 trial (ISRCTN 01852072). *Journal of Clinical Oncology* 2015;33(15):iv117-iv18.

78. Al-Batran S, Homann N, Pauligk C, Goetze TO, Meiler J, Kasper S, et al. Perioperative chemotherapy with fluorouracil plus leucovorin, oxaliplatin, and docetaxel versus fluorouracil or capecitabine plus cisplatin and epirubicin for locally advanced, resectable gastric or gastro-oesophageal junction adenocarcinoma (FLOT4): a randomised, phase 2/3 trial. *The Lancet* 2019;393(10184):1948-57.

79. Macdonald JS, Smalley SR, Benedetti J, Hundahl SA, Estes NC, Stemmermann GN, et al. Chemoradiotherapy after surgery compared with surgery alone for adenocarcinoma of the stomach or gastroesophageal junction. *New England Journal of Medicine* 2001;345(10):725-30.

80. van Hagen P, Hulshof MCCM, van Lanschot JJB, Steyerberg EW, van Berge Henegouwen MI, Wijnhove BPL, et al. Preoperative Chemoradiotherapy for Esophageal or Junctional Cancer. *New England Journal of Medicine* 2012;366(22):2074-84.

81. Stahl M, Walz MK, Stuschke M, Lehmann N, Meyer HJ, Riera-Knorrenschild J, et al. Phase III comparison of preoperative chemotherapy compared with chemoradiotherapy in patients with locally advanced adenocarcinoma of the esophagogastric junction. *Journal of Clinical Oncology* 2009;27(6):851-56.

82. Wang DB, Zhang X, Han HL, Xu YJ, Sun DQ, Shi ZL. Neoadjuvant chemoradiotherapy could improve survival outcomes for esophageal carcinoma: a meta-analysis. *Digestive Diseases & Sciences* 2012;57(12):3226-33.

83. Ronellenfitsch U, Schwarzbach M, Hofheinz R, Kienle P, Kieser M, Slanger TE, et al. Perioperative chemo(radio)therapy versus primary surgery for resectable adenocarcinoma of the stomach, gastroesophageal junction, and lower esophagus. *The Cochrane database of systematic reviews* 2013;5(5):CD008107.

84. Mukherjee S, Hurt CN, Gwynne S, Sebag-Montefiore D, Radhakrishna G, Gollins S, et al. NEOSCOPE: A randomised phase II study of induction chemotherapy followed by oxaliplatin/capecitabine or carboplatin.paclitaxel based pre-operative chemoradiation for resectable oesophageal adenocarcinoma. *European Journal of Cancer* 2017;74:38-46.

85. Leong T, Smithers BM, Hausterman K, Michael M, Gebski V, Miller DL, et al. TOPGEAR: A Randomized, Phase III Trial of Perioperative ECF Chemotherapy with or Without Preoperative Chemoradiation for Resectable Gastric Cancer: Interim Results from an International, Intergroup Trial of the AGITG, TROG, EORTC and CCTG. *Annals of Surgical Oncology* 2017;24:2252-58.

86. Fuchs CS, Niedzwiecki D, Mamon HJ, Tepper JE, Ye X, Swanson RS, et al. Adjuvant Chemoradiotherapy With Epirubicin, Cisplatin, and Fluorouracil Compared With Adjuvant Chemoradiotherapy With Fluorouracil and Leucovorin After Curative Resection of Gastric Cancer: Results From CALGB 80101 (Alliance) *Journal of Clinical Oncology* 2017;35(32):3671-77.

87. Keegan N, Keane F, Cuffe S, Cunningham M, Ravi N, Lee G, et al. ICORG 10-14: Neo-AEGIS: A randomized clinical trial of neoadjuvant and adjuvant chemotherapy (modified MAGIC regimen) versus neoadjuvant chemoradiation (CROSS protocol) in adenocarcinoma of the esophagus and esophagogastric junction. *Journal of Clinical Oncology* 2014;1).

88. Hoeppner J, Lordick F, Brunner T, Glatz T, Bronsert P, Rothling N, et al. ESOPEC: prospective randomized controlled multicentre phase III trial comparing perioperative chemotherapy (FLOT protocol) to neoadjuvant chemoradiation (CROSS protocol) in patients with adenocarcinoma of the oesophagus (NCT02509286). *BMC Cancer* 2016;16:503.

89. Cunningham D, Stenning SP, Smyth EC, Okines AF, Allum WH, Rowley S, et al. Peri-operative chemotherapy with or without bevacizumab in operable oesophagogastric adenocarcinoma (UK Medical Research Council ST03): primary analysis results of a multicentre, open-label, randomised phase 2 -3 trial. *The Lancet Oncology* 2017;18(3):357-70.

90. Wagner AD, Grabsch HI, Mauer ME, Marreaud S, Caballero C, Thuss-Patience P, et al. EORTC-1203-GITCG - The "INNOVATION"-trial: Effect of Chemotherapy Alone Versus Chemotherapy Plus Trastuzumab, Versus Chemotherapy Plus Trastuzumab Plus Pertuzumab, in the Perioperative Treatment of HER2 Positive, Gastric and Gastroesophageal Junction Adenocarcinoma on Pathologic Response Rate: A Randomized Phase II-intergroup Trial of the EORTC-Gastrointestinal Tract Cancer Group, Korean Cancer Study Group and Dutch Upper GI-Cancer Group. *BMC Cancer* 2019;19(1):494.

91. Longley DB, Harkin DP, Johnston PG. 5-fluorouracil: mechanisms of action and clinical strategies. *Nat Rev Cancer* 2003;3(5):330-8.

92. Dasari S, Tchounwou PB. Cisplatin in cancer therapy: molecular mechanisms of action. *Eur J Pharmacol* 2014;740:364-78.

93. Manual BCACD. Epirubicin, 2017:1-9.

94. Horwitz SB. Taxol (paclitaxel): mechanisms of action. *Annals of Oncology* 1994;5 Suppl 6:S3-6.

95. Organization WH. WHO Handbook for reporting results of cancer treatment. Geneva, Switzerland: World Health Organization, 1979.

96. Group RW, Cancer EOfRaTo, States NCIotU, Group CCT. *RECIST (Response Evaluation Criteria in Solid Tumours)*. http://recist.eortc.org/ (accessed 19/07/2017).

97. Park JO, Lee SI, Song SY, Kim K, Kim WS, Jung CW, et al. Measuring response in solid tumors: comparison of RECIST and WHO response criteria. *Japanese Journal of Clinical Oncology* 2003;33(10):533-7.

98. Tirkes T, Hollar MA, Tann M, Kohli MD, Akisik F, Sandrasegaran K. Response criteria in oncologic imaging: review of traditional and new criteria. *RadioGraphics* 2013;33(5):1323-41.

99. Schwartz LH, Colville JAC, Ginsberg MS, Wang L, Mazumdar M, Kalaigian J, et al. Measuring tumor response and shape change on CT: esophageal cancer as a paradigm. *Annals of oncology : official journal of the European Society for Medical Oncology / ESMO* 2006;17:1018-23.

100. Kurokawa Y, Shibata T, Ando N, Seki S, Mukaida H, Fukuda H. Which is the optimal response criteria for evaluating preoperative treatment in esophageal cancer: RECIST or histology? *Annals of Surgical Oncology* 2013;20(9):3009-14.

101. Choi H. Response evaluation of gastrointestinal stromal tumors. *Oncologist* 2008;13 Suppl 2(suppl 2):4-7.

102. Choi H, Charnsangavej C, S. DCF, Tamm EP, Benjamin RS, Johnson MM, et al. CT evaluation of the response of gastroinestinal stromal tumors after imatinib mesylate treatment: a quantitative analyses correlated with FDG PET findings. *AJR Am J Roentgenol* 2004;183(6):1619-28.

103. Stacchiotti S, Collini P, Messina A, Morosi C, Barisella M, Mertulli R, et al. High-grade soft-tissue sarcomas: tumor response assessment - pilot study to assess the coorelation between radiologic and pathologic response by using RECIST and Choi criteria. *Radiology* 2009;251(2):447-56.

104. Wahl RL, Jacene H, Kasamon Y, Lodge MA. From RECIST to PERCIST: Evolving Considerations for PET response criteria in solid tumors. *J Nucl Med* 2009;50 Suppl 1:122S-50S.

105. Yanagawa M, Tatsumi M, Miyata H, Morii E, Tomiyama N, Watabe T, et al. Evaluation of response to neoadjuvant chemotherapy for esophageal cancer: PET response criteria in solid tumors versus response evaluation criteria in solid tumours. *J Nucl Med* 2012;53(6):872-80.

106. Hoos A, Parmiani G, Hege K, Sznol M, Loibner H, Eggermont A, et al. A clinical development paradigm for cancer vaccines and related biologics. *J Immunother* 2007;30(1):1-15.

107. Wolchok JD, Hoos A, O'Day S, Weber JS, Hamid O, Lebbe C, et al. Guidelines for the evaluation of immune therapy activity in solid tumors: immune-related response criteria. *Clinical Cancer Research* 2009;15(23):7412-20.

108. Davies AR, Gossage JA, Zylstra J, Mattsson F, Lagergren J, Maisey N, et al. Tumor stage after neoadjuvant chemotherapy determines survival after surgery for adenocarcinoma of the esophagus and esophagogastric junction. *Journal of Clinical Oncology* 2014;32(27):2983-90.

109. Becker K, Mueller JD, Schulmacher C, Ott K, Fink U, Buch R, et al. Histomorphology and grading of regression in gastric carcinoma treated with preoperative chemotherapy. *Cancer* 2003;98:1521-30.

110. Becker K, Langer R, Reim D, Novotney A, Meyer zum Buschenfelde C, Engel J, et al. Significance of histopathologial tumor regression after neoadjuvant chemotherapy in gastric adenocarcinomas: a summary of 480 cases. *Annals of Surgery* 2011;253(5):934-39.

111. Schneider PM, Baldus SE, Metzger R, Kocher M, Bongartz R, Bollschweiler E, et al. Histomorphologic tumor regression and lymph node metastases determine prognosis following neoadjuvant radiochemotherapy for esophageal cancer: Implications for response classification. *Annals of Surgery* 2005;242(5):684-92.

112. Wu TT, Chirieac LR, Abraham SC, Krasinskas AM, Wang H, Rashid A, et al. Excellent interobserver agreement on grading the extent of residual carcinoma after preoperative chemoradiation in esophageal and esophagogastric junction carcinoma: a reliable predictor for patient outcome. *Am J Surg Pathol* 2007;31(1):58-64.

113. Society JE. Japnese Classification of Esophageal Cancer, 11th Edition: part I. *Esophagus* 2017;14(1-36).

114. Guo K, Cai L, Zhang Y, Zhu JF, Rong TH, Lin P, et al. The predictive value of histological tumor regression grade (TRG) for therapeutic evaluation in locally advanced esophageal carcinoma treated with neoadjuvant chemotherapy. *Chinese Journal of Cancer* 2012;31(8):399-408.

115. Mandard AM, Dalibard F, Mandard JC, Marnay J, Henry-Amar M, Petiot JF, et al. Pathologic assessment of tumor regression after preoperative chemoradiotherapy of esophageal carcinoma. Clinicopathologic correlations. *Cancer* 1994;73(11):2680-6.

116. Noble F, Nolan L, Bateman AC, Byrne JP, Kelly JJ, Bailey IS, et al. Refining pathological evaluation of neoadjuvant therapy for adenocarcinoma of the esophagus. *World Journal of Gastroenterology* 2013;19(48):9282-93.

117. Smyth EC, Fassan M, Cunningham D, Allum WH, Okines AFC, Lampis A, et al. Effectof pathologic tumor response and nodal status on survival in the medical research council adjuvant gastric infusional chemotherapy trial. *Journal of clinical oncology : official journal of the American Society of Clinical Oncology* 2016;34(23):2721-27.

118. Noble F, Lloyd MA, Turkington RC, Griffiths E, O'Donovan M, O'Neill JR, et al. Multicentre cohort study to define and validate pathological assessment of response to neoadjuvant therapy in oesophagogastric adenocarcinoma. *British Journal of Surgery* 2017;104(13):1816-28.

119. Davies AR, Myoteri D, Zaylstra J, Baker CR, Wulaningsih W, Van Hemelrijck M, et al. Lymph node repgression and survival following neoadjuvant chemotherapy in oesophageal adenocarcinoma. *British Journal of Surgery* 2018;105(12):1639-49.

120. Fareed KR, Kaye P, Soomro IN, Ilyas M, Martin S, Parsons SL, et al. Biomarkers of response to therapy in oesophago-gastric cancer. *Gut* 2009;58(1):127-43.

121. van Heijl M, Omloo JM, van Berge Henegouwen MI, Busch OR, Tilanus HW, Bossuyt PM, et al. NEOadjuvant therapy monitoring with PET and CT in Esophageal Cancer (NEOPEC-trial). *BMC Med Phys* 2008;8:3.

122. Mueller MM, Fusenig NE. Friends or foe - bipolar effets of the tumour stroma in cancer. *Nat Rev Cancer* 2004;4(839-849).

123. Duluc C, Moatassim-Billah S, Chalabi-Dchar M, Perraud A, Samain R, Breibach F, et al. Pharmacological targeting of the protein synthesis mTOR/4E-BP1 pathway in

cancer-associated fibroblasts abrogates pancreatic tumour chemoresistance. *EMBO Mol Med* 2015;7(6):735-53.

124. Wang K, Ma W, Wang J, Yu L, Zhang X, Wang Z, et al. Tumor-stroma ratio is an independent predictor for survival in esophageal squamous cell carcinoma. *Journal of Thoracic Oncology: Official Publication of the International Association for the Study of Lung Cancer* 2012;7(9):1457-61.

125. Courrech Staal EF, Wouters MW, van Sandick JW, Takkenberg MM, Smit VT, Junggeburt JM, et al. The stromal part of adenocarcinomas of the oesophagus: does it conceal targets for therapy? *European Journal of Cancer* 2010;46(4):720-8.

126. Andre F, Berrada N, Desmedt C. Implication of tumor microenvironment in the resistance to chemotherapy in breast cancer patients. *Current Opinion in Oncology* 2010;22(6):547-51.

127. Pietras K, Ostman A, Sjoquist T, Sjo M, Arne O, Buchdunger E, et al. Inhibition of platelet-derived growth factor receptors reduces interstital hypertension and increases transcapillary transport in tumors. *Cancer Research and Clinic* 2001;61:2929-34.

128. Pietras K, Rubin K, Sjoblom T, Buchdunger E, Sjoquist M, Heldin CH, et al. Inhibition of PDGF receptor signaling in tumor stroma enhances antitumor effect of chemotherapy. *Cancer Research* 2002;62(19):5476-84.

129. Sethi T, Rintoul RC, Moore SM, MacKinnon AC, Salter D, Choo C, et al. Extracellular matrix proteins protect small cell lung cancer cells against apoptosis: a mechanism for small cell lung cancer growth and drug resistance in vivo. *Nature Medicine* 1999;5(6):662-8.

130. Castells M, Thibault B, Delord JP, Couderc B. Implication of tumor microenvironment in chemoresistance: tumor-associated stromal cells protect tumor cells from cell death. *Int J Mol Sci* 2012;13(8):9545-71.

131. Mao Y, Keller ET, Garfield DH, Shen K, Wang J. Stromal cells in tumor microenvironment and breast cancer. *Cancer & Metastasis Reviews* 2013;32(1-2):303-15.

132. Hanahan D, Weinberg RA. Hallmarks of cancer: the next generation. *Cell* 2011;144(5):646-74.

133. Matsushita H, Hosoi A, Ueha S, Abe J, Fujieda N, Tomura M. Cytotoxic T lymphocytes block tumor growth both by lytic activity and IFN-gamma-dependent cell-cycle arrest. *Cancer Immunol Immunother* 2015;3(26-36).

134. Noble F, Mellows T, McCormick Matthews LH, Bateman AC, Harris S, Underwood TJ, et al. Tumour infiltrating lymphocytes correlate with improved survival in patients with oesophageal adenocarcinoma. *Cancer Immunol Immunother* 2016;65(6):651-62.

135. Facciabene A, Motz GT, Coukos G. T-regulatory cells: key players in tumor immune escape and angiogenesis. *Cancer Research* 2012;72(9):2162-71.

136. Werb Z, Lu P. The Role of Stroma in Tumor Development. *Cancer Journal* 2015;21(4):250-3.

137. Liu H, Zhang T, Ye J, Li H, Huang J, Li X, et al. Tumor-infiltrating lymphocytes predict response to chemotherapy in patients with advance non-small cell lung cancer. *Cancer Immunol Immunother* 2012;61(10):1849-56.

138. Bhome R, Bullock MD, Al Saihati HA, Goh RW, Primrose JN, Sayan AE, et al. A top-down view of the tumor microenvironment: structure, cells and signaling. *Front Cell Dev Biol* 2015;3:33.

139. Jain RK. Normalizing tumor microenvironment to treat cancer: bench to bedside to biomarkers. *Journal of Clinical Oncology* 2013;31(17):2205-18.

140. Facciabene A, Peng X, Hagemann IS, Balint K, Wang LP, Gimotty PA, et al. Tumour hypoxia promotes tolerance and angiogenesis via CCL29 and T(reg) cells. *Nature* 2011;475:226-30.

141. Semenza GL. Hypoxia-inducible factorsL Mediators of cancer progression and tagets for cancer therapy. *Trends Pharmacol Sci* 2012;33:207-14.

142. Ward PS, Thompson CB. Metabolic reprogramming: A cancer hallmark even Warburg did not anticipate. *Cancer Cell* 2012;21:297-308.

143. Wilson WR, Hay MP. Targeting hypoxia in cancer therapy/ *Nature Review Cancer* 2011;11:393-410.

144. Hale MD, Hayden JD, Grabsch HI. Tumour-microenvironment interactions: role of tumour stroma and proteins produced by cancer-associated fibroblasts in chemotherapy response. *Cellular Oncology* 2013;36(2):95-112.

145. Kharaishvili G, Simkova D, Bouchalova K, Gachechiladze M, Narsia N, Bouchal J. The role of cancer-associated fibroblasts, solid stress and other microenvironmental factors in tumor progression and therapy resistance. *Cancer Cell Int* 2014;14:41.

146. Mitsiades N, Yu WH, Poulaki V, Tsokos M, Stamenkovic I. Matrix metalloproteinase-7-mediated cleavage of Fas ligand protects tumor cells from chemotherapeutic drug cytotoxicity. *Cancer Research* 2001;61(2):577-81.

147. Schrohl AS, Meijer-van Gelder ME, Holten-Andersen MN, Christensen IJ, Look MP, Mouridsen HT, et al. Primary tumor levels of tissue inhibitor of metalloproteinase-I are predictive of resistance to chemotherapy in patients with metastatic breast cancer. *Clinical Cancer Research* 2006;12:7054-58.

148. Sorensen NM, Bystrom P, Christensen IJ, Berglund A, Nielsen HJ, Brunner N, et al. TIMP-1 is significantly associated with objective response and survival in metastatic colorectal cancer patients receiving combination of irinotecan, 5-fluorouracil, and folinic acid. *Clinical Cancer Research* 2007;45:4117-22.

149. Cirri P, Chiarugi P. Cancer associated fibroblasts: the dark side of the coin. *Am J Cancer Res* 2011;1(4):482-97.

150. Huang L, Xu AM, Liu S, Liu W, Li TJ. Cancer-associated fibroblasts in digestive tumors. *World Journal of Gastroenterology* 2014;20(47):17804-18.

151. Aboussekhra A. Role of cancer-associated fibroblasts in breast cancer development and prognosis. *Int J Dev Biol* 2011;55:841-49.

152. Kiaris H, Chatzistamou I, Trimis G, Frangou-Plemmenou M, Pafiti-Kondi A, Kalofoutis A. Evidence for nonautonomous effect of p53 tumor suppressor in carcinogenesis. *Cancer Research* 2005;65(5):1627-30.

153. Trimboli AJ, Cantemir-Stone CZ, Li F, Wallace JA, Merchant A, Creasap N, et al. Pten in stromal fibroblasts suppressed mammary epithelial tumors. *Nature* 2009;461(7267):1084-91.

154. Trimmer C, Sotgia F, Whitaker Menezes D, Balliet RM, Eaton G, Martinez Outschoorn UE, et al. Caveolin-1 and mitochondrial SOD2 (MnSOD) function as tumor suppressors in the stromal environment: a new genetically tractable model for human cancer associated fibroblasts. *Cancer Biology & Therapy* 2011;11(4):383-94.

155. Moskovits N, Kalinkovich A, Bar J, Lapidot T, Oren M. p53 attenuates cancer cell migration and invasion through repression of SDF-1/CXCL12 expression in stromal fibroblasts. *Cancer Research* 2006;66(22):10671-76.

156. Grugan KD, Miller CG, Yao Y, Michaylira CZ, Ohashi S, Klein-Szanto AJ, et al. Fibroblast-secreted hepatocyte growth factor plays a functional role in esophageal squamous cell carcinoma invasion. *Proceedings of the National Academy of Sciences of the United States of America* 2010;107(24):11026-31.

157. Jedeszko C, Victor BC, Podgorski I, Sloane BF. Fibroblast hepatocyte growth factor promotes invasion of human mammary ductal carcinoma in situ. *Cancer Research* 2009;69:9148-55.

158. Erkan M, Adler G, Apte MV, Bachem MG, Buchholz M, Detlefsen S, et al. StellaTUM: current consensus and discussion on pancreatic stellate cell research. *Gut* 2012;61(2):172-78.

159. Schulz WA, Burchardt M, Cronauer MV. Molecular biology of prostate cancer. *Mol Hum Reprod* 2003;9(8):437-48.

160. Noma K, Smalley KSM, Lioni M, Naomoto Y, Tanaka N, El-Deiry W, et al. The essential role of fibroblasts in esophageal squamous cell carcinoma-induced angiogenesis. *Gastroenterology* 2008;134(7):1981-93.

161. Orimo A, Gupta PB, Sgroi DC, Arenzana-Seisdedos F, Delaunay T, Naeem R, et al. Stromal fibroblasts present in invasive human breast carcinomas promote tumor growth and angiogenesis through elevated SDF-1/CXCL12 secretion. *Cell* 2005;121(3):335-48.

162. Underwood TJ, Hayden AL, Derouet M, Garcia E, Noble F, White MJ, et al. Cancer-associated fibroblasts predict poor outcome and promote periostin-dependent invasion in oesophageal adenocarcinoma. *Journal of Pathology* 2015;235:466-77.

163. Henry LR, Lee HO, Lee JS, Klein-Szanto A, Watts P, Ross EA, et al. Clinical implications of fibroblast activation protein in patients with colon cancer. *Clinical Cancer Research* 2007;13:1736-41.

164. Porta C, De Amici M, Quaglini S, Paglino C, Tagliani FB, A. , Moratti R, et al. Circulating interleukin-6 as a tumour marker for hepatocellular carcinoma. *Annals of Oncology* 2008;19:353-58.

165. Valcz G, Sipos F, Tulassay Z, Molnar B, Yagi Y. Importance of carcinoma-associated fibroblast-derived proteins in clinical oncology. *Journal of Clinical Pathology* 2014;67(12):1026-31.

166. Paraiso KH, Smalley KS. Fibroblast-mediated drug resistance in cancer. *Biochemical Pharmacology* 2013;85(8):1033-41.

167. Aoudjit F, Vuori K. Integrin signalling in cancer cell survival and chemoresistance. *Chemother Res Pract* 2012;2012:283181.

168. Witta SE, Gemmill RM, Hirsch FR, Coldren CD, Hedman K, Ravedel L, et al. Restoring E-cadherin expression increases sensitivity to epidermal growth factor receptor inhibitors in lung cancer cell lines. *Cancer Research* 2006;66:944-50.

169. Wang W, Li Q, Yamada T, Matsumoto K, Matsumoto I, Oda M, et al. Crosstalk to stromal fibroblasts induces resistance of lung cancer to epidermal growth factor receptor tyrosine kinase inhibitors. *Clinical Cancer Research* 2009;15:6630-38.

170. Crawford Y, Kasman I, Yu L, Zhong C, Wu X, Modrusan Z, et al. PDGF-C mediates the angiogenic and tumorigenic properties of fibroblasts associated with tumors refractory to anti-VEGF treatment. *Cancer Cell* 2009;15(1):21-34.

171. Rong G, Kang H, Wang Y, Hai T, Sun H. Candidate markers that associate with chemotherapy resistance in breast cancer through the study on Taxotere-induced damage to tumor microenvironment and gene expression profiling of carcinoma-associated fibroblasts (CAFs). *PLoS ONE [Electronic Resource]* 2013;8(8):e70960.

172. Sonnenberg M, van der Kuip H, Haubeis S, Fritz P, Schroth W, Friedel G, et al. Highly variable response to cytotoxic chemotherapy in carcinoma-associated fibroblasts (CAFs) from lung and breast. *BMC Cancer* 2008;8:364.

173. Flach EH, Rebecca VW, Herlyn M, Smalley KS, Anderson AR. Fibroblasts contribute to melanoma tumor growth and drug resistance. *Molecular Pharmaceutics* 2011;8(6):2039-49.

174. Tiago M, de Oliveira EM, Brohem CA, Pennacchi PC, Paes RD, Haga RB, et al. Fibroblasts protect melanoma cells from the cytotoxic effects of doxorubicin. *Tissue engineering. Part A.* 2014;20(17-18):2412-21.

175. Yoshida T, Ishii G, Goto K, Neri S, Hashimoto H, Yoh K, et al. Podoplanin-positive cancer-associated fibroblasts in the tumor microenvironment induce primary resistance to EGFR-TKIs in lung adenocarcinoma with EGFR mutation. *Clinical Cancer Research* 2015;21(3):642-51.

176. Pontiggia O, Sampayo R, Raffo D, Motter A, Xu R, Bissell MJ, et al. The tumor microenvironment modulates tamoxifen resistance in breast cancer: a role for soluble stromal factors and fibronectin through beta1 integrin. *Breast Cancer Research & Treatment* 2012;133(2):459-71.

177. Mueller KL, Madden JM, Zoratti GL, Kuperwasser C, List K, Boerner JL. Fibroblast-secreted hepatocyte growth factor mediates epidermal growth factor receptor tyrosine kinase inhibitor resistance in triple-negative breast cancers through paracrine activation of Met. *Breast Cancer Research* 2012;14(4):R104.

178. Yamada T, Matsumoto K, Wang W, Li Q, Nishioka Y, Sekido Y, et al. Hepatocyte growth factor reduces susceptibility to an irreversible epidermal growth factor receptor inhibitor in EGFR-T790M mutant lung cancer. *Clinical Cancer Research* 2010;16(1):174-83.

179. Ying L, Zhu Z, Xu Z, He T, Li EM, Guo Z, et al. Cancer associated fibroblast-derived hepatocyte growth factor inhibits the paclitaxel-induced apoptosis of lung cancer A549 cells by up-regulating the PI3K.Akt and GRP78 signaling on a microfluidic platform. *PLoS ONE [Electronic Resource]* 2015;10(6):e0129593.

180. Saito S, Morishima K, Ui T, Hoshino H, Matsubara D, Ishikawa S, et al. The role of HGF/MET and FGF/FGFR in fibroblast-derived growth stimulation and lapatinib-resistance of esophageal squamous cell carcinoma. *BMC Cancer* 2015;15:82.

181. Wang W, Li Q, Yamada T, Matsumoto K, Matsumoto I, Oda M, et al. Crosstalk to stromal fibroblasts induces resistance of lung cancer to epidermal growth factor receptor tyrosine kinase inhibitors. *Clinical Cancer Research* 2009;15(21):6630-8.

182. Yamada T, Takeuchi S, Kita K, Bando H, Nakamura T, Matsumoto K, et al. Hepatocyte growth factor induces resistance to anti-epidermal growth factor receptor antibody

in lung cancer. *Journal of Thoracic Oncology: Official Publication of the International Association for the Study of Lung Cancer* 2012;7(2):272-80.

183. Yamada T, Takeuchi S, Nakade J, Kita K, Nakagawa T, Nanjo S, et al. Paracrine receptor activation by microenvironment triggers bypass survival signals and ALK inhibitor resistance in EML4-ALK lung cancer cells. *Clinical Cancer Research* 2012;18(13):3592-602.

184. Kim SM, Kwon OJ, Hong YK, Kim JH, Solca F, Ha SJ, et al. Activation of IL-6R/JAK1/STAT3 signaling induces de novo resistance to irreversible EGFR inhibitors in non-small cell lung cancer with T790M resistance mutation. *Molecular Cancer Therapeutics* 2012;11(10):2254-64.

185. Muerkoster S, Wegehenkel K, Arlt A, Witt M, Sipos B, Kruse ML, et al. Tumor stroma interactions induce chemoresistance in pancreatic ductal carcinoma cells involving increased secretion and paracrine effects of nitric oxide and interleukin-1beta. *Cancer Research* 2004;64(4):1331-7.

186. Muerkoster SS, Werbing V, Koch D, Sipos B, Ammerpohl O, Kalthoff H, et al. Role of myofibroblasts in innate chemoresistance of pancreatic carcinoma--epigenetic downregulation of caspases. *International Journal of Cancer* 2008;123(8):1751-60.

187. Johansson AC, Ansell A, Jerhammar F, Lindh MB, Grenman R, Munck-Wikland E, et al. Cancer-associated fibroblasts induce matrix metalloproteinase-mediated cetuximab resistance in head and neck squamous cell carcinoma cells. *Molecular Cancer Research: MCR* 2012;10(9):1158-68.

188. Martinez-Outschoorn UE, Lin Z, Ko YH, Goldberg AF, Flomenberg N, Wang C, et al. Understanding the metabolic basis of drug resistance: therapeutic induction of the Warburg effect kills cancer cells. *Cell Cycle* 2011;10(15):2521-8.

189. Martinez-Outschoorn UE, Goldberg A, Lin Z, Ko YH, Flomenberg N, Wang C, et al. Anti-estrogen resistance in breast cancer is induced by the tumor microenvironment and can be overcome by inhibiting mitochondrial function in epithelial cancer cells. *Cancer Biology & Therapy* 2011;12(10):924-38.

190. Amornsupak K, Insawang T, Thuwajit P, P OC, Eccles SA, Thuwajit C. Cancer-associated fibroblasts induce high mobility group box 1 and contribute to resistance to doxorubicin in breast cancer cells. *BMC Cancer* 2014;14:955.

191. Kinugasa Y, Matsui T, Takakura N. CD44 expressed on cancer-associated fibroblasts is a functional molecule supporting the stemness and drug resistance of malignant cancer cells in the tumor microenvironment. *Stem Cells* 2014;32(1):145-56.

192. Kharaziha P, Rodriguez P, Li Q, Rundqvist H, Bjorklund AC, Augsten M, et al. Targeting of distinct signaling cascades and cancer-associated fibroblasts define the efficacy of Sorafenib against prostate cancer cells. *Cell Death & Disease* 2012;3:e262.

193. Mink SR, Vashistha S, Zhang W, Hodge A, Agus DB, Jain A. Cancer-associated fibroblasts derived from EGFR-TKI-resistant tumors reverse EGFR pathway inhibition by EGFR-TKIs. *Molecular Cancer Research: MCR* 2010;8(6):809-20.

194. Shekhar MP, Santner S, Carolin KA, Tait L. Direct involvement of breast tumor fibroblasts in the modulation of tamoxifen sensitivity. *American Journal of Pathology* 2007;170(5):1546-60.

195. Matsuoka Y, Yoshida R, Nakayama H, Nagata M, Hirosue A, Tanaka T, et al. The tumour stromal features are associated with resistance to 5-FU-based

chemoradiotherapy and a poor prognosis in patients with oral squamous cell carcinoma. *Apmis* 2015;123(3):205-14.

196. Tanaka K, Miyata H, Sugimura K, Fukuda S, Kanemura T, Yamashita K, et al. miR-27 is associated with chemoresistance in esophageal cancer through transformation of normal fibroblasts to cancer-associated fibroblasts. *Carcinogenesis* 2015;36(8):894-903.

197. Zhang H, Xie C, Yue J, Jiang Z, Zhou R, Xie R, et al. Cancer-associated fibroblasts mediated chemoresistance by a FOXO1/TGFb1 signaling loop in esophageal squamous cell carcinoma. *Molecular Carcinogenesis* 2017;56(3):1150-63.

198. Galvan JA, Wiprachtiger J, Slotta-Huspenina J, Feith M, Ott K, Kroll D, et al. Immunohistochemical analysis of the expression of cancer-associated fibroblast markers in esophageal cancer with and without neoadjuvant therapy. *Virchows Archiv* 2020;476(5):725-34.

199. Che Y, Wang J, Li Y, Lu Z, Huang J, Sun SJ, et al. Cisplatin-activated PAI-1 secretion in the cancer-associated fibroblasts with paracrine effects promoting esophageal squamous cell carcinoma progression and causing chemoresistance. *Cell Death & Disease* 2018;9(7):759.

200. Qiao Y, Zhang C, Li A, Wang D, Luo Z, Ping Y, et al. IL6 derived from cancer-associated fibroblasts promotes chemoresistance via CXCR7 in esophageal squamous cell carcinoma. *Oncogene* 2018;37(7):873-83.

201. Longley DB, Johnston PG. Molecular mechanisms of drug resistance. *Journal of Pathology* 2005;205(2):275-92.

202. Ashdown ML, Robinson AP, TYatomi-Clarke SL, Ashdown ML, Allison A, Abbott D, et al. Chemotherapy for Late-Stage Cancer Patients: Meta-Analysis of Complete Rates. *F1000Res* 2015;4:232.

203. Smith G, Ng MTH, Shepherd L, Herrington CS, Gourley C, Ferguson MJ, et al. Individuality in FGF1 expression significantly influences platinum resistance and progression-free survival in ovarian cancer. *British Journal of Cancer* 2012;107(8):1327-36.

204. Liau SS, Whang E. HMGA1 is a molecular determinany of chemoresistance to gemcitabine in pancreatic adenocarcinoma. *Clinical Cancer Research* 2008;14(5):1470-77.

205. Wang XJ, Li J, Luo L, Wang H, Chi Z, Xin A, et al. Oxaliplatin activates the Keap1/Nrf2 antioxidant system conferring protection against the cytotoxicity of anticancer drugs. *Free Radic Biol Med* 2014;70:68-77.

206. Gan PP, Pasquier R, Kavallaris M. Class III (beta)-tubulin mediates sensitivity to chemotherapeutic drugs in non small cell lung cancer. *Cancer Research and Clinic* 2007;67:9356-63.

207. Izzo JG, Malhotra U, Wu TT, Ensor J, Luthra R, Lee JH, et al. Association of activated transcription factor nuclear factor kappaB with chemoradiation resistance and poor outcome in esophageal carcinoma. *Journal of Clinical Oncology* 2006;24(5):748-54.

208. Langer R, Specht K, Becker K, Ewald P, Bekesch M, Sarbia M, et al. Association of pretherapeutic expression of chemotherapy-related genes with response to neoadjuvant chemotherapy in Barrett carcinoma. *Clinical Cancer Research* 2005;11(20):7462-69.

209. Roninson IB. The role of the MDR1 (p-glycoprotein) gene in multidrug resistance in vitro and in vivo. *Biochemical Pharmacology* 1992;43(1):95-102.

210. Florea A, Bussellberg D. Cisplatin as an anti-tumor drug: Cellular mechanisms of activity, drug resistance and induced side effects. *Cancers* 2011;3:1351-71.

211. Iqbal S, Labonte MJ, Yang D, Zhang W, Bohanes PO, Ning Y, et al. Polymorphisms in EGF a+61G, GSTP1 Ile105Val, and MTHFR A1298C to predict response and survival in a phase II study for patients with metastatic or unresectable gastric (G) or gastroesophageal junction (GEJ) cancer treated with capecitabine, oxaliplatin (XELOX), and cetuximab. *Journal of Clinical Oncology* 2011;1).

212. Joshi MBM, Shirota Y, Danenberg KD, Conlon DH, Salonga DS, Herndon IJE, et al. High gene expression of TS1, GSTP1, and ERCC1 are risk factors for survival in patients treated with trimodality therapy for esophageal cancer. *Clinical Cancer Research* 2005;11(6):2215-21.

213. Lee JM, Wu MT, Lee YC, Yang SY, Chen JS, Hsu HH, et al. Association of GSTP1 polymorphism and survival for esophageal cancer. *Clinical Cancer Research* 2005;11(13):4749-53.

214. Schneider S, Uchida K, Brabender J, Baldus SE, Yochim J, Danenberg KD, et al. Downregulation of TS, DPD, ERCC1, GST-Pi, EGFR, and HER2 gene expression after neoadjuvant three-modality treatment in patients with esophageal cancer. *Journal of the American College of Surgeons* 2005;200(3):336-44.

215. Warnecke-Eberz U, Metzger R, Miyazono F, Baldus SE, Neiss S, Brabender J, et al. High specificity of quantitative excision repair cross-complementing 1 messenger RNA expression for prediction of minor histopathological response to neoadjuvant radiochemotherapy in esophageal cancer. *Clinical Cancer Research* 2004;10(11):3794-99.

216. Kim MK, Cho KJ, Kwon GY, Park SI, Kim YH, Kim JH, et al. ERCC1 predicting chemoradiation resistance and poor outcome in oesophageal cancer. *European Journal of Cancer* 2008;44(1):54-60.

217. Hong J, Peng D, Chen Z, Sehdev V, Belkhiri A. ABL regulation by AXL promotes cisplatin resistance in esophageal cancer. *Cancer Research* 2013;73(1):331-40.

218. Myers AL, Lin L, Nancarrow DJ, Wang Z, Ferrer-Torres D, Thomas DG, et al. IGFBP2 modulates the chemoresistant phenotype in esophageal adenocarcinoma. *Oncotarget* 2015;6:25897-916.

219. Langer R, Specht K, Becker K, Ewald P, Ott K, Lordick F, et al. Comparison of pretherapeutic and posttherapeutic expression levels of chemotherapy-associated genes in adenocarcinomas of the esophagus treated by 5-fluorouracil- and cisplatin-based neoadjuvant chemotherapy. *American Journal of Clinical Pathology* 2007;128(2):191-97.

220. Hong J, Maacha S, Belkhiri A. Transcriptional upregulation of c-MYC by AXM confers epirubicin resistance in esophageal adenocarcinoma. *Molecular Oncology* 2018;12(12):2191-208.

221. Wang Y, Chen Q, Jin S, Deng W, Li S, Tong Q, et al. Up-regulation of P-glycoprotein is involved in the increased paclitaxel resistance in human esophageal cancer radioresistant cells. *Scandinavian Journal of Gastroenterology* 2012;47(7):802-08.

222. Liu L, Zuo LF, Guo JW. ABCG2 gene amplification and expression in esophageal cancer cells with acquired adriamycin resistance. *Molecular Medicine Reports* 2014;9(4):1299-304.

223. Sohda M, Ishikawa H, Masuda N, Kato H, Miyazaki T, Nakajima M, et al. Pretreatment evaluation of combined HIF-1alpha, P53 and P21 expression is a useful and sensitive indicator of response to radiation and chemotherapy in esophageal cancer. *International Journal of Cancer* 2004;110(6):838-44.

224. Loeffler M, Kruger JA, Niethammer AG, Reisfeld RA. Targeting tumor-associated fibroblasts improves cancer chemotherapy by increasing intratumoral drug uptake. *Journal of Clinical Investigation* 2006;116(7):1955-62.

225. Senthebane DA, Jonker T, TRowe A, Thomford NE, Munro D, Dandara C, et al. The role of tumor microenvironment in chemoresistance: 3D extracellular matrices as accomplices. *International Journal of Molecular Sciences* 2018;19(10):2861.

226. Luthra R, Wu TT, Luthra MG, Izzo J, Lopez-Alvarez E, Zhang L, et al. Gene expression profiling of localized esophageal carcinomas: Association with pathologic response to preoperative chemoradiation. *Journal of Clinical Oncology* 2006;24(2):259-67.

227. Luthra MG, Ajani JA, Izzo J, Ensor J, Wu TT, Rashid A, et al. Decreased expression of gene cluster at chromosome 1q21 defines molecular subgroups of chemoradiotherapy response in esophageal cancers. *Clinical Cancer Research* 2007;13(3):912-19.

228. Zenzmaier C, Kern J, Sampson N, Heitz M, Plas E, Untergasser G, et al. Phosphodiesterase type 5 inhibition reverts prostate fibroblast-to-myofibroblast trans-differentiation. *Endocrinology* 2012;153(11):5546-55.

229. Zenzmaier C, Sampson N, Pernkopf D, Plas E, Untergasser G, Berger P. Attenuated proliferation and trans-differentiation of prostatic stromal cells indicate suitability of phosphodiesterase type 5 inhibitors for prevention and treatment of benign prostatic hyperplasia. *Endocrinology* 2010;151(8):3975-84.

230. Catalano S, Panza S, Augimeri G, Giordano C, Malivindi R, Gelsomino L, et al. Phosphodiesterase 5 (PDE5) ia highly expressed in cancer-associated fibroblasts and enhances breast tumor progression. *Cancers* 2019;11:1740.

231. Pratt S, Shepard RL, Kandasamy RA, Johnston PA, Perry III W, Dantzig AH. The multidrug resistance protein 5 (ABCC5) confers resistance to 5-fluorouracil and transports its monophosphorylated metabolites. *Molecular Cancer Therapeutics* 2005;4(5):855-63.

232. Chen JJ, Sun YL, Tiwari AK, Xiao ZJ, Sodani K, Yang DH, et al. PDE5 inhibitors, sildenafil and vardenafil, reverse multidrug resistance by inhibiting the efflux function of multidrug resistance protein 7 (ATP-binding Cassette C10) tranporter. *Cancer Science* 2012;103(8):1531-37.

233. Das A, Durrant D, Mitchell C, Mayton E, Hoke NN, Salloum FN, et al. Sildenafil increases chemotherapeutic efficacy of doxorubicin in prostate cancer and ameliorates cardiac dysfunction. *Proceedings of the National Academy of Sciences of the United States of America* 2010;107(42):18202-07.

234. Das A, durrant D, Mitchell C, Dent P, Batra SK, Kukreja RC. Sildenafil (Viagra) sensitizes prostate cancer cells to doxorubicin-mediated apoptosis through CD95. *Oncotarget* 2016;7:4399-413.

235. Chang J, Hsu J, Sheng Y, Lau W, Yu C, Chan S, et al. Phosphodiesterase Type 5 (PDE5) inhibitors in killing prostate cancer through PDE-independent impairment of HR and NHEJ DNA repair systems. *Frontiers in Oncology* 2019;8:681.

236. Catalano S, Campana A, Giordano C, Gyorffy B, Tarallo R, Rinaldi A, et al. Expression and function and phosphodiesterase type 5 in human breast cancer cell lines and

tissues: Implications for targeted therapy. *Clinical cancer research : an official journal of the American Association for Cancer Research* 2016;22(9):2271-82.

237. Klutzny S, Anurin A, Nicke B, Regan JL, Lange M, Schulze L, et al. PDE5 inhibition eliminates cancer stem cells via induction of PKA signalling. *Cell Death and Disease* 2018;9:192.

238. Singh M, Kasna S, TRoy S, Aldosary S, Saeedan AS, Ansari MN, et al. Repurposing mechanistic insight of PDE-5 inhibitor in cancer chemoprevention through mitochondrial-oxidative stress intervention and blockage of DuCLOX signalling. *BMC Cancer* 2019;19(1):996.

239. Sponziello M, Verrienti A, Rosignolo F, De Rose RF, Pecce V, Maggisano V, et al. PDE5 expression in human thyroid tumors and effects of PDE5 inhibitors on growth and migration of cancer cells. *Endocrine* 2015;50(2):434-41.

240. Li N, Xi Y, Tinsley HN, Gurpinar E, Gary BD, Zhu B, et al. Sulindac selectively inhibits colon tumor cell growth by activating the cGMP/PKG pathway to suppress Wnt/beta-catenin signaling. *Molecular Cancer Therapeutics* 2013;12(9):1848-59.

241. Li N, Chen X, Zhu B, Ramirez-Alcantara V, Canzoneri JC, Lee K, et al. Suppression of beta-catenin/TCF transcriptional activity and colon tumor cell growth by dual inhibition of PDE5 and 10. *Oncotarget* 2015;6(29):27403-15.

242. Li Q, Shu Y. Pharmacological modulation of cytotoxicity and cellular uptake of anti-cancer drugs by PDE5 inhibitors in lung cancer cells. *Pharm Res* 2014;31(1):86-96.

243. Tuttle TR, Mierzwa ML, Wells SI, Fox SR, Ben-Jonathan N. The cyclic GMP/protein kinase G pathway as a therapeutic target in head and neck squamous cell carcinoma. *Cancer Letters* 2016;370(2):279-85.

244. Califano JA, Khan Z, Noonan KA, Rudraraju L, Zhang Z, Wang H, et al. Tadalafil augments tumor specific immunity in patients with head and neck squamous cell carcinoma. *Clinical Cancer Research* 2015;21(1):30-8.

245. Garcia E, Hayden AL, Birts C, Britton E, Cowie A, Pickard KM, et al. Authentication and characterisation of a new oesophageal adenocarcinoma cell line: MFD-1. *Scientific Reports* 2016;6:32417.

246. Shi Z, Tiwari AK, Shukla S, Robey RW, Singh S, Kim IW, et al. Sildenafil reverses ABCB1- and ABCG2-mediated chemotherapeutic drug resistance. *Cancer Research* 2011;71(8):3029-41.

247. Das A, Durrant D, Salloum FN, Xi L, Kukreja RC. PDE5 inhibitors as therapeutics for heart disease, diabetes and cancer. *Pharmacology & Therapeutics* 2015;147:12-21.

248. Rosen RC, Kostis JB. Overview of phosphodiesterase 5 inhibition in erectile dysfunction. *The American Journal of Cardiology* 2003;92(9):9-18.

249. Formulary BN. *British National Formulary* https://bnf.nice.org.uk/ (accessed 29 August).

250. Humbert M, Ghofrani HA. The molecular targets of approved treatments for pulmonary arterial hypertension. *Thorax* 2016;71(1):73-83.

251. Varma A, Das A, Hoke NN, Durrant DE, Salloum FN, Kukreja RC. Anti-inflammatory and cardioprotective effects of tadalafil in diabetic mice. *PLoS ONE [Electronic Resource]* 2012;7(9):e45243.

252. . *2015 ACR/ARHP Annual Meeting*, *San Francisco, California*.

253. Tiwari AK, Chen ZS. Repurposing phosphodiesterase-5 inhibitors as chemoadjuvants. *Front Pharmacol* 2013;4:82.

254. Booth L, Roberts JL, Cruickshanks N, Conley A, Durrant DE, Das A, et al. Phosphodiesterase 5 inhibitors enhance chemotherapy killing in gastrointestinal/genitourinary cancer cells. *Molecular Pharmacology* 2014;85(3):408-19.

255. Li EM, Chen WY, Chen AY, Wu JY, Xu LY. Identification of overexpressed genes induced by nitric oxid in human esophageal carcinoma cell line. [Chinese]. *Ai zheng = Aizheng = Chinese journal of cancer* 2002;21(6):610-14.

256. Ding PR, Tiwari AK, Ohnuma S, Lee JW, An X, Dai CL, et al. The phosphodiesterase-5 inhibitor vardenafil is a potent inhibitor of ABCB1/P-glycoprotein transporter. *PLoS ONE [Electronic Resource]* 2011;6(4):e19329.

257. Shi Z, Tiwari AK, Patel AS, Fu LW, Chen ZS. Roles of sildenafil in enhancing drug sensitivity in cancer. *Cancer Research* 2011;71(11):3735-8.

258. Sampson N, Koziel R, Zenzmaier C, Bubendorf L, Plas E, Jansen-Durr P, et al. ROS signaling by NOX4 drives fibroblast-to-myofibroblast differentiation in the diseased prostatic stroma. *Mol Endocrinol* 2011;25(3):503-15.

259. McCormick Matthews LH, Noble F, Tod J, Jaynes E, Harris S, Primrose JN, et al. Systematic review and meta-analysis of immunohistochemical prognostic biomarkers in resected oesophageal adenocarcinoma. *British Journal of Cancer* 2015:1-12.

260. Boonstra JJ, Van Marion R, Beer DG, Lin L, Chaves P, Ribeiro C, et al. Verification and unmasking of widely used human esophageal adenocarcinoma cell lines. *Journal of the National Cancer Institute* 2010;102:271-74.

261. Weaver JMJ, Shannon NB, Smith M, Dunning M, Ong CA, Ross-Innes C, et al. Defining the genetic landscape of oesophageal adenocarcinoma by next-generation sequencing. *Gut* 2012;61:A3-A4.

262. Fitzgerald R, Fitzgerald RC. Early detection biomarkers for oesophageal cancer. *European Journal of Cancer* 2014;50:S14.

263. Menyhart O, Harami-Papp H, Sukumar S, Schafer R, Magnani L, de Barrios O, et al. Guidelines for the selection of functional assays to evaluate the hallmarks of cancer. *Biochimica et Biophysica Acta* 2016:300-19.

264. Cheng C, Liu ZG, Zhang H, Xie JD, Chen XG, Zhao XQ, et al. Enhancing chemosensitivity in ABCB1- and ABCG2-overexpressing cells and cancer stem-like cells by an Aurora kinase inhibitor CCT129202. *Molecular Pharmaceutics* 2012;9(7):1971-82.

265. Rockett JC, Larkin K, Darnton SJ, Morris AG, Matthews HR. Five newly established oesophageal carcinoma cell lines: phenotypic and immunological characterization. *British Journal of Cancer* 1997;75:258-63.

266. Pantziarka P, Sukhatme V, Crispino S, Bouche G, Meheus L, Sukhatme VP. Repurposing drugs in oncology (ReDO) - selective PDE5 inhibitors as anti-cancer agents. *E cancer medical science* 2018;12:824.

267. Cowie A. *PDE5 expression in oesophageal adenocarcinoma*. University of Southampton, 2018.

268. Kwon Y. Periostin (POSTN), highly expressed gene only in stromal cells around ESCC. *Diseases of the Esophagus* 2010;23:16A.

269. Ruan K, Bao S, Ouyang G. The multifaceted role of periotin in tumorigenesis. *Cell Mol Life Sci* 2009;66(14):2219-30.

270. Saadi A, Shannon NB, Lao-Sirieix P, O'Donovan M, Walker E, Clemons NJ, et al. Stromal genes discriminate preinvasive from invasive disease, predict outcome, and highlight inflammatory pathways in digestive cancers. *Proceedings of the National Academy of Sciences of the United States of America* 2010;107(5):2177-82.

271. Coculova M, Imrichova D, Seres M, Messingerova L, Bohacova V, Sulova Z, et al. The expression of P-glycoprotein in leukaemia cells is associated with the upregulated expression of nestin, a class 6 filament protein. *Leukaemia Research* 2016;48:32-39.

272. Sarlomo-Rikala M, Tsujimura T, Lendahl U, Miettinen M. Patterns of nestin and other intermediate filament expression distinguish between gastrointestinal stromal tumors, leiomyomas and schwannomas. *Apmis* 2002;110(6):499-507.

273. Ishiwata T, Matsuda Y, Naito Z. Nestin in gastrointestinal and other cancers: Effects on cells and tumor angiogenesis. *World Journal of Gastroenterology* 2011;17(4):409-18.

274. Su P, Wang T, Wong Z, Huang B, Yang H. The expression of nestin delineates skeletal muscle differentiation in the developing rat esophagus. *Journal of Anatomy* 2011;218:311-23.

275. Jacekiewicz K, Izycka-Ewieszewska E, Janiak M, Lysiak-Szydlowska W, Adrych K, Reinartz J, et al. Platelet 12-lipoxygenase and stem cells in Barrett's oesophagus. *Oncology Letters* 2010;1(5):789-91.

276. Zhong B, Wang T, Lun X, Zhang J, Zheng S, Yang W, et al. Contribution of nestin positive esophageal squamous cancer cells on malignant proliferation, apoptosis, and poor prognosis. *Cancer Cell International* 2014;14:57.

277. Zhang H, Zhong J, Yu J, Li J, Di W, Lu P, et al. Nestin expression involves invasiveness of esophageal carcinoma and its downregulation enhances paclitaxel sensitivity to esophageal carcinoma cell apoptosis. *Oncotarget* 2017;8(39):65056-63.

278. Manousopoulou A, Hayden AL, Mellone M, Garay-Baquero DJ, White CH, Noble F, et al. Quantitative proteomic profiling of primary cancer-assocaited fibroblasts in oesophageal adenocarcinoma. *British Journal of Cancer* 2018;118:1200-07.

279. Liu J, Xu B, Zheng C, Gong Y, Garibaldi J, Soria J, et al. An end-to-end deep learning histochemical scoring system for breast cancer TMA. *IEEE Trans Med Imaging* 2019;38(2):617-28.

280. Koning JJ, Konijn T, Lakeman KA, O'Toole T, Kenswil KJ, Raaijmakers MH, et al. Nestin-expressing precursors give rise to both endothelial as well as non-endothelial lymph node stromal cells. *Journal of Immunology* 2016;197(7):2686-94.

281. M. ML, Altman DG, Sauerbrei W, Taube SE, Gion M, Clark GM. REporting recommendations for tumour MARKer prognostic studies (REMARK). *European Journal of Cancer* 2005;41(12):1690-96.

282. Evans RA, Tian YC, Steadman R, Phillips AO. TGF-B1-mediated fibroblast-myofibroblast terminal differentiation - The role of Smad proteins. *Exp Cell Res* 2003;282(2):90-100.

283. Ebbing EA, Van der Zalm AP, Steins A, Creemers A, Hermsen S, Rentenaar R, et al. Stromal-derived interleukin 6 drives epithelial-to-nesenchymal transition and therapy resistance in esophageal adenocarcinoma. *Proceedings of the National Academy of Sciences of the United States of America* 2019;116(6):2237-42.

284. M G, C N, Shaker A. Isolation of myofibroblasts from mourse and human esophagus. *Journal of Visualized Experiments* 2015;95:e52215.